ERDC/EL TR-07-21

Environmental Laboratory

US Army Corps of Engineers®
Engineer Research and Development Center

Pre-Construction Biogeochemical Analysis of Mercury in Wetlands Bordering the Hamilton Army Airfield (HAAF) Wetlands Restoration Site. Part 2

Elly P. H. Best, Herbert L. Fredrickson, Holger Hintelmann, Olivier Clarisse, Brian Dimock, Charles H. Lutz, Gui R. Lotufo, Rod N. Millward, Anthony J. Bednar, and John S. Furey

September 2007

Approved for public release; distribution is unlimited.

ERDC/EL TR-07-21
September 2007

Pre-Construction Biogeochemical Analysis of Mercury in Wetlands Bordering the Hamilton Army Airfield (HAAF) Wetlands Restoration Site. Part 2

Elly P. H. Best, Herbert L. Fredrickson, Charles H. Lutz, Gui R. Lotufo, Anthony J. Bednar, and John S. Furey

Environmental Laboratory
U.S. Army Engineer Research and Development Center
3909 Halls Ferry Road
Vicksburg, MS 39180-6199

Holger Hintelmann, Olivier Clarisse, and Brian Dimock

Trent University
Department of Chemistry
Peterborough, Ontario, Canada

Rod N. Millward

Applied Research Associates, Inc.
Vicksburg, MS 39180

Interim report

Approved for public release; distribution is unlimited. [or a restricted statement]

Prepared for U.S. Army Corps of Engineers
Washington, DC 20314-1000

Monitored by U.S. Army Engineer Research and Development Center
3909 Halls Ferry Road, Vicksburg, MS 39180-6199

Abstract: Over 90% of the coastal wetlands in San Francisco Bay have been lost since the industrial revolution. With funding from the Long Term Management Strategy team, the U.S. Army Corps of Engineers (USACE) is working with the San Francisco Basin Regional Water Board, California State Coastal Conservancy, and San Francisco Bay Conservation and Development Commission to reconstruct wetlands at the former Hamilton Army Airfield (HAAF) on San Pablo Bay. This 203-ha site will provide tidal habitat to endangered species such as the clapper rail and the saltmarsh harvest mouse. Because HAAF has subsided well below mean sea level, it will require 8.1 million cubic meters of material to elevate the site to the point where emergent marsh vegetation can become established. This is a critical process that will reestablish natural sediment trapping, marsh building, and physical dynamics. However, wetlands are generally considered a source of monomethylmercury (MeHg) production, and the association of mercury with gold mining legacies of the Bay Basin raises particular concerns. HAAF represents only 203 ha of the additional 26,325 ha of wetlands to be established around the bay between 2005 and 2055. Means to mitigate MeHg magnification in bay aquatic food webs are needed not only for HAAF but other SF Bay restoration sites as well. Those means are currently unknown.

This interim technical report describes studies primarily performed in 2004 and 2005 and completed in the first half of 2006. Work during this period focused on (1) site-specific rates of methylation and demethylation, as well as characterizations of sedimentary microbial communities; (2) mercury dynamics in decomposing plant litter; (3) mercury dynamics in food webs; and (4) bioavailability of sediment-associated mercury of existing marsh sediments to macrobenthos. In addition, a new time-integrative method for measuring and monitoring mercury cycle-related biogeochemical parameters in marshes was developed, and the role of marsh vegetation as a vector in mercury species transport was quantified.

DISCLAIMER: The contents of this report are not to be used for advertising, publication, or promotional purposes. Citation of trade names does not constitute an official endorsement or approval of the use of such commercial products. All product names and trademarks cited are the property of their respective owners. The findings of this report are not to be construed as an official Department of the Army position unless so designated by other authorized documents.

DESTROY THIS REPORT WHEN NO LONGER NEEDED. DO NOT RETURN IT TO THE ORIGINATOR.

Contents

Figures and Tables vii

Executive Summary xiii

Preface xix

1 Report Summary 1

Problem 1

Study 1 (Chapter 3): Mercury Cycle-Related Dynamics in Wetland Sediments of San Pablo Bay: Methylation, Demethylation, and Microbial Biomass 4

Study 2 (Chapter 4): Diffusive Gradient in Thin Film Sentinels for Monitoring Methylmercury Production in Tidal Wetlands on San Pablo Bay 5

Study 3 (Chapter 5): Marsh Vegetation as a Vector in Mercury Species Transport in San Pablo Bay Tidal Marshes—Understanding the Entry of Mercury Into the Aquatic Food Web 6

Study 4 (Chapter 6): Dynamics of Mercury, Methylmercury, and Stable Isotope Signatures in Decomposing Macrophytes from a Tidal Marsh on San Pablo Bay 7

Study 5 (Chapter 7): Mercury Dynamics in Food Webs Associated With Tidal Salt Marshes on San Pablo Bay 8

Study 6 (Chapter 8): Bioavailability of Sediment-Associated Mercury to Macrobenthos 9

2 Background Monomethylmercury Study 11

3 Mercury Cycle-Related Dynamics in Wetland Sediments of San Pablo Bay: Methylation, Demethylation, and Microbial Biomass 15

Introduction 15

Objectives 19

Study sites 19

Materials and methods 21

Approach 21

Sediment sampling 22

Redox and pH measurements 22

Stable mercury isotopic tracer studies 23

Core processing 24

Total mercury determination 24

Methylmercury determination 25

Mercury analysis QA/QC 25

Measurements of mercury methylation and methylmercury demethylation 25

Polar lipid fatty acid methylester analysis 27

Data analysis 28

Results 29

Spatial distribution of mercury and processes in wetlands bordering San Pablo Bay 29

Seasonal changes in methylation and demethylation and potential consequences for net methylmercury production ... 33
Microbial signatures in sediments and their association with net methylmercury production ... 39
Availability of mercury species for uptake by marsh plants ... 43
Discussion ... 45
Measuring rates of methylation and demethylation ... 45
Spatial differences in mercury parameters ... 46
Relationships between microbes and rates of methylation and demethylation ... 47
Seasonal changes in methylation and demethylation rates ... 47
Factors potentially affecting net methylmercury production ... 47
Updating wetland mass balance calculations with recently collected data ... 48
Concluding remarks ... 59

4 Diffusive Gradient in Thin Film Sentinels for Monitoring Methylmercury Production in Tidal Wetlands on San Pablo Bay ... 61
Introduction ... 61
Objectives ... 65
DGT background ... 65
Development of a DGT technique to measure methylmercury in water - chemical calibration ... 68
Methylmercury accumulation as function of deployment time ... 68
Methylmercury accumulation as function of the diffusion layer thickness ... 68
Diffusion coefficient determination ... 69
Effect of dissolved organic matter on methylmercury diffusion in DGT ... 70
Field validation experiment ... 71
Exploration of the use of DGT to characterize key geochemical parameters in sediment ... 71
Methods ... 72
Results and discussion ... 76
Conclusions ... 82

5 Marsh Vegetation as a Vector in Mercury Species Transport in San Pablo Bay Tidal Marshes—Understanding the Entry of Mercury into the Aquatic Food Web ... 84
Introduction ... 84
Objectives ... 85
Study site ... 86
Materials and methods ... 86
Sampling methods ... 86
Total mercury determinations ... 89
Methylmercury determinations ... 89
Mercury analysis QA/QC ... 90
Results and discussion ... 90
Standing crop ... 90
Mercury and methylmercury concentrations in plant tissues ... 95
Net primary production, mortality, fragmentation/leaching, and consequences for the fluxes of mercury species ... 97

Annual mass balances *104*
Entry of mercury into the food web *107*
Conclusions 107

6 Dynamics of Mercury, Methylmercury, and Stable Isotope Signatures in Decomposing Macrophytes from a Tidal Marsh on San Pablo Bay 109
Introduction 109
Objectives 111
Study site 111
Materials and methods 113
Materials *113*
Methods *116*
Results and discussion 119
Change in dry mass *119*
Changes in stable isotope ratios and elemental concentrations in the decomposing litter *125*
Changes in microbial biomass in the decomposing litter *129*
Potential impact of decomposing macrophyte litter on food chains *133*
Conclusions 134

7 Mercury Dynamics in Food Webs Associated with Tidal Salt Marshes on San Pablo Bay 135
Introduction 135
Objectives 138
Study sites 138
Materials and methods 140
Field collection *140*
Laboratory processing *144*
Elemental and stable isotope analysis *145*
Total mercury determinations *145*
Methylmercury determinations *146*
Mercury analysis QA/QC *146*
Statistical comparisons and models *146*
Results 147
Particulate matter isotopic composition *147*
Primary producer isotopic composition *148*
Consumer isotopic composition *151*
Associations among producer and consumer ratios *154*
Mercury species concentrations and MeHg:THg ratios in producers and consumers *158*
General discussion *162*
Conclusions 164

8 Bioavailability of Sediment-Associated Mercury to Macrobenthos 167
Introduction 167
Objectives 168
Study sites 168
Methods 169

Experimental organisms *169*
Sediment sampling *169*
Uptake kinetics experiment *169*
Bioavailability reduction experiment *170*
Chemical analyses of invertebrate tissue *171*
Statistical analysis *172*
Results and discussion 172
Sediment chemistry *172*
Uptake kinetics experiment *172*
Bioavailability reduction experiment *177*
Conclusions 178

References 180

Appendix A 194

Report Documentation Page

Figures and Tables

Figures

Figure 1-1. Location of San Pablo Bay within San Francisco Bay (left) and location of the Hamilton Army Airfield Restoration Site, China Camp reference, and other sites (right). 3

Figure 2-1. Map of sampling locations HAAF and China Camp (inset). 14

Figure 3-1. Site map showing the location of San Pablo Bay within San Francisco Bay (left) and the location of the Hamilton Army Airfield Restoration Site, China Camp, Sonoma Marsh, Sonoma Baylands, and Petaluma River (right). 20

Figure 3-2. Levels of THg versus MeHg (left) and rates of methylation versus level of MeHg (right) measured in surface sediments from various wetlands bordering San Pablo Bay in July 2004. 32

Figure 3-3. Rates of methylation, demethylation, and net MeHg production in non-vegetated sediments of existing marshes on San Pablo Bay measured in July 2004. 34

Figure 3-4. Rates of methylation, demethylation, and net methylmercury production in the sediments of existing marshes on San Pablo Bay measured in June 2003, March and July 2004. 36

Figure 3-5. Relationships between methylation rates, demethylation rates, and *Desulfovibrio* biomass, and the presence of a vegetative cover in sediments of China Camp, HAAF, Sonoma Fringe Marsh, Sonoma Baylands, and Petaluma River sampled in July 2004 expressed in a box-whisker plot. 37

Figure 3-6. Relationships between methylation rates, and redox potential and pH in nonvegetated and vegetated July 2004 sediments of China Camp, HAAF, Sonoma Marsh, Sonoma Baylands, and Petaluma River. 39

Figure 3-7. Relationships between microbial biomass and other characteristics in nonvegetated and vegetated sediments of China Camp, HAAF, Sonoma Marsh, Sonoma Baylands, and Petaluma River sampled in July 2004. 44

Figure 3-8. Annual mass balances of THg and MeHg calculated for a nonvegetated Hamilton Army Airfield wetland. 54

Figure 4-1. Principles of DGT assembly and illustration of diffusion processes in the gel. 67

Figure 4-2. Perspex strips with DGTs are inserted vertically in the sediment, exposing the gels to mercury species at two depths within the sediment and to the above-standing water column. 67

Figure 4-3. Mass of MeHg accumulated by the DGT unit over time. Mean values and standard deviations (N=3). 69

Figure 4-4. Mass of MeHg accumulated by the DGT unit as function of the thickness of the diffusive layer. Mean values and standard deviations (N=3). 69

Figure 4-5. MeHg uptake by DGT in the presence of humic acid 70

Figure 4-6. Sulfide concentrations (μmol L^{-1}) in pore water of Petaluma River sediment (July 2005) measured by the DGT technique. 73

Figure 4-7. Principles of DET assembly and illustration of diffusion processes in the gel. 74

Figure 4-8. Iron and manganese concentrations (μmol L^{-1}) in pore water of Petaluma River sediment (July 2005). 76

Figure 4-9. Sulfate consumption (mmol L^{-1}) in pore water at China Camp (July 2005). 78

Figure 4-10. Sulfide concentrations (μmol L^{-1}) in pore water of Petaluma River sediment (July 2005). 79

Figure 4-11. Key geochemical species in the San Pablo Bay showing manganese, iron, sulfide concentration, and sulfate consumption in sediment pore water (July 2005). 79

Figure 4-12. Sulfide and MeHg in sediment pore water of San Pablo Bay (July 2005). 81

Figure 5-1. Site map showing the location of San Pablo Bay within San Francisco Bay (left) and the location of the Hamilton Army Airfield Restoration Site and the China Camp reference site (right). 87

Figure 5-2. Seasonal changes in the live and dead aboveground standing crop at low marsh site R-44 of the China Camp State Park 90

Figure 5-3. Seasonal changes in the aboveground biomass, concentrations of THg and MeHg, MeHg:THg ratio, and THg and MeHg mass of *Spartina foliosa* at low marsh site R-44 of the China Camp State Park. 93

Figure 5-4. Seasonal changes in the aboveground biomass, concentrations of THg and MeHg, MeHg:THg ratio, and THg and MeHg mass of *Salicornia virginica* at low marsh site R-44 of the China Camp State Park. 94

Figure 5-5. Conceptual model of the role of marsh plants as vectors in mercury species dynamics. 98

Figure 5-6. Flow chart of the flux of dry matter through live *Spartina foliosa* and the community associated with the attached dead plants at low marsh site R-44 of the China Camp State Park. 99

Figure 5-7. Flow chart of the flux of mercury through live *Spartina foliosa* and the community associated with the attached dead plants at low marsh site R-44 of the China Camp State Park. 101

Figure 5-8. Seasonal changes in the estimated net aboveground production, uptake rates of THg and MeHg, and the mortality and fragmentation/leaching rates of *Spartina foliosa* at low marsh site R-44 of the China Camp State Park. 102

Figure 5-9. Seasonal changes in the estimated net aboveground production, uptake rates of THg and MeHg, and the mortality and fragmentation/leaching rates of *Salicornia virginica* at low marsh site R-44 of the China Camp State Park. 103

Figure 6-1. Site map showing the location of San Pablo Bay within San Francisco Bay (left) and the location of the Hamilton Army Airfield Restoration Site and the China Camp reference site (right). 112

Figure 6-2. *Spartina foliosa* (upper) and *Salicornia virginica* (lower) in March 2004. 113

Figure 6-3. Incubations of *Spartina foliosa* and *Salicornia virginica* plant materials in litter bags with sediment and seawater in the laboratory under aerobic and anaerobic conditions. 115

Figure 6-4. Changes over time of mass loss, C:N ratio, concentrations of THg and MeHg, and MeHg:THg ratio in decomposing litter of *Spartina foliosa*. 120

Figure 6-5. Changes over time of mass loss, C:N ratio, concentrations of THg and MeHg, and MeHg:THg ratio in decomposing litter of *Salicornia virginica*. 122

Figure 6-6. Changes in stable isotope means ($\delta^{13}C$, $\delta^{15}N$, and $\delta^{34}S$) of decomposing litter of *Spartina foliosa* (left-hand side) and *Salicornia virginica* (right-hand side) under aerobic and anaerobic conditions. 127

Figure 6-7. Changes over time of microbial biomass and relative contributions of sulfur reducing bacterial strains in decomposing litter of *Spartina foliosa*. 130

Figure 6-8. Changes over time of microbial biomass and relative contributions of sulfur reducing bacterial strains in decomposing litter of *Salicornia virginica*. 132

Figure 7-1. Site map showing the location of San Pablo Bay within San Francisco Bay (left) and the location of the Hamilton Army Airfield Restoration Site and the China Camp reference site (right). 139

Figure 7-2. Habitat types at the China Camp State Park from which samples were collected (upper). Reference site and zones dominated by *Spartina foliosa* and *Salicornia virginica*, respectively, marked (lower). 141

Figure 7-3. Sites of phytoplankton collection in San Pablo Bay (upper) and of phytoplankton and filamentous algae in the marsh pool of the China Camp site (mid and lower). 142

Figure 7-4. Site of epipelic algae collection of the China Camp site. 143

Figure 7-5. Stable isotope ratios, THg and MeHg concentrations, and MeHg:THg ratios of organic material groups collected from the China Camp marsh and adjacent San Pablo Bay area. 150

Figure 7-6. Stable isotope ratios, THg and MeHg concentrations, and MeHg:THg ratios of consumer groups collected from the China Camp marsh and adjacent San Pablo Bay area. 153

Figure 7-7. Trophic level estimation for invertebrates, fish, and avian consumers collected from the China Camp marsh and adjacent San Pablo Bay area based on mean (± standard error of the mean) ranked nitrogen isotopic distributions ($\delta^{15}N$)-Upper left-hand side. 155

Figure 7-8. Dual isotope plots of $\delta^{13}C$, $\delta^{15}N$, and $\delta^{34}S$ mean values for particulate organic matter (POM), primary producers, and consumers collected from the China Camp marsh and adjacent San Pablo Bay area. 157

Figure 8-1. Mean body burdens of THg in *Nereis virens* exposed to Hamilton Army Airfield (HAAF), China Camp (CC), Sonoma Marsh (SM), and Sonoma Baylands (SB) sediment for increasing periods.. 173

Figure 8-2. Mean body burdens of MeHg in *Nereis virens* exposed to Hamilton Army Airfield (HAAF), China Camp (CC), Sonoma Marsh (SM), and Sonoma Baylands (SB) sediments for increasing periods.. 174

Figure 8-3. Effect of 3.4% GAC contact on the 56-d bioaccumulation of THg and MeHg in *Nereis virens* 178

Tables

Table 3-1. THg, MeHg, rates of methylation, demethylation, and net MeHg production in the vegetated sediments of the existing marsh at China Camp on San Pablo Bay, March 2004. 27

Table 3-2. THg, MeHg, rates of methylation, demethylation, and net MeHg production in the sediments of existing marshes on San Pablo Bay, July 2004. 31

Table 3-3. THg, MeHg, rates of methylation, demethylation, and methylation:demethylation ratio in the sediments of existing marshes on San Pablo Bay, June 2003–July 2004. 35

Table 3-4. Relationships between methylation rates, demethylation rates, and microbial communities, and presence of a vegetative cover measured in July 2004 sediment samples, as demonstrated by ANOVA. 36

Table 3-5. Relationships between methylation and demethylation rates, redox potential, pH, and microbial biomass in nonvegetated and vegetated July 2004 sediment samples, as demonstrated by regression analysis. 38

Table 3-6. Total microbial biomass and relative contributions (in percent) of sulfate reducing microbial strains in the sediments of existing marshes on San Pablo Bay, July 2004. 40

Table 3-7. Total microbial biomass and relative contributions (in percent) of sulfate reducing microbial strains in the sediment depth profiles affected by *Spartina foliosa* and *Salicornia virginica* at China Camp, March and July 2004. 40

Table 3-8. Redox potential and pH in the sediments of existing marshes on San Pablo Bay, July 2004. 42

Table 3-9. Relationships between microbial biomass and other characteristics in July 2004 sediment samples, as demonstrated by regression analysis. 43

Table 3-10. Estimated mercury and methylmercury standing stocks of tidal marsh areas in a restored HAAF, based on the assumption that a restored HAAF would turn into a system like the tidal marsh at the China Camp reference site. 50

Table 3-11. Estimated potential methylmercury export of tidal marsh areas in a restored HAAF based on the assumption that a restored HAAF would turn into a system like the tidal marsh at China Camp, using values from the current study. 52

Table 3-12. Estimated potential methylmercury export of tidal marsh areas in a restored HAAF, based on the assumption that a restored HAAF would turn into a system like the tidal marsh at China Camp, using Marvin-DiPasquale et al. (2003) values for methylation and demethylation rates. 57

Table 3-13. Estimated potential methylmercury production and export from tidal marsh areas in San Pablo Bay. 58

Table 4-1. Comparison of MeHg diffusion coefficients obtained by different methods. 69

Table 4-2. Comparison of MeHg measurements by conventional and DGT techniques. 71

Table 4-3. Diffusive flux of MeHg measured in Petaluma River sediment compared to other locations. 82

Table 5-1. Seasonal changes in measured aboveground live and dead standing crop, and calculated net primary production, uptake rates of THg and MeHg, and mortality and fragmentation/leaching rates of *Spartina foliosa* at low marsh site R-44 of the China Camp State Park. 91

Table 5-2. Seasonal changes in measured aboveground live and dead standing crop, and calculated net primary production, uptake rates of THg and MeHg, and mortality and fragmentation/leaching rates of *Salicornia virginica* at low marsh site R-44 of the China Camp State Park. 92

Table 5-3. Coefficients of equations representing the curves of live and dead standing crop for *Spartina foliosa* and *Salicornia virginica* at the low marsh site R-44 of the China Camp State Park (for the means of seven replicates). 95

Table 5-4. Summary of estimated annual net primary production (NPP) of *Spartina foliosa* and *Salicornia virginica* in San Francisco Bay tidal marshes. 105

Table 5-5. Annual net primary production and mercury species mass balances. 106

Table 6-1. Changes in decomposing plant litter of *Spartina foliosa* under aerobic and anaerobic conditions: mass, THg, MeHg concentrations, and MeHg:THg ratio. 121

Table 6-2. Changes in decomposing plant litter of *Salicornia virginica* under aerobic and anaerobic conditions: mass, THg, MeHg concentrations, and MeHg:THg ratio. 123

Table 6-3. Changes in oxygen concentration and pH of the seawater in which the plant litter of *Spartina foliosa* decomposed.

Table 6-4. Changes in oxygen concentration and pH of the seawater in which the plant litter of *Salicornia virginica* decomposed. 125

Table 6-5. Changes in decomposing plant litter of *Spartina foliosa* under aerobic and anaerobic conditions: concentrations and stable isotope ratios of carbon, nitrogen, sulfur, and C:N ratio. 126

Table 6-6. Changes in decomposing plant litter of *Salicornia virginica* under aerobic and anaerobic conditions: concentrations and stable isotope ratios of carbon, nitrogen, sulfur, and C:N ratio. 128

Table 6-7. Changes in decomposing plant litter of *Spartina foliosa* under aerobic and anaerobic conditions: total microbial biomass, and relative contributions of sulfur reducing microbial strains. 129

Table 6-8. Changes in decomposing plant litter of *Salicornia virginica* under aerobic and anaerobic conditions: total microbial biomass, and relative contributions of sulfur reducing microbial strains. 131

Table 7-1. Stable isotope ratios of suspended particulate organic material (POM), primary producers, and vascular plant litter (including habitat type, where sampled) collected from the China Camp marsh and adjacent San Pablo Bay area. 148

Table 7-2. Stable isotope ratios of invertebrate, fish, mammals, and avian consumers (including habitat type, where sampled) collected from the China Camp marsh, HAAF, and adjacent San Pablo Bay area. 152

Table 7-3. Estimated trophic levels for invertebrate, fish, mammals, and avian consumers collected from the China Camp marsh, HAAF, and adjacent San Pablo Bay area, calculated using SOURCE and STEP with $\delta^{13}C$, $\delta^{15}N$, and $\delta^{34}S$. 158

Table 7-4. THg, MeHg, and MeHg:THg ratios of suspended particulate organic material (POM), primary producers, and vascular plant litter (including habitat type, where sampled) collected from the China Camp marsh and adjacent San Pablo Bay area. 159

Table 7-5. THg, MeHg, and MeHg:THg ratios of invertebrate, fish, mammals, and avian consumers (including habitat type, where sampled) collected from the China Camp marsh, HAAF, and adjacent San Pablo Bay area. 161

Table 8-1. Mean THg and MeHg concentrations in the upper 10 cm of sediment from four sites bordering San Pablo Bay. 172

Table 8-2. Toxicokinetic model parameters estimates for THg and MeHg calculated for *Nereis virens* exposed to Hamilton Army Airfield, China Camp, Sonoma Baylands, and Sonoma Marsh sediments. 175

Table A5-1. Seasonal changes in biomass of *Spartina foliosa* at low marsh site R-44 of the China Camp State Park. 194

Table A5-2. Seasonal changes in the concentrations of THg, MeHg, and MeHg:THg ratio in biomass of *Spartina foliosa* at low marsh site R-44 of the China Camp State Park. 195

Table A5-3. Seasonal changes in biomass of *Salicornia virginica* at low marsh site R-44 of the China Camp State Park. 196

Table A5-4. Seasonal changes in the concentrations of THg, MeHg, and MeHg:THg ratio in biomass of *Salicornia virginica* at low marsh site R-44 of the China Camp State Park. 197

Table A7-1. C, N, and S contents of suspended particulate organic material (POM), primary producers, and vascular plant litter (including habitat type where sampled) collected from the China Camp marsh and adjacent San Pablo Bay area. 198

Table A7-2. C, N, and S contents of invertebrate, fish, mammals, and avian consumers (including habitat type where sampled) collected from the China Camp marsh, HAAF, and adjacent San Pablo Bay area. 199

Executive Summary

Over 90% of the coastal wetlands in San Francisco Bay have been lost since the industrial revolution. With funding from the Long Term Management Strategy team, the U.S. Army Corps of Engineers (USACE) is working with the San Francisco Basin Regional Water Board, California State Coastal Conservancy, and San Francisco Bay Conservation and Development Commission to reconstruct wetlands at the former Hamilton Army Airfield (HAAF) on San Pablo Bay. This 203-ha site will provide tidal habitat to endangered species such as the clapper rail and the saltmarsh harvest mouse. Because HAAF has subsided well below mean sea level, it will require 8.1 million cubic meters of material to elevate the site to the point where emergent marsh vegetation can become established. This is a critical process that will reestablish natural sediment trapping, marsh building, and physical dynamics. However, wetlands are generally considered a source of monomethylmercury (MeHg) production, and the association of mercury with gold mining legacies of the Bay Basin raises particular concerns. HAAF represents only 203 ha of the additional 26,325 ha of wetlands to be established around the bay between 2005 and 2055. Means to mitigate MeHg magnification in bay aquatic food webs are needed not only for HAAF but other SF Bay restoration sites as well. Those means are currently unknown.

This interim technical report describes studies primarily performed in 2004 and 2005 and completed in the first half of 2006. Work during this period focused on (1) site-specific rates of methylation and demethylation, as well as characterizations of sedimentary microbial communities; (2) mercury dynamics in decomposing plant litter; (3) mercury dynamics in food webs; and (4) bioavailability of sediment-associated mercury of existing marsh sediments to macrobenthos. In addition, a new time-integrative method for measuring and monitoring mercury cycle-related biogeochemical parameters in marshes was developed, and the role of marsh vegetation as a vector in mercury species transport was quantified.

The levels of total mercury (THg) in the surface sediments of wetlands bordering San Pablo Bay, which were studied by the authors of this report in the period 2001-2004, are in the order of 300 ng g^{-1} dry weight (DW) and are comparable to those generally found in San Francisco Bay. No

strong correlations were demonstrated between levels of THg and MeHg. Results of field studies using a heavy-labeled mercury isotope approach indicated that methylation and demethylation rates are rapid and that current rates of methylation would double the standing pool size of MeHg within a day if this rate was not counter balanced by demethylation. The current rates of demethylation would deplete the standing MeHg pool size to null within a few days if methylation ceased. This produces a dynamic MeHg pool with respect to time and space. No consistent trend in net MeHg production rates (methylation rate minus demethylation rate) was found in SF Bay wetlands ranging from the China Camp State Park (24‰ salinity) to the Petaluma River (7‰). Analysis of variance indicated that net MeHg production was significantly less in vegetated than in bare sediments in July 2004 (0.72 versus 4.4 ng MeHg g^{-1}DW d^{-1}), but relative abundance of the sulfate-reducing bacterial (SRB) *Desulfovibrio* was significantly greater. A significant relationship between microbial biomass and relative abundances of the SRB genera *Desulfobacter* (+ *Desulfobacterium*) and *Desulfovibrio* and MeHg pool size was found, but no significant relationships between THg and other sediment characteristics were demonstrated.

A new method, Diffusive Gradient in Thin Film (DGT) technique, was developed to monitor bioavailable MeHg in the water column and sediment pore water. This method uses 3–mercaptopropyl–functionalized silica gel to bind MeHg. The detection limit of the overall method, 0.001 ng of MeHg, corresponds approximately to 0.030 ng L^{-1} of MeHg in a water sample when deployed for 24 hours. Field tests have indicated that DGT measurements of dissolved MeHg provide comparable results to conventional methods of sample collection and measurement. The DGT technique provides an alternative in situ sampling method for MeHg with the added advantage that it integrates exposure levels over a time period. This may dampen the wide fluctuations in MeHg levels often observed and may provide more reliable data required for monitoring and management decisions. Field data collected using this method formed the basis for estimates of MeHg diffusion fluxes from sediment to water of 1,500-6,900 ng m^{-2} y^{-1} in China Camp and of 15,000 ng m^{-2} y^{-1} in the Petaluma River. Therefore, the river sediment potentially represents a significant source of MeHg for SF Bay. The DGT technique was also used in July 2005 to sample key geochemical species in sediment pore water to characterize and understand the biogeochemistry of SF Bay sediment and to investigate the mobility of associated MeHg. In combination with other gel-based

sampling techniques (DET, Diffusional Equilibration in Thin Film) ancillary parameters, such as dissolved sulfide, sulfate, manganese, and iron, were measured at a millimeter-scale. This allowed a detailed characterization of redox zones in the sediments and identification of mercury methylation hot spots, which are typically confined to thin horizons in the sediment layer (few millimeters).

The potential for marsh plants to be vectors in the transport of mercury species was studied in the China Camp salt marsh. The fluxes of organic matter, THg, and MeHg were studied in natural stands of *Spartina foliosa* and *Salicornia virginica*. Seasonal fluxes from the sediment into aboveground biomass of live plants and subsequent transfer into the dead plant community by mortality were measured. Disappearance of THg and MeHg from the latter community through fragmentation, leaching, and excretion were calculated. Seasonal data were used to calculate annual input-output budgets. Based on data that covered the period April to October 2005, annual fluxes were estimated. In *S. foliosa*, annual net production was approximately 1,499 g DW m^{-2}, and the annual uptakes in the aboveground biomass of THg and MeHg were, respectively, 34.897 µg m^{-2} and 0.784 µg m^{-2}. In *S. virginica*, annual net production was approximately 1,361 g DW m^{-2}, and the annual uptakes in the aboveground biomass of THg and MeHg were, respectively, 9.422 µg m^{-2} and 0.018 µg m^{-2}. Since *S. foliosa* had a similar production rate but greater mercury species uptake and loss rates than *S. virginica*, *S. foliosa*-matter is expected to affect the local and possibly the regional food web more than *S. virginica*.

Decomposition of *S. foliosa* and *S. virginica* plant litter, harvested in March 2004 from the China Camp salt marsh, was studied under laboratory conditions. Dried plant materials, weighing 12-15 g, were incubated in litter bags within vessels, filled with San Pablo Bay water and inoculated with local sediment, under aerobic or anaerobic conditions for up to 150-day periods. Total mass loss, mercury species, and carbon, nitrogen, and sulfur stable isotopes were used to characterize the changes in the plant litter during the decomposition process. Total microbial biomass and the contributions of two SRB groups to the total microbial biomass, i.e., *Desulfobacter* sp. (+*Desulfobacterium* sp.) and *Desulfovibrio desulfuricans*, in the decomposing plant litter were determined using polar lipid fatty acid methylesters (PLFAME) to explore their involvement in the mercury dynamics. Plant materials decomposed with different rates, with a dry weight loss of maximally 66% in *S. foliosa* under aerobic conditions

and 84% in *S. virginica* under anaerobic conditions. Oxygen concentration affected decomposition rates differentially, in that aerobic conditions increased mass loss in *S. foliosa* litter but decreased it in *S. virginica* litter. The THg concentration (ng g^{-1}DW) in the litter increased during the decomposition process, but the THg mass contained in the litter did not. The temporarily increased MeHg portion of THg in the decomposing plant litter, up to 17.9 ng g^{-1} (in 10-day, anaerobically incubated *S. foliosa* litter), supports the hypothesis that THg in and on the surface of the plant litter is methylated during decomposition. In a later decomposition phase, the MeHg concentration decreased, and, thus, demethylation of MeHg associated with the litter occurred also. This indicates that plant litter from coastal marshes can act as a transient source of MeHg. This finding may help explain the seasonal pattern of MeHg production observed in wetland habitats. However, some portion of the decrease in MeHg in the decomposing plant litter may be caused by loss to the water column or the sediment. The $\delta^{13}C$ ratio proved to be a reliable indicator of plant material source. The C:N ratio generally decreased during decomposition and exceeded the value of 35 temporarily and only in *S. foliosa* litter. Because a C:N ratio of $\geq$35 is indicative of low food quality for animals (Elser et al. 2000), litter of *S. foliosa* may have a lower food quality than that of *S. virginica* during part of the decomposition process.

Carbon, nitrogen, and sulfur stable isotopes were used to characterize the food webs (i.e., sources of carbon and trophic status of consumers) of the China Camp tidal salt marsh and adjacent San Pablo Bay area. Trends in the collective isotopic distributions suggest that inputs from bay macroalgae, C_4 grasses (largely *S. foliosa*), marsh-diatoms, marsh-cyanobacteria, and marsh-pool filamentous algae provide the organic matter that forms the base of the food web, supporting invertebrates, fishes, mammals (*Reithrodontomys raviventris* and *Microtus californicus*), and birds (*Melospiza melodia samuelis* and *Laterallus jamaicensis coturniculus*). These producers together occupy four habitat types, i.e., the bay, the low-, mid- and high-salt marsh. It remains to be demonstrated if connectivity between these habitats exists. Mean THg and MeHg concentrations of primary producers and particulate organic matter (POM) appeared to be less related to habitat than to organismal characteristics. Levels were greatest in phytoplankton (ranges 578 to 654 ng THg g^{-1} DW and 16.9 to 41.0 ng MeHg g^{-1} DW), intermediate in POM and marsh microalgae (ranges 38 to 276 ng THg g^{-1} DW and 1.05 to 8.87 ng MeHg g^{-1} DW), and least in marsh vascular plants (live and litter) and bay macroalgae (ranges

9 to 61 ng THg g^{-1} DW and 0.30 to 1.48 ng MeHg g^{-1} DW). The MeHg:THg ratio was significantly greater in phytoplankton and marsh microalgae than in marsh vascular plant litter, with the other groups having intermediate MeHg:THg ratios. Mean THg levels were significantly greater in birds with 1,670 ng g^{-1} DW, than in all other consumer groups, with 1,670 ng g^{-1} DW. The mean THg levels in the other consumer groups were far less, notably 274 ng g^{-1} in invertebrates, 185 ng g^{-1} in fish, and 27 ng g^{-1} in mammals. However, the mean THg level in birds was even exceeded by the THg concentration of 1,820 ng g^{-1} DW in an unidentified worm species from the bay. The MeHg levels in birds were also significantly greater than in the other consumer groups, i.e., 1,290 ng g^{-1}. The mean MeHg levels in the other consumer groups were far less than those for THg, notably 190 ng g^{-1} in fish, 119 ng g^{-1} in invertebrates, and 17 ng g^{-1} in mammals. Among the consumers, the greatest MeHg:THg ratio was found in fish, where almost 100% of THg had accumulated in the form of MeHg. MeHg:THg ratios in the other consumer groups decreased in the order of birds and mammals with 75% and invertebrates with 64%. There was a scale difference between the overall mean MeHg:THg ratio in primary producers and in consumers of a factor of 12. Ranking the consumers into their approximate trophic levels based on their $\delta^{15}N$-values did not indicate an increase in MeHg concentration with increasing trophic level for most consumers. Fish ranked at the greatest, fourth, trophic level and also exhibited elevated MeHg levels (mean MeHg level 215 ng g^{-1} DW). Although birds ranked below fish at the third trophic level, they demonstrated by far the greatest MeHg concentrations (mean MeHg level 1,290 ng g^{-1} DW). Mammals ranked at a trophic level below both other consumer groups and exhibited lesser MeHg concentrations (mean MeHg level 199 ng g^{-1} DW). Further analysis of the associations among producers and consumers using multiple-source mixing models to approximate the relative inputs of each source into the food web of the China Camp marsh and adjacent San Pablo Bay area is expected to elucidate these relationships. Following this different approach the consumers will be organized by their position in the food web in terms of their diets, rather than by habitat.

Measures to decrease bioavailability were explored as a management tool. The bioavailability characteristics of Hg species in sediments of HAAF and other marshes bordering San Pablo Bay were evaluated experimentally using a bioassay. This type of assessment may also be suitable to evaluate the bioavailability of mercury species in dredged material used as fill for

the HAAF wetland restoration project. The bioaccumulation factor (BAF) values were greater for MeHg than for THg. The THg and MeHg body burdens of *Nereis virens (*polychaete worm) experimentally exposed for 56 days were similar to body burdens determined for crabs and mussels field-collected from the HAAF and China Camp sites. The bioavailabilities of THg and MeHg to *N. virens* were not significantly decreased by sediment amendment with 3.4% granular activated carbon (GAC), in contrast to results obtained earlier where amendment decreased the bioavailability of freshly-spiked THg and MeHg on sediments to the clam *Macoma nasuta*.

Preface

The work reported herein was conducted by the Environmental Laboratory (EL) of the U.S. Army Engineer Research and Development Center (ERDC), Vicksburg, MS.

With funding from the Long-Term Management Strategy, research staffs from the U.S. Army Corps of Engineers (USACE) are working with the San Francisco Basin Regional Water Board, the California State Coastal Conservancy, and the San Francisco Bay Conservation and Development Commission to reconstruct wetlands at the former Hamilton Army Airfield (HAAF).

In March 2003, the U.S. Army Engineer District, San Francisco, requested that EL provide an expansion of pre-construction monitoring of total mercury and methylmercury concentrations in sediments and soils of existing wetlands bordering the Hamilton Army Airfield (HAAF) Wetlands Restoration Site on San Pablo Bay, California. The purpose of the expanded activities was to gain site-specific knowledge of the geochemical/geophysical, microbial, and predominant plant- and animal-related interactions that affect the stabilization and mobilization of mercury and methylmercury in the sediments and soils of the area. Exploratory research data from 2003 resulted in a first-generation site-specific screening-level model created for estimating mercury and methylmercury mobility during wetlands reconstruction.

The current report describes

1. Detailed research analyses of data collected during 2004 on methylation and demethylation rates and tentatively involved microbial groups; mercury dynamics in food webs; and bioavailability of sediment-associated mercury to macrobenthos.
2. The results of data collected from three work units funded in 2005, titled: “Size and determinants of the sedimentary mercury pool available for methylation – minimizing methylmercury production,” “Diffusive gradient thin film (DGT) sentinels for long-term monitoring,” and “Transfer of mercury from primary producers to primary consumers – quantifying the entry of mercury into the aquatic food web.”

The project leader of this work was Dr. H. L. Fredrickson, Environmental Processes Branch (EPB), of the Environmental Processes and Engineering Division (EPED), EL. The multidisciplinary team was composed by multiple principal investigators. Dr. Fredrickson; Dr. Elly P. H. Best, Environmental Risk Assessment Branch (ERAB), EL; and Dr. H. Hintelmann (Trent University, Department of Chemistry, Peterborough, Ontario, Canada), conducted the study on mercury cycle-related dynamics in wetland sediments of San Pablo Bay. Drs. O. Clarisse and Hintelmann (Trent University) and Dr. Fredrickson conducted the study on diffusive gradient in thin film. Dr. Best, Dr. A. J. Bednar (Environmental Chemistry Branch, EL), Dr. Hintelmann, and Dr. B. Dimock (Trent University) conducted the study on marsh vegetation as vector in mercury species transport in San Pablo Bay tidal marshes. Drs. Best and Fredrickson, John S. Furey (EPB), and Drs. Hintelmann and Dimock conducted the study on dynamics of mercury and methylmercury and stable isotope signatures in decomposing macrophytes from a tidal wetland on San Pablo Bay. Dr. Best, C. H. Lutz (ERAB), Dr. Fredrickson, and Dr. Hintelmann conducted the study on mercury dynamics in food webs associated with tidal salt marshes on San Pablo Bay. Dr. G. R. Lotufo (ERAB), Dr. R. N. Millward (Applied Research Associates, Inc., Vicksburg, MS), and Dr. Hintelmann conducted the study on the bioavailability of sediment-associated mercury to macrobenthos. Dr. Best served as technical editor of this report.

We gratefully acknowledge the external reviews by staff at Moss Landing Marine Laboratory, Moss Landing, CA, and San Francisco Estuary Institute, Oakland, CA.

Special thanks go to the following Corps personnel who gave generously of their time and expertise to review the drafts of this report: Drs. J. C. Pennington, R. P. Jones, and G. L. Ray.

The study was conducted under the direct supervision of Dr. Richard E. Price, Chief, EPED, and under the general supervision of Dr. Beth Fleming, Director, EL.

COL Richard B. Jenkins was Commander and Executive Director of ERDC. Dr. James R. Houston was Director.

1 Report Summary

Problem

Over 90% of the wetlands bordering San Francisco Bay was lost between 1850 and 1990 (USGS 2002; 80% between 1800 and 1988 according to Valiela et al. 2004). Habitats for wildlife and fish species are being threatened and coastal shore erosion mitigation greatly diminished due to human activities and, possibly, sea level rise. Long-term goals for San Francisco Bay development, formulated in a report of habitat recommendations by the San Francisco Bay Area Habitat Ecosystem Goals Project, include extensive wetland restoration. The tidal marshes bordering San Francisco Bay are to be increased from 16,200 ha in 1999 to 42,525 ha by the year 2055 (San Francisco Bay Area Wetlands Ecosystem Goals Project 1999a). Dikes currently protect most of the areas targeted for restoration. Drying and oxidation of the soils on the landward side of the dikes have resulted in subsidence such that current soil elevations are often meters below the mean tide level. Simply breaching the dikes would result in lakes, not wetlands. Considerable amounts of fill material are required to raise the elevation of subsided areas to a level that would support aquatic macrophytes that would in turn trap sediments required to sustain the elevation of the wetland. Sediments derived from operations and maintenance of navigation channels in the SF Bay could be used for this purpose. This beneficial use of locally dredged sediment would reduce the cost of obtaining other fill material or transporting the material to more distant disposal sites.

The elevated levels of mercury currently present in the San Francisco Bay fishery and birds constrain environmental management. The San Francisco Bay watershed is impacted by the legacy of mercury mines in the coastal range and placer style gold mining in parts of the Sierra Nevada watershed. Wetlands, particularly tidal wetlands, are recognized for their potential to convert mercury into monomethylmercury (CH_3Hg^+). Monomethylmercury is referred to as methylmercury (MeHg) in this report. MeHg is a potent toxin that efficiently biomagnifies in many aquatic food webs.

In this context, the immediate concern of the U.S. Army Corps of Engineers (USACE) focuses on the use of mercury containing dredged

material for the restoration of wetlands. The larger environmental issue is the contribution of SF Bay salt marshes to mercury mitigation in the SF Bay fishery, regardless of the source of the mercury. For example, wetland restoration at the Hamilton Army Airfield (HAAF) site will require approximately 8.1 million cubic meters of dredged material to attain an elevation of approximately 0.5 ft above mean sea level where the marsh macrophyte *Spartina foliosa* would colonize. The first 1.6 to 1.9 million cubic meters of material came from the Oakland Harbor Navigation Improvement Project, and was deposited in the HAAF site from spring 2006 onwards, and does not contain elevated mercury levels. Additional material will come from efforts to maintain existing shipping channels in San Francisco Bay, is expected to be in place by 2014, and may contain mercury levels typical of that found in the majority of SF Bay sediment (300 ng g^{-1} dry weight, with MeHg typically being 1% of total mercury; Beijer and Jernelow 1979; Best et al. 2005; this report).

Most of the work in this interim report was designed to address consensus technical questions formulated at the CALFED[1] Stakeholders' Workshop on Mercury in San Francisco Bay, held 8-9 October 2002 at Moss Landing Marine Laboratories (Wiener et al. 2003). These included the following:

- What are the present levels of MeHg in San Francisco Bay wetlands with respect to biota, sub-habitats, and location within the SF Bay?
- What are the rates of MeHg production?
- What factors control MeHg production? Can these be managed?
- Are some wetlands larger mercury exporters than others?
- Can we model/predict the effects of wetland restoration on MeHg production and export?

In partial response to these questions, and building on prior research, six major studies were designed and executed and the resulting information is presented in the current report. Peer-reviewed publications are currently being prepared from these six studies.

A site map is provided in Figure 1-1.

[1] The CALFED Bay-Delta Program is a cooperative effort among 18 state and federal agencies and diverse interest groups to address environmental and water management issues in the Bay-Delta, the Sacramento and San Joaquin Rivers, and the watersheds that feed them. It was initiated in 1995 by California Governor Pete Wilson and the William J. Clinton Administration.

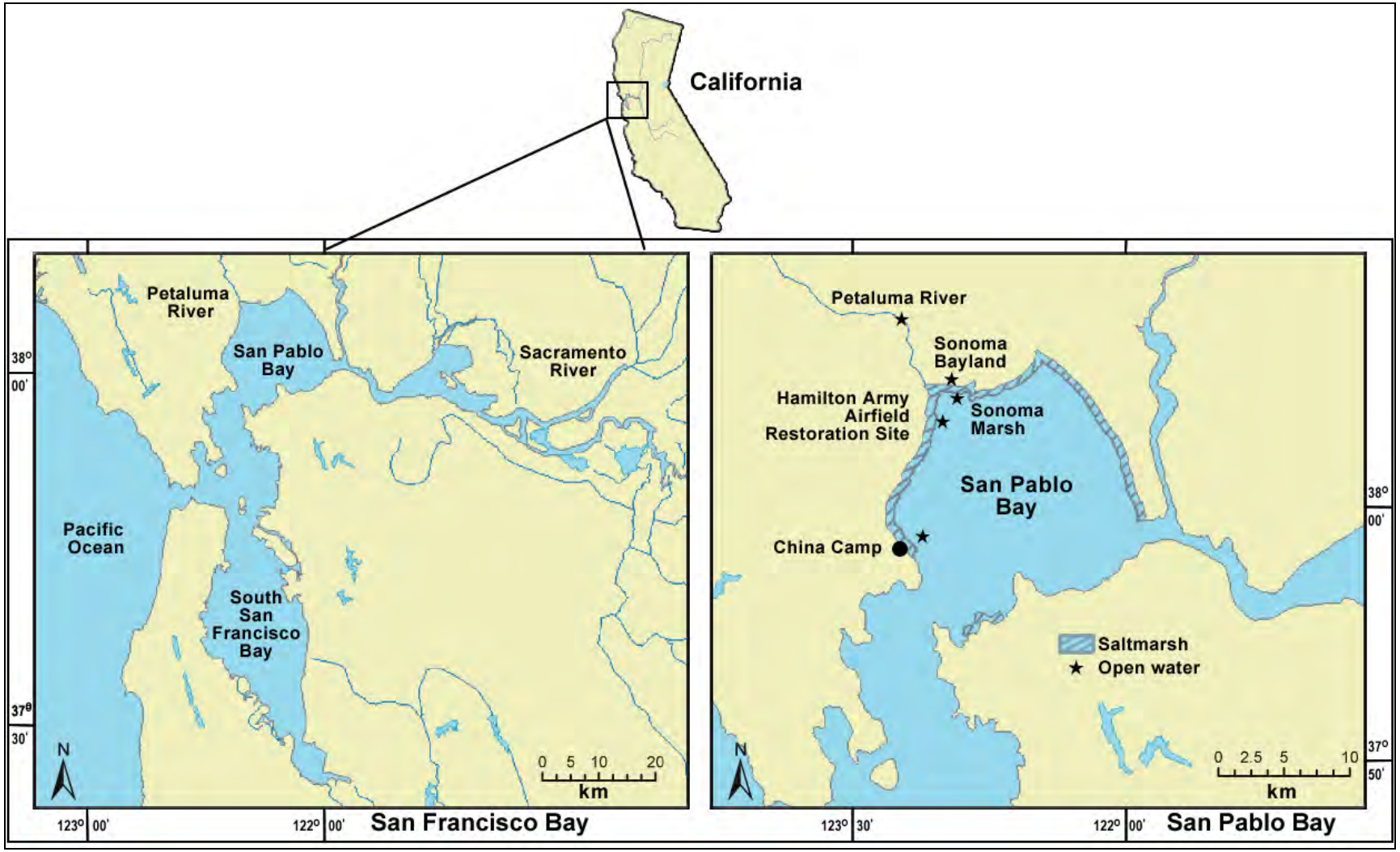

Figure 1-1. Location of San Pablo Bay within San Francisco Bay (left) and location of the Hamilton Army Airfield Restoration Site, China Camp reference, and other sites (right).

Study 1 (Chapter 3): Mercury Cycle-Related Dynamics in Wetland Sediments of San Pablo Bay: Methylation, Demethylation, and Microbial Biomass

The levels of total mercury (THg) in the surface sediment of wetlands bordering San Pablo Bay, which were studied by the authors of this report in the period 2001-2004, are in the order of 300 ng g^{-1} DW and are roughly comparable to those found throughout San Francisco Bay. MeHg is the mercury species of greatest concern because it is a toxin that biomagnifies up the aquatic food webs. The relationships between THg and MeHg in aquatic systems are unclear and, thus, are the primary focus of this study. Methods for simultaneous in situ measurements of methylation and demethylation rates, based on the injection of mercury stable isotopes into sediment were used and evaluated. The rates of both these juxtaposed processes were rapid. Current rates of methylation would double the standing pool size of MeHg within a day if this rate was not counter balanced by demethylation. The current rates of demethylation would deplete the standing MeHg pool size to null within a few days if methylation ceased. These processes produce a dynamic MeHg pool with respect to time and space. Many statistically significant differences in net MeHg production rates (methylation rate minus demethylation rate) were shown but revealed no consistent trend in SF Bay wetlands ranging from the China Camp State Park (24‰ salinity) to the Petaluma River (7‰). Potentially, even small changes to local factors that affect rates of methylation, demethylation, or both can rapidly alter standing pool sizes of MeHg. Analysis of variance indicated that net MeHg production was significantly less in vegetated than in bare sediments in July 2004 (0.72 versus 4.4 ng MeHg g^{-1}DW d^{-1}), but relative abundance of the sulfate-reducing bacterial (SRB) *Desulfovibrio* was significantly greater in vegetated sediments. A significant relationship between microbial biomass and relative abundances of the SRB genera *Desulfobacter (+Desulfobacterium)* and *Desulfovibrio*, and MeHg pool size was found, but no significant relationships between THg and other sediment characteristics were demonstrated. However, indirect relationships via the sulfur cycle are being examined. Mechanisms that link the methylation and demethylation processes are not understood but warrant further study in support of wetland environmental management.

Study 2 (Chapter 4): Diffusive Gradient in Thin Film Sentinels for Monitoring Methylmercury Production in Tidal Wetlands on San Pablo Bay

A new method, Diffusive Gradient in Thin Film (DGT) technique, was developed to monitor bioavailability MeHg in the water column and sediment pore water. This method uses 3–mercaptopropyl–functionalized silica gel to bind MeHg. A polyacrylamide gel and the binding agent are enclosed in a small plastic device that is immersed in the solution. The new resin was characterized and calibrated. Basic performance tests of the new DGT device confirmed the applicability of Fick's first law for such DGT measurements. Diffusion coefficients vary slightly as a function of the actual methylmercury species present in solution. MeHgCl, the predominant species in seawater, diffuses at a rate of $D = 5.0 \times 10^{-6}$ cm^{-2} s^{-1} (at 20 °C), while the rate for large MeHg-DOC complexes is only $D = 1.25 \times 10^{-6}$ cm^{-2} s^{-1}. The detection limit of the overall method is 0.001 ng of MeHg, whereas corresponds to approximately 0.030 ng L^{-1} of MeHg in a water sample, when deploying a typical DGT device for 24 hours. Lower MeHg concentrations are measurable using longer deployment times or a thinner diffusive gel layer. Field tests have indicated that DGT measurements of dissolved MeHg provide comparable results to conventional methods of sample collection and measurement. The DGT technique represents, therefore, an alternative in situ sampling method for MeHg. It provides the added advantage that integrated samples are collected over prolonged periods of time in contrast to conventional snap-shot sampling approaches. This advantage results in more reliable data upon which to base monitoring and management decisions. The DGT technique was also used in July 2005 to sample key geochemical species in sediment pore water to characterize and understand the biogeochemistry of San Francisco Bay sediment and to investigate the mobility of associated MeHg. In combination with other gel-based sampling techniques (DET, Diffusional Equilibration in Thin Film) ancillary parameters, such as dissolved sulfide, sulfate, manganese, and iron, were measured at a millimeter-scale. This allowed a detailed characterization of redox zones in the sediments and identification of mercury methylation hot spots, which are typically confined to thin horizons in the sediment layer (few millimeters). Often, sulfide concentrations and sulfate consumption peaked concurrently with MeHg, indicating that sulfate reduction is correlated with mercury methylation and that sulfate-reducing bacteria are driving methylmercury levels in the SF Bay area. Field data collected using DGT formed the basis for estimates of MeHg diffusion fluxes from sediment to water of 1,500-6,900 ng m^{-2} y^{-1} in China Camp and of 15,000 ng m^{-2} y^{-1} in

the Petaluma River. Therefore, the river sediment potentially represents a significant source of MeHg for the SF Bay.

Study 3 (Chapter 5): Marsh Vegetation as a Vector in Mercury Species Transport in San Pablo Bay Tidal Marshes—Understanding the Entry of Mercury Into the Aquatic Food Web

The potential for marsh plants to be vectors in the transport of mercury species was studied in the natural, tidal China Camp salt marsh on San Pablo Bay. The fluxes of organic matter, THg, and MeHg were studied in natural stands of *Spartina foliosa* and *Salicornia virginica*. Seasonal fluxes from the sediment into aboveground biomass of live plants and subsequent transfer into the dead plant community by mortality were measured. Disappearance of THg and MeHg from the dead plant community through fragmentation, leaching, and excretion were calculated. Seasonal data were summed up to calculate annual input-output budgets. Annual fluxes were estimated based on data collected during the period April to October 2005. In *S. foliosa*, annual net production was approximately 1,499 g DW m^{-2}, and the annual uptakes in the aboveground biomass were 34.897 µg THg m^{-2} and 0.784 µg MeHg m^{-2}. In *S. virginica*, annual net production was approximately 1,361 g DW m^{-2}, and the annual uptakes in the aboveground biomass were 9.422 µg THg m^{-2} and 0.018 µg MeHg m^{-2}. Mercury species uptake rates in this study were less than those of other metals determined in another tidal marsh on the Pacific coast. Of both plant species studied, *S. foliosa* had a similar production rate but greater mercury species uptake and loss rates than *S. virginica*, and, consequently, it is to be expected that *S. foliosa*-matter may affect the local and possibly the regional food web more than *S. virginica*. However, the actual effects of the input of mercury-species-containing plant-derived particulate matter into the food webs would depend on trophic level, food preference, seasonal cycle of the consumer, total sediment surface area vegetated, location of the vegetation in the marsh landscape (elevation relative to sea level, distance to subtidal area), and estuary-bay landscape. Since the levels of mercury species in dead plant material greatly exceed those in live plant material (on a dry weight basis), detritivores would ingest greater mercury concentrations than herbivores, and consumers of *S. foliosa* would ingest more MeHg than those of *S. virginica*. When full-year data become available, the estimates made in the current chapter may require modification.

Study 4 (Chapter 6): Dynamics of Mercury, Methylmercury, and Stable Isotope Signatures in Decomposing Macrophytes from a Tidal Marsh on San Pablo Bay

Chemical changes in the standing, aboveground plant litter of *S. foliosa* and *S. virginica*, harvested in March 2004 from the natural, tidal China Camp salt marsh on San Pablo Bay, were studied during decomposition under laboratory conditions. The dried plant materials, weighing 12-15 g, were incubated in litter bags within vessels filled with San Pablo Bay water and inoculated with local sediment under aerobic or anaerobic conditions for up to 150-day periods. Total mass loss, mercury species (THg and MeHg), carbon, nitrogen, and sulfur stable isotopes were used to characterize changes in the plant litter during the decomposition process. Total microbial biomass and the contributions of two SRB genera (*Desulfobacter* sp. + *Desulfobacterium* sp., and *Desulfovibrio)* to the total microbial biomass in the decomposing plant litter were determined using polar lipid fatty acid methylesters (PLFAME) to explore SRB involvement in the mercury dynamics. Plant materials decomposed with different rates, with a dry weight loss of maximally 66% in *S. foliosa* under aerobic conditions and 84% in *S. virginica* under anaerobic conditions. Oxygen concentration affected decomposition rates differentially. Aerobic conditions increased mass loss in *S. foliosa* litter but decreased it in *S. virginica* litter. The THg concentration (ng g^{-1}DW) in the litter increased during the decomposition process, but the total THg mass contained in the litter did not. The temporarily increased MeHg content in the decomposing plant litter, up to concentrations of 17.9 ng g^{-1} (in 10-day, anaerobically incubated *S. foliosa* litter) supports the hypothesis that THg in and on the surface of the plant litter is methylated during the decomposition process when in contact with sediment and water from the site. However, in later phases of the decomposition process, the MeHg concentration decreased, and, thus, demethylation of MeHg occurred also under both aerobic and anaerobic conditions. This phenomenon indicates that plant litter from coastal marshes can act as a transient source of MeHg, the amount depending on litter quantity and quality (plant species), environmental conditions (oxygen level), and stage within the decomposition process (time). This finding may help explain the seasonal pattern of MeHg production observed in wetland habitats. However, some portion of the decrease in MeHg in the decomposing plant litter may be caused by loss to the water column or the sediment. Among the stable isotope ratios determined, the $\delta^{13}C$ ratio proved to be a reliable indicator of the plant material source, since $\delta^{13}C$ remained stable at approximately -15.6‰ in *S. foliosa* litter and approximately -26.1‰ in *S. virginica* litter. Shifts in the $\delta^{15}N$ ratios were greater than

3.0‰ to 3.6‰ considered as indicative for trophic transfer by one level and typical for specialized diets within food webs. Even greater shifts in the $\delta^{34}S$ ratios were observed, i.e., up to 7‰. The C:N ratio generally decreased during decomposition and exceeded the value of 35 only in *S. foliosa* litter in the period between initial and 10 to 50 days of decomposition. A C:N ratio of $\geq$35 is considered to be indicative of low food quality for animals (Elser et al. 2000). Thus, *S. foliosa* litter may be considered as having a lesser food quality than *S. virginica* litter during part of the decomposition process.

Study 5 (Chapter 7): Mercury Dynamics in Food Webs Associated With Tidal Salt Marshes on San Pablo Bay

Carbon, nitrogen, and sulfur stable isotopes were used to characterize the food webs (i.e., sources of carbon and trophic status of consumers) of the China Camp tidal salt marsh and adjacent San Pablo Bay area. Trends in the collective isotopic distributions suggest that inputs from bay macroalgae, C_4 grasses (largely *S. foliosa*), marsh-diatoms, marsh-cyanobacteria, and marsh-pool filamentous algae provide the organic matter that forms the base of the food web, supporting invertebrates, fishes, mammals (*Reithrodontomys raviventris* and *Microtus californicus*), and birds (*Melospiza melodia samuelis* and *Laterallus jamaicensis coturniculus*). These producers together occupy four habitat types, i.e., the bay, the low-, mid-, and high-salt marsh. It remains to be demonstrated if connectivity between these habitats exists.

Mean THg and MeHg concentrations of primary producers and particulate organic matter (POM) appeared to be less related to habitat than to organismal characteristics. Levels were greatest in phytoplankton (ranges 578 to 654 ng THg g^{-1} DW and 16.9 to 41.0 ng MeHg g^{-1} DW), intermediate in particulate organic matter (POM) and marsh microalgae (ranges 38 to 276 ng THg g^{-1} DW and 1.05 to 8.87 ng MeHg g^{-1} DW), and least in marsh vascular plants (live and litter) and bay macroalgae (ranges 9 to 61 ng THg g^{-1} DW and 0.30 to 1.48 ng MeHg g^{-1} DW). The MeHg:THg ratio was significantly greater in phytoplankton and marsh microalgae than in marsh vascular plant litter, with the other groups having intermediate MeHg:THg ratios. Among the primary producers and POM, two groups were distinguished based on their MeHg:THg ratios. The group with the greatest MeHg:THg ratio, ranging from 7 to 8, included bay phytoplankton and marsh pool filamentous algae. The other group with a MeHg:THg ratio of 1 to 5 included all other primary producers, POM, and marsh vascular plant litter.

The mean THg level (1,670 ng g^{-1} DW) was significantly greater in birds than in all other consumer groups. The mean THg level in the other consumer groups was far less, notably 274 ng g^{-1} in invertebrates, 185 ng g^{-1} in fish, and 27 ng g^{-1} in mammals. However, the mean THg level in birds was exceeded by the THg concentration of 1,820 ng g^{-1} DW in an unidentified worm species from the bay. The MeHg level (1,290 ng g^{-1}) in birds was also significantly greater than the level in the other consumer groups. The mean MeHg level (190 ng g^{-1} in fish, 119 ng g^{-1} in invertebrates, and 17 ng g^{-1} in mammals) in the other consumer groups was far less than that for THg. Among the consumers, the greatest MeHg:THg ratio was found in fish, where almost 100% of THg had accumulated in the form of MeHg. MeHg:THg ratios in the other consumer groups decreased in the order of birds and mammals with 75% and invertebrates with 64%. There was a scale difference of a factor of 12 between the overall mean MeHg:THg ratio in primary producers and in consumers.

Ranking the consumers into their approximate trophic levels based on their $\delta^{15}N$-values did not indicate an increase in MeHg concentration with increasing trophic level for most consumers. Fish ranked at the greatest, fourth, trophic level and also exhibited elevated MeHg levels (mean MeHg level 215 ng g^{-1} DW). Although birds ranked below fish at the third trophic level, they demonstrated by far the greatest MeHg concentrations (mean MeHg level 1,290 ng g^{-1} DW). Mammals ranked at a trophic level below both other consumer groups and exhibited lesser MeHg concentrations (mean MeHg level 199 ng g^{-1} DW). Further analysis of the associations among producers and consumers using multiple-source mixing models (Lubetkin and Simenstad 2004) to approximate the relative inputs of each source into the food web of the China Camp marsh and adjacent San Pablo Bay area is expected to elucidate these relationships. Following this different approach the consumers will be organized by their position in the food web in terms of their diets, rather than by habitat.

Study 6 (Chapter 8): Bioavailability of Sediment-Associated Mercury to Macrobenthos

The bioavailability of sediment-associated THg and MeHg from HAAF and other San Francisco Bay non-restored marshes was compared with data from a similar marsh that was restored using dredged sediment. The bioavailability of Hg and MeHg was examined by determining sediment uptake and clearance rates of those compounds in the benthic polychaete worm *Nereis virens* using laboratory exposures. This type of assessment may also be suitable to evaluate the bioavailability of mercury species in

dredged material used as fill for the HAAF wetland restoration project. Sediments from the HAAF bay edge site SM-10 (HAAF), China Camp State Park R-44, and the natural (Sonoma Marsh) and restored Sonoma Bayland salt marshes were assessed. *Nereis virens* accumulated increasing concentrations of THg and MeHg over a 56-day exposure to San Francisco Bay area sediments. Two-compartment-model-fitted estimates of uptake clearance rate coefficient (k_u) for THg were similar for the HAAF, China Camp, and Sonoma Marsh sediments but were greater for the Sonoma Bayland sediment. For MeHg, k_u estimates were similar for the HAAF, China Camp, and Sonoma Bayland sediment but were greater for the Sonoma Marsh sediment. The rate of metal uptake from sediment or soil has been used as a reliable indicator of metal bioavailability and indicates that bioavailability was greatest in the Sonoma Bayland sediment for THg and in the Sonoma Marsh sediment for MeHg. Estimates of elimination rate (k_e) in *N. virens* were much less, similar to previous observations with other invertebrates. The 56-day THg and MeHg tissue concentrations in *N. virens* were relatively similar to body burdens determined for crabs and mussels field-collected from the HAAF and China Camp sites. The bio-accumulation factor (BAF, tissue-to-sediment concentration ratio) values were greater for MeHg than for THg. Overall, the bioavailability of Hg and MeHg to *N. virens* in laboratory exposures appears to be similar to the bioavailability of those compounds in the field for HAAF and China Camp sediments.

Sediment from the HAAF site was used to test the effects of granular activated carbon (GAC) on the bioaccumulation of THg and MeHg. Activated carbon has strong affinity for non-polar and ionic compounds and has been suggested as a viable sorbent for the removal of contaminants from sediments. Sediment amended with GAC at 3.4% on a dry weight basis and stored for 84 days at 20 °C failed to promote a significant decrease in the bioaccumulation of aged THg or MeHg to *N. virens*. In contrast, treatment with GAC promoted decreased bioavailability of freshly-spiked Hg in a similar earlier study. Therefore, Hg is less available for sorption to GAC compared to spiked Hg which is more labile.

2 Background Monomethylmercury Study

The potential for methylation of mercury in sediments and soils of tidal marsh and seasonal wetlands bordering the HAAF Wetlands Restoration Site at San Pablo Bay, CA, was assessed by same-sample analysis for THg and MeHg during the dry season (McFarland et al. 2002; and appendices therein) and during the wet season in 2002–2003 (McFarland et al. 2002, 2003). Surficial 1-2 cm of sediments at 60 sites (replicated five times) divided among seven locations were sampled. Results served as the basis for selection of sites for subsequent intensive study.

In March 2003, the U.S. Army Engineer District, San Francisco (CESPN) requested an expansion of pre-construction monitoring of THg and MeHg concentrations in sediment and soils of existing wetlands bordering the HAAF Wetlands Restoration Site. Sampling locations are shown in Figure 2-1. The purpose of the expanded activities was to gain site-specific knowledge of the geochemical/geophysical, microbial, and predominantly plant- and animal-related interactions that affect the stabilization and mobilization of THg and MeHg there.

Results of studies conducted in 2003 have been published (Best et al. 2005) and are summarized here. In June 2003, THg and MeHg levels in the sediment were measured in relation to depth at tidal sites at HAAF and the China Camp State Park (as a reference), as well as at inland sites at HAAF and Bel Marin Creek. Other parameters important for the cycling of Hg and MeHg in sediments were measured also to establish site-specific relationships between these parameters and THg and MeHg. In the cores from the tidal sites, the greatest MeHg concentrations (range 0.8-4.4 ng g^{-1} DW) were found in the upper 2.5 – 5.1 cm and levels decreased with depth. THg levels (range 160 – 550 ng g^{-1}) increased with depth, correlating inversely with MeHg. MeHg correlated directly with redox potential (E_h), total organic carbon, and phosphorus. Net MeHg production is the result of methylation and demethylation rates in the sediment. Methylation and demethylation rates were determined by on site incubations of mud- and vegetated-mud-cores (open at top and bottom) with stable Hg isotopes at the tidal HAAF and China Camp sites. Methylation rates were 1.44 ng MeHg g^{-1} d^{-1} in nonvegetated sediments of HAAF. Rates were usually less in vegetated than in nonvegetated sediments. Rates were usually greater in cores incubated exposed to sun light than in darkened cores. Methylation rates varied with location within the bay on bare and epipelon-vegetated

sites and were less at HAAF than at China Camp. Epipelon is the complex of microalgae, bacteria, and detritus on the sediment surface. Demethylation rates were 1.281 ng MeHg g^{-1} d^{-1} in nonvegetated sediments at HAAF and 0.78 ng MeHg g^{-1} d^{-1} at China Camp.

Mean THg concentrations in the macrophytic vegetation, predominated by *S. foliosa* and *S. virginica*, ranged from 13 to 158 ng g^{-1} in shoots and from 217 to 297 ng g^{-1} in roots. Mean MeHg concentration ranged from 0.55 to 4.75 ng g^{-1} in shoots and from 2.83 to 5.26 ng g^{-1} in roots. Plant levels of MeHg usually exceeded those in the sediments in which they rooted (roots and sediment originating from the same 9.5-cm-diameter sediment core). The THg and MeHg levels in plant detritus were far greater than in live shoots, i.e., by a factor of 5 to 8.

Macrofauna specimens were hand-collected at tidal sites at HAAF and at China Camp. Three species were found in sufficient abundance for analysis, i.e., yellow shore crab (*Hemigrapsus oregonensis*), ribbed mussel (*Geukinsia demissa*), and a mud snail (*Nassarius obsoletus*) only in a small tidal creek. Significant levels of mercury species were detected in the macrofauna tissues. THg levels ranged from 56.0 to 69.6 ng g^{-1} in crabs, from 115 to 187 ng g^{-1} DW in mussels, and of 401 ng g^{-1} in mud snails. MeHg levels ranged from 11.8 to 44.5 ng g^{-1} in crabs, from 28.9 to 105 ng g^{-1} DW in mussels, and averaged 153 ng g^{-1} in mud snails. MeHg comprised 19.9 to 67.4% of THg in crabs, 20.5 to 53.8% in mussels, and 39.9 in mud snails. Biota to sediment accumulation factors (BAFs) for MeHg ranged from 3.3 to 10.1 in crabs, 8.8 to 29.1 in mussels, and 46.0 in mud snails. The snail bioaccumulated the most THg and MeHg. Since the diet of these animals is composed largely by plant material, it is likely that MeHg in plants represents an important MeHg source for trophic transfer in the marsh. A preliminary annual MeHg mass balance for a 203-ha HAAF system indicated a net MeHg production of 12.8 kg and MeHg export in the order of 0.1 kg with tidal waters to the bay. These values serve as the basis for research hypotheses and future work.

Measures to decrease bioavailability were explored as a management tool. The bioavailability characteristics of Hg species in HAAF sediments were evaluated experimentally. Of the body burdens of 2-56 days exposed *Macoma nasuta* clams, THg showed a distinct pattern but MeHg varied considerably between replicates. Uptake and elimination kinetics of THg both showed a biphasic pattern, composed by a rapid initial phase and slower subsequent phase. Since final body burdens were only

approximately half of those recorded in previously collected *Modiolus* clams inhabiting HAAF bay edge sediments, it was concluded that exposure periods longer than 56 days are needed for Hg to approach apparent steady state in clam tissues. It is also possible that native clams had been exposed to greater THg concentrations than the test clams. Two sorbents were tested for their potential to decrease the bioavailability of mercury species, i.e., GAC and sulfonated Kraft-lignin. Bioavailability decreased more by sediment amendment with GAC than with Kraft-lignin.

A first-generation screening-level computer model was developed to estimate the mobility of THg and MeHg during wetlands reconstruction and management. The model is based on the mass balance principle. The THg and MeHg pools in the sediment are central to the model and may change over time with time-steps of 1 hour to 1 day due to methylation and demethylation, uptake and release of Hg species by organisms, and by export. Methylation and demethylation are influenced by tidal action, wet and dry season, and daylight. The initial model version, QnD:HAAF version 1.0 utilizes four stylized spatial areas representing the major salt marsh habitats, i.e., "Subtidal," "Mud flat," "*S. foliosa* marsh," and "*S. virginica* marsh." Ultimately the model is expected to simulate ecosystem pool sizes and processes for an entire map of linked spatial areas. The current version is site-specific and calibrated on data collected in the field and laboratory pertaining to HAAF in 2003. The model was run to simulate two 14-day scenarios, representing the wet and dry season of 2003. Simulated sediment MeHg concentrations exceeded the measured levels whereas simulated methylation and demethylation rates were in the same order of magnitude as measured values. Net MeHg production varied greatly with elevation relative to mean sea level. The differences between the simulated and measured THg and MeHg levels in sediment and biota are expected to provide leads to identify areas for further research.

Results of studies largely conducted in 2004 are described in the current annual Technical Report.

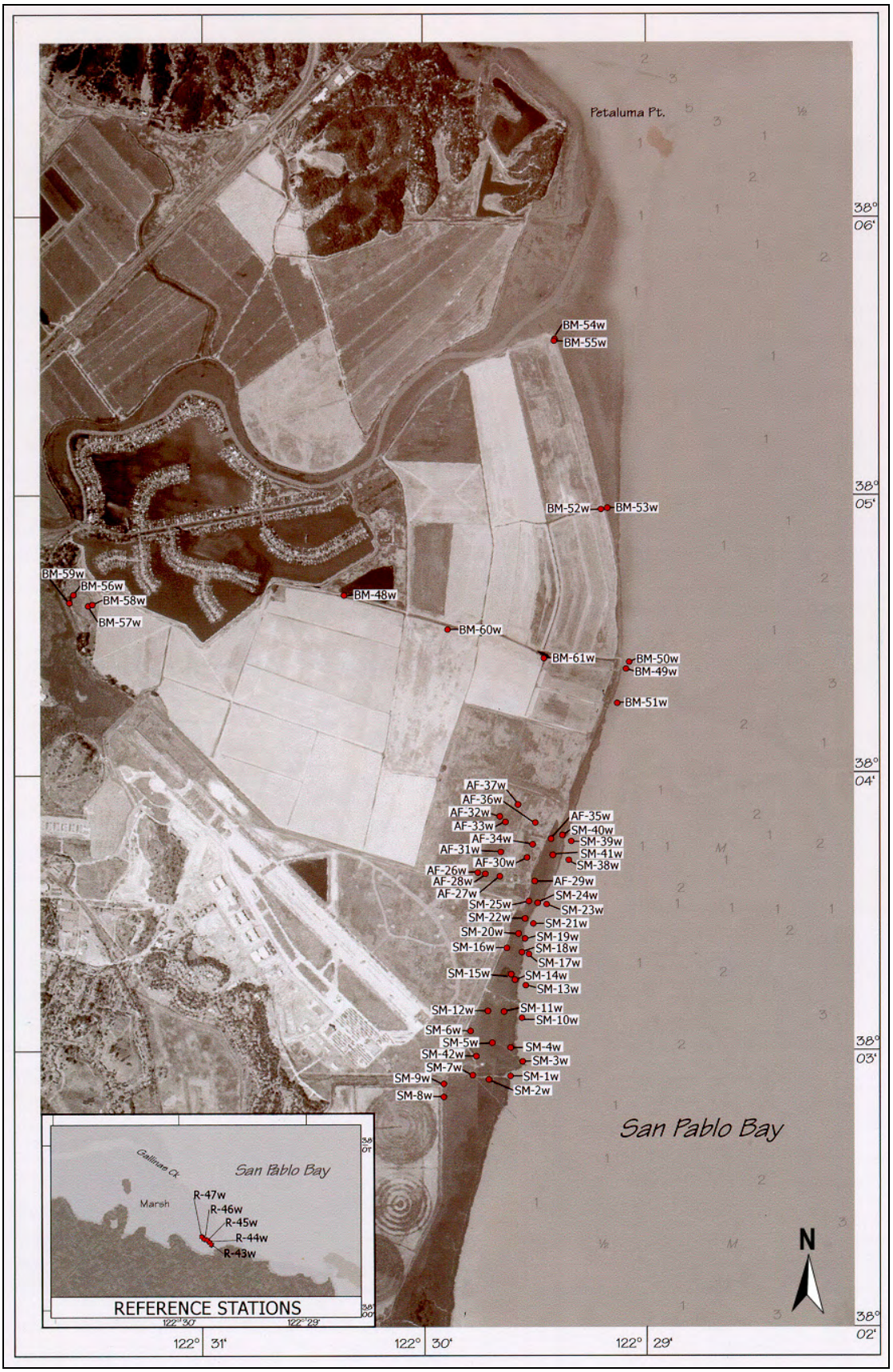

Figure 2-1. Map of sampling locations HAAF and China Camp (inset).

3 Mercury Cycle-Related Dynamics in Wetland Sediments of San Pablo Bay: Methylation, Demethylation, and Microbial Biomass

Introduction

Due to a history of placer type gold and mercury mining, San Francisco Bay's watershed contains elevated levels of THg in its sediment and in particles transported by river water. The THg levels in San Francisco Bay sediment range from 400 to 1,080 ng g^{-1} DW with means in the order of 300 ng g^{-1} DW (Best et al. 2005; this report). Levels of THg in SF Bay sediment are still elevated although slowly decreasing since the 1970s (Hornberger et al. 1999) mainly due to export via the Golden Gate. Although levels of THg are the most commonly measured value and most environmental regulations are based on THg levels, monomethylmercury (MeHg) is one of the most toxic mercury species and causes great environmental and human health concern. The relationships between levels of THg measured in river-borne particulates and sediment and MeHg levels in aquatic biomass are very complicated. The elevated levels and widespread distribution of THg in San Francisco Bay and its watersheds would make removal of the THg source difficult and costly. Effective environmental management options for controlling MeHg production and uptake into the aquatic food web will probably come from improvements in the fundamental understanding of (1) chemical and biological mechanisms responsible for the production of MeHg in San Francisco Bay surface sediment, (2) its bioaccumulation into biota, and (3) biomagnification in aquatic food webs. This chapter focuses on aspects of the first issue, the development of a mechanistic geochemical and microbiological understanding of the production of MeHg in wetlands that border San Pablo Bay, the northern part of San Francisco Bay.

Wetland conditions can be conducive to MeHg production, and certain natural wetlands have been identified as contributors of MeHg to downstream lakes and streams (St. Louis et al. 1994; St. Louis et al. 1996; Rudd 1995; Hurley et al. 1995; Branfireun et al. 1996; Branfireun et al. 1998). More specifically, this process has been linked to the activity of SRB (Compeau and Bartha 1985; Devereux et al. 1996; Gilmour and Henry

1991; Gilmour et al. 1998; King et al. 2000; Macalady et al. 2000; Batten and Scow 2003) which thrive under anoxic wetland conditions. Mercury methylation occurs when bioavailable inorganic mercury is taken up by SRB, but knowledge of the biochemistry and physiology of this process, mediated by the SRB, remains fragmentary (Berman et al. 1990; Choi and Bartha 1993; Choi et al. 1994).

In anoxic sediment, SRB use sulfate (SO_4^{2-}) as the terminal electron acceptor for their respiration. This dissimilatory sulfate reduction process produces hydrogen sulfide (H_2S), which is responsible for the rotten egg smell associated with salt marshes. Under anoxic conditions, H_2S rapidly reacts with cationic metals such as mercury to form extremely insoluble precipitates (e.g., HgS) that generally are not available for biological uptake or methylation. As long as these sediments remain anoxic, the precipitated HgS is effectively removed from the biological system. This was the likely situation in the San Francisco Bay watershed before the HgS ore was mined from geological formations and thermally converted to elemental mercury (Hg^0) for gold mining and other industrial applications.

SRB affect the biogeochemical sulfur and mercury cycles. Under conditions that favor sulfate respiration and where the re-oxidation of sulfide to sulfate is limited, elevated levels of sulfide persist. Reactive mercury species could form the precipitate, HgS, but reactive mercury is also suspected to be most easily methylated into monomethylmercury or dimethylmercury. The SRB of the genus *Desulfovibrio* are able to withstand sulfide concentrations that are toxic to other microbes and are believed to dominate under salt marsh conditions. In an estuary, dissolved sulfate levels generally diminish along with salinity. Sulfate levels ≤1 mM in the upper estuary can limit dissimilatory sulfate respiration and sediment sulfide levels (Marvin-DiPasquale and Capone 1998). SRB can successfully compete for sulfate in low sulfide environments. SRB of the genus *Desulfobacter* (+*Desulfobacterium*) are believed to be more abundant in this sediment type. Accordingly, rates of MeHg production would be predictably greater in sediment with low levels of sulfate and sulfide where sulfate respiration still occurs. This logic was used to explain the elevated levels of MeHg in fish caught in Water Conservation Areas 2B and 3A of the Everglades system (Gilmour et al. 1998).

There are also other determinants for the levels of MeHg in sediment. The demethylation of methylated mercury is also an important process.

Aerobic and anaerobic bacteria belonging to a number of different genera are capable of establishing the MeHg bond. Estuarine sediment can be rich in organic carbon and the respiration of the microbial community in such sediment is high, generally limiting the oxic part of the sediment horizon to the top few millimeters. In estuarine sediment, demethylation takes place in both oxic and anoxic horizons but demethylation in oxic sediments was found most significant (Oremland et al. 1991). In the same sediment type, aerobic demethylation appears to proceed by the organomercurial-lyase pathway, with methane as the sole organic product (Robinson and Tuovinen 1984; Summers 1986; Walsh et al. 1988). In contrast, in freshwater sediment demethylation in the oxic layer was insignificant. In this sediment type, demethylation in the anoxic layer was linked to sulfate-reducing and methane-producing bacteria since it ceased when metabolic inhibitors were added experimentally (Oremland et al. 1991).

The measured standing pool levels of MeHg in sediment represent the effects of differences between rates of methylation and demethylation (Beijer and Jernelow 1979; Ullrich et al. 2001). Since both rates of these juxtaposed processes are rapid (see below), relatively small changes in either rate can rapidly and significantly affect the measured standing pool size of MeHg. This effect is believed to be a major reason for large variations in MeHg pool sizes (Best et al. 2005). Confronted with the resulting real spatial and temporal differences in standing MeHg pool sizes, sufficiently dense additional MeHg sampling and analyses rapidly become cost prohibitive. Means to aggregate samples before analysis to integrate MeHg levels over time (see Chapter 4) would help reduce this variability.

In addition to the factors affecting the opposing rates of methylation and demethylation, the physical location of MeHg pools in the sediment must also be considered in the context of the benthic community. Benthic organisms are exposed to MeHg via the dissolved and particulate fractions of pore water and water column, and via the ingestion of food. Filter-feeding benthic infauna may get their largest exposure via MeHg sorbed to suspended particulates. Deposit-feeders would be exposed to MeHg on particles processed from the mud-water interface. Aquatic macrophytes can absorb MeHg up from the pore water in deeper sediment layers with roots and transport it to their shoots to a limited extent (Heller and Weber 1998). MeHg appears to accumulate progressively in higher trophic levels of food webs, while nonmethyl Hg declines (Back and Watras 1995; Baeyens et al. 2003). The reason for this preferential accumulation in fish

has its source at the phytoplankton level. Mercury species enter phytoplankton by diffusion, with MeHg entering the cytoplasm and inorganic Hg mainly bound to the cell membrane (Mason et al. 1993). Planktonic consumers, such as planktivorous fish, digest the dissolved cytoplasmic but defecate the membrane material, thus, poorly assimilating inorganic Hg (Mason et al. 1993). Further discrimination up the food chain can result from the functioning of the metabolic system, particularly the liver, which in turn is affected by age of the organisms and by the intensity and the period of Hg exposure. Recently published Hg levels in fish species at the top of the food chain in San Francisco Bay are 0.80 $\mu g\ g^{-1}$ wet weight (WW) in leopard shark and 0.32 $\mu g\ g^{-1}$ WW in striped bass. These levels exceed the threshold for human health concern (data 2000, SFEI 2005a). MeHg is one of the forms of Hg that is of great concern with respect to ecological and human health. Knowledge of the environmental factors that control the standing pool size of MeHg (and its introduction into and magnification up food chains) is needed for assessing the potential impacts of MeHg in the San Francisco Bay system. It is logical to begin this analysis at the base of the aquatic food web. This need is particularly acute for assessing the environmental risk posed by tidal wetlands construction, systems that are known to produce MeHg.

A large part of the research included in this study was designed to address consensus technical questions formulated at the CALFED Stakeholders' Workshop on Mercury in San Francisco Bay, held 8-9 October 2002 at Moss Landing Marine Laboratories (Wiener et al. 2003).

These included the following:

- What are the present levels of MeHg in San Francisco Bay wetlands with respect to biota, sub-habitats, and location within SF Bay?
- What are the rates of MeHg production?
- What factors control MeHg production? Can these be managed?
- Are some wetlands larger mercury exporters than others?
- Can we model/predict the effects of wetland restoration on MeHg production and export?

The first determinations of in situ methylation and demethylation rates using a stable mercury isotope approach in San Pablo Bay wetlands are from June 2003 (Best 2005; Chapter 3). Results of a short-term study on THg and MeHg concentrations in sediments of the fringe marsh bordering the HAAF Wetlands Restoration Site and its environs in the wet and dry

season, respectively, indicated that THg levels were similar, but that MeHg levels were greater in the wet than in the dry season (McFarland et al. 2003). Therefore, the data thus far on methylation and demethylation rates were expected to be relatively low and not representative for year-round net MeHg production. Largely based on these observations, recommendations for future research were formulated. The current study addresses the recommendation to quantify net MeHg production in wetland sediments with respect to subhabitats and location within SF Bay.

Objectives

In the present study, the three following questions relating to mercury cycling are addressed:

1. Are methylation and demethylation rates in San Pablo Bay wetlands sediments affected by season?
2. Are there spatial differences in methylation and demethylation rates in San Pablo Bay wetland sediments?
3. Are methylation and demethylation rates related to microbial parameters?

In this chapter results are described of in situ determinations largely made in 2004. A more integrated view will be reported in a subsequent report.

Study sites

The HAAF on San Pablo Bay is part of the San Francisco Baylands. It is located in the North Bay. The Baylands consist of shallow water habitats around the San Francisco Bay. The Baylands ecosystem includes the areas of maximum and minimum fluctuations, adjacent habitats, and their associated plants and animals. The boundaries of the ecosystem vary with the bayward and landward movements of fish and wildlife that depend upon the baylands for survival. Many habitats of the Baylands are wetlands. Habitat goals selected for the planned restored HAAF include the restoration of tidal marshes, with natural transitions into upland areas with seasonal wetlands. The restored HAAF area is expected to increase the habitats of the regionally rare and protected clapper rail and salt marsh harvest mouse; because it is adjacent to existing populations, it will contain a large tidal wetland and is remote from predator outposts and corridors (San Francisco Bay Area Wetlands Ecosystem Goals Project 1999). The test site representative for the tidal part of HAAF was situated at the HAAF bay edge (SM-10; 38° 03.116′ N, 122° 29.55′ W; Figure 3-1).

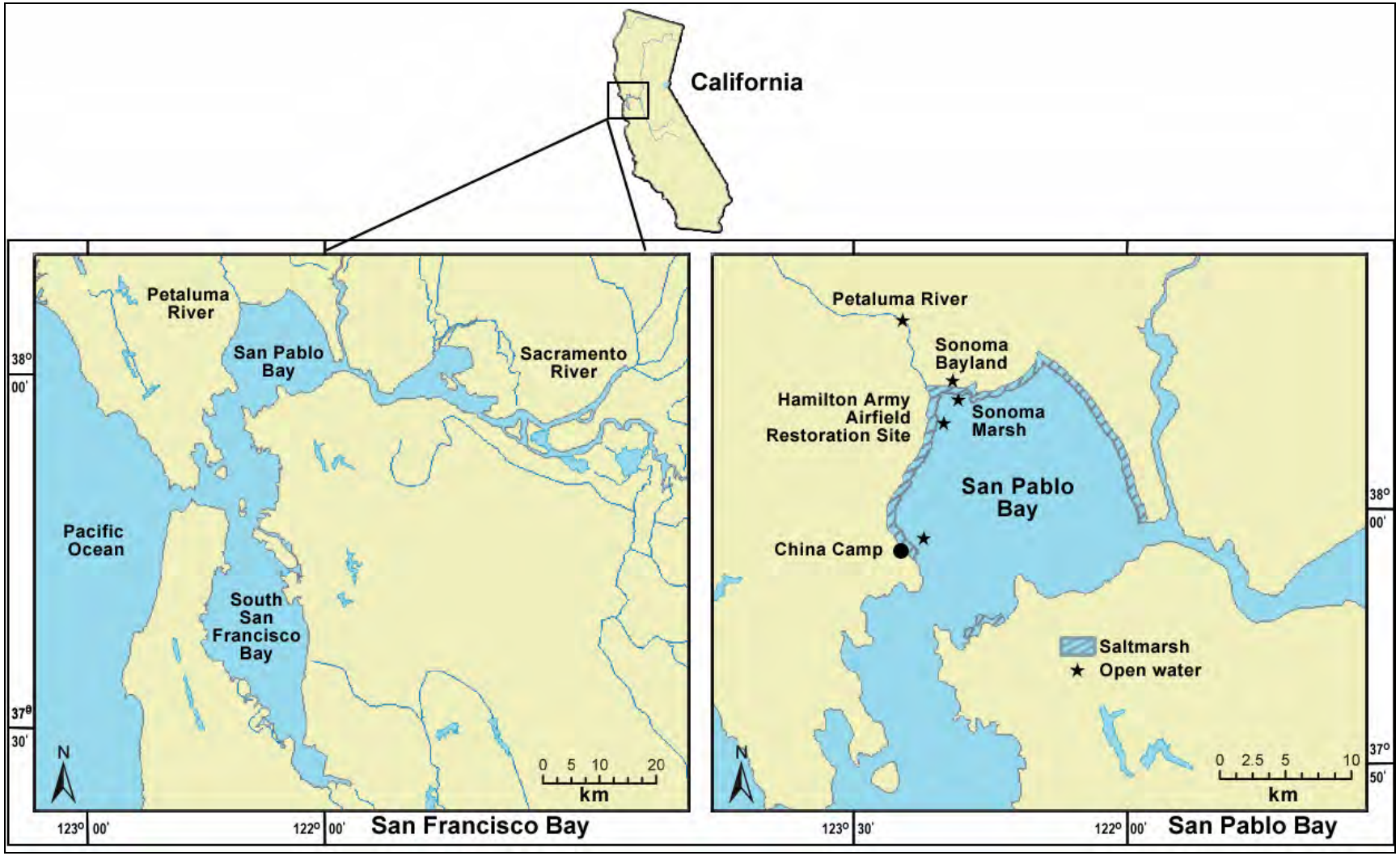

Figure 3-1. Site map showing the location of San Pablo Bay within San Francisco Bay (left) and the location of the Hamilton Army Airfield Restoration Site, China Camp, Sonoma Marsh, Sonoma Baylands, and Petaluma River (right).

The restored HAAF is expected to cover ca. 203 ha. The nearby tidal salt marsh at the China Camp State Park, chosen as a reference (R44; 38°° 00.411′ N, 122° 28.758′ W), covers ca. 45 ha (Hopkins and Parker 1984) and is frequently immersed by tidal waters (salinity 25-32‰; Figure 3-1). The tidal salt marsh at China Camp is predominated by *Spartina foliosa* (Pacific cordgrass) on the low marsh between mean tidal level (MTL) and mean high water level (MHW), and by *Salicornia virginica* (common pickleweed*)* at somewhat higher levels and above MHW. Other sites for nonvegetated low marsh sediment sampling were selected along a decreasing gradient in salinity and included Sonoma Fringe Marsh (SM; 38° 06.769′ N, 122° 28.950′ W), Sonoma Baylands (SB; 38° 07.26′ N, 122° 29.31′ W), and Petaluma River (PR; 38° 06.76′ N, 122° 28.95′ W). Net MeHg production is expected to reach a maximum at intermediate sulfate (SO_4^{2-}) concentrations that occur at intermediate salinities (Gilmour and Henry 1991). The Sonoma Baylands site was chosen because it is a recently restored coastal wetland with characteristics similar to those expected at a restored HAAF.

Materials and methods

Approach

From 22 to 25 March 2004, the wet season, methylation and demethylation were evaluated in different vegetated sediment cores. Several experiments were conducted to explore if (1) length of incubation period affected the methylation and demethylation rates in the sediment, and (2) plant uptake, upward transport, and leaching from foliage of the mercury isotopes injected into the rhizosphere were detectable in field incubations. To provide answers to these questions, cores vegetated by *S. foliosa* and cores vegetated by *S. virginica* were collected at China Camp and incubated in situ for periods of 5, 24, 48, and 72 h, using one replicate each time, and mercury isotope amendments approximately ten times greater than previously employed. Replications were limited by budgetary constraints. On 26 July 2004, the dry season, methylation and demethylation rates were determined in vegetated and nonvegetated cores at China Camp by 5-h in situ incubations that were replicated three times. The nonvegetated cores were collected adjacent to the vegetation, and nonvegetated and vegetated cores were up to several meters apart.

On 27 and 28 July 2004, spatial variation in methylation and demethylation rates were assessed and replicated three times in nonvegetated

sediment cores at HAAF, Sonoma Marsh, Sonoma Baylands, and a site up the Petaluma River. Determinations in nonvegetated sediment at China Camp carried out the previous day were used for comparison.

Sediment sampling

Sediment cores with a diameter of 9.5 cm were collected using a special sediment corer, described by Best et al. (2005) and used for the sediment incubations to derive methylation and demethylation rate measurements. This corer was placed over an intact plant, twisted into the sediment to a depth of approximately 20 cm, and used to extract the entire plant, roots, and adjacent sediment. The cores were capped at the bottom, and a solution of $^{199}Hg^{2+}$ and $CH_3{}^{200}Hg^{+}$ was injected through pre-drilled ports in the acrylic tube liner of each core. After injection of isotopes, all cores were set back into their original location within a frame with handles and incubated in place for 5 h, unless stated otherwise. At the end of the incubation period, the cores were pulled up by the handles; the aboveground plant material was contained within the upper part of the core; and cores were capped at the top and quick-frozen with dry ice in the field. Samples remained frozen until analysis in the laboratory.

Smaller diameter (5-cm) PVC cores were collected immediately adjacent to the large diameter cores. Sediment samples from 0- to 5-cm depths of these cores were analyzed for PLFAME analyses. PLFAME analyses provide a measure of sedimentary microbial community biomass and taxonomic composition mostly at the genus but sometimes at the species level. This procedure is described below.

Redox and pH measurements

Sediment redox potential and pH were measured at the end of the incubation period using an Orion pH/mV meter (Model 250A) adapted with a self-manufactured platinum (Pt) tip redox electrode (Boehn 1971; Faulkner et al. 1989) and a pH electrode (Orion, Model 91-05), as described earlier (Best et al. 2005, Chapter 3). Electrodes were inserted into the sediment of the incubated cores with the tips contacting sediment at 5-cm depths at the beginning of the incubation period. The pH was measured only in the surface sediment of the incubated cores.

Stable mercury isotopic tracer studies

$^{199}HgCl_2$ was used for the methylation assay. ^{199}HgO (Oak Ridge National Laboratories) was converted into $^{199}HgCl_2$ by dissolving ^{199}Hg enriched (91.95% purity) HgO in 1 mL of hydrochloric acid (10 mM), resulting in a solution with a concentration of 758,000,000 ng/L ^{199}Hg. $CH_3{}^{200}HgCl$ was prepared for the demethylation assay. ^{200}Hg enriched (96.41% purity) HgO (Oak Ridge National Laboratories) was synthesized using the methyl-cobalamin method as described in Hintelmann et al. (2000), resulting in a solution with a concentration of 594,000 ng/L $CH_3{}^{200}HgCl$. Appropriate aliquots of the two isotopic stock solutions were combined in the field and diluted with filtered seawater to yield the working standards used for spiking cores. For the experiments conducted in March 2004, final concentrations were 13,240,000 ng/L of $^{199}Hg^{2+}$ and 44,800 ng/L $CH_3{}^{200}Hg^+$. In July, the concentrations were 30,400,000 ng/L of $^{199}Hg^{2+}$ and 89,600 ng/L $CH_3{}^{200}Hg^+$. The pH in the final solution was near neutral and the authors did not expect the small volume of injected isotope solution to change sediment pH.

The solution (100 µL) of $^{199}Hg^{2+}$ and $CH_3{}^{200}Hg^+$ was injected through pre-drilled ports in the acrylic tube every cm for the first 5 cm of each of the vegetated cores. For the March (and July) experiments a total of 5 × 1,324 ng (5 × 3,040) = 6,620 ng (15,200) $^{199}Hg(II)$ and 5 × 4.48 ng (5 × 8.96) = 22.4 (44.8) ng of $Me^{200}Hg$ were injected into the top 5 cm. For the methylation/demethylation (M/D) experiments conducted 27-28 July, the solution was injected every centimeter for the first 3 cm of the non-vegetated cores (a total of 3 × 3,040 ng = 9,120 ng of $^{199}Hg(II)$ and 3 × 8.94 ng = 26.9 ng of $Me^{200}Hg$). While these amounts appear to be high, the isotopes were dispersed as evenly as possible into each 1-cm layer upon injection. Furthermore, the authors were using large-diameter cores, so that each centimeter of the core contains approximately 40 g DW of sediment. Therefore, the final concentration of isotopes injected per centimeter was still lower than corresponding ambient concentrations.

After injection of isotopes, all cores were set back into their original location and incubated in place for 5 h at the beginning of low tide. The March experiments included additional single replicates incubated in sediment for 24, 48, and 72 h. Incubation was terminated by quick-freezing of cores, including plants, with dry ice in the field. Samples remained frozen until analysis in the laboratory.

Core processing

The aboveground plant material was cut off from the sediment core and weighed. The frozen cores were extruded from the plastic tube and the top 5 cm of the vegetated and the top 3 cm of the nonvegetated cores were sliced off with a diamond-tipped cutting blade. The area injected with mercury isotopes was further isolated by cutting a 1.25-cm slice from the center area around the injection point resulting in a sub-core containing the injected solution of isotopes. This sub-core was further homogenized and subsamples were taken for the various measurements. Root material was obtained by washing a subsample of the isolated core over a fine meshed sieve to remove clay and silt particles. The relative amounts of sediments and root material (wet weight) were determined at this stage. Wet sediment was dried at 50 °C overnight or until weight consistency was obtained to determine the dry/wet weight ratio (% solids). The loss on ignition (LOI) was determined by ashing the dried sample at 500 °C for 4 h or until weight consistency was obtained.

Total mercury determination

About 0.2 g of sample was weighed into 30 mL acid washed glass vials. Typically, 12.2 ng of $^{201}HgCl_2$ was added as an internal standard. After addition of 5 mL of concentrated H_2SO_4/HNO_3, the mixture was left to react for 1 h at room temperature. Digestion was finished by heating vials in an Al block at 120 °C on a hot plate for 3 h or until formation of brown nitrous gases had ceased. The digest was diluted with Milli-Q water to the mark.

The concentration of Hg isotopes in the digest was quantified using continuous-flow cold-vapor generation with ICP/MS detection (Finnigan MAT, Model Element 2). The acidified sample was continuously mixed with a solution of stannous chloride by means of a peristaltic pump. The formed mercury vapor was separated from the liquid in a gas-liquid separator (Model L1-2) and the elemental mercury swept into the plasma of the ICP/MS. The following isotopes of Hg were measured: ^{199}Hg (added isotope for the methylation assay), ^{200}Hg (added isotope for the demethylation assay), ^{201}Hg (internal standard) and ^{202}Hg (to calculate ambient THg). Concentrations of individual isotopes were calculated as described in Hintelmann and Ogrinc (2003).

Methylmercury determination

MeHg concentrations were determined according to Hintelmann and Evans (1997). Approximately 0.2 g of sample was weighed into 30 mL Teflon vials and suspended with an additional 10 mL of distilled water. $CH_3{}^{201}HgCl$ (55 pg) was added as an internal standard. After 200 µL of H_2SO_4 (9 M) and 500 µL of KCl (20%) were added, the vessel was placed into a heating block at 140 °C. MeHg was distilled from the sample under a supporting nitrogen stream (80 mL min^{-1}). Distillation time was approximately 60-90 min per sample.

A reaction vessel was filled with 100 mL Milli-Q water, and the distillate was added for measurement of MeHg. Next, 0.2 mL of acetate buffer (2 M) was added to adjust the pH to 4.9. Sodium tetraethylborate (100 µL, 1% w/v) was added and the solution sat at room temperature for 20 min while the tetraethylborate reacted. Tenax adsorber traps were connected to the reaction vessel and the generated methylethylmercury was purged for 20 min from the solution using nitrogen (200 mL min^{-1}) and collected on the Tenax trap. Finally, all mercury species were thermally desorbed from the trap (250 °C), separated with gas chromatography and quantified by ICP/MS (Micromass Platform). The following isotopes of Hg were measured: ^{199}Hg (methylated Hg), ^{200}Hg (MeHg demethylation assay), ^{201}Hg (internal standard) and ^{202}Hg (to calculate ambient MeHg). Peak areas were used for quantification and concentrations of individual isotopes were calculated as described in Hintelmann and Ogrinc (2003).

Mercury analysis QA/QC

For each batch of samples the following set of QA/QC samples was measured: three reagent blanks (THg) or bubbler blanks (MeHg) and a certified reference material (IAEA 356 marine sediment and MESS-3 marine estuary sediment for sediment analysis and NIST 1515 apple leaves for plant analysis). Individual distillation yields were determined using the added internal ^{201}Hg isotope standard. Typically, one triplicate sample was analyzed (i.e., triplicate distillation or digestion) per batch.

Measurements of mercury methylation and methylmercury demethylation

For the current study the best methods available at this time to determine the rates of methylation and demethylation are being used. Use of stable isotopes of mercury species enables the addition of labeled mercury

species at tracer levels. This is particularly important for determining MeHg demethylation rates. Due to detection limit considerations, radio-labeled $^{14}CH_3$-Hg usually must be added at levels that may exceed the total sedimentary MeHg pool. These levels cannot be considered tracer levels as the mass of added MeHg can alter in situ reaction kinetics. Addition of lower levels of $^{14}CH_3$-Hg can increase the analytical error of the analysis. In the current study, therefore, a method is employed whereby a cocktail of $^{199}HgCl_2$ and CH3^{200}Hg is injected at tracer level to select depth horizons of an undisturbed sediment core contained in a polyvinyl chloride (PVC) sleeve. Rates of methylation and demethylation are measured in the same volume of sediment during the same period of time so that they are directly comparable. The core is placed back into the sediment on site, incubated for a predetermined period, then removed and quickly frozen in dry ice. This incubation is designed to measure processes under on site conditions. Upon returning to the laboratory, cores are sectioned. Sections of the appropriate horizon are thawed and homogenized. Separate samples are taken for THg and MeHg analysis as described above. $^{201}HgCl_2$ or $CH_3{}^{201}Hg$ is added as internal standard in the respective analyses. 202Hg is measured to calculate the ambient THg levels. These methods typically produce results with less than 3% standard analytical error.

In addition to knowing the strengths of the technical methods used to determine rates of methylation and demethylation, it is also important to know their limits. The study of mercury biogeochemistry is technically difficult and caution must be used when interpreting data of in situ rates of methylation and demethylation. In the current study, the effects of on site incubation times ranging from 5 to 72 h were evaluated (Table 3-1). Generally, the China Camp State Park marsh is exposed to two tides per day. The 5-h incubations were started as the water receded from the marsh surface sediment and collected before the next tide had reached a level that was too high to recover the incubated cores. Longer incubations were subject to two or more high tides before recovery at low tide. The length of the sediment incubation period and tides affected both the apparent methylation and demethylation rates. The net conversion rates (expressed as % Hg converted) tended to decrease with increasing incubation times in both cores containing *S. foliosa* and *S. virginica* root zones. To obtain gross conversion rates, it was decided to standardize subsequent rate measures using 5-h sediment incubations. All subsequent methylation and demethylation rate measures were based on this incubation time unless otherwise stated.

Table 3-1. THg, MeHg, rates of methylation, demethylation, and net MeHg production in the vegetated sediments of the existing marsh at China Camp on San Pablo Bay, March 2004. Single values, overall means, and standard deviations (N=4).

Sediment	THg (ng g^{-1} DW)	MeHg (ng g^{-1} DW)	Methylation		Demethylation		Net MeHg Production
			100 × k_M (% Hg^{2+} per day)	M (ng g^{-1} DW per day)	Dm (% $Me^{200}Hg$ degraded per day)	D (ng g^{-1} DW per day)	M-D (ng g^{-1} DW per day)
Spartina root zone sediment							
China Camp, 0-5 cm							
5-h inc	337	9.47	1.13	4.03	96	3.86	0.18
24-h inc	334	7.71	0.87	3.13	56	1.76	1.37
48-h inc	380	5.58	1.66	5.94	26	1.52	4.42
72-h inc	385	3.35	0.81	2.91	16	0.46	2.45
Overall mean	358 (27)	6.53 (2.65)	1.12 (0.38)	4.00 (1.38)	48 (36)	1.90 (1.42)	2.11 (1.80)
Salicornia root zone sediment							
China Camp, 0-5 cm							
5-h inc	284	5.04	2.76	6.20	78	4.86	1.34
24-h inc	307	5.29	0.87	2.31	20	0.46	1.86
48-h inc	331	10.41	0.57	1.74	33	0.57	1.17
72-h inc	300	5.44	0.38	1.17	22	0.26	0.91
Overall mean	305 (19)	6.54 (2.58)	0.93 (0.75)	2.85 (2.27)	38 (27)	1.54 (2.21)	1.31 (0.40)

Polar lipid fatty acid methylester analysis

PLFAME has been detailed elsewhere (Fredrickson et al. 1986). Briefly, 2-g (WW) sediment samples were collected from the frozen cores at depths of 2, 5, and 10 cm. These samples were extracted and placed for 3 h at room temperature into 6 mL of a dichloromethane:methanol:water (1:2:0.8 on a volume basis) mixture. Amino-propyl solid phase extraction columns (Supelco, Bellefonte, PA) were used to separate the total lipid into neutral, glyco-, and polar lipid fractions. Phospholipid fatty acid methyl esters (from the polar lipid fraction) were prepared for gas chromatography/mass spectrometry (GC/MS) by mild alkaline methanolic transesterification. The resulting phospholipid fatty acid methyl esters were dissolved in hexane containing methyl nonadecanoate (50 pmol μL^{-1}) as an internal standard and analyzed using a GC equipped with a 50 m × 0.25 mm (ID) DB-1 capillary column (0.1 µm film thickness, J&W Scientific, Folsom, CA) and a flame ionization detector. Peak identities were confirmed using a GC-mass selective detector (Hewlett Packard GC6890-5973 MSD) with electron impact ionization at 70 eV.

Areas under the peaks were converted to concentrations, summed, and then normalized to the gram weight extracted for biomass determinations. For community comparisons, the percentage contribution of each peak was calculated and then normalized using an arcsine square root transformation. The following SRB's were distinguished by their unique FA biomarkers: both, *Desulfobacter hydrogenophilus* and *Desulfobacterium autotrophicum* by 10-Methyl 16:0 (10Me16:0) and *Desulfovibrio desulfuricans* by iso17:0 (i17:0) (Boon et al. 1977; Taylor and Parkes 1983; Vainshtein et al. 1992). Because *Desulfobacter* and *Desulfobacterium* biomasses were indistinguishable from each other using this biomarker approach, their combined biomass is further referred to as *Desulfobacter* biomass in this chapter. No other SRB biomarkers were available to allow distinction of more than these two groups. For comparison with literature data, 1 pmole PLFAME is considered as equivalent to 2.5×10^4 microbial cells (Fredrickson et al. 1986).

Data analysis

Calculations of methylation and demethylation rates

Rates for mercury methylation and demethylation were calculated assuming first-order kinetics for both processes (Hintelmann et al. 2000). Consequently, the methylation rate constant, k_M, is simply the ratio of newly formed $Me^{199}Hg$ over the total concentration of added $^{199}Hg(II)$, per time: $k_M = [Me^{199}Hg] / [^{199}Hg]$ / incubation time (in days). k_M is expressed in units of d^{-1}. Since the newly formed $Me^{199}Hg$ is eventually subject to the demethylation process, the gross rate constant of k_M is best obtained from measurements early in the assay, where demethylation will not significantly deplete the pool of $Me^{199}Hg$ and, therefore, will not significantly affect the methylation rate constant. An exact solution would be obtained by using the approach outlined in Hintelmann et al. (2000). However, the variability of measured rates within replicate cores is far greater than the difference between the simplified approach used here and the exact method described by Hintelmann et al. (2000). Hence, the authors chose to equate net methylation rates (i.e., the measured MeHg formation during the initial 5 h) with the gross rate. Consequently, final net MeHg production is a conservative estimate, as actual production is likely less. The rate of ambient MeHg production, M (in ng g^{-1} d^{-1}), is obtained by multiplying the measured rate constant by the concentration of total ambient Hg (in ng/g): $M = [THg] \times k_M$.

Being a first-order process, spike $Me^{200}Hg$ concentrations decrease exponentially over time. Hence, a demethylation rate constant, k_{Dm}, expressed in units of d^{-1}, is calculated by linear regression of $\ln[Me^{200}Hg]$ versus time, with the slope of the regression being k_{Dm}. The percentage of MeHg degradation per day, Dm (expressed in units of %), is then calculated as $Dm = 1\text{-}e^{-kDm} \times 100\%$. The rate of MeHg demethylation, D (in ng g^{-1} d^{-1}), is obtained by multiplying the percentage degradation by the concentration of newly methylated MeHg: $D = Dm \times [THg] \times k_M$.

Eventually, combining both rates allows estimating the net amount of MeHg, net_{MeHg} (in ng g^{-1} d^{-1}), that is newly generated from the pool of ambient inorganic THg:

$$net_{MeHg} = M - D = [THg] \times k_M - Dm \times [THg] \times k_M = (1 - Dm) \times [THg] \times k_M.$$

Statistics

Statistical analyses were conducted with the software STATGRAPHICS Plus for Windows version 32S package (Manugistics, Rockville, MD). Normal distribution of the data was tested using the Shapiro-Wilk's test. Analysis of variance (ANOVA) was expanded with a multiple range test using the Fisher's least significant difference procedure. The p-value in the ANOVA is a measure of the significance of the analysis; it was set at a 95% confidence level (p-value of ≤ 0.05). Regression analyses were conducted using the least squares method. Linear equations were fitted with the linear module and non-linear equations with the exponential or polynomial modules. The p-value in the regression models was set at a 95% confidence level (p-value of ≤ 0.05) unless stated otherwise. The R^2-value of the regression model indicates the proportion of the variance explained by the model. Regression models explaining at least 50% of the variability in the data set, i.e., $R^2 \geq 0.50$, were considered as providing a good fit.

Results

Spatial distribution of mercury and processes in wetlands bordering San Pablo Bay

A large part of previous mercury studies by ERDC have centered on reconstruction of tidal wetlands on the HAAF site and a control site at China Camp (Best et al. 2005). The scope is expanded in the current study to include a range of wetland sites bordering San Pablo Bay along a salinity

gradient (24‰ – 7‰) from China Camp, through HAAF, the recently reconstructed Sonoma Baylands, and the Sonoma Fringe Marsh, up to a marsh on the Petaluma River (Figure 3-1). Data collected there provide a context for comparing the biogeochemical processes in the China Camp and HAAF wetlands to those at other locations on San Pablo Bay.

This wider perspective enables the assessment of trends that may be useful in making decisions with respect to creating wetlands around San Pablo Bay and allows effective management of the new wetlands, once constructed. The majority of the THg in surface sediments of San Pablo Bay wetlands comes from deposition of contaminated particles from the watershed. As a result, THg contamination is ubiquitous and the levels of THg are generally not significantly different in any particular San Pablo Bay wetland surface (0-3 cm) sediment (Best et al. 2005). Current data (Table 3-2) support this with the exception of sediment in the newly created Sonoma Baylands. It is unclear whether these lower THg levels are due to cleaner sediment used to construct the wetland, contemporary inefficiency at trapping contaminated sediment particles, or both. From this wider spatial perspective no relationship between levels of THg and levels of MeHg was apparent when surface sediments from the various San Pablo Bay wetlands were compared (Figure 3-2).

Additionally, no apparent relationships were found between levels of THg and rates of methylation and demethylation, respectively, in these San Pablo Bay surface sediments. The data demonstrate that THg is not a good predictor of MeHg levels in sediments and underscores the current inability to identify and measure the mercury species within the THg measurable pool that are subject to methylation. Although the reduction of particle-borne THg into the SF Bay intuitively appears a rational management action, the absence of this relationship brings into question the potential efficacy of efforts to control levels of mercury in SF Bay birds and fish by focusing solely on reducing THg in watershed sediment loads (SFEI 2005b).

Table 3-2. THg, MeHg, rates of methylation, demethylation, and net MeHg production in the sediments of existing marshes on San Pablo Bay, July 2004. Mean values and standard deviations (N = 3).

Sediment	THg (ng g^{-1} DW)	MeHg (ng g^{-1} DW)	Methylation		Demethylation		Net MeHg Production
			100 × kM (% $Hg2^+$ per day)	M (ng g^{-1} DW per day)	Dm (% $Me^{200}Hg$ degraded per day)	D (ng g^{-1} DW per day)	M-D (ng g^{-1} DW per day)
Nonvegetated sediment							
China Camp, 0-5 cm	362 (35)B[1]	3.71 (0.59)DE	2.63 (0.25)	9.43 (0.16)CD	88 (4)	8.29 (0.36)C	1.13 (0.38)BC
HAAF, 0-5 cm	379 (38)B	1.97 (0.89)BC	2.35 (1.30)	6.59 (3.97)BC	80 (2)	5.36 (4.08)BC	1.23 (0.79)C
Sonoma Marsh, 0-5 cm	358 (10)B	0.49 (0.07)A	0.78 (0.07)	2.80 (0.23)AB	83 (15)	2.31 (0.32)AB	0.48 (0.47)AB
Sonoma Baylands, 0-5 cm	296 (10)A	2.75 (0.16)CD	4.49 (1.20)	13.21 (2.59)D	96 (3)	12.73 (3.35)D	0.48 (0.23)AB
Petaluma River, 0-5 cm	397 (2)B	1.33 (0.32)AB	1.95 (0.55)	7.74 (1.80)C	95 (7)	7.29 (2.12)C	0.45 (0.54)AB
Vegetated sediment							
Spartina root zone sediment							
China Camp, 0-3 cm	393 (11)B	3.00 (0.26)BC	0.41 (0.08)	1.63 (0.33)A	89 (1)	1.45 (0.29)A	0.17 (0.05)A
Salicornia root zone sediment							
China Camp, 0-3 cm	322 (9)AB	3.91 (1.80)E	0.49 (0.37)	1.56 (1.11)A	89 (4)	1.36 (0.91)A	0.21 (0.20)A

[1] ANOVA results of THg, MeHg, methylation, and demethylation data, using site as factors and vegetation cover as covariate (site and vegetation cover entered as numbers in the analysis). Mean values followed by the same letter are not statistically different according to Fisher's least significant difference procedure.

In this wider spatial context, many statistically significant differences in levels of MeHg and in methylation rates were found among San Pablo Bay wetland surface sediments as indicated by analysis of variance followed by multiple range test, using Fisher's least significant difference procedure to demonstrate between-site differences (Table 3-2). Unknown local conditions appear to be affecting both the MeHg standing pool sizes and rates of methylation. Rates of mercury methylation correlate with MeHg levels at vegetated sites and at nonvegetated sites. Although methylation rates at vegetated sites are lower, the slope of the regression is much steeper compared to nonvegetated sites, suggesting greater demethylation rates at the vegetated sites (Figure 3-2). A similar relationship was demonstrated in the Florida Everglades along a gradient of eutrophic water in the north (agricultural runoff) to relative oligotrophic water in the south (Gilmour et al. 1998). The standing pool size of MeHg is the result of the methylation

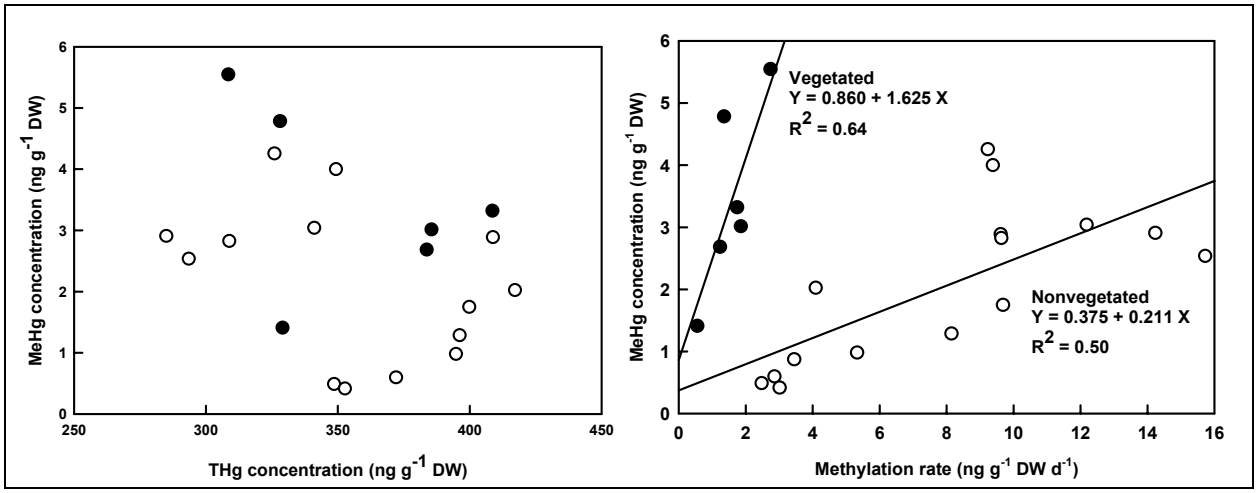

Figure 3-2. Levels of THg versus MeHg (left) and rates of methylation versus level of MeHg (right) measured in surface sediments from various wetlands bordering San Pablo Bay in July 2004. Open circles represent nonvegetated and closed circles vegetated sediments. Regression equation, significance (p), and proportion of variance explained (R^2) by the fitted model indicated.

reaction that produces MeHg and the demethylation reaction that reduces this pool size, and the rates of these juxtaposed reactions are rapid. Like the methylation rates, the demethylation rates in most sediments also differed significantly (Table 3-2), again suggesting control by local conditions. MeHg concentration increased linearly with methylation (Figure 3-2). Taken together, the rates of methylation and demethylation were similar in the sample volume of bare surface sediment from marshes bordering San Pablo Bay and indicate that rates of net MeHg production ranged from 0.45 to 1.23 ng g^{-1} DW d^{-1} (Table 3-2).

Demethylation rates, and the factors that drive them, are important to consider because they help to control net MeHg production rates (Table 3-2). Frequently, demethylation rates are increased at sites with elevated mercury methylation activity. This suggests that the MeHg demethylating microbial communities in these sediments are able to respond to a greater MeHg pool size by increasing their demethylation activities and thus limit the MeHg pool size. The mechanism by which this self-regulation occurs is not currently understood but warrants further investigation. In the Florida Everglades, the greatest net MeHg production rates have been reported in Water Conservation Areas 2B and 3A and have been correlated to intermediate dissolved sulfate levels (50-100 µM) derived from sulfur added to agricultural fields in the north (Gilmour et al. 1998). This correlation was called the Goldie Locks Effect because high sulfate/sulfide levels in the eutrophic north are believed to decrease the levels of mercury species available for methylation and lack of sulfate in

the oligotrophic south limited sulfate respiration (Benoit et al. 1999). In the current study, no such analogous trend was demonstrated in San Pablo Bay marshes ranging from those at China Camp near the Golden Gate (24‰ salinity) to those up the Petaluma River (7‰; Figure 3-3). Salinity classes were assigned according to salinity measured in surface waters bordering the marshes in 2002 (San Francisco Regional Water Quality Control Board 2006).

It was conspicuous that the daily production of MeHg in the majority of sediment measured to date is usually in the same order of magnitude, but always less, than the starting sediment pool size of MeHg (Table 3-2). This means, if the demethylation rate were zero, the sediment pool of MeHg may have the potential to double in one day or faster. Additionally, the rates on the demethylation reactions generally tend to match the rates of methylation. This means, if the methylation rate were zero, the sediment microbial community has the potential to deplete the MeHg pool in a few days or faster. Thus, the mercury species dynamics of this sediment system are substantial and the possibility of relatively small changes in either rate can quickly affect standing MeHg pool sizes.

Seasonal changes in methylation and demethylation and potential consequences for net methylmercury production

In addition to spatial factors affecting net MeHg production, potential seasonal factors were investigated. Seasonal changes in temperature and rainfall are important macro-drivers for most SF Bay processes — with the wet season lasting from November to March and the dry season from April to October. These factors greatly affect growth of the macrophytic wetland vegetation, which in turn has profound effects on microbial communities and root zone processes as well as on organic matter inputs that largely fuel the food web.

2003 to 2004 comparisons

Mercury values for a particular surface sediment and season in 2003 were compared to the analogous measures in 2004 to determine year to year fluctuations (Table 3-3, Figure 3-4). The levels of THg remained in the same order of magnitude in 2003 to 2004, except for the *S. virginica*-vegetated sediments with low THg levels in 2003. MeHg pool sizes tended to be greater in 2004 than in 2003, but differences were not statistically significant in China Camp.

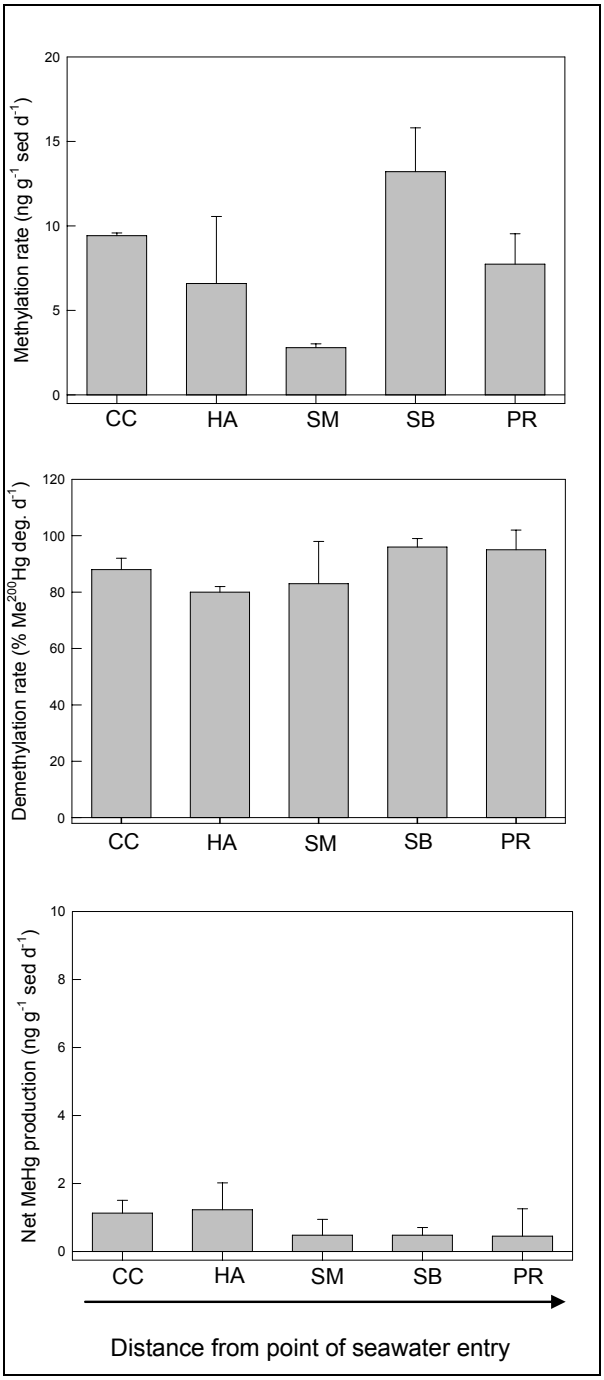

Figure 3-3. Rates of methylation, demethylation, and net MeHg production in nonvegetated sediments of existing marshes on San Pablo Bay measured in July 2004. Mean values and standard deviations (N=3). Relative distance to the point of sea-water entry into the bay indicated. Abbreviations: CC = China Camp; HA = HAAF; SM = Sonoma Fringe Marsh; SB = Sonoma Baylands; PR = Petaluma River.

Table 3-3. THg, MeHg, rates of methylation, demethylation, and methylation:demethylation ratio in the sediments of existing marshes on San Pablo Bay, June 2003–July 2004. Mean values and standard deviations (N=3).

Sediment	THg (ng g^{-1} DW)	MeHg (ng g^{-1} DW)	Methylation		Demethylation		Net MeHg Production
			100 × k_M (% Hg^{2+} per day)	M (ng g^{-1} DW per day)	Dm (% $Me^{200}Hg$ degraded per day)	D (ng g^{-1} DW per day)	M-D (ng g^{-1} DW per day)
China Camp							
Nonvegetated sediment							
June 2003[1]	333 (9)	1.05 (0.19)	0.42 (0.18)	1.40 (0.60)	59 (52)	0.83 (0.81)	0.57 (1.00)
March 2004	ND[3]	ND	ND	ND	ND	ND	ND[3]
July 2004	362 (35)	3.71 (0.59)	2.63 (0.25)	9.43 (0.16)	88 (4)	8.29 (0.36)	1.13 (0.38)
Vegetated sediment							
Spartina-rz[2], June 2003[1]	323 (23)	2.77 (1.37)	0.70 (0.34)	2.26 (1.11)	46 (41)	1.04 (1.06)	1.22 (1.53)
Spartina-rz[2], March 2004	358 (27)	6.53 (2.65)	1.12 (0.38)	4.00 (1.38)	48 (36)	1.90 (1.42)	2.11 (1.80)
Spartina-rz[2], July 2004	393 (11)	3.00 (0.26)	0.41 (0.08)	1.63 (0.33)	89 (1)	1.45 (0.29)	0.17 (0.05)
Salicornia-rz[2], June 2003[1]	276 (27)	2.40 (2.42)	0.60 (0.12)	1.66 (0.37)	83 (16)	1.37 (0.41)	0.28 (0.55)
Salicornia-rz[2], March 2004	305 (19)	6.54 (2.58)	0.93 (0.75)	2.85 (2.27)	38 (27)	1.54 (2.21)	1.31 (0.40)
Salicornia-rz[2], July 2004	322 (9)	3.91 (1.80)	0.49 (0.37)	1.56 (1.11)	89 (4)	1.36 (0.91)	0.21 (0.20)
HAAF							
Nonvegetated sediment							
June 2003[1]	350 (92)	1.11 (0.82)	0.88 (0.82)	3.08 (2.98)	59 (51)	1.82 (2.36)	1.26 (3.80)
July 2004	379 (38)	1.97 (0.89)	2.35 (1.30)	6.59 (3.97)	80 (2)	5.36 (4.08)	1.23 (0.79)
Vegetated sediment							
Spartina-rz, June 2003[1]	393 (35)	3.21 (0.29)	0.72 (0.28)	2.83 (1.13)	65 (56)	1.84 (1.75)	0.99 (2.08)
Salicornia-rz, June 2003[1]	280 (14)	1.07 (0.63)	0.70 (0.42)	1.96 (1.18)	63 (55)	1.24 (1.310	0.73 (1.76)

[1] Data 2003 upper 2-cm sediment, incubations in the light only (Best et al. 2005); [2] rz, root zone; [3] ND, not determined.

Seasonal changes in mercury parameters

Values of mercury parameters were measured in March (wet season) and July (dry season) 2004 only in the vegetated surface sediment of China Camp to determine seasonal influences on the mercury biogeochemical cycle (Table 3-3). There was no significant difference in THg levels with respect to season, but there was a substantial decrease in the standing MeHg pool sizes of both the *S. foliosa* and *S. virginica* root zones in July compared to March. This decrease was due to lower methylation and greater demethylation (Dm) rates. ANOVA of the July data indicated that net MeHg production was significantly less in vegetated than in bare sediments in July 2004 (0.72 versus 4.4 ng MeHg g^{-1}DW d^{-1}), but relative abundance of the SRB *Desulfovibrio* was significantly greater (Table 3-4, Figure 3-5).

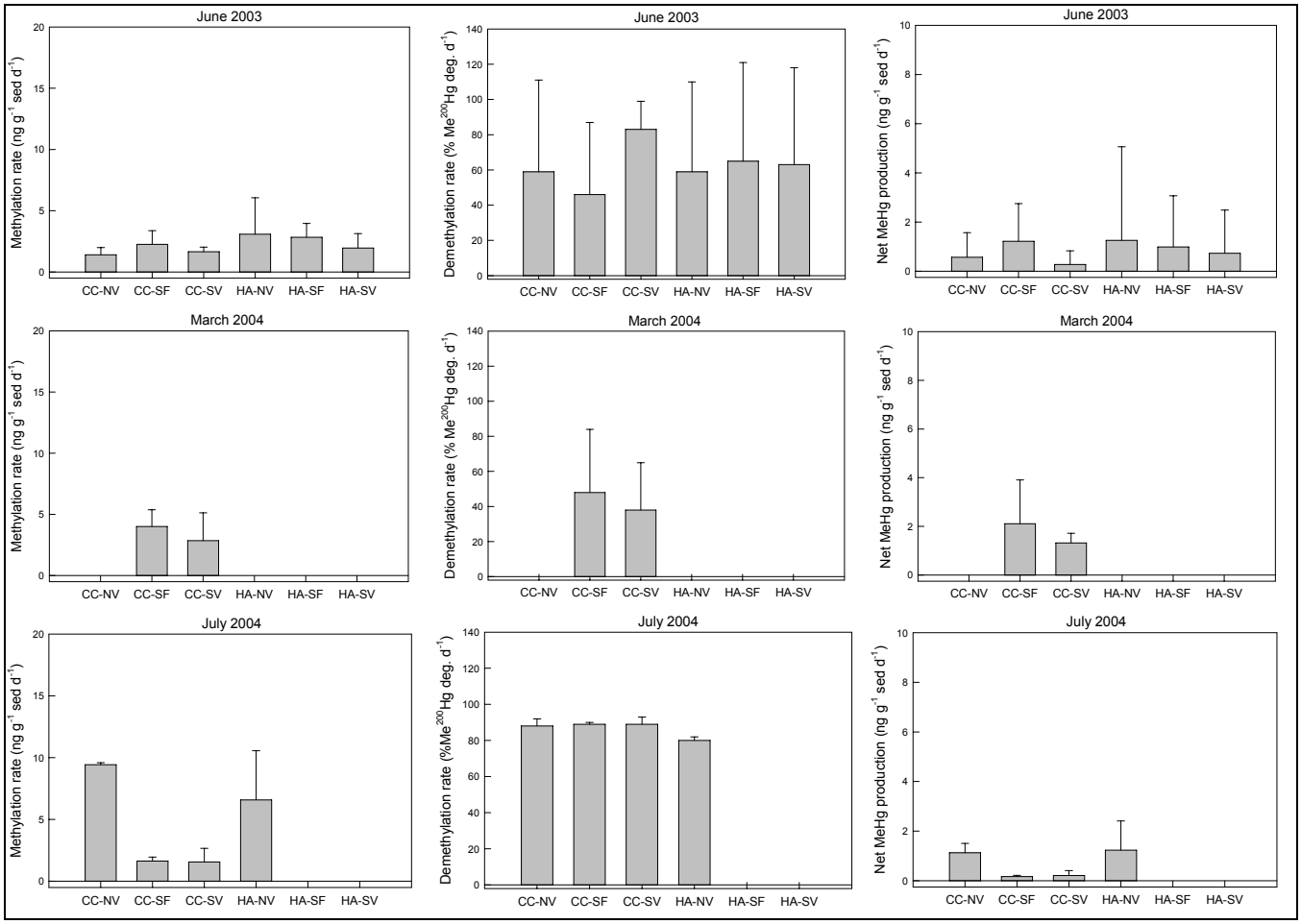

Figure 3-4. Rates of methylation, demethylation, and net methylmercury production in the sediments of existing marshes on San Pablo Bay measured in June 2003, March and July 2004. Mean values and standard deviations (N=3). Abbreviations: CC-NV = China Camp-nonvegetated; CC-SF = China Camp-*S. foliosa* vegetated; CC-SV = China Camp *S. virginica* vegetated; HA-NV = HAAF nonvegetated; HA-SF = HAAF *S. foliosa* vegetated, HA-SV = HAAF *S. virginica* vegetated.

Table 3-4. Relationships between methylation rates, demethylation rates, and microbial communities, and presence of a vegetative cover measured in July 2004 sediment samples, as demonstrated by ANOVA. Significant p-values underlined.

Parameter	Vegetative Cover	Mean	Standard Error	p-Value
Methylation rate (ng g^{-1} DW d^{-1})	+	1.60	1.50	0.002
	-	7.95	0.95	
Demethylation rate (% $Me^{200}Hg$ degraded d^{-1})	+	55.66	4.51	0.048
	-	44.40	2.86	
Total microbial biomass (pmol g^{-1} DW)	+	107,124	18,473	0.865
	-	111,812	20,237	
Desulfobacter biomass (% total microbial biomass)	+	17.59	0.80	0.157
	-	19.30	0.87	
Desulfovibrio biomass (% total microbial biomass)	+	1.56	0.11	0.008
	-	1.11	0.12	

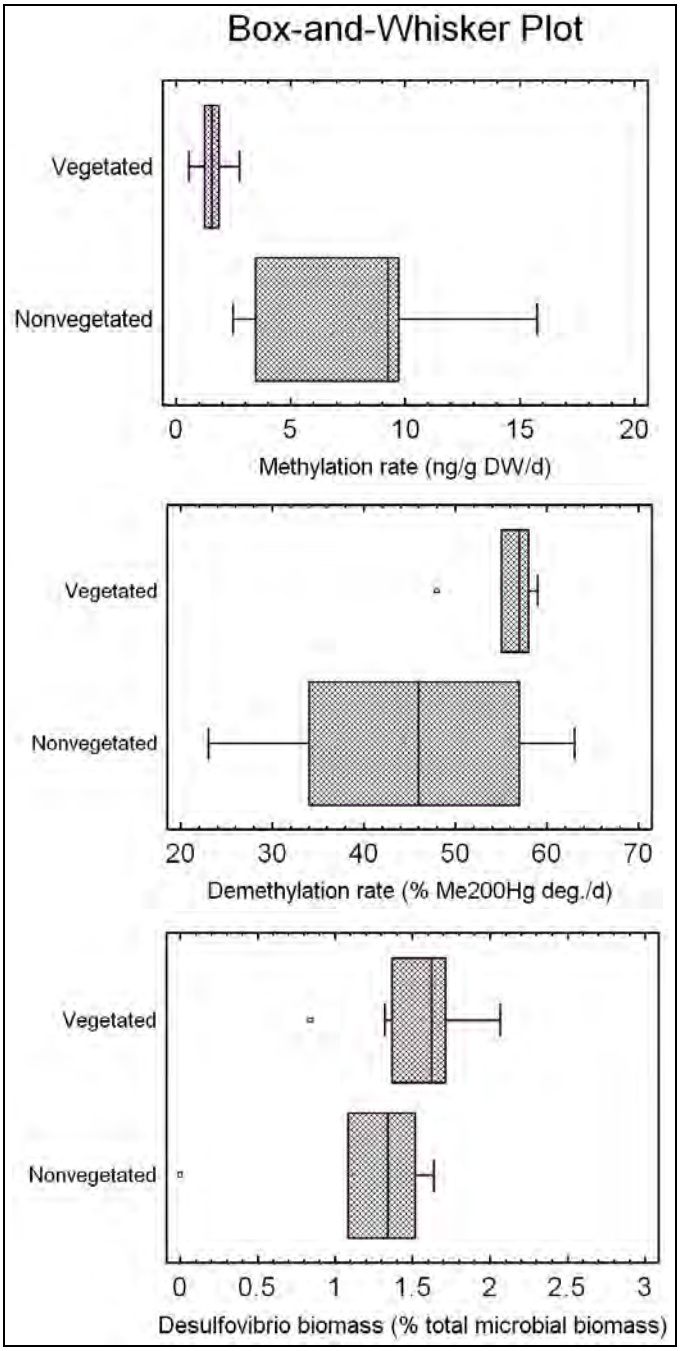

Figure 3-5. Relationships between methylation rates, demethylation rates, and *Desulfovibrio* biomass, and the presence of a vegetative cover in sediments of China Camp, HAAF, Sonoma Fringe Marsh, Sonoma Baylands, and Petaluma River sampled in July 2004 expressed in a box-whisker plot. The box is drawn with ends through the points for the first and third quartile, a horizontal line representing the median, and a vertical line from each end of the box to the smallest and largest values.

Relationships between methylation, demethylation, and sediment redox potential and pH

The relationships between methylation and demethylation rates and factors potentially affecting these in nonvegetated and vegetated sediment were explored using regression analysis. The methylation rate increased exponentially with the redox potential becoming less negative, but the regression model that best fitted the data explained only 24% of the variability in the data set, suggesting a highly variable response (Table 3-5, Figure 3-6). The methylation rate also tended to increase with increasing pH, but the regression models did not provide a significant fit (Table 3-5, Figure 3-6). No further significant relationships between methylation and other factors were found. No significant relationships between the demethylation rates and sediment redox potential and pH were found, but demethylation increased exponentially with total microbial biomass and with relative abundance of *Desulfovibrio* but not with relative abundance of *Desulfobacter* (Table 3-4).

Table 3-5. Relationships between methylation and demethylation rates, redox potential, pH, and microbial biomass in nonvegetated and vegetated July 2004 sediment samples, as demonstrated by regression analysis. Regression equation, significance (p-value) and proportion of variance explained (R^2) by the fitted model indicated. Y is the process rate and X is the sediment characteristic. Significant regression models underlined.

Characteristic	R^2	p-Value	Equation
Methylation rate (ng g^{-1} DW d^{-1})			
E_h (mV)	0.24	<u>0.014</u>	$Y = e^{(3.572 + 0.013X)}$
pH	0.13	0.059	Y = -16.191 + (3.241X)
Total microbial biomass (pmol g^{-1} DW)	0		No fit
Desulfobacter biomass (% total microbial biomass)	0.03	0.224	$Y = e^{(2.688 - 0.063X)}$
Desulfovibrio biomass (% total microbial biomass)	0		No fit
Demethylation rate (% $Me^{200}Hg$ degraded d^{-1})			
E_h (mV)	0.08	0.113	Y = 29.18 – 0.11X
pH	0.08	0.121	Y = 95.75 – 6.99X
Total microbial biomass (pmol g^{-1} DW)	0.25	<u>0.013</u>	$Y = e^{(3.582 + 0.000002X)}$
Desulfobacter biomass (relative abundance)	0.05	0.158	$Y = e^{(4.271 - 0.023X)}$
Desulfovibrio biomass (relative abundance)	0.40	<u>0.001</u>	$Y = e^{(3.407 + 0.332X)}$

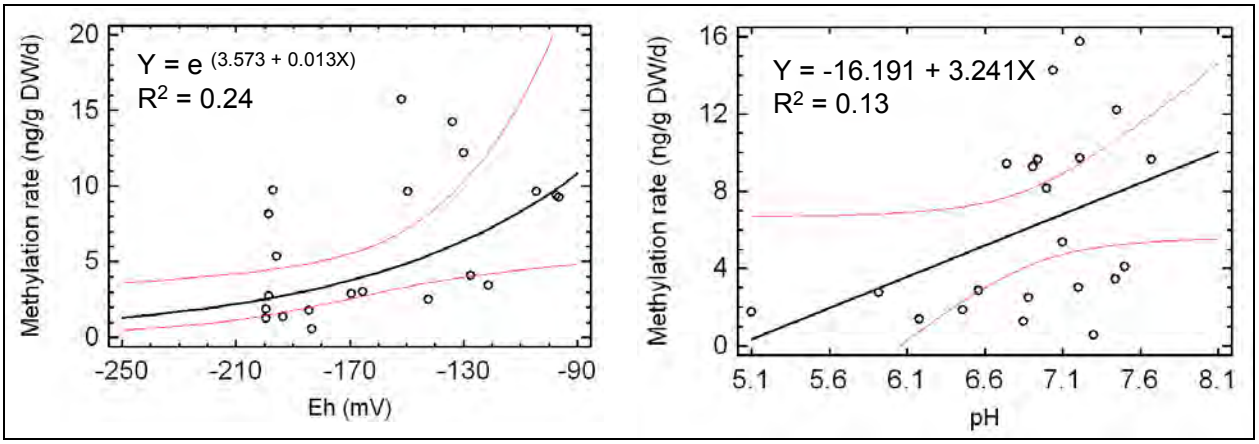

Figure 3-6. Relationships between methylation rates, and redox potential and pH in nonvegetated and vegetated July 2004 sediments of China Camp, HAAF, Sonoma Marsh, Sonoma Baylands, and Petaluma River. Lines represent regression lines and 95% confidence limits. Regression equation and proportion of variance explained (R^2) by the fitted model indicated.

Microbial signatures in sediments and their association with net methylmercury production

Sedimentary microbial community biomass was characterized using PLFAME derived from membrane lipid bilayers. This approach circumvents the gross underestimations (99%) and bias of culture-based microbiological methods and produces good estimates of total microbial community biomass (total pmoles PLFAME g^{-1} DW). It also produces a multivariate PLFAME profile of the microbial community, which can be used to show differences between communities. When a PLFAME or groups of PLFAME can be associated with particular microbial taxa, PLFAME-defined operational taxonomic units can provide information on changes in specific groups of microorganisms. Herein, the relative abundance of the sulfate-reducing genera *Desulfobacter* (+*Desulfobacterium*) was calculated from the concentration of a fatty acid marker (10-methylhexadoate) relative to the total membrane lipid fatty acids in the sample. Analogously, iso-heptadecenoate was used as a biomarker for the genus *Desulfovibrio*.

Geographic distribution of microbial biomass in surface sediments of San Pablo Bay Wetlands

The level of total microbial community biomass in the surface sediment in San Pablo Bay wetlands ranged from 13,657 pmol g^{-1} DW in the nonvegetated sediments in the fringe wetlands at Sonoma Baylands to 194,534 pmol g^{-1} DW in nonvegetated surface sediments at China Camp (Table 3-6). Using the cellular content of PLFAME in a single cell as a benchmark, the range of PLFAME levels is comparable to cell counts of

3.414×10^8 to 4.863×10^9 g^{-1} DW. SRB cell counts ranged from 4×10^3 to 39×10^3 cells g^{-1} DW (Tables 3-6 and 3-7), which is relatively low compared to the SRB range of 2.5×10^2 to 10^6 cells g^{-1} DW estimated earlier in surface sediments of San Francisco marsh soils by Murray and Horne (1979; derived from 10^2 to 10^6 cells g^{-1} WW, using a dry weight:wet weight ratio of 0.40 as commonly found by the authors in China Camp sediment). Although some statistically significant differences were shown in the distribution of total sedimentary microbial community biomass and the relative abundance of the sulfate-reducing genera *Desulfobacter* and *Desulfovibrio*, at this spatial scale there appears to be a generally continuous but patchy microbial distribution. Because *Desulfobacter* and *Desulfobacterium* biomasses were indistinguishable from each other using this biomarker approach, their combined biomass is further referred to as *Desulfobacter* biomass in this chapter.

Table 3-6. Total microbial biomass and relative contributions (in percent) of sulfate reducing microbial strains in the sediments of existing marshes on San Pablo Bay, July 2004. Polar lipid fatty acids methyl ester content (PLFAME) is taken as a measure for total microbial biomass. Mean values and standard deviations (N=8).

Sediment	Microbial Biomass (pmole g^{-1} DW)	*Desulfobacter* (relative abundance)	*Desulfovibrio* (relative abundance)
China Camp	194,534 (8,656) C[1]	18.48 (1.01) A	1.39 (0.13) B
HAAF	79,074 (16,527) AB	18.12 (1.12) A	1.42 (0.01) B
Sonoma Marsh	13,657 (2,482) A	26.60 (2.17) B	0.00 (0.00) A
Sonoma Baylands	120,208 (63,640) BC	17.64 (0.50) A	1.33 (0.16) B
Petaluma River	151,586 (36,600) BC	15.65 (3.82) A	1.42 (0.24) B

[1] ANOVA results of microbial biomass, using site as factor. Mean values followed by the same letter are not statistically different (95% confidence level) according to Fisher's least significant difference procedure.

Table 3-7. Total microbial biomass and relative contributions (in percent) of sulfate reducing microbial strains in the sediment depth profiles affected by *Spartina foliosa* and *Salicornia virginica* at China Camp, March and July 2004. Polar lipid fatty acids methyl ester content (PLFAME) is taken as a measure for total microbial biomass. Mean values and standard deviations (N=3).

Sediment	Microbial Biomass (pmole g^{-1} DW)	*Desulfobacter* (relative abundance)	*Desulfovibrio* (relative abundance)
March 2004			
Spartina root zone sediment			
0-2.5 cm	154,069 (82,717) CD[1]	18.76 (7.12) AB	1.73 (0.47) BC
2.5-5 cm	228,290 (63,245) E	18.16 (5.63) AB	1.42 (0.41) AB
5-10 cm	252,743 (113,118) E	19.65 (2.43) AB	1.29 (0.58) A

Sediment	Microbial Biomass (pmole g-1 DW)	*Desulfobacter* (relative abundance)	*Desulfovibrio* (relative abundance)
Salicornia root zone sediment			
0-2.5 cm	79,156 (25,608) AB	23.83 (1.92) C	2.33 (0.43) D
2.5-5 cm	90,272 (23,495) ABC	20.70 (1.73) ABC	2.09 (0.29) CD
5-10 cm	136,259 (91,913) BCD	21.86 (2.58) BC	1.84 (0.56) BC
July 2004			
Spartina root zone sediment			
0-3 cm	174,713 (82,649) CDE	19.38 (3.44) ABC	1.37 (0.38) AB
3-8 cm	73,031 (28,485) ABC	17.11 (0.38) AB	1.62 (0.04) ABC
8-13 cm	39,990 (14,290) A	16.64 (0.37) A	1.44 (0.15) AB
Salicornia root zone sediment			
0-3 cm	222,848 (32,592) DE	18.50 (1.53) AB	1.48 (0.15) AB
3-8 cm	96,813 (26,515) ABC	17.08 (0.92) AB	1.77 (0.12) ABCD
8-13 cm	35,347 (5,871) A	16.83 (1.74) AB	1.72 (0.29) ABC

[1] ANOVA results of microbial biomass, using site as factor and vegetation cover as covariate. Mean values followed by the same letter are not statistically different (95% confidence level) according to Fisher's least significant difference procedure.

Seasonal changes in sedimentary microbial biomass

Total microbial community biomass was greatest in the deeper parts of both the *S. foliosa* and *S. virginica* root zones (Table 3-7) at the onset of the wetland macrophyte growth season in March. This could be due to the macrophytes pumping oxygen and nutrients to the deeper sediments, the grazing of microorganisms in the upper sediments, and combinations of the two processes. Microbial biomass associated with the *S. foliosa* root zone was generally greater than that of *S. virginica*. In July the distribution of sedimentary microbial biomass had completely changed. The total microbial community biomass was greatest in the top 3 cm and decreased with depth. ANOVA was used to determine the relationships between months, plant cover, sediment depth, total microbial biomass, and the relative abundances of *Desulfobacter* and *Desulfovibrio* (Table 3-7). Depth-averaged microbial biomass in the sediment was greater in March (156,798 pmole PLFAME g^{-1} DW) than in July 2004 (109,255 pmole g^{-1} DW), but the difference between these averages was not statistically significant ($p > 0.05$). The relative abundances of the sulfate-reducing genera *Desulfobacter* and *Desulfovibrio* were significantly greater in March than in July. The relative abundance of *Desulfovibrio* was significantly elevated in the *S. foliosa* and *S. virginica* root zones when compared to bare sediment (Figure 3-4, Table 3-4).

Exploration of relationships between microbial biomass and other sediment characteristics

The data set on microbial biomass collected in July 2004 was most complete with respect to measured sediment characteristics (Table 3-2, and Tables 3-4 through 3-8). This data set and linear and nonlinear regressions were used to explore and mathematically describe the relationships between the major physico-chemical and microbiological variables of surface sediment from San Pablo Bay wetlands. No strong relationship could be derived but the exercise was, nonetheless, informative. Total microbial biomass decreased linearly with depth within the sediment, and increased logarithmically with MeHg concentration, with both models providing significant fits to the measured data (Table 3-9). The contributions of the *Desulfobacter* and *Desulfovibrio* strains to total microbial biomass did not show a specific trend with depth. The relative abundances of *Desulfobacter* and *Desulfovibrio* were significantly related to MeHg concentration in the sediment, with that of *Desulfobacter* decreasing logarithmically but of *Desulfovibrio* increasing logarithmically with

Table 3-8. Redox potential and pH in the sediments of existing marshes on San Pablo Bay, July 2004. Mean values and standard deviations (N=3).

Sediment	E_h (mV)	pH
Nonvegetated sediment		
China Camp, -5 cm	- 99 (4) E1	6.9 (0.1) BC
HAAF, -5 cm	-126 (4) D	7.5 (0.0) D
Sonoma Marsh, -5 cm	-159 (12) C	6.9 (0.3) BC
Sonoma Baylands, -5 cm	-145 (8) CD	7.3 (0.3) CD
Petaluma River, -5 cm	-197 (1) B	7.1 (0.1) BCD
Vegetated sediment		
Spartina root zone sediment		
China Camp, -3 cm	-194 (8) B	6.9 (0.3) BC
China Camp, -8 cm	-209 (21) AB	6.7 (0.1) B
China Camp, -13 cm	-227 (18) A	7.1 (0.1) BCD
Salicornia root zone sediment		
China Camp, -3 cm	-192 (6) B	5.7 (0.5) A
China Camp, -8 cm	-206 (5) AB	6.0 (0.1) A
China Camp, -13 cm	-206 (7) AB	6.9 (0.4) BC

[1] ANOVA results of redox potential and pH, using site as factor and vegetation cover as covariate. Mean values followed by the same letter are not statistically different (95% confidence level) according to Fisher's least significant difference procedure.

Table 3-9. Relationships between microbial biomass and other characteristics in July 2004 sediment samples, as demonstrated by regression analysis. Regression equation, significance (p-value), and proportion of variance explained (R^2) by the fitted model indicated. Y is the microbial biomass and X is the sediment characteristic. Significant regression models underlined. No relationship could be established between microbial biomass and redox potential, pH, and THg concentration.

Characteristic	R^2	p-Value	Equation
Total microbial biomass (pmol g^{-1} DW)			
Depth (cm)	0.32	<0.001	Y = 19714 – (13244 X)
MeHg concentration (ng g^{-1} DW)	0.51	<0.001	Y = 83496 + (79128LnX)
Desulfobacter biomass (relative abundance)			
Depth (cm)	0.05	0.104	Y = 20.29 – (0.29X)
MeHg concentration (ng g^{-1} DW)	0.16	0.039	Y = 20.81 – (2.399LnX)
Desulfovibrio biomass (relative abundance)			
Depth (cm)	0.05	0.111	Y = 1.08 + (0.04X)
MeHg concentration (ng g^{-1} DW)	0.45	<0.001	Y = 0.87 + (0.496LnX)

increasing MeHg concentration (Figure 3-7; Table 3-9). No significant relationship was demonstrated between the total microbial biomass, and relative abundances of *Desulfobacter* and *Desulfovibrio*, respectively, and rates of methylation or demethylation. No relationship or trend was found between microbial biomass, redox potential, pH, and THg concentration (relationships not shown).

Availability of mercury species for uptake by marsh plants

A pilot experiment was conducted in March 2004 to explore THg and MeHg uptake, upward transport and leaching from foliage in marsh plants in the field. A summary of the data is provided here. The ^{199}Hg of the $^{199}HgCl_2$ added to the root zone was rapidly taken up by *S. foliosa,* and ^{199}Hg was translocated to the roots, stems, and leaves. Transpiration of ^{199}Hg to the leaf surface was assayed using a wipe test (Windham et al. 2001) but none was detected within a 72-h incubation period. For a wipe test plants are temporarily covered by a transparent plastic tent supported by four 1.5-m poles inserted into the sediment to shield plants from atmospheric deposition but let sunlight through. At the beginning of the incubation period, three leaves of each plant that were situated above the tide during the incubation period were wiped on both surfaces twice with filter paper (Whatman 1) that had been soaked in deionized water, and leaves were tagged. At the end of the incubation period, the same leaves were wiped again and filter papers were quick-frozen in the field until subsequent processing and mercury species analysis in the laboratory.

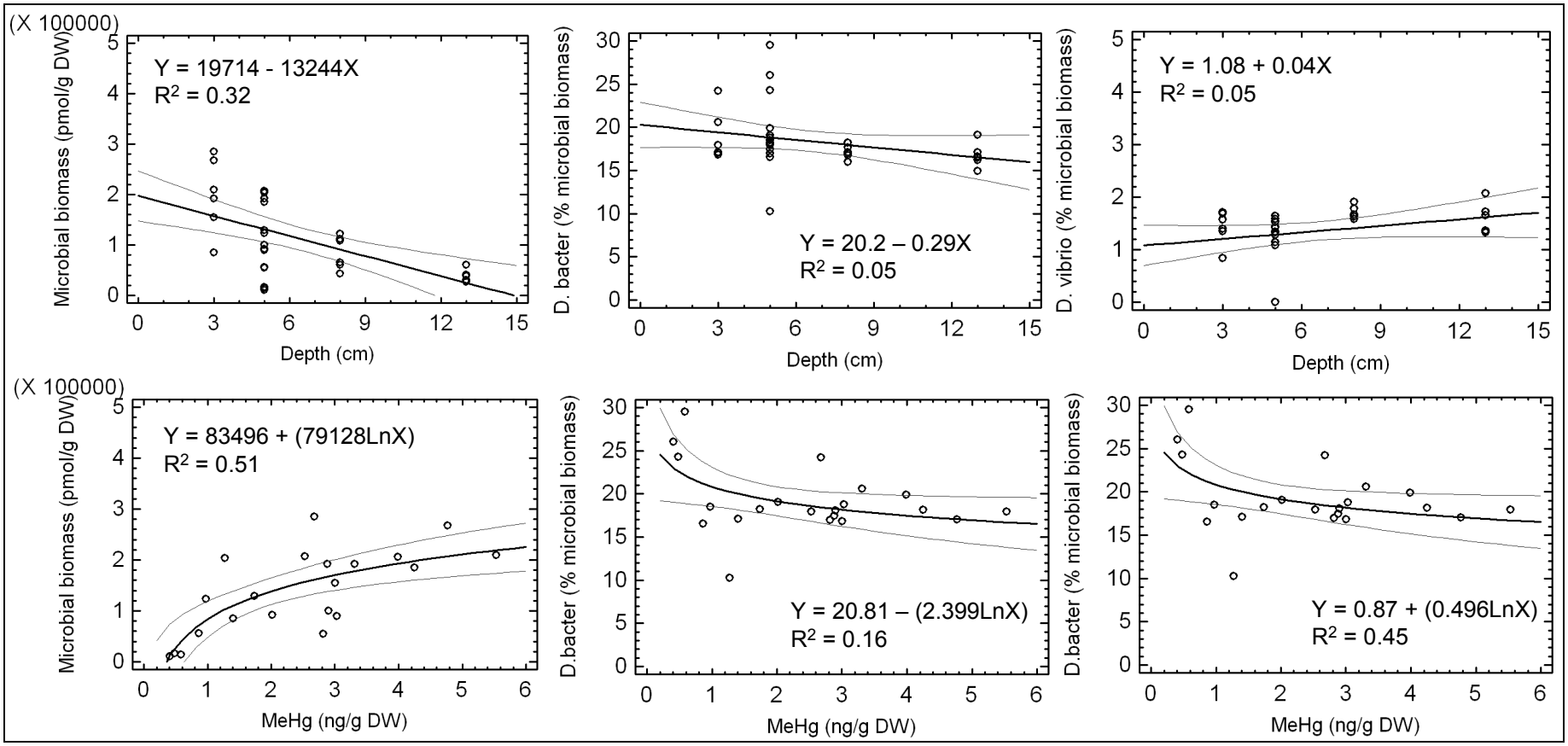

Figure 3-7. Relationships between microbial biomass and other characteristics in nonvegetated and vegetated sediments of China Camp, HAAF, Sonoma Marsh, Sonoma Baylands, and Petaluma River sampled in July 2004. Lines represent regression lines and 95% confidence limits. Regression equation and proportion of variance explained (R^2) by the fitted model indicated. No relationship or trend was found between microbial biomass, and redox potential, pH, and THg concentration.

$^{199}HgCl_2$ was only taken up via the roots and not through other plant tissues. $CH_3{}^{200}HgCl$ added to the root zone of *S. foliosa* was also taken up, rapidly reaching a constant level in the roots that became detectable in stems and leaves after 72 h of incubation. Although the uptake of both $^{199}HgCl_2$ and $CH_3{}^{200}HgCl$ by *S. foliosa* over a 72-h period of field incubation was successfully demonstrated, the absolute levels of mercury uptake were low. The uptake of heavy-labeled mercury species by *S. virginica* in parallel experiments was below detection. Transfer of mercury via both plant species into the base of the marsh-associated food web is significant (see Chapters 6 and 7). Therefore, additional experiments are needed to understand mercury uptake, translocation, and possible transpiration processes.

Discussion

Measuring rates of methylation and demethylation

The mercury stable isotope tracer approach used in the current study provides a method for the simultaneous determination of methylation and demethylation rates in the same volume of sediment which is incubated in-place under field conditions. These experiments were designed to provide data on rates of methylation and demethylation that are directly comparable and subjected to environmental influences that may affect these rates. The use of the specially designed corer minimizes the physical disturbance of sediment core removal and replacement. Sediment incubation times were limited to 5 h to assess instantaneous, net conversion rates and to preclude enclosure effect artifacts. Longer incubation times decreased net Hg conversion rates as described in the “Materials and methods” section. Tracer studies are based on the mixing of negligible levels (below 1% of the standing pool size) of tagged molecules into a known environmental pool size and measuring the rate of conversion of the tagged chemical. Multiplication of the rate of conversion of the tagged molecule by the size of the pool at the time when the tagged molecules are added gives the rate of change for the entire pool. The details of the method actually used in this study are more complex (Hintelmann and Ogrinc 2003) but are based on this principle. Since it is known that MeHg constitutes the relevant mercury species and MeHg can be accurately measured, the experimentally derived demethylation rates are probably good estimates of these rates in nature. Currently, required assumptions introduce uncertainty into the derivation of methylation rates. It is assumed that the added isotopic mercury tracers will behave in the

sediment the way that the relevant mercury species (THg, reactive Hg, bioavailable Hg) behave. However, it is not known what these relevant mercury species are, and they have not been measured in the volumes of sediment tested in this study. In the current case, it is assumed that all measured THg is available for methylation, and this value is used for the required multiplication. This may result in overestimating the natural methylation rate.

In the March samples, both methylation and demethylation rates decreased with incubation period increasing from 5 to 72 h. Although elevated initial rates could be attributed to a lingering effect of disturbance from inserting the core sampler into the sediment increasing activity of the microbial community, low final rates may be attributed to the reassimilation of both mercury isotopes injected into the sediment cores prior to in situ incubation. Secondly, the counter-current process (e.g., demethylation of newly methylated $CH_3{}^{199}HgCl$) will eventually occur and reduce the net amount of $CH_3{}^{199}HgCl$. In the vegetated July samples methylation was relatively low compared to a very effective demethylation process, which may suggest that the $^{199}Hg^{2+}$ amended for methylation was less available than the $CH_3{}^{200}HgCl$ amended for demethylation by microbes. Similar results have been observed in samples from the Florida Everglades, the heavily contaminated Carson River Superfund site, and in another study on San Pablo Bay sediment (Marvin-DiPasquale and Oremland 1998; Marvin-DiPasquale et al. 2003). The methylation and demethylation rates reported in the current study are in the same range as those published rates for open-water sediments and one marsh site in San Pablo Bay (Marvin-DiPasquale et al. 2003) and for open-water sediments in the San Francisco Bay Delta (Marvin-DiPasquale and Agee 2003).

Spatial differences in mercury parameters

Linear relationships between rates of methylation and MeHg were shown for surface sediments of wetlands bordering San Pablo Bay, and these relationships had strong spatial components (Figure 3-2). Points representing rates in nonvegetated sediment from the respective wetlands tended to group, but the arrangement of these points along the regression line did not correspond to salinity or other known physico-chemical gradient. The presence of vegetation decreased rates of both methylation and demethylation (Figures 3-2, 3-4).

In contrast, no relationship, including a spatial component, between the levels of THg and MeHg in the surface sediments of wetlands bordering San Pablo Bay was apparent (Figure 3-2). The lack of this relationship in the data set and in that of larger San Francisco Bay surveys brings into question one of the main assumptions of the proposed mercury Total Maximum Daily Load for the San Francisco Bay basin (http://www.waterboards.ca.gov/sanfranciscobay/TMDL/sfbaymercurytmdl.htm), namely, that lowering the particulate Hg load will necessarily reduce MeHg levels in fish and birds.

Relationships between microbes and rates of methylation and demethylation

Although sulfate-reducing bacteria are widely believed to be the major agents of mercury methylation and a number of different groups of bacteria have been shown to demethylate MeHg, it remains a challenge to demonstrate strong relationships between sedimentary microbial community characteristics and measures of the mercury biogeochemical cycle. In the current study, demethylation increased significantly with total microbial biomass and relative abundance of *Desulfovibrio*, but not with that of *Desulfobacter* (+ *Desulfobacterium*). In contrast, methylation did not increase significantly (statistically) with microbial biomass.

Seasonal changes in methylation and demethylation rates

In 2004 methylation and demethylation rate measurements in the wet (March) and the dry season (July) were made in vegetated sediments of China Camp. Both methylation and demethylation were greater in March than in July in sediment vegetated by *S. foliosa* and *S. virginica*. The resulting net MeHg production was also greater in vegetated China Camp surface sediment during the wet season. Analogous measures of bare sediments were not performed, so no information of seasonal effects on mud flats is currently available.

Factors potentially affecting net methylmercury production

The results of this study suggest that an elevated net MeHg production is caused by elevated methylation rates rather than by small demethylation rates. It was found that methylation was greater, demethylation less, and microbial biomass also less in bare (0-3 cm) than in vegetated sediments. Methylation and demethylation rates increased exponentially with redox

potential becoming less negative. Rates also tended to increase with increasing pH.

Thus, it appears as if methylation in situ is regulated largely by season and by redox potential, provided a certain level of microbial biomass containing SRB besides other microbes is present. The latter prerequisite is indicated by the fact that exceptionally low methylation and demethylation rates were found at the Sonoma Marsh site where microbial biomass was also extremely low. This site was unusual as it was strongly exposed to wave action and close to the outlet of the Petaluma River where erosion may have been substantial. The elevated methylation in the wet season may be caused by (1) a greater bioavailable fraction of THg since most Hg from wet aerial deposition, which is largely bioavailable, enters the system with rain in the wet season (dry deposition is expected to contribute also, but no quantitative data were available at the time that this report was written); and/or (2) a lowering of the otherwise elevated and rate-limiting concentration of SO_4^{2-}, being diluted by rain water. In the growth season, between April and October, methylation increases when redox potential becomes less negative through aeration of the sediment surface by benthic microalgae and by aeration of the rhizosphere during photosynthesis of taller plants. In the same period, part of MeHg and Hg^{2+} were taken up from the sediment by taller plants (this study), with Hg^0 being released by this vegetation into the atmosphere. MeHg previously absorbed by roots is not known to be volatilized. Demethylation in situ is regulated by microbial biomass of which both SRB groups distinguished are important, with greater demethylation occurring with greater microbial biomass. Among the SRB, *Desulfovibrio* has more impact than *Desulfobacter*, despite the fact that the *Desulfovibrio* contribution to total microbial biomass was about 10 times less than that of *Desulfobacter*. Data indicate that pH may affect methylation, in that pH decreases due to the production of organic acids by SRB, with pH 7.3 being optimum for methylation and pH 5.8 for demethylation. Thus, regular oscillations in the contributions of both SRB groups are expected, depending on their sensitivity to pH. Such oscillations have been found in the course of the decomposition process of both *S. foliosa* and *S. virginica* litter types (Chapter 6).

Updating wetland mass balance calculations with recently collected data

A mass balance of mercury for the HAAF wetlands would be useful for two reasons. As stated in our former Technical Report (Best et al. 2005), the environmental risk posed by the potential transport of mercury from

dredged material into the HAAF food web is of immediate concern. In addition, the potential cumulative impact of Hg from dredged sediments and other sources in the context of numerous ongoing and proposed wetland restorations on San Francisco Bay is a concern. The discussion here is meant to stimulate thought and identify critical gaps in knowledge of wetland mercury biogeochemistry with respect to physical/biological processes and trophic transfer of mercury from reconstructed wetlands into San Francisco Bay. The numerical values on these processes have changed because more data have been collected, and several assumptions have been replaced by measured or calculated values.

Methylmercury balance for a hypothetical HAAF wetland revised

Based on the levels of mercury measured in the current study, a projection of the levels and distribution of mercury species in the HAAF marsh, once it is reconstructed, was calculated (Table 3-10). In this projection, it is assumed that the 8.1 million cubic meters of dredged sediment needed to elevate the HAAF site (Phillip Williams and Associates 1998) will contain the same levels of THg and MeHg as currently found in the China Camp reference site surface sediment, and that this will be the primary source of Hg. This assumption is simplistic. If the source of the dredged material is the geological formation to be excavated for the expansion of the Oakland Harbor, the level of Hg in this material will be far lower. Sediment trapped by the HAAF wetland as it develops will originate from North Bay rivers and contain levels of Hg comparable to those currently in North Bay surficial sediment. Amounts and bioavailability for methylation of atmospherically deposited mercury are currently unclear, and depositing dredged material may continue until 2012. These aspects are still being discussed (interview, E. Polson, Eric Polson Engineering, Novato, CA; Landers 2005).

If all required dredged sediment were deposited in 2005, as originally planned, into the target area and the initial wetland construction activities were completed, the total surface of the HAAF wetland would measure approximately 203 ha. The top 0-5 cm of sediment weighs 40.6×10^6 kg (DW), and (based on the above assumption) contains 14.3 kg of THg and 0.107 kg of MeHg (Table 3-10).

The standing crop and amounts of THg and MeHg contained within the macrophytic vegetation were measured partly in 2005. Standing crop values were greater and mercury species contents lower than estimated in

the previous mass balance for a hypothetical HAAF wetland (Best et al. 2005). Standing crop values of live and dead aboveground plant biomass have been measured (Chapter 5, Tables 5-1, 5-2). Belowground standing crop is estimated as equal to aboveground. Maximum standing crops were 37,860 kg DW ha^{-1} for *S. foliosa*, occupying 117 ha in 2015, and 27,320 kg DW ha^{-1} for *S. virginica*, occupying 86 ha in 2015. Standing crops will represent the following mercury species concentrations: for *S. foliosa*, 152.1 µg THg m^{-2} and 3.4 µg MeHg m^{-2} (Chapter 5, Table 5-1), representing 117.9 g THg and 4.0 g MeHg per 115-ha HAAF system in 2015; for *S. virginica*, 79.9 µg THg m^{-2} and 2.2 µg MeHg m^{-2} (Chapter 5, Table 5-2), representing 68.8 g THg and 1.9 g MeHg per 86-ha HAAF system in 2015.

The mass balance of mercury in HAAF during 2055 shown in Table 3-10 assumes little change from the current distributions and levels in sediment and vegetation due to the increase in wetland surface area. This table puts into perspective the mass of THg and MeHg in the surface sediments that is potentially available to the HAAF food web. It shows macrophytic marsh vegetation as a dominant biological presence in the marsh. Contents in macrophytes amount to 1.1% THg and 0.5% MeHg of the contents in surficial sediments. Perhaps most significantly, given the role of macrophyte biomass in wetland trophodynamics, it shows that the sediment/plant exposure route is potentially an important route for Hg to enter the wetland food web.

Table 3-10. Estimated mercury and methylmercury standing stocks of tidal marsh areas in a restored HAAF, based on the assumption that a restored HAAF would turn into a system like the tidal marsh at the China Camp reference site.

Compartment	Area HAAF (ha)	THg (ng g^{-1} DW)	MeHg (ng g^{-1} DW)	Mass (kg DW ha^{-1})	Mass (kg DW)	THg (g)	THg (% system)	MeHg (g)	MeHg (% system)
Year 2005									
Sediment nonveg. (0->5 cm)[1]	203	353	2.64	200,000	40.6×10^6	14,331.8	100.0	107.2	100.0
Spartina vegetation	0	0	0	0	0	0	0	0	0
Salicornia vegetation	0	0	0	0	0	0	0	0	0
Total	203					14,331.8	100.0	107.2	100.0
Year 2015									
Sediment nonveg. (0->5 cm)[1]	203	353	2.64	200,000	40.60×10^6	14,331.8	98.7	107.2	94.8
Spartina	117	Table 5-1	Table 5-1	37,860	4.43×10^6	117.9	0.8	4.0	3.5

Compartment	Area HAAF (ha)	THg (ng g^{-1} DW)	MeHg (ng g^{-1} DW)	Mass (kg DW ha^{-1})	Mass (kg DW)	THg (g)	THg (% system)	MeHg (g)	MeHg (% system)
vegetation									
Salicornia vegetation	86	Table 5-2	Table 5-2	27,320	2.35×10^6	68.8	0.5	1.9	1.7
Total	203					14,518.5	100	113.1	100.0
Year 2055									
Sediment nonveg. (0->5 cm)[1]	203	353	2.64	200,000	40.60×10^6	14,331.8	98.9	107.2	99.5
Spartina vegetation	0	0	0	0	0	0	0	0	0
Salicornia vegetation	203	Table 5-2	Table 5-2	27,320	5.55×10^6	162.3	1.1	4.6	0.5
Total	203					14,494.1	100.0	111.8	100.0

Note: [1], Sediment: The dry mass contained in surficial 0- to 5-cm layer estimated at 20 kg dry sediment m^{-2}. THg and MeHg concentrations: nonvegetated, mean values June-03, July-04 China Camp. [2], Vegetation, data 2005 China Camp, maximum live + dead standing crop (aboveground +belowground; aboveground measured, Chapter 5, Tables 5-1, 5-2; belowground estimated to be equal to aboveground).

Effects of wetland restoration on methylmercury production and export

Predicting HAAF wetland results. After placing the dredged sediment into the HAAF and breaching the dike, suspended sediments from the bay will enter HAAF. HAAF must be engineered to trap sediments if the salt marsh is to become sustainable. During the initial 10 years (2005-2015), the marsh plain will be composed largely by nonvegetated sediment (Phillip Williams and Associates 1998). This sediment will be exposed to regular tides at elevations below mean high water. Sediment at higher elevations will be wetted by higher tides and storms. During this period, a sedimentation rate in the order of 1.8 cm sediment y^{-1} would be expected as measured recently in the nearby Muzzi Marsh at a distance of 15 km from HAAF (Orr et al. 2003). During this initial period, elevations will be primarily vegetated by epipelon that can greatly affect the cycling of Hg and MeHg in and out of the wetland. In studies conducted in 2003, it was found that the methylation:demethylation ratio in epipelon-vegetated sediment was far greater than that of bare or macrophyte-vegetated sediment (Best et al. 2005). An elevated net MeHg production would be expected, and these superior food quality algal mats would probably be associated with efficient MeHg trophic transfer. However, data on the biomass of epipelon per square meter basis and efficiency of trophic transfer are sparse. Thus, it is currently not possible to estimate how large

the epipelon-vegetated part will be. Therefore, these values have not been used in the current projections.

To identify gaps in knowledge required to produce useful estimates of MeHg export from salt marshes, initial estimates of MeHg export from HAAF have been made. Assuming that the entire HAAF will be tidal and nonvegetated, as will be the case initially, and that the tides will export the same amount of MeHg as diffuses from submersed sediment in the San Francisco Bay Delta of 2.2×10^{-6} g MeHg m^{-2} y^{-1} (Choe et al. 2004), a potential net export of 4.47 g MeHg y^{-1} was calculated (Table 3-11). This is a conservative estimate, since storms are expected to increase the amounts of THg and MeHg exported into the SF Bay, when sediment layers deeper

Table 3-11. Estimated potential methylmercury export of tidal marsh areas in a restored HAAF based on the assumption that a restored HAAF would turn into a system like the tidal marsh at China Camp, using values from the current study.

Compartment	Area HAAF (ha)	Total Mass (kg DW)	Methylation Rate[1] (µg/kg DW/d)	Demethylation Rate (µg/kg DW/d)	Net MeHg Production Rate (µg/kg DW/d)	Net MeHg Production Rate (g/system/y)	MeHg Plant Decomp. Rate[3] (g/system/y)	Total MeHg Potential Export to Bay (g/system/y)
Year 2005								
Sediment nonveg. (0->5 cm)[1]	203	40.6x106	7.23	4.56	0.85	12,596	0	
Potential export[2]						4.47	0	4.47
Year 2015								
Sediment nonveg. (0->5 cm)[1]	0	0	7.23	4.56	0.85	0		
Spartina-veg. sed.	117	23.4×10^6	2.01	1.46	1.17	9,993		
Salicornia-veg. sed.	86	17.2×10^6	0.55	1.42	0.60	3,767		
Spartina-vegetation	117	2.34×10^6					0.69	
Salicornia-vegetation	86	1.72×10^6					0.02	
Potential export[2]						4.47	0.71	5.18
Year 2055								
Sediment non veg. (0->5 cm)1	0		7.23	4.56	0.85	0		
Spartina-veg. sed.	0		2.01	1.46	1.17	0		
Salicornia-veg. sed.	203	40.6×10^6	0.55	1.42	0.60	8,891		
Spartina-vegetation	0						0	
Salicornia-vegetation	203	4.06×10^6					0.04	
Potential export[2]						4.47	0.04	4.51

Note: [1], Sediment: The dry mass contained in surficial 0- to 5-cm layer estimated at 20 kg dry sediment m^{-2}. THg and MeHg concentrations: nonvegetated, mean values June-03, July-04 China Camp; veg., mean values June-03, March-July-04. [2], MeHg flux in SF Bay Delta 2.2 x 10^{-6} g m^{-2} y^{-1} (Choe et al. 2004); [3], Release of MeHg during decomposition expected to be equal to uptake measured in 2005-aboveground only (Chapter 5, Tables 5-1, 5-2).

than 5 cm within the sediment are contacted by waves. Moreover, the work described by Choe et al. (2004) primarily pertained to the MeHg flux from fine grain sediment throughout the tidally influenced channels in the San Francisco Bay Delta, not deep inside (vegetated) marshes. Fine grain sediment tends to be much more homogeneous than marsh sediment.

The value of 2.2×10^{-6} g MeHg m^{-2} y^{-1} is obviously a critical value that must be validated with marsh sediment. Moreover, marsh produced MeHg may stay or may leave with the tidal waters. Even if only a small part would leave with the tidal waters, i.e., to the order of 1% per year, a net production of 12.5 kg MeHg per system y^{-1} would provide an input of 0.125 kg MeHg in the bay, based on the mean net MeHg production rates determined in this study.

Unlike most other heavy metals, the global cycle of mercury is dominated by atmospheric transport. Significant quantities are released by volatilization from vegetation, land, and water surfaces (Schroeder and Munthe 1998). These processes occur largely in the light. Volatilization from vegetation would lower bioavailable THg concentrations within the rhizosphere from 0- to 25-cm depths within the sediment. Volatilization from the sediment surface would significantly decrease the THg concentration in the upper centimeters of sediment. Volatilization from the water surface would lower the THg concentration in the surficial water layer. Volatilization has not yet been included in the current mass balances, but estimates are presented below that give an indication of the order of magnitude based on available literature. Volatilization from vegetation was recently measured in the freshwater wetlands in the Everglades and ranged from 17 to 31 ng THg m^{-2} h^{-1} (Lindberg et al. 2002). Assuming a mean volatilization rate of 24 ng THg m^{-2} h^{-1}, a 12-h light day, and a 180-d growth season, annual volatilization above a completely vegetated HAAF system would be $\geq$105.23 g THg y^{-1} (51,840 ng m^{-2} y^{-1}). Volatilization above fresh water was 8 to 15 times less than above vegetation, i.e., 1-2 ng THg m^{-2} h^{-1} (Lindberg et al. 2002). Conservatively assuming a mean volatilization rate of 2 ng THg m^{-2} h^{-1}, a 12-h light day and 365-d year, annual volatilization above a completely inundated HAAF system would be 17.7 g THg y^{-1} (8,724 ng m^{-2} y^{-1}). The estimated volatilization above the vegetation exceeds the range, and above the water close to the lower limit of the range of 6,664 and 24,600 ng THg m^{-2} y^{-1} estimated by Conaway et al. (2003) above San Francisco Bay. Volatilization from anoxic sediments exposed to solar radiation was determined recently in the Tagus estuary by Canario

and Vale (2004) and ranged from 46 to 332 ng THg g^{-1} sediment h^{-1}, depleting not only surficial THg locally, but also significantly decreasing THg concentrations in pore water. The latter process appears to be independent of the degree of sediment contamination, as was inferred from the large proportion (>50%) of THg that escaped from low- to highly contaminated sediments included in the experiments. The estimated volatilization values of 105.23 ng THg m^{-2} above vegetated and 17.7 ng THg m^{-2} above inundated sediment are great when comparing them with the recently measured annual THg deposition of 23,200 ng THg m^{-2} in the San Francisco Bay area (Tsai and Hoenicke 2001), as that would be equivalent to an annual deposition of 47.09 g THg for a HAAF-size system. A completely vegetated HAAF may volatilize about 2.5 times the amount of THg that would be deposited on a HAAF-size surface area. A graphical representation of THg and MeHg mass balances of a hypothetical HAAF-size wetland is provided in Figure 3-8.

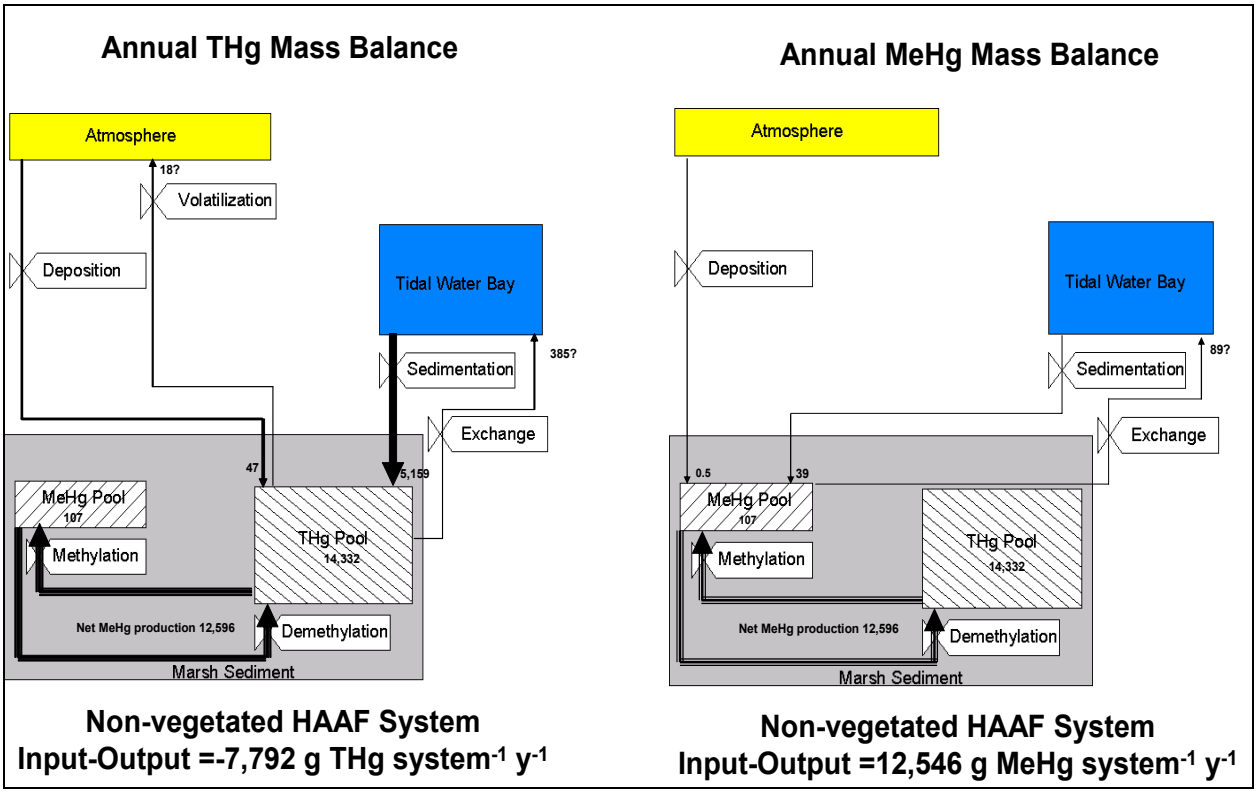

Figure 3-8. Annual mass balances of THg and MeHg calculated for a nonvegetated Hamilton Army Airfield wetland.

Colonization by macrophytic communities of HAAF is predicted to result in a system vegetated largely by *S. foliosa* and partly by *S. virginica* by 2015, and in a *S. virginica*-dominated system by 2055 (Philip Williams and Associates 1998). The vegetation contributes via three different routes to the export of MeHg from the wetland. Daily, the standing biomass will contribute relatively small amounts of THg and MeHg to the export by leaching processes. These amounts are expected to be at least 10% of the internal THg and MeHg concentrations in the aboveground plant material, values commonly published for nutrients. Far greater values for Hg-leaching have been found for another plant species commonly found in salt marshes, *S. alterniflora* (Windham et al. 2001). It is not clear if leached mercury species are available for export or directly re-absorbed by the vegetation upon reaching the sediment. Therefore, they have not been included in the current export estimates. In addition, a large part of plant biomass will senesce. Almost all aboveground *S. foliosa* plant litter will move into the SF Bay during storms in winter and spring, a common characteristic of salt marshes (Odum 1980). Senescence and decomposition of *S. virginica* will be a more gradual but continuous process throughout the year. The contribution of vegetation to the MeHg export from the marsh via fragmentation would amount to 0.71 g MeHg y^{-1} in 2015 and 0.04 g MeHg y^{-1} in 2055 (Table 3-11). These amounts are less than estimated earlier (Best et al. 2005). They include the amounts of aboveground plant material lost by fragmentation with their estimated mercury species contents (see Chapter 5). However, during decomposition the MeHg concentration in the litter increases for periods that depend on the litter quality (see Chapter 6). These transient phenomena may be responsible for great exposures of detritivorous organisms not included in this mass balance calculation. Net MeHg production in vegetated sediment was in the same order of magnitude as in bare sediment, i.e., ranging from 600 to 1,170 ng MeHg kg^{-1} DW d^{-1} versus 850 ng MeHg kg^{-1} DW d^{-1}. If part of this net MeHg production would be exchanged with tidal waters at a greater rate than by diffusion alone (the latter process is only considered in the diffusion values according to Choe et al. 2004), the potential MeHg export would increase significantly. Finally, volatilization of THg from the vegetation is expected, as discussed above.

The current goal of these mass balance estimates is to identify the key processes and values required to make useful estimates of MeHg export and to provide initial estimates for this purpose. **These initial estimates are not intended to be used as quantitative values.** From the

current estimates on MeHg standing stocks and potential export from a restored HAAF wetland, it is obvious that values of net MeHg production in surficial sediments are crucial. Aside from the values provided here, little other data are available. However, one recent study reports values on methylation, demethylation, and net MeHg production rates measured in surficial bay sediment and in one marsh site. These values were obtained using the less sensitive ^{14}C-method (Marvin-DiPasquale et al. 2003). In the study by Marvin-DiPasquale et al., net MeHg production in bare sediment is four times less, and in marsh sediments three to four times greater than in the current study. If the latter values are used, a 1% loss of net production per year of a bare HAAF system would generate a far smaller input of 0.003 kg MeHg, whereas a vegetated system would generate an input of 0.50 kg MeHg in the bay, in the same order of the estimate as the current study (Table 3-12). Reasons for the differences in methylation, demethylation, and net MeHg production rates in the current study and in the Marvin-DiPasquale et al. (2003) study may be the following. The current study uses a more sensitive stable isotope approach than the radioactive isotope approach used by Marvin-DiPasquale et al.

The methylation rates in the current study are above the method detection level, whereas the methylation rates measured by Marvin-DiPasquale et al. (2003) in San Pablo Bay sediments are below detection level. The non-vegetated SF Bay sediment assayed in the current study originates from the China Camp marsh, which is richer in organic matter than the SF Bay sediments assayed by Marvin-DiPasquale et al., possibly causing greater methylation rates. This comparison demonstrates the sensitivity of MeHg export projections in different study approaches.

Since the current study is the only one in which vegetated sediment cores have been incubated in situ and stable isotopes have been used to track methylation and demethylation rates, the generated values are currently unique.

Table 3-12. Estimated potential methylmercury export of tidal marsh areas in a restored HAAF, based on the assumption that a restored HAAF would turn into a system like the tidal marsh at China Camp, using Marvin-DiPasquale et al. (2003) values for methylation and demethylation rates.

Compartment	Area HAAF (ha)	Total Mass (kg DW)	Methylation Rate[1] (µg/kg DW/d)	Demethylation Rate[1] (µg/kg DW/d)	Net MeHg Production Rate (µg/kg DW/d)	Net MeHg Production Rate (g/system/y)	MeHg Plant Decomp. Rate[3] (g/system/y)	Total MeHg Potential Export (g/system/y)
Year 2005								
Sediment nonveg. (0->5 cm)	203	40.6×10^6	0.108	0.087	0.021	311.199	0	
Potential export[2]						4.47	0	4.47
Year 2015								
Sediment nonveg. (0->5 cm)	0	0	0.108	0.087	0.021	0		
Spartina-veg. sed.	117	23.4×10^6	4.824	1.442	3.382	28,886		
Salicornia-veg. sed.	86	17.2×10^6	4.824	1.442	3.382	21,232		
Spartina-vegetation	117	2.34×10^6					0.69	
Salicornia-vegetation	86	1.72×10^6					0.02	
Potential export[2]						4.47	0.71	5.18
Year 2055								
Sediment nonveg. (0->5 cm)	0		0.108	0.087	0.021	0		
Spartina-veg. sed.	0		4.824	1.442	3.382	0		
Salicornia-veg. sed.	203	40.6×10^6	4.824	1.442	3.382	50,118		
Spartina-vegetation	0						0	
Salicornia-vegetation	203	4.06×10^6					0.04	
Potential export[2]						4.47	0.04	4.51

Note: [1], Sediment: The dry mass contained in surficial 0- to 5-cm layer estimated at 20 kg dry sediment m^{-2}. THg and MeHg concentrations: nonvegetated, mean values June-03, July-04 China Camp; veg., mean values June-03, March-July-04. [2], MeHg flux in SF Bay Delta 2.2×10^{-6} g m^{-2} y^{-1} (Choe et al. 2004); [3], Release of MeHg during decomposition expected to be equal to uptake measured in 2005-aboveground only (Chapter 5, Table 5-1, 5-2).

Potential export of methylmercury from restoration of whole target salt marsh area in San Pablo Bay. Large uncertainties in projections of MeHg export from HAAF will be multiplied when calculating total MeHg exports from all salt marshes bordering San Pablo Bay. In spite of these uncertainties, it is still useful to perform these calculations for the purpose of identifying key variables and initial attempts to delimit the solution space. Recommendations for salt marsh restoration in the San Pablo Bay (San Francisco Bay Area Wetlands Ecosystem Goals Project 1999) include the restoration of salt marshes from a total area of 16,200 ha in 2005 to 42,525 ha in the future while keeping an open-water area of 102,870 ha in the SF Bay intact. The net MeHg production rates of

vegetated China Camp sediment determined in the current study are several times greater (600-1,170 versus 21 ng MeHg kg^{-1} DW d^{-1}) and of nonvegetated sediment less (850 versus 1,442 ng MeHg kg^{-1} DW d^{-1}) than those measured by Marvin-DiPasquale et al. in open-water San Pablo Bay sediment. Based on net MeHg production rates determined in this study, one would expect that a 42% increase in surface area of wet estuarine sediment would result in a 42% increase in the production of MeHg in San Pablo Bay (Table 3-13). In this context it is critically important to determine what part of the net MeHg production in bordering salt marshes is exported into San Pablo Bay in a manner that impacts the food web. If one chooses to assume that only 1% of the net MeHg production in the top 0-5 cm of sediment is exported to the SF Bay with out-flowing tides and all of the MeHg produced in the open SF Bay sediments impacts the food web, then 42,525 ha of restored wetland would contribute only 0.29% of San Pablo Bay MeHg (Table 3-13). However, the percentage of net MeHg production leaving the sediment and entering the tidal waters is currently unknown, and it may be greater. This estimate does not include a trophic transfer link and is simplistic. In this context, comprehensive information

Table 3-13. Estimated potential methylmercury production and export from tidal marsh areas in San Pablo Bay. Open water and salt marsh areas according to San Francisco Bay Area Wetlands Ecosystem Goals Project (1999).

Compartment	Area (ha)	Mass (kg DW/ha)	Mass (kg DW)	Net MeHg Production Rate (µg/kg DW/d)	Net MeHg Production Rate (g/system/y)	MeHg Plant Decomposition Rate (g/system/y)	Total MeHg Potential Export (g/system/y)	Export/Bay MeHg Production (%)
Year 2005								
Bay	102,870	200,000	$20,574 \times 10^6$	0.85	6,383,083			
Tidal marsh vegetated sediment[1]	16,200	200,000	$3,240 \times 10^6$	0.60	709,560			
Tidal marsh vegetation[1]	16,200	27,320	443×10^6			3		
Tidal marsh export[1]							358	<0.001
Total Baylands	119,070							
Target for Future								
Bay	102,870	200,000	$20,574 \times 10^6$	0.85	6,383,083			
Tidal marsh vegetated sediment[1]	42,525	200,000	$8,505 \times 10^6$	0.60	1,862,597			
Tidal marsh vegetation[1]	42,525	20,000	850.5×10^6			3		
Tidal marsh export[1]							940	0.002
Total Baylands	145,395							

Note: [1], Based on estimates for HAAF 2055, colonized completely by *S. virginica* (Tables 3-10, 3-11).

on the spatial sedimentary distribution of net MeHg production rates in San Pablo Bay is needed. The impact on the trophic system of 1 mole of MeHg produced in open-water sediment relative to 1 mole produced in a bordering salt marsh must be determined. This impact will require analysis of volatilization of mercury from wetlands and their subhabitats (bare exposed sediment, open water, vegetation zones) because volitalization has been shown to be a major route of export from other wetland systems (Lindberg et al. 2002).

Concluding remarks

1. Despite the fact that coastal wetlands have a considerable potential for MeHg production, the actual amount of MeHg produced within a wetland's sediment is determined by complex, juxtaposed processes, and so is the proportion of MeHg and MeHg produced during in-marsh decomposition processes that leaves the marsh.
2. Results of field studies using a heavy-labeled mercury isotope approach indicated that methylation and demethylation rates are rapid, and that current rates of methylation would double the standing pool size of MeHg within a day if this rate was not counter balanced by demethylation. The current rates of demethylation would deplete the standing MeHg pool size to null within a few days if methylation ceased. This produces a dynamic MeHg pool with respect to time and space. Insights into the size and behavior of those Hg fractions that are amenable to either leave the THg pool by volatilization (reactive Hg), or by microbial conversion (bioavailable, methylation), or by plant uptake (bioavailable, uptake), are urgently needed. MeHg concentrations in SF Bay water are usually low, in the order of 0.044 ng L^{-1} (9 ng THg L^{-1}; median values 2004; SFEI 2004), and MeHg concentrations in surface water do not necessarily reflect MeHg concentrations in pore water (Harmon et al. 2004).
3. Net MeHg production was significantly less in vegetated than in bare sediments in July 2004 (0.72 versus 4.4 ng MeHg g^{-1}DW d^{-1}), but relative abundance of the SRB *Desulfovibrio* was significantly greater in vegetated sediments. A significant relationship between microbial biomass and relative abundances of the SRB genera *Desulfobacter (+Desulfobacterium)* and *Desulfovibrio* and MeHg pool size was found, but no significant relationships between THg and other sediment characteristics were demonstrated.
4. Intuitively, it appears that during the wet season, most MeHg produced stays within the less porous sediment, while during the dry season most MeHg produced would leave the more porous sediment and either

volatilize or enter the tidal waters. The latter case is supported by a recent observation from the current study. Water from the incoming tide reaching the China Camp wetland in March 2004 contained far greater concentrations than usually measured in bulk water from the bay, i.e., 1.10 ng MeHg L^{-1} (463 ng THg L^{-1}; Chapter 6), possibly due to colloidal complexes with MeHg and THg (Choe et al. 2003a, 2003b).

5. Whatever the reason, animals and plants in the marsh and in the adjacent bay are exposed to the greater concentrations via characteristic pathways, and several fish species have significantly enhanced Hg levels that exceed the threshold for human health concern (SFEI 2005a, data 2000; Grenier et al. 2007). Data presented in Chapter 7 of this report indicate that fish can even be less impacted than birds. It is, therefore, important to quantify if and how food webs in the marsh itself and in the adjacent bay are impacted, and to design and manage wetlands targeted to minimize net MeHg production. New insights within the current project are gained into the influence of marsh plants in fueling food chains and serving as vectors for mercury species (Chapters 5 and 6), mercury food web dynamics (Chapter 7), and methods to help monitor the bioavailability of mercury species (Chapters 4 and 8), while the recently developed screening-level model QnD:HAAF serves for data integration and explores management scenarios (Best et al. 2005).

POINT OF CONTACT CHAPTER 3:

Dr. Elly P. H. Best
U.S. Army Engineer Research and Development Center
Environmental Laboratory, Vicksburg, MS
Ph: 601-634-4246; E-mail: elly.p.best@erdc.usace.army.mil

4 Diffusive Gradient in Thin Film Sentinels for Monitoring Methylmercury Production in Tidal Wetlands on San Pablo Bay

Introduction

Monitoring ongoing restoration efforts with sentinels that would serve as leading edge indicators of potential impacts of monomethylmercury (MeHg) on threatened and endangered species and the SF Bay fishery would provide feedback to environmental regulators and enable them to adaptively manage the progress in wetland restoration. Direct analysis of THg and MeHg in water, sediment, and biota samples using established standard methods has indicated complex relationships that are not fully understood. THg levels in sediments are consistently in the order of 300 ng g^{-1} DW (Best et al. 2005; this report) and do not reflect the levels of MeHg in adjacent biota. Such measurements will typically only yield concentrations of total or total dissolved mercury species. Ideally though, those mercury species that are available to organisms should be measured. Uptake of trace metals across living membranes is determined by the total concentration of labile species able to cross biological membranes as the first step of biomagnification. Standing pool sizes of MeHg reflect the differences between rapid and competing methylation and demethylation reactions and are extremely variable in both space and time. Levels of MeHg in punctual samples are so variable that a large number of samples will have to be analyzed to obtain representative estimates of MeHg levels.

Sorption devices have been used to monitor levels of other contaminants. Solid phase extraction materials have been developed and used to monitor exposure of fish (Brenner et al. 2004) and benthic fauna (Kraaij et al. 2001) to hydrophobic organic contaminants (Fredrickson et al. 2004). Hydrophobic organic contaminants (petroleum hydrocarbons, polynuclear aromatic hydrocarbons, and polychlorinated biphenyls) dissolved in the water column and sediment pore water partition to hydrophobic solid phase materials that act as instantaneous and infinite sinks. DGT devices are currently being developed as comparable sentinels for metals.

Biogeochemical processes in sediment play an important role in the geochemistry of mercury, as sulfate reduction in sediment is thought to be the

principal mechanism in the conversion of dissolved mercury to MeHg, a toxin and bioaccumulated form of mercury. For many decades, geochemists have studied the chemistry of pore water to attempt to understand biogeochemical processes occurring in sediments (Berner 1971, 1980). The enrichment or depletion of various chemical species in pore water can indicate the nature of ongoing biogeochemical processes in the sediment, processes that are not readily apparent from studies of the solid phase geochemistry. Pore water chemical data also provide the basis for quantitative estimates of the rates of biogeochemical processes occurring in the sediment (Berner 1980).

Most bacteria in marine sediment meet their need for energy by decomposing organic matter, a process that in turn drives many other sedimentary geochemical processes. To obtain energy in this way, bacteria chemically oxidize the organic matter (commonly written as CH_2O)

$$CH_2O + \text{Oxidant} \rightarrow CO_2 + \text{Reductant} + H_2O \qquad (4\text{-}1)$$

This reaction yields carbon dioxide, water, and the conversion of the oxidant to a reduced form (reductant). Depending on the oxidant available, decomposition yields different amounts of energy for microbial growth and metabolism. The effects of utilizing different oxidants can be seen more clearly by dividing reaction (Equation 4-1) into distinct oxidation and reduction steps. In the oxidation step, bacteria remove electrons shared by the carbon atoms in organic compounds, as written here for the decomposition of a generic unit of organic matter:

$$CH_2O + H_2O \rightarrow CO_2 + 4H^+ + 4e^- \qquad (4\text{-}2)$$

The electrons produced by this process cannot be released to solution but must be transferred to an available electron-poor molecule, termed the oxidant or electron acceptor. In marine sediments, the most important electron acceptors are oxygen (O_2), manganese oxide ($MnO_{2(s)}$), iron oxides ($Fe(OH)_{3(s)}$), and sulfate (SO_4^{2-}), which undergo the following reactions when supplied with electrons:

$$\begin{array}{ll} \text{Aerobic respiration} & O_2 + 4H^+ + 4e^- \rightarrow 2H_2O \\ \text{Manganese reduction} & MnO_{2(s)} + 4H^+ + 2e^- \rightarrow Mn^{2+} + 2H_2O \\ \text{Iron reduction} & Fe(OH)_{3(s)} + 3H^+ + e^- \rightarrow Fe^{2+} + 3H_2O \\ \text{Sulfate reduction} & SO_4^{2-} + 10H^+ + 8e^- \rightarrow H_2S + 4H_2O \end{array} \quad (4\text{-}3)$$

These reduction reactions are listed in order of decreasing energy yield when coupled with the oxidation of organic matter. Oxygen, which yields the most energy by a large margin, is always consumed first and is generally not measurable below the first few millimeters to centimeters of muddy sediments. At greater depth in the sediments, Mn-oxides, Fe-oxides and then sulfate are utilized as oxidants, resulting in vertical segregation (with some blurring of boundaries) of these processes. Note that reactions in Equation 4-3 are greatly simplified since multiple steps, different minerals, and many different bacterial species may be involved. Reactions between the various end-products of microbial processes also occur. For purposes of this study, one of the most important reactions is the precipitation of iron sulfide ($FeS_{(s)}$):

$$Fe^{2+} + H_2S \longleftrightarrow 2H^+ + FeS_{(s)} \quad (4\text{-}4)$$

This reaction occurs in zones of sulfate reduction when sufficient Fe^{2+} is available, as is generally the case in this study.

Variations in these microbial processes influence sedimentary Hg methylation in several ways. One of the most important processes is the alteration of Hg solubility and bioavailability in environments where SRB produce hydrogen sulfide (H_2S) (Benoit et al. 1999). Also important are the associated changes in microbial community composition and consequent biochemical capability to methylate Hg. In particular, SRB are thought to be the principal methylating bacteria in the environment. Both of these considerations highlight the central role of SRB in methylation and suggest the possibility of modeling Hg methylation as a function of sulfate reduction, a process that can be modeled without reference to specific SRB.

Moreover, MeHg concentrations are often greater in pore water than in the overlying water; where a vertical concentration gradient of MeHg in pore water and in the overlying water is established which can physically drive the release of MeHg from the sediment to the bay water (this study). It is, therefore, important to measure the concentration gradient of MeHg in sediment pore water to determine the diffusive flux of MeHg from the sediment.

However, pore water sampling is still a challenge. Conventional techniques typically start with sediment coring followed by pore water separation by centrifugation, squeezing, or dialysis. Such techniques face major problems including contamination, artifacts in the sampling procedure, and sampling of a limited volume of pore water. To overcome these limitations, the new gel techniques (DGT and Diffusional Equilibration in Thin Film (DET)) developed here will be applied in sediments to sample key species to examine the biogeochemistry of mercury methylation in San Francisco Bay sediments and to characterize the diffusive flux of MeHg from the sediment.

DGT-based measurement methods have been developed by Davison and Zhang (1994). The DGT device is comprised of an ion-exchange resin immobilized in a gel (resin gel), which is separated from the test solution by an ion-permeable gel (diffusive gel). Concentration gradients develop across the diffusive gel and the contaminants are transported to the resin gel where they are fixed (in the case of MeHg by an ion-exchange reaction) and accumulate during the deployment time. The DGT approach has several advantages over other techniques proposed for measuring trace metals in natural waters:

1. The device can be mass produced and is easy to use.
2. It can provide information about the actual MeHg species present in the water by varying the thickness and pore size of the diffusion gel layer.
3. It concentrates MeHg in situ.
4. It yields time-averaged concentrations over the length of the deployment period.
5. The analysis of the devices can be optimized for high-throughput analyses.

DGT devices accumulate only certain forms of metal, i.e., mainly the labile metal species able to pass through the diffusion layer and able to be bound by the resin layer. After the DGT device is removed from the sampling site,

the mass of metal in the resin layer is determined analytically. The well-defined geometry of the DGT device enables quantitative interpretation of the mass accumulated, either in terms of dissolved concentrations, or remobilization fluxes from sediments to pore waters. In waters that are reasonably well mixed, the interpretation of DGT-measured fluxes as labile metal concentrations in solution external to the DGT device is relatively straightforward (Zhang and Davison 1995). In sediments and saturated soils, interpretations are more complicated due to the interaction of metal in solution with metal associated with the solid phase. Simple interpretations can provide estimates of a time-averaged remobilization flux from solid phase to solution and estimates of pore water concentrations (Zhang et al. 1995). A numerical modeling approach (Harper et al. 1998) is used to provide a more quantitative interpretation in terms of the rate of supply from sediment to solution (i.e., the exchangeable MeHg associated with sediment particles). It enables the determination of the characteristic sorption-desorption reactions, together with information on the size of the exchangeable fraction associated with the solid phase.

Objectives

This study has the following objectives:

1. Development of a DGT technique to measure MeHg in water (chemical calibration)
2. Exploration of the use of DGT to characterize key geochemical parameters in sediment
3. Testing the ability of the DGT technique to mimic the exposure to MeHg by common filter-feeding clams (*Macoma baltica*) and fish, and application of the device as a sentinel for monitoring MeHg in San Pablo Bay area (biological calibration).

The results pertaining to the first and second objectives are presented in this chapter. The results of bioaccumulation testing and application of the DGT technique in the field will be reported in a subsequent report.

DGT background

DGT employs a binding agent that accumulates solutes quantitatively after their passage through a well-defined diffusion layer (Zhang and Davison 1995). A polyacrylamide gel and a membrane filter (for protecting the gel) considered as an extension of the gel (Davison and Zhang 1994), of known

thickness Δd, are commonly used as the diffusive layer, whereas for trace metals a resin, incorporated into a second gel layer, serves as a binding agent (Figure 4-1). The two gels are enclosed in a small plastic device of approximately 3-cm diameter that is immersed in the solution (Figure 4-2). For a fixed time (t) of deployment, knowing the surface area (A) of the diffusive layer in contact with the solution or the sediment and measuring the mass of accumulated metals (M) in the resin layer associated, the flux (F) of metals from solution to the DGT probe can be calculated (Equation 4-5).

$$F = \frac{M}{At} \tag{4-5}$$

According to Fick's first law of diffusion, this flux can also be interpreted as the mean concentration (C_i) at the surface of the probe

$$F = D\frac{\left(C_i - C\right)}{\Delta d} \tag{4-6}$$

If the metal ions bind rapidly and efficiently to the resin, C is effectively equal to zero provided that the resin is not saturated. Therefore, Equation 4-6 can be simplified to

$$F = D\frac{C_i}{\Delta d} \tag{4-7}$$

The accumulated amount of metal by DGT is, therefore, equal to

$$M = D\frac{C_i At}{\Delta g} \tag{4-8}$$

C_i can be calculated from the mass of metal accumulated by the DGT resin, as long as gel thickness, exposure time, and diffusion coefficient of the analyte are known:

$$C_i = \frac{M\Delta d}{DAt} \tag{4-9}$$

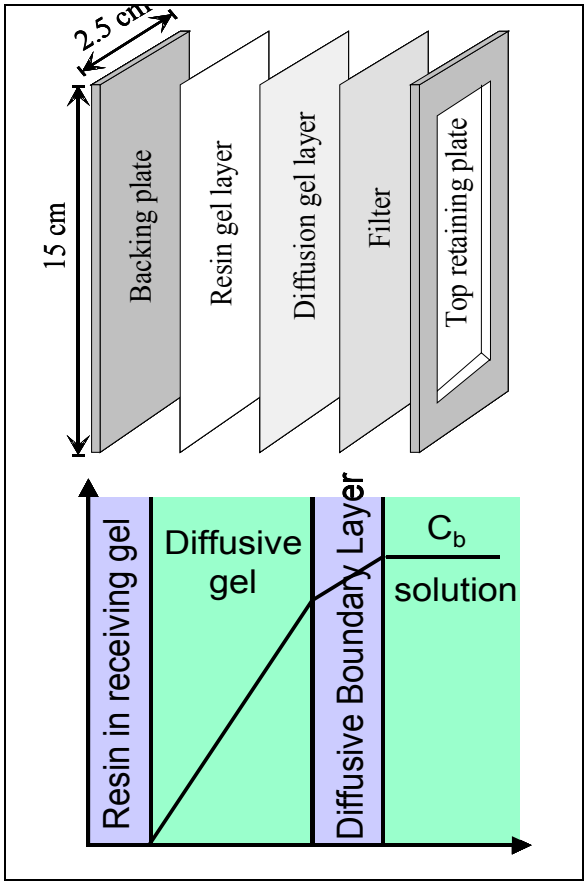

Figure 4-1. Principles of DGT assembly and illustration of diffusion processes in the gel.

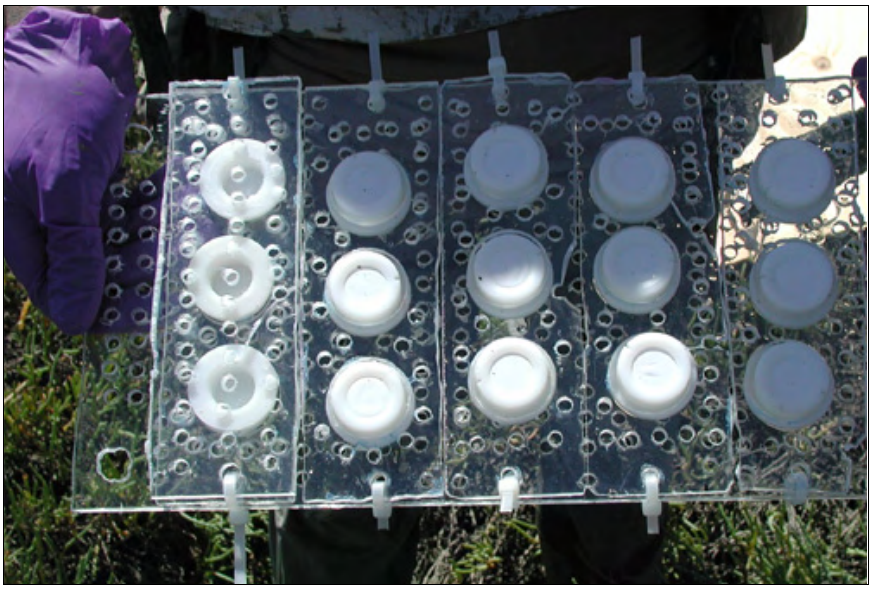

Figure 4-2. Perspex strips with DGTs are inserted vertically in the sediment, exposing the gels to mercury species at two depths within the sediment and to the above-standing water column.

Development of a DGT technique to measure methylmercury in water - chemical calibration

Conventionally used chelex resins are not effective to concentrate MeHg on DGT devices. Instead, a novel mercaptopropyl functionalized resin was developed for monitoring in the field. The new resin was initially characterized, optimized, and calibrated. To test the validity of DGT measurements for MeHg monitoring, a series of standard tests as recommended by Zhang and Davison (1995) were conducted using a MeHg standard solution (5,000 ng L^{-1}, prepared in 0.1 mol L^{-1} NaCl).

Methylmercury accumulation as function of deployment time

The DGT units were assembled with resin and diffusive gels, then covered by a membrane filter. The device was submerged in the stirred MeHg solution for different periods of time (6, 8, 24, and 32 h) and the concentration of MeHg in the test solution was monitored. At each sampling interval, three DGT units were removed from the solution, the resin gels were extracted, and the mass of MeHg determined (Figure 4-3). In accordance with DGT theory, the mass of MeHg accumulated by DGT is proportional to the deployment time.

Methylmercury accumulation as function of the diffusion layer thickness

To confirm that the DGT devices sample MeHg in agreement with Fick's first law (i.e., the accumulated mass of MeHg in the resin is inversely proportional to the thickness of the diffusive gel) five different polyacrylamide diffusive gels were evaluated (thickness Δd = 0.53, 0.93, 1.33, 1.73, 2.13 mm). The DGT units were deployed for 16 h in a stirred MeHg solution. After 16 h of exposure, DGT units were removed, resin gels were extracted, and the mass of MeHg was measured (Figure 4-4).

The amount of MeHg by DGT was proportional to the reciprocal thickness of the diffusive layer and confirmed the DGT theory (Equation 4-9). Binding of MeHg by the DGT unit is controlled by the geometry of the DGT unit (thickness of the diffusive layer and area of the DGT unit), the time deployment, and the concentration of MeHg in solution.

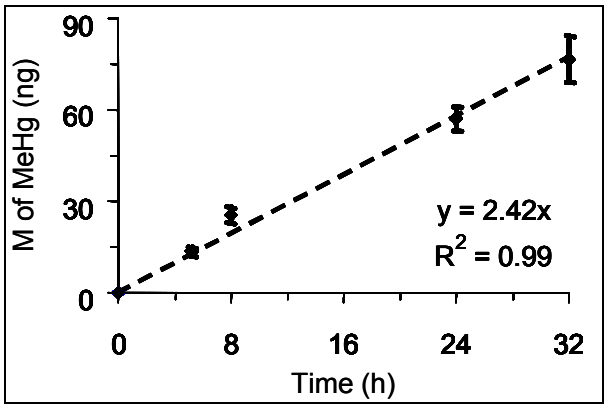

Figure 4-3. Mass of MeHg accumulated by the DGT unit over time. Mean values and standard deviations (N=3). pH = 6; [NaCl] = 0.1 M; V = 1 L; T = 20 °C; Δd = 0.093 cm.

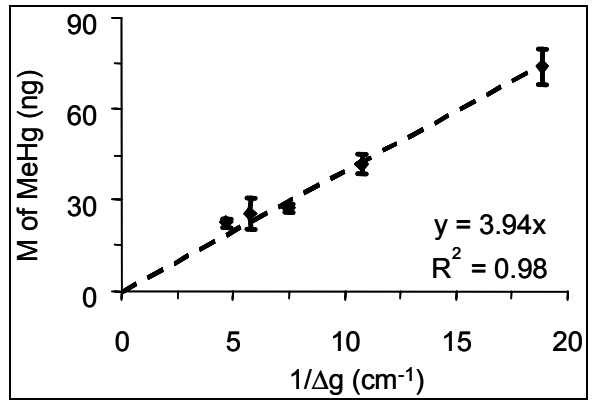

Figure 4-4. Mass of MeHg accumulated by the DGT unit as function of the thickness of the diffusive layer. Mean values and standard deviations (N=3). pH = 6; [NaCl] = 0.1 M; V = 1 L; T = 18 °C; t = 16 h.

Diffusion coefficient determination

It is possible to deduce the diffusive coefficient of MeHg in the polyacrylamide gel from the two previous experiments: the coefficient is provided by the slope of the relationship between the amount of MeHg accumulated by the DGT unit and the thickness of the diffusive layer or the deployment time (Equation 9).

Both experiments provide a similar diffusion coefficient for MeHg in the polyacrylamide gel, which is close to its theoretical value in seawater. Previous studies using the DGT technique generally showed a good agreement between diffusion coefficients of metals in water and in polyacrylamide gels (Zhang and Davison 1999).

The concentration of MeHg in an aqueous solution can be calculated from the measured mass of MeHg accumulated by the resin if the diffusion coefficient is known and a temperature correction is applied (Table 4-1).

Table 4-1. Comparison of MeHg diffusion coefficients obtained by different methods. Mean values and standard deviations (N=4).

Method	Media	T (°C)	D (*10^{-6} cm^2 s^{-1})
Deployment time experiment	polyacrylamide gel	20	5.1 ± 0.3
Diffusive layer thickness experiment	polyacrylamide gel	18	4.7 ± 0.3
Bothner et al. 1980; Gobeil and Cossa 1993; Mason et al. 1993	seawater	20	5.0

Effect of dissolved organic matter on methylmercury diffusion in DGT

To investigate the influence of dissolved organic matter (DOM) on MeHg accumulation 12 DGT units were deployed in a standard solution of MeHg and humic acids. Humic acids were added in excess to bind all of the MeHg in solution.

For each experiment, the apparent diffusive coefficient was deduced from the slope of the experimental trend line.

$$\text{slope} = D_{\text{apparent}} * [\text{MeHg}] * A / \Delta d$$

In both experiments, the apparent diffusive coefficient is equal to 1.25×10^{-6} cm^2 s^{-1}, which is approximately 75% lower than the coefficient obtained from diffusion of MeHgCl (Figure 4-5). The slower diffusion suggests that the excess humic substance completely complexed the MeHg, resulting in larger MeHg-"molecules" diffusing into the gel. Consequently, the presence of DOM affects the DGT technique by slowing down the diffusion of MeHg through the diffusive gel. MeHg accumulated by the resin is lower and dissolved concentrations of MeHg are potentially underestimated. On the other hand, the MeHg measured by the DGT technique may very well represent the labile MeHg concentration that is available to biota.

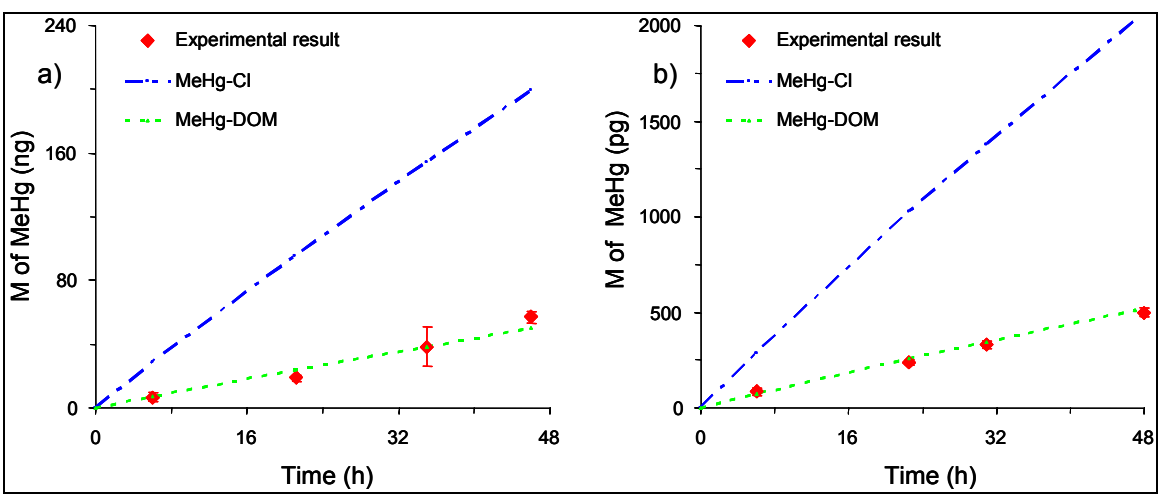

Figure 4-5. MeHg uptake by DGT in the presence of humic acid: a) DOM = 38.7 mg C L^{-1} ([HA] = 100 mg L^{-1}), [MeHg] = 3.3 µg L^{-1}, [NaCl] = 1 g L^{-1}, Δd = 0.043 cm; b) DOM = 37.3 mg C L^{-1} ([HA] = 100 mg L^{-1}), [MeHg] = 70 ng L^{-1}, [NaCl] = 1 g L^{-1}, Δd = 0.093 cm. Mean values and standard deviations (N=3).

Field validation experiment

In July 2004, four DGT units were deployed close to the sediment-water interface in a tidal creek of the China Camp salt marsh. Two DGT units were exposed for 32 h and two units for 56 h. After retrieval from the field, the DGT units were rinsed with distilled water and kept in clean polyethylene bags for transport to the laboratory. In the laboratory, resin gels were extracted using thiourea/HCl solution (0.005% in 0.1 M HCl) and analyzed for MeHg. Water from the creek was sampled at the beginning and the end of the experiment. Seawater samples of 150 mL were collected, acidified with 100 µL of concentrated HCl (aq) and stored under refrigeration until analysis.

Although the direct measurement resulted in a greater mean value of MeHg, it also exhibited a larger uncertainty and was statistically not different from the DGT derived values (Table 4-2). Considering that the DGT technique distinguishes between species both kinetically (according to their lability) and by size (they have to pass through the diffusive gel layer), MeHg concentrations determined by the DGT technique and by direct measurement of the seawater are in good agreement.

Table 4-2. Comparison of MeHg measurements by conventional and DGT techniques. Samples were taken in a tidal creek of the China Camp salt marsh (N=2); water samples were collected at the beginning and at the end of the DGT deployment.

Method	MeHg (ng L^{-1})	
	Replicate 1	Replicate 2
Creek water; grab sample	0.345 (t = 0);	0.271 (t = 56 h)
DGT 32 h	0.244	0.265
DGT 56 h	0.254	0.278

Exploration of the use of DGT to characterize key geochemical parameters in sediment

The parameters for MeHg and sulfide in sediment were investigated using the DGT technique. Other techniques were also employed, i.e., the DET for the determination of iron, manganese, and anions, and pore water centrifugation of core sections for the determination of MeHg, sulfide, iron, manganese, and anions. Two sites were selected to test the ability of the DGT technique to explore the pore water geochemistry in San Pablo Bay. Sites were chosen to represent different salinities in the SF Bay region. The

China Camp State Park site (R44; 38° 04.379′ N, 122° 28.758′ W) has been selected as a site with a greater salinity and the mouth of the Petaluma River as a site with less salinity.

Methods

DGT-methylmercury

DGT-probes for sampling Hg species in pore water of marine sediment have been previously deployed for the measurement of Hg^{2+} (Divis et al. 2005). DGT-probes for accumulating MeHg were constructed with standard filter membranes (cellulose nitrate), diffusive gels (Δd = 0.013 and 0.08 cm) and a binding resin consisting of mercapto-propyl functionalized silica gel embedded in a 0.05-cm thick polyacrylamide gel. The probe was deployed after de-aeration and retrieved in the standard manner for DGT-sediment probes (see Figure 4-2), just as the sulfide probe. The diffusive gel was removed from the binding resin, which was cut into 1-cm sections and placed in clean glass vials. The resin sections were preserved by refrigeration. In the laboratory, the resins were leached using a thiourea/HCl solution (0.005% in 0.1 M HCl) and analyzed by inductively coupled plasma/mass spectrometry (ICP/MS). Pore water MeHg concentrations were computed using the recorded incubation times of 24-49 h. Calculated concentrations correspond to the interval from 5 mm above to 5 mm below the indicated nominal depth in the cores.

DGT-sulfide (S^{2-})

Sulfide in sediment pore water was determined by deploying an AgI sensor strip in a DGT probe. After deploying the strip for a predetermined duration and retrieval from the sediment, the sensor strip was optically scanned and the color density measured using commercially available software (Scion Image for Windows, Scioncorp; Teasdale et al. 1999). From a previously determined calibration curve, the amount of accumulated sulfide is calculated. Dissolved sulfide concentrations are obtained from known diffusion rates in the diffusive gel layer of the sediment probe. Depending on the scan definition, a resolution of approximately 300 μm^2 is achievable and a 2-dimensional cross section of sulfide levels is generated. To obtain a simpler vertical profile and to minimize effect of pore water heterogeneity at the sub-millimeter scale, results were integrated horizontally and vertically over 1-cm sections. Reported sulfide values thus correspond to an average over the 1.75-cm width of the probe. With the selected

geometry of the DGT device (Δd = 0.093 cm), the limit of detection (LOD) of the densitometric procedure for a 24-h deployment is 0.13 µmol L^{-1} or 4.73 µg L^{-1}, and the maximum concentration measurable is 60 µmol L^{-1} or 1,926 µg L^{-1} (Figure 4-6).

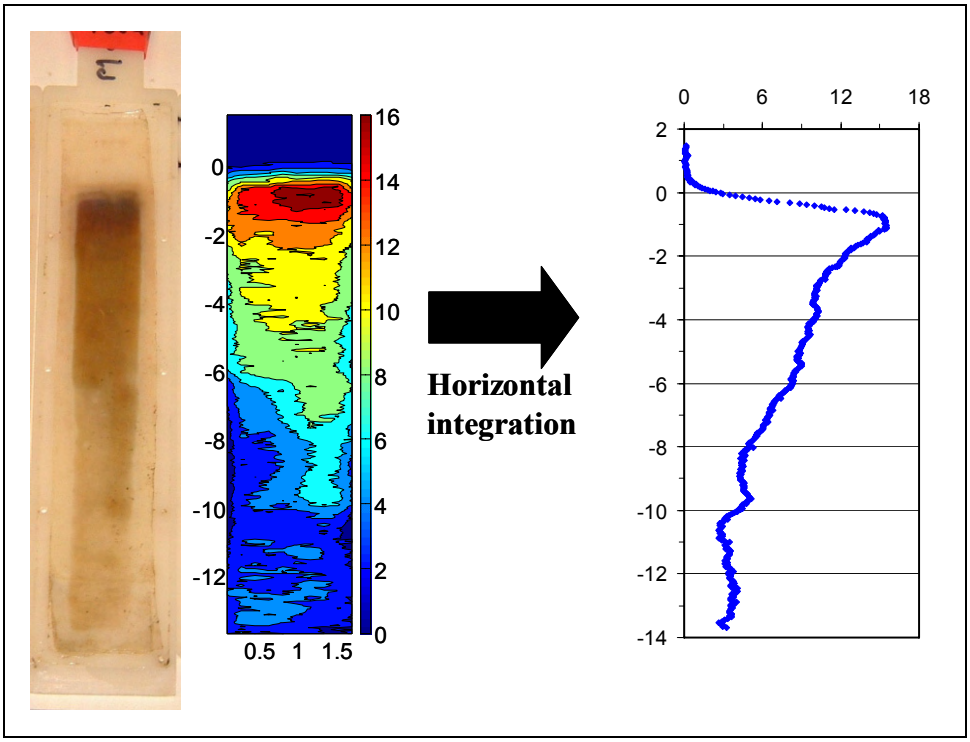

Figure 4-6. Sulfide concentrations (µmol L^{-1}) in pore water of Petaluma River sediment (July 2005) measured by the DGT technique. Vertical scale, depth in cm.

DET diffusional equilibration in thin film

The DET principle, developed by Davison et al. in 1991, is similar to dialysis except that the chamber volumes are filled with a gel instead of water. Solutes in the surrounding solution diffuse into the gel until the concentrations in the gel and in the water are equal. Compared with dialysis, this technique presents the advantage of relatively fast response times (within a day) and the ability to perform measurements at detailed spatial resolution (Figure 4-7). Similar to DGT, the DET principle is based on diffusion of target molecules into the gel. However, there is no resin where these target molecules are accumulated. The DET technique is an equilibration technique and is limited to the measurements of Fe, Mn, and other major anions and cations in the environment.

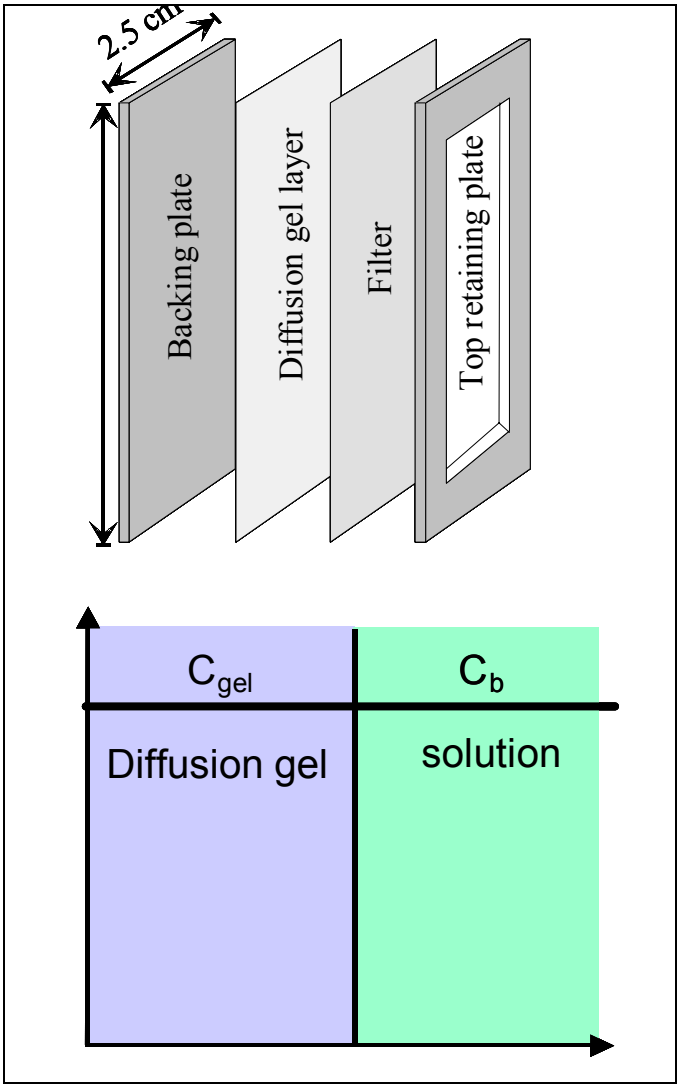

Figure 4-7. Principles of DET assembly and illustration of diffusion processes in the gel.

After de-aeration, DET probes were deployed and incubated inserted into sediments (Figure 4-2) for at least 24 h to allow the equilibration of target solutes between the gel and the sediment pore water. Then, DET probes were removed, the gels sectioned and each 2-mm (vertical dimension) piece of agarose gel placed in a 1.5-mL centrifuge vial for shipment back to the laboratory. Iron and manganese were later dissolved from the agarose gel pieces by adding HNO_3 solution (1 M) and measured by ICP-MS analysis (Element 2, Thermo-Finnigan) (Docekalova et al. 2002). Anions were leached from the agarose gels with Milli-Q water and determined by ion chromatography (Dionex EG 40).

Core sampling procedure

To validate the DGT and DET techniques in sediment, a sediment core was sampled at each site in July 2005, and pore water was extracted by centrifugation and analyzed. At each site, samples were collected with a stainless steel coring device (10-cm i.d. × 30 cm). Clear polyacrylamid liners (with plastic covers at the bottom to prevent loss of the core when extracting the sampler from the sediment) were inserted into the sampling device. A stainless steel head was attached to hold the liner and cover in place during the sampling process. The sampler was pushed into the sediment until the top was even with the sediment surface. The core was extracted by slowly withdrawing the sampler with the aid of a T-shaped handle on the top of the sampler. Cores collected in this manner typically measured 15 to 20 cm in length. The core liner containing the sample was immediately removed from the sampling device, labeled, capped, cut in a nitrogen glove box at a 2-cm resolution scale and shipped to Trent University, Canada (refrigerated). Pore water was extracted by centrifugation and filtered (0.45 µm). Different aliquots were measured for MeHg, sulfide, iron, manganese, and anions.

Methylmercury analysis

A method modified from Hintelmann and Evans (1997) was used. A reaction vessel was filled with 100 mL Milli-Q water, and the sample was added for measurement of MeHg. As an addition, 0.2 mL of acetate buffer (2 M) was mixed into the solution to adjust the pH to 4.9. Sodium tetraethylborate (100 µL, 1% w/v) was added and the solution sat at room temperature for 20 min while the tetraethylborate reacted. Tenax adsorber traps were connected to the reaction vessel and the generated MeHg was purged for 20 min from the solution using nitrogen (200 mL min^{-1}) and collected on the Tenax trap. Finally, all mercury species were thermally desorbed from the trap (250 °C), separated by gas chromatography, and quantified by ICP/MS (Micromass Platform). The following isotopes of Hg were measured: ^{201}Hg (internal standard) and ^{202}Hg (to calculate ambient MeHg). Peak areas were used for quantification, and concentrations of individual isotopes were calculated using an Excel spreadsheet as described in Hintelmann and Ogrinc (2003).

Results and discussion

DET-core comparison

To understand the biogeochemistry of San Francisco Bay sediments, key parameters such as iron and manganese (Figure 4-8) in pore water were measured using the DET technique and an alternative technique (core extraction/centrifugation). These two dissolved species are commonly used as markers of major biogeochemical processes in sediments.

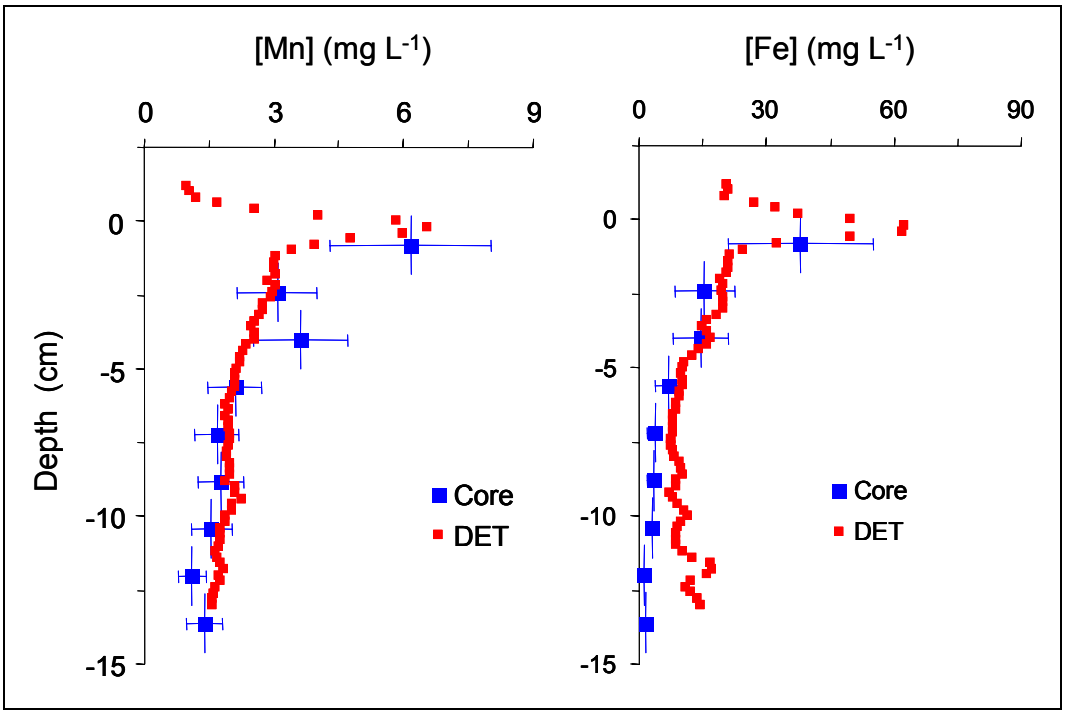

Figure 4-8. Iron and manganese concentrations (µmol L^{-1}) in pore water of Petaluma River sediment (July 2005). Mean values and standard deviations (N=3).

The increase in dissolved metal concentrations reveals the reduction of manganese and iron oxide used by bacteria to oxidize particulate organic matter (Berner 1980). At greater depths, the dissolved metals are more likely to react with sulfide and precipitate. Manganese and iron oxide reduction zones are generally defined by the sediment layer showing a maximum of dissolved metals.

The DET technique and the conventional core sampling/pore water extraction method gave similar results, confirming that iron and manganese oxide reduction occurs in Petaluma River sediment. However, only the high resolution of DET profiles reveals the distinct peaks of manganese

and iron oxide reduction just a few millimeters below the sediment-water interface.

Sulfate is also used by bacteria as a source of energy to decompose particulate organic matter. This biogeochemical process known as sulfate reduction can be investigated by following the decrease in sulfate concentration or the appearance of sulfides in pore water. Using the DET technique, the depletion of sulfate in pore water with depth as a result of SRB activity was followed. Sulfate consumption is expressed as the difference of sulfate concentration in seawater and sulfate concentration in the sample. In order to minimize analytical errors in the high performance liquid chromatography (HPLC) method, sulfate concentrations were normalized to chloride.

$$\Delta SO_4^{2-} = \left[\left(\frac{\left[SO_4^{2-} \right]}{\left[Cl^- \right]} \right)_{seawater} - \left(\frac{\left[SO_4^{2-} \right]}{\left[Cl^- \right]} \right)_{sample} \right] \times \left[Cl^- \right]_{sample} \tag{4-10}$$

Sulfate consumption can be used as an indicator of sulfate reducing activity because sulfate consumption increases with greater SRB activity. Since sulfides are the product of this biological process, the sulfide profile should be correlated to the sulfate consumption. However, sulfides could also precipitate with heavy metals (especially iron) and disappear from the pore water. Hence, some differences between the profiles of these two species are to be expected.

The core measurements in Figure 4-9 show a slight increase of sulfate consumption with depth at China Camp, indicating an increase in sulfate reduction activity. This increase is consistent with the sulfide profile at this location (see Figure 4-11). Areas of high sulfate reducing activity are revealed by DET profiles at +1 and -4 cm. At the same depths, the sulfide concentration shows maxima, confirming the existence of these sulfate reduction high-activity areas.

Sulfate consumptions measured by the DET technique or directly in the pore water extracted from the sediment core were similar at China Camp. The DET technique is, therefore, suitable as an alternative technique to measure major elements such as sulfate, iron, or manganese in pore water.

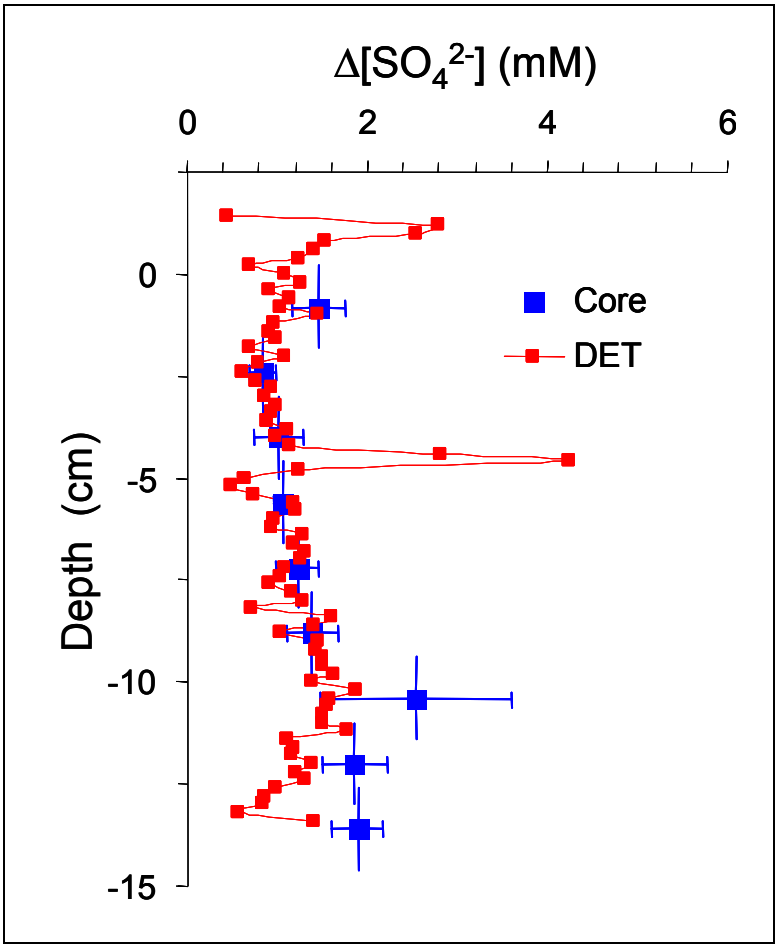

Figure 4-9. Sulfate consumption (mmol L^{-1}) in pore water at China Camp (July 2005). Cores: mean values and standard deviations (N=3).

DGT-core comparison

Sulfate consumption by bacteria generates some sulfides in pore water. Another way to study sulfate reduction is to measure sulfide concentrations. DGT sulfides were used for this purpose and results were compared with direct sulfide measurements in pore water extracted from a sediment core from the Petaluma River.

The pore water sulfide concentrations measured by DGT and directly in the pore water extracted from the sediment core agreed closely (Figure 4-10). This agreement between the DGT and pore water concentrations lends strong support to the reliance on the DGT sulfide results in this study. Not only do the mean results for the two methods concur, but the peaks and valleys in the profiles generally are aligned.

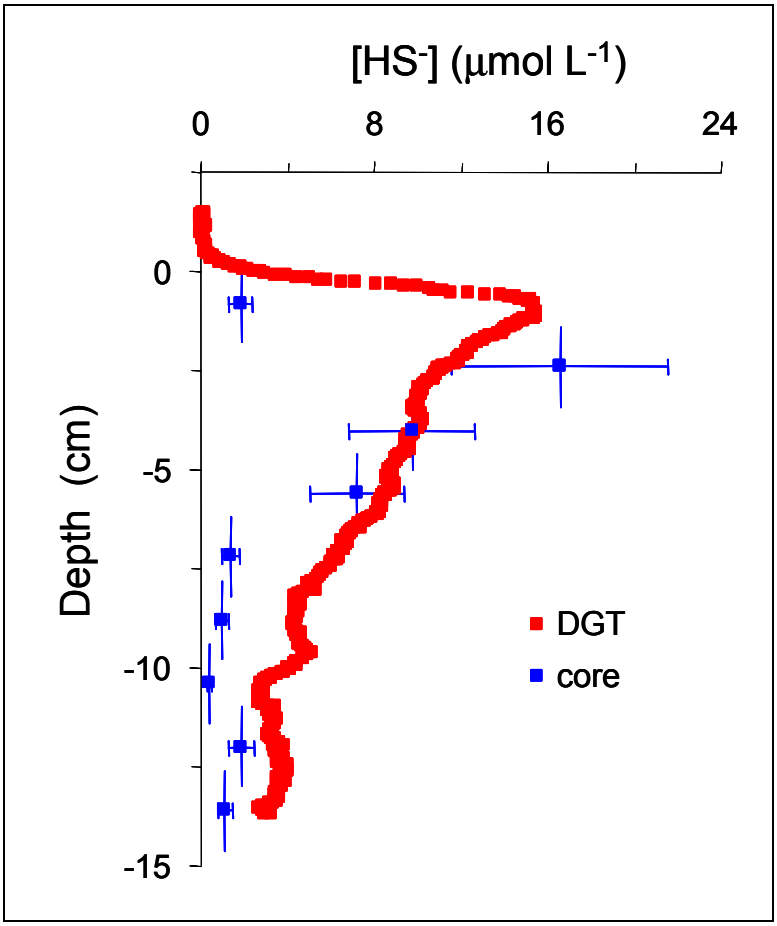

Figure 4-10. Sulfide concentrations (µmol L^{-1}) in pore water of Petaluma River sediment (July 2005). Cores: mean values and standard deviations (N=3).

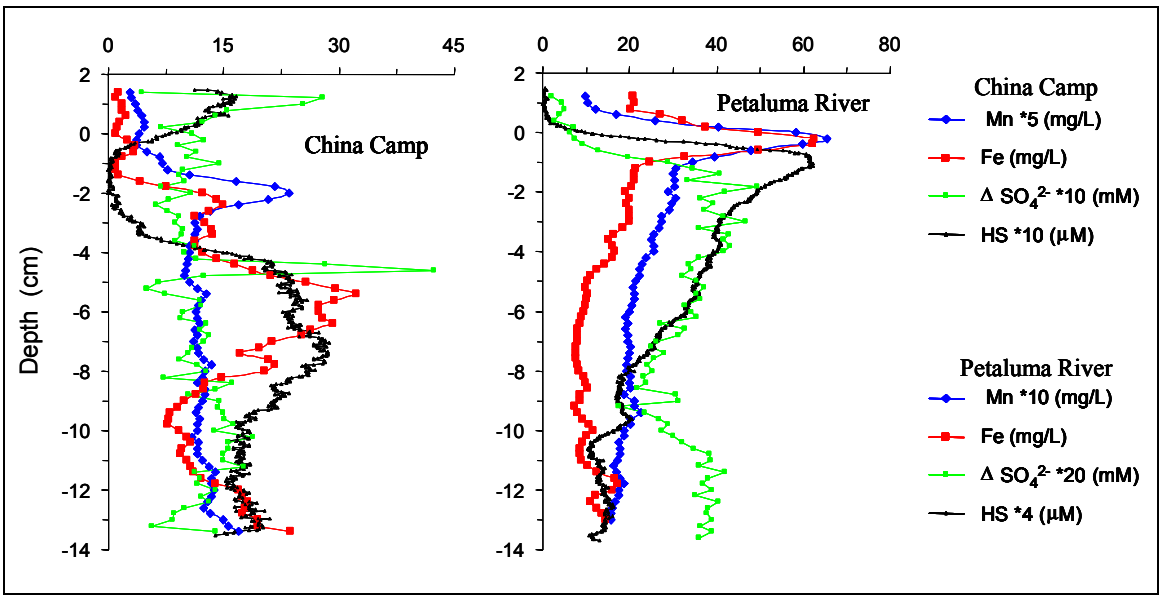

Figure 4-11. Key geochemical species in the San Pablo Bay showing manganese, iron, sulfide concentration, and sulfate consumption in sediment pore water (July 2005).

Sediment heterogeneity could be one of the reasons for the difference observed between DGT profiles and core data: for DGT, only the target ions in the vicinity of the probe (few millimeters to a centimeter) are sampled. The volume of sediment affected by the DGT probe is, therefore, limited. DGT measurement could be highly affected by sediment heterogeneity.

Representativity of the DGT measurements could potentially be an issue and were addressed in 2006. In comparison, sediment cores are quite large (10-cm diameter), and the slices from where pore water is extracted by centrifugation are quite thick. Pore water from the sediment core is virtually homogenized and is certainly more representative of the sediment than DGT. However, pore water homogenization can also hide certain information (MeHg – sulfides relation for example) and do not reveal completely all the biogeochemical processes.

A second reason could explain the difference observed between DGT and core data: Pore water sampling is still a challenge and very difficult. During the long and fastidious process of pore water extraction, there is always a risk to introduce oxygen into ours samples and to induce a reoxydation of redox sensitive species (Fe or HS^- for example). Their concentration in pore water would be, therefore, depleted and would not be representative of the environmental reality.

DGT/DET results and core data match well and validate these new pore water sampling techniques and their application to study mercury biogeochemistry in sediment.

Gel techniques appear to be an alternative method to sample sediment pore water. Moreover, the high resolution of theses techniques provides more detail of redox-active element profiles, which is essential for a better understanding of the sediment biogeochemistry.

Sediment processes investigation

The sedimentary biogeochemistry of mercury is closely coupled to that of the redox-active elements iron, manganese, and sulfur, which in turn are all driven by carbon cycling. The microbial oxidation of these compounds in sediments leads to the accumulation of chemically reduced iron, manganese, and sulfur solutes and minerals (Berner 1971, 1980).

Using the different chemical measurements in pore water, a vertical segregation (with some blurring of boundaries) of biogeochemical processes was established for San Pablo Bay sediments. Reduction of Mn oxide occurs simultaneously with the reduction of Fe oxide but at a greater depth by the reduction of sulfate (Figure 4-11). These reduction reactions occur in the order of decreasing energy yield when coupled with the oxidation of organic matter.

Methylmercury-sulfide interaction

MeHg also has been measured in pore water using the DGT method. MeHg profiles with depth are presented in Figure 4-12 and appear to be related to sulfide profiles. Peaks and valleys of sulfide concentrations are generally followed at a greater depth by similar peaks and valleys in MeHg concentrations.

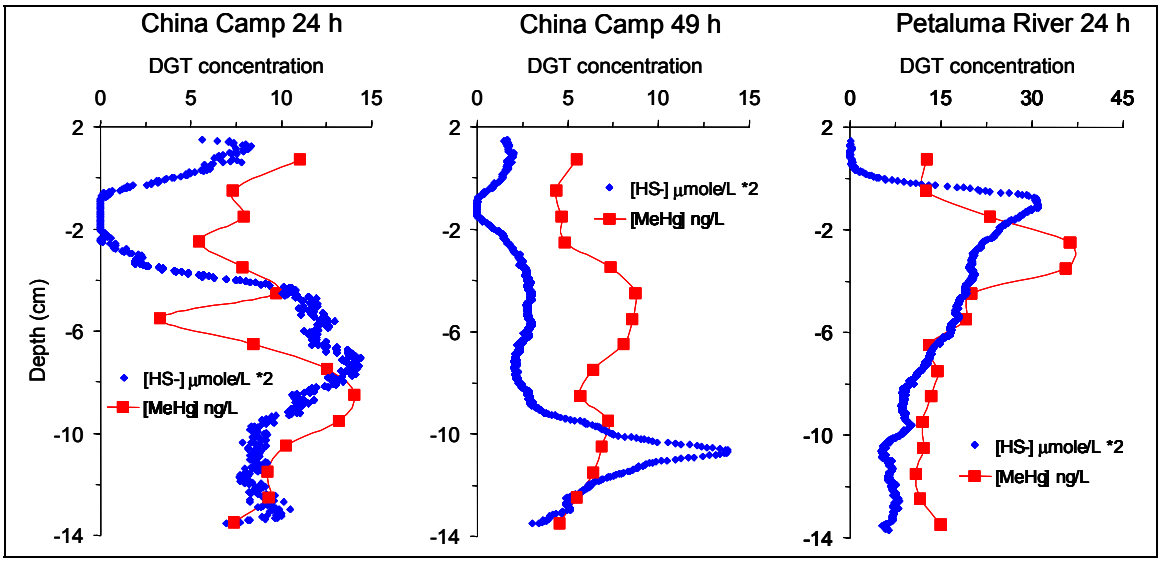

Figure 4-12. Sulfide and MeHg in sediment pore water of San Pablo Bay (July 2005).

Similar patterns were observed in all three profiles indicating a causal relationship between sulfide peaks closely followed by a MeHg maximum. In addition, the MeHg profile of the Petaluma River sediment showed a concentration gradient that peaks close to the sediment-water interface, indicating a release of MeHg to the river water by diffusive flux. Calculations using Fick's first law of diffusion (and a diffusive coefficient of MeHg in pore water of 5×10^{-6} cm^2 s^{-1}) resulted in diffusive fluxes of 1,500-6,900 ng m^{-2} y^{-1} in China Camp and of 15,000 ng m^{-2} y^{-1} in the Petaluma River. Thus, of these sites the river sediment potentially represents a significant source of MeHg for the SF Bay. Similar MeHg diffusive fluxes have

been determined in other studies, which are summarized in Table 4-3. Spatial variability could be one explanation between the results from the DGTs incubated at China Camp for 24 h and 49 h. However, DGT probes act as a local sink for MeHg: the MeHg concentration in the vicinity of the probe is affected and could deplete with time. Thus, the DGT equation becomes more complicated, and the direct calculation of MeHg accumulated by the resin in terms of pore water concentration could be underestimated. This issue was been investigated in 2006 (see relation between DGT measurement in sediment and methylation rate).

Nevertheless, further investigations are needed to determine seasonal and spatial variations of diffusive fluxes of MeHg from sediment pore water, to clarify the MeHg/sulfide relationship in sediment pore water, and to understand the biogeochemistry of mercury in San Pablo Bay sediment.

Table 4-3. Diffusive flux of MeHg measured in Petaluma River sediment compared to other locations.

Site	Diffusion Flux of MeHg (ng m^{-2} y^{-1})	Reference
Petaluma River	15,000	This study
China Camp (creek)	1,500 – 1,800	This study
China Camp (nonvegetated sediment)	4,100 – 6,900	This study
Freshwater Lake (Minnesota)	60	Hines et al. 2004
San Francisco Bay Delta	10 – 10,000	Choe et al. 2004
Long Island Sound (New York)	5,500	Hammerschmidt et al. 2004
Lavaca Bay (Texas)	15,300	Gill et al. 1999

Conclusions

1. The MeHg concentrations in San Pablo Bay water vary to a large extent. There are several hypotheses as to why this occurs. Research in this report, and in other studies, indicates that several dynamic, juxtaposed processes influence the seasonal pattern, including vegetation growth and decomposition, microbial life cycles, temperature, light levels, and changes in chemical parameters such as pH and dissolved oxygen concentrations.
2. The DGT and DET probes enable representative and rapid sampling in ambient water and pore water of chemicals at low concentrations and at rapidly fluctuating levels. The probes are a clever approach to sampling pore water geochemical constituents because pore water presents many challenges for accurate sampling of chemical concentrations.

3. However, spot sampling only provides a snapshot of the current MeHg exposure, and biological monitoring programs are often put in place to gauge contaminant exposure. For the DGT technique to become a valid alternative to biomonitoring programs, the DGT technique has to be calibrated with organisms that are currently proposed as mercury biosentinels. This phase of the project is still in progress and will eventually correlate the MeHg measured by DGT devices to those accumulated by biomonitoring sentinels. This phase of the project will further establish the necessary frequency and duration of DGT deployments in the field.

POINT OF CONTACT CHAPTER 4:

Dr. Holger Hintelmann
Trent University, Department of Chemistry
Peterborough, Ontario, Canada
Ph: 715-748-1011 ext. 7659 ; E-mail: hhintelmann@trentu.ca

5 Marsh Vegetation as a Vector in Mercury Species Transport in San Pablo Bay Tidal Marshes—Understanding the Entry of Mercury into the Aquatic Food Web

Introduction

North American Pacific coastal marshes are generally small compared to those associated with most Atlantic and Gulf of Mexico shores. On the western coast, the gradient between land and sea is steep and the intertidal zone is small. The Pacific coast is a high energy zone, and marshes can only develop in protected embayments. As in the Atlantic and gulf coast areas, the nature of the soils in the marshes depends on the sediment load in the water entering the marsh rather than the original substrate. In general, the marshes are associated with emerging coastal areas. Sediment deposited on intertidal bars and flats elevate the surface to a position where emergent macrophytes can colonize. The stems of the plants act as filters to trap sediment more effectively and elevate the surface more rapidly. In areas of rapid sedimentation, or rapid resuspension and deposition from rivers, the upper layers of the soil are mineral in nature. Soils in marshes developed in areas with little sediment input are very rich in organic matter. These differences greatly influence the nature of the soil phase in trace metal cycling in these systems.

For the studies aimed at providing baseline information on cycling of mercury species, i.e., THg and MeHg, in a tidal wetland at San Pablo Bay, Hamilton Army Airfield (HAAF), the nearby tidal salt marsh at China Camp State Park was chosen as a reference. This tidal salt marsh is traversed by several tidal channels, and *Spartina foliosa* (Pacific cordgrass) and *Salicornia virginica* (common pickleweed) are the dominant plant species. *S. foliosa* is usually the primary colonizer on the tidal mud flats that fringe the tidal marsh plain and occurs in virtually pure stands on the low marsh between mean tidal level (MTL) and mean high water level (MHW). At somewhat higher elevations near and above MHW, *S. foliosa* intermixes and gradually yields to *S. virginica*. According to Mahall and Park (1976b), the transition zone between these two dominant species is at about 24‰, with *S. virginica* being more resistant to elevated salinities by

excluding ions from entering its roots. At elevations between MHW and the maximum height of the tides, *S. virginica* is found in association with peripheral halophytes including *Distichlis spicata* (saltgrass) and *Atriplex triangularis* (fathen). The history, physical setting, and ecological relationships in several Baylands ecosystems have been previously outlined by the San Francisco Bay Area Wetlands Ecosystem Goals Project (1999).

The food web in Pacific coastal marshes as in Atlantic coastal marshes is primarily detritus based, with microbes, insects, and amphipods as the most important heterotrophs. Once detrital material plus the community of microorganisms leave the attached dead plant, the food web in the Pacific Northwest marshes may include copepods, mollusks, and salmonid fishes (Sibert 1977). In addition, a strong food web linkage between salt marsh plants and nearshore fish consumers has been identified for many North American coastal ecosystems, including the Atlantic, the Pacific Northwest, and San Francisco Bay (Naiman and Sibert 1979; Kistritz and Yesaki 1979; Wainwright et al. 2000; Grenier 2004). In contrast, other researchers report that coastal and estuarine food webs are fueled by algal production, i.e., either phytoplankton (Nixon et al. 1976; Haines 1977; Gleason and Wellington 1988; Kimmerer 2004), submersed macrophytes, epiphytes, and macroalgae (Simenstad and Wissmar 1985); or epibenthic microalgae (Sullivan and Moncreiff 1990). A recent food web analysis of Southern California coastal wetlands indicates that salt marsh plants can be the major organic matter source for fish, and macroalgae for invertebrates and selected bird species, but that in the absence of abundant marsh plants, inputs of macroalgae and microalgae support fishes (Kwak and Zedler 1997).

Objectives

The current study addresses two questions on the role of marsh plants:

1. What is the natural cycle of transfer of mercury (a) into the live plant, (b) from the live plants to the dead plant material, and (c) from the standing dead plant community to the rest of the ecosystem via fragmentation?
2. Is there a difference in the effectiveness of the predominant plant species (*S. foliosa* or *S. virginica*) to act as vectors for the transfer of mercury from mercury-contaminated sediments into the aboveground plant parts and hence into the food chain?

The results pertaining to part of an annual cycle are presented in this chapter. The results pertaining to the complete annual cycle will be reported in a later report.

Study site

The Hamilton Army Airfield (HAAF) Wetlands Restoration Site on San Pablo Bay is part of the San Francisco Baylands. It is located in the North Bay. The Baylands consist of shallow water habitats around the San Francisco Bay. The Baylands ecosystem includes the areas of maximum and minimum tidal fluctuations, adjacent habitats, and their associated plants and animals. The ecosystem boundaries vary with the bayward and landward movements of fish and wildlife that depend upon the Baylands for survival. Many habitats of the Baylands are wetlands. Habitat goals selected for the planned restored HAAF wetland, with a surface area of 203 ha, include the restoration of tidal marshes, with natural transitions into upland areas with seasonal wetlands. The restored HAAF area is expected to increase the habitat of the regionally rare and protected clapper rail and salt marsh harvest mouse because it is adjacent to existing populations, will contain a large tidal wetland, and is remote from predator outposts and corridors (San Francisco Bay Area Wetlands Ecosystem Goals Project 1999).

The test site representative for the HAAF was situated at the HAAF bay edge (SM-10; 38° 03.116′ N, 122° 29.55′ W; Figure 5-1). The nearby tidal salt marsh at the China Camp State Park (R44; 38° 00.411′ N, 122° 28.758′ W), chosen as a reference, covers approximately 45 ha (110 acres according to Hopkins and Parker 1984), and is frequently immersed by tidal waters (salinity 25‰–32‰; Figure 5-1).

Materials and methods

Sampling methods

For this study on mercury species flow through the predominant vegetation, samples were collected in the tidal marsh at the reference site China Camp. To answer both questions, an approach similar to that published by Gallagher and Kibby (1980) was chosen. This approach combines estimates of dry matter production and disappearance based on measurements of live biomass, dead biomass, and mortality with seasonal metal

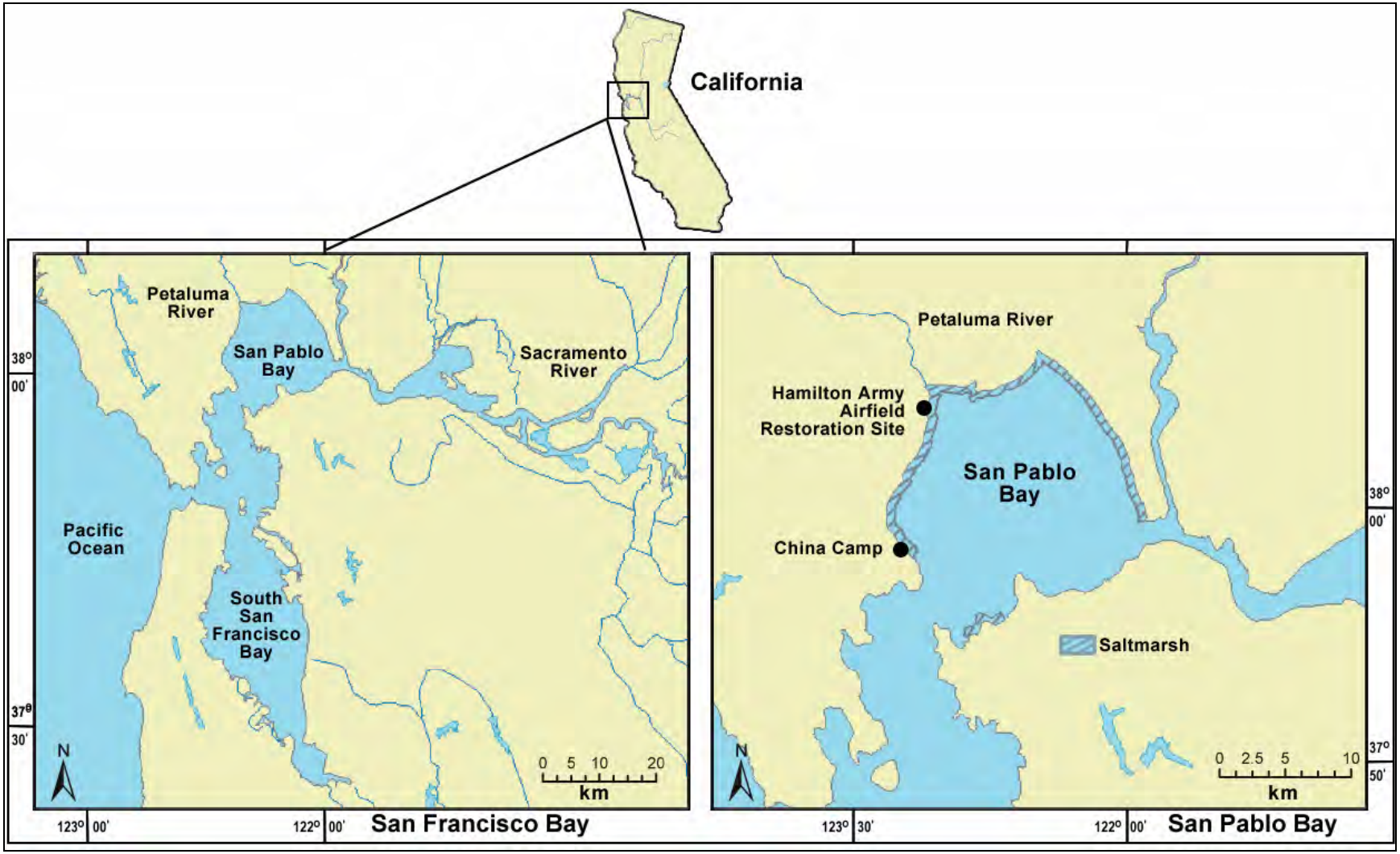

Figure 5-1. Site map showing the location of San Pablo Bay within San Francisco Bay (left) and the location of the Hamilton Army Airfield Restoration Site and the China Camp reference site (right).

concentrations in plant tissues. Relationships between concentrations of mercury species in sediment and those in particulate plant material were emphasized, but gaseous transpiration (volatilization) of mercury in the form of Hg^0 was not taken into account.

Live and dead shoot biomass measurements in stands of *S. foliosa* and *S. virginica* were made by harvesting the aboveground plant biomass in seven randomly placed quadrat frames of 0.0256 m^2 at regular intervals, ranging from 4-week intervals during April to November 2005 to 6- to 8-week intervals during November 2005 to April 2006. Seven replicates were taken because wetland vegetation is notoriously variable in density. More frequent sampling including both live and dead components is usually referred to as the Smalley (1958) method. The method yields greater estimates of primary production than either a single end-of-season harvest or estimates based on the difference between minimum and maximum aboveground biomass.

Mortality was determined in two extra Lomnicki plots, similar to two of the seven plots randomly harvested by the modified Wiegert-Evans method for estimation of net primary production, as described by Lomnicki et al. (1968). On the Lomnicki plots only dry weights were determined and mercury species concentrations were not measured. For conversion of mortality in terms of dry weight into terms of mercury species, the concentrations measured in the live aboveground biomass were used in contrast to Galagher and Kibby (1980), who used the concentrations found in the dead biomass. This was done because the mercury species levels associated with the dead plant material were greater than those in the live plant material and appeared to originate largely from encrustation on the outside of the plant material, possibly due to exposure to seawater. Mortality was determined as follows. At time=0 the dead aboveground plant biomass was removed from two 0.0256-m^2, tagged Lomnicki plots per plant species, and the live biomass was left in place. At time=1 all aboveground plant material was harvested from the same two previously-tagged Lomnicki plots, and the dead biomass generated over time interval t_1-t_0, the mortality, was measured. This method required a time interval small enough to prevent the disappearance of material that died. For grassland communities, a time interval of 1 month proved to be short enough to avoid errors in estimation due to disappearance of material dying within that period (Lomnicki et al. 1968). Some loss at

longer time intervals may occur, but it was not quantified in the current study.

After harvest, plant samples were cleaned from adhering sediment by thoroughly washing with tap water, followed by one rinse with demineralized water. Then samples were dried to constant weight at 60 °C and ground in a Cyclone Mill (UDY Corp., Fort Collins, CO) to pass a 1-mm screen.

Total mercury determinations

Total mercury was determined in the ground plant samples following USEPA method 7471 (USEPA 1992; USEPA 1994). Approximately a 0.52-g sample of the plant tissue was weighed to the nearest 0.1 mg in Teflon digestion vessels and heated at 115 °C with 5 mL of concentrated sulfuric acid and 2.5 mL of concentrated nitric acid for 15 min until the tissue dissolved. Subsequently, 8 mL of 5% potassium persulfate and 15 mL of 5% potassium permanganate were added and heated to 95 °C for 2 h. The excess potassium permanganate was reduced with hydroxylamine hydrochloride and sodium chloride solution. The digestate was then diluted to 100 mL with deionized water. Mercury was determined using a PS Analytical Atomic Fluorescence Mercury Analyzer. Typical reporting and method detection limits for this sample size are 0.004 and 0.001 ng g^{-1}, respectively.

Methylmercury determinations

MeHg was determined by species-specific isotope dilution ICP/MS according to Hintelmann and Evans (1997). For this, a 0.2-g sample was weighed into 30-mL Teflon vials and suspended with an additional 10 mL of distilled water. $CH_3{}^{201}HgCl$ (55 pg) was added as an internal standard. Then 200 µL of H_2SO_4 (9 M) and 500 µL of KCl (20%) were added. The vessel was placed into a heating block at 140 °C. MeHg was distilled from the sample under a supporting nitrogen stream (80 mL min^{-1}) over a period of approximately 60-90 min per sample.

A reaction vessel was filled with 100 mL Milli-Q water, and the distillate was added for measurement of methylmercury. A 0.2-mL acetate buffer (2 M) was added to adjust the pH to 4.9. Sodium tetraethylborate (100 µL, 1% w/v) was added and the solution sat at room temperature for 20 min while the tetraethylborate reacted. Tenax adsorber traps were connected to

the reaction vessel and the generated methylethylmercury was purged for 20 min from the solution using nitrogen (200 mL min^{-1}) and collected on the Tenax trap. Finally, all mercury species were thermally desorbed from the trap (250 °C), separated by gas chromatography, and quantified by ICP/MS (Micromass Platform). The following isotopes of Hg were measured: ^{201}Hg (internal standard) and ^{202}Hg (to calculate ambient methylmercury). Peak areas were used for quantification and concentrations of individual isotopes were calculated as described in Hintelmann and Ogrinc (2003).

Mercury analysis QA/QC

For each batch of samples, the following set of QA/QC samples was measured: three reagent blanks (THg) or bubbler blanks (MeHg) and a certified reference material (IAEA 356 marine sediment and MESS-3 marine estuary sediment for sediment analysis and NIST 1515 apple leaves for plant analysis). Individual distillation yields were determined using the added internal ^{201}Hg isotope standard. Typically, one triplicate sample was analyzed (i.e., triplicate distillation or digestion) per batch.

Results and discussion

Standing crop

Figure 5-2 shows the changes in aboveground standing crop of live and dead plant material for the field data as well as for the fitted curves of both plant species. In *S. foliosa*, the live standing crop increased very rapidly

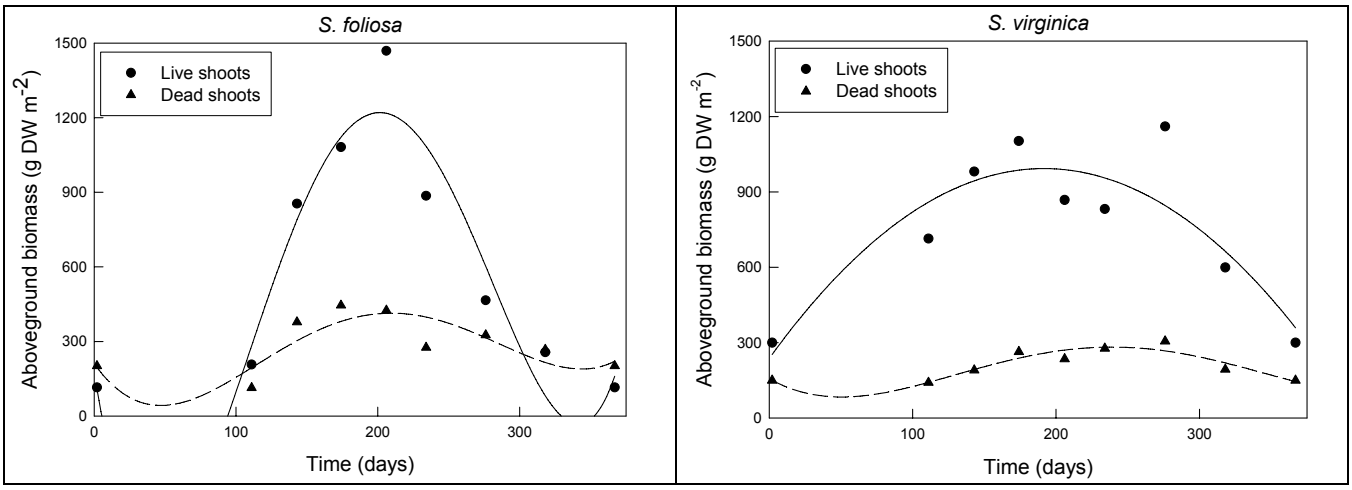

Figure 5-2. Seasonal changes in the live and dead aboveground standing crop at low marsh site R-44 of the China Camp State Park. Julian Day 1 is January 1. Mean values 2005 (N=7). Solid lines give the regression curves for live standing crop, dashed lines for dead standing crop.

from almost 0 to 1,468 g DW m^{-2} between the beginning of April and the end of July and decreased steeply to very low values at the end of the year. The dead standing crop fluctuated less, showing a maximum of 445 g DW m^{-2} in July and becoming negligible in March (Table 5-1).

Table 5-1. Seasonal changes in measured aboveground live and dead standing crop, and calculated net primary production, uptake rates of THg and MeHg, and mortality and fragmentation/leaching rates of *Spartina foliosa* at low marsh site R-44 of the China Camp State Park.

S. foliosa	Standing Crop-Live	Standing Crop-Dead	Net Primary Production	Net Uptake	Mortality	Fragmentation/ Leaching
	Biomass					
Period (days)	(g DW m^{-2})	(g DW m^{-2})	(g DW m^{-2} d^{-1})		(g DW m^{-2} d^{-1})	(g DW m^{-2} d^{-1})
111-142	207	114	20.97		0.75	0 (-7.50)
143-173	854	378	10.36		3.02	0.84
174-205	1,081	445	15.80		3.71	4.34
206-233	1,468	425	2.92		23.74	29.09
234-275	885	275	1.35		11.36	10.15
276-317	465	326	TBD		TBD	TBD
318-1	TBD	TBD	TBD		TBD	TBD
2-53	TBD	TBD	TBD		TBD	TBD
Annual			≥1,499		TBD	TBD
	THg					
Period	(µg m^{-2})	(µg m^{-2})		(µg m^{-2} d^{-1})	(µg m^{-2} d^{-1})	(µg m^{-2} d^{-1})
111-142	2.21	17.08		0.455	0.008	0 (-1.532)
143-173	16.18	66.37		0.0.23	0.057	0 (-0.133)
174-205	15.10	72.26		0.273	0.052	0.626
206-233	22.16	53.87		0	0.356	1.153
234-275	9.90	31.59		0.060	0.125	0 (-1.413)
276-317	7.17	56.89		TBD	TBD	TBD
318-1	TBD	TBD		TBD	TBD	TBD
2-53	TBD	TBD		TBD	TBD	TBD
Annual[1]				≥26.173	TBD	TBD
	MeHg					
Period	(µg m^{-2})	(µg m^{-2})		(µg m^{-2} d^{-1})	(µg m^{-2} d^{-1})	(µg m^{-2} d^{-1})
111-142	0.06	0.25		0.005	0	0 (-0.029)
143-173	0.22	1.18		0.004	0.001	0 (-0.003)
174-205	0.32	1.31		0.009	0.001	0.006
206-233	0.56	1.14		0.001	0.009	0.029
234-275	0.33	0.57		0	0.004	0.018
276-317	TBD	TBD		TBD	TBD	TBD
318-1	TBD	TBD		TBD	TBD	TBD
2-53	TBD	TBD		TBD	TBD	TBD
Annual[1]				≥0.588	TBD	TBD

Note: TBD = to be determined.

[1] Sum uptake April-August × 1.33 (see text). Mean values 2005 and standard deviations (N=7). Belowground biomass was 1184.65 ± 470.43 g DW m^{-2} on 25 July 2005 (N=3).

Table 5-2. Seasonal changes in measured aboveground live and dead standing crop, and calculated net primary production, uptake rates of THg and MeHg, and mortality and fragmentation/leaching rates of *Salicornia virginica* at low marsh site R-44 of the China Camp State Park.

S. virginica	Standing Crop-Live	Standing Crop-Dead	Net Primary Production	Net Uptake	Mortality	Fragmentation/ Leaching
	Biomass					
Period	(g DW m^{-2})	(g DW m^{-2})	(g DW m^{-2} d^{-1})		(g DW m^{-2} d^{-1})	(g DW m^{-2} d^{-1})
111-142	714	141	11.663		3.315	1.778
143-173	981	190	7.866		3.954	1.585
174-205	1,102	264	4.571		11.894	12.794
206-233	868	235	21.351		22.639	21.131
234-275	832	277	TBD		TBD	TBD
276-317	1,160	306	TBD		TBD	TBD
318-1	TBD	TBD	TBD		TBD	TBD
2-53	TBD	TBD	TBD		TBD	TBD
Annual			≥1,361		TBD	TBD
	THg					
Period	(µg m^{-2})	(µg m^{-2})		(µg m^{-2} d^{-1})	(µg m^{-2} d^{-1})	(µg m^{-2} d^{-1})
111-142	32.80	7.17		0	0.123	0.146
143-173	22.18	6.45		0.010	0.079	0 (-0.074)
174-205	20.06	11.19		0	0.069	0.037
206-233	16.07	12.22		0.325	0.258	0 (-0.016)
234-275	17.94	19.91		TBD	0.226	TBD
276-317	TBD	TBD		TBD	TBD	TBD
318-1	TBD	TBD		TBD	TBD	TBD
2-53	TBD	TBD		TBD	TBD	TBD
Annual[1]				≥9.422	TBD	TBD
	MeHg					
Period	(µg m^{-2})	(µg m^{-2})		(µg m^{-2} d^{-1})	(µg m^{-2} d^{-1})	(µg m^{-2} d^{-1})
111-142	0.80	0.18		0	0.003	0.004
143-173	0.50	0.14		0.012	0.002	0 (-0.004)
174-205	0.81	0.31		0	0.003	0.003
206-233	0.58	0.30		0.006	0.009	0.008
234-275	0.50	0.34		TBD	TBD	TBD
276-317	TBD	TBD		TBD	TBD	TBD
318-1	TBD	TBD		TBD	TBD	TBD
2-53	TBD	TBD		TBD	TBD	TBD
Annual[1]				≥0.018	TBD	TBD

Note: TBD = to be determined.

[1] Sum uptake April-August × 1.33 (see text). Mean values 2005 and standard deviations (N=7). Belowground biomass was 3147.81 ± 1543.82 g DW m^{-2} on 25 July 2005 (N=3).

The leaves contributed a smaller proportion than the stems to the live standing crop, while the reverse was true for the dead standing crop (Figure 5-3).

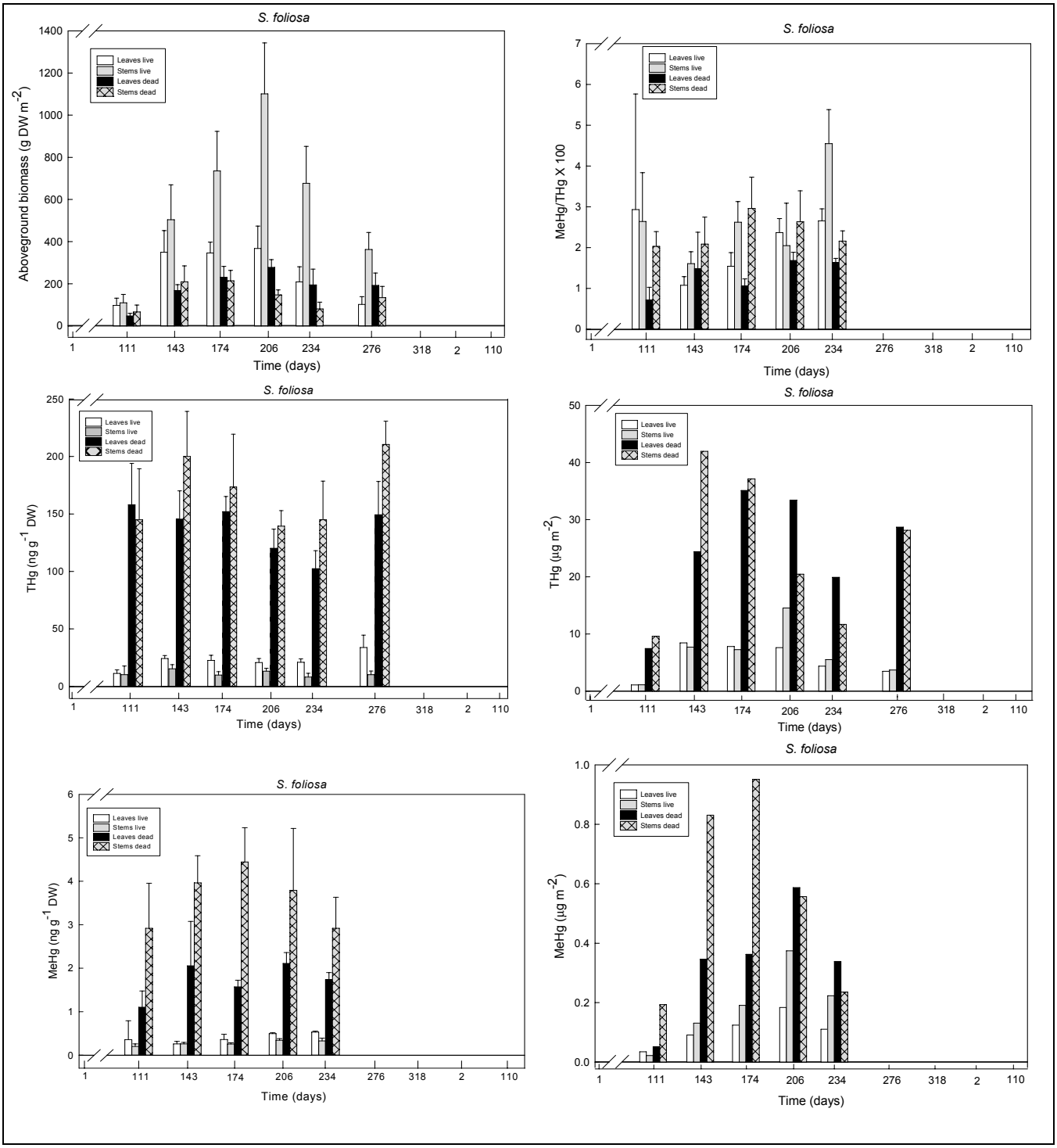

Figure 5-3. Seasonal changes in the aboveground biomass, concentrations of THg and MeHg, MeHg:THg ratio, and THg and MeHg mass of *Spartina foliosa* at low marsh site R-44 of the China Camp State Park. Mean values 2005-2006 and standard deviations (N=5).

In *S. virginica* live and dead standing crop fluctuated less and maxima were generally less than in *S. foliosa*. The maxima of live and dead

standing crop were, respectively, 1,102 g DW m^{-2} and 306 g DW m^{-2} (Table 5-1). In this species, the stems contributed the greatest proportion to both the live and dead standing crop (Figure 5-4).

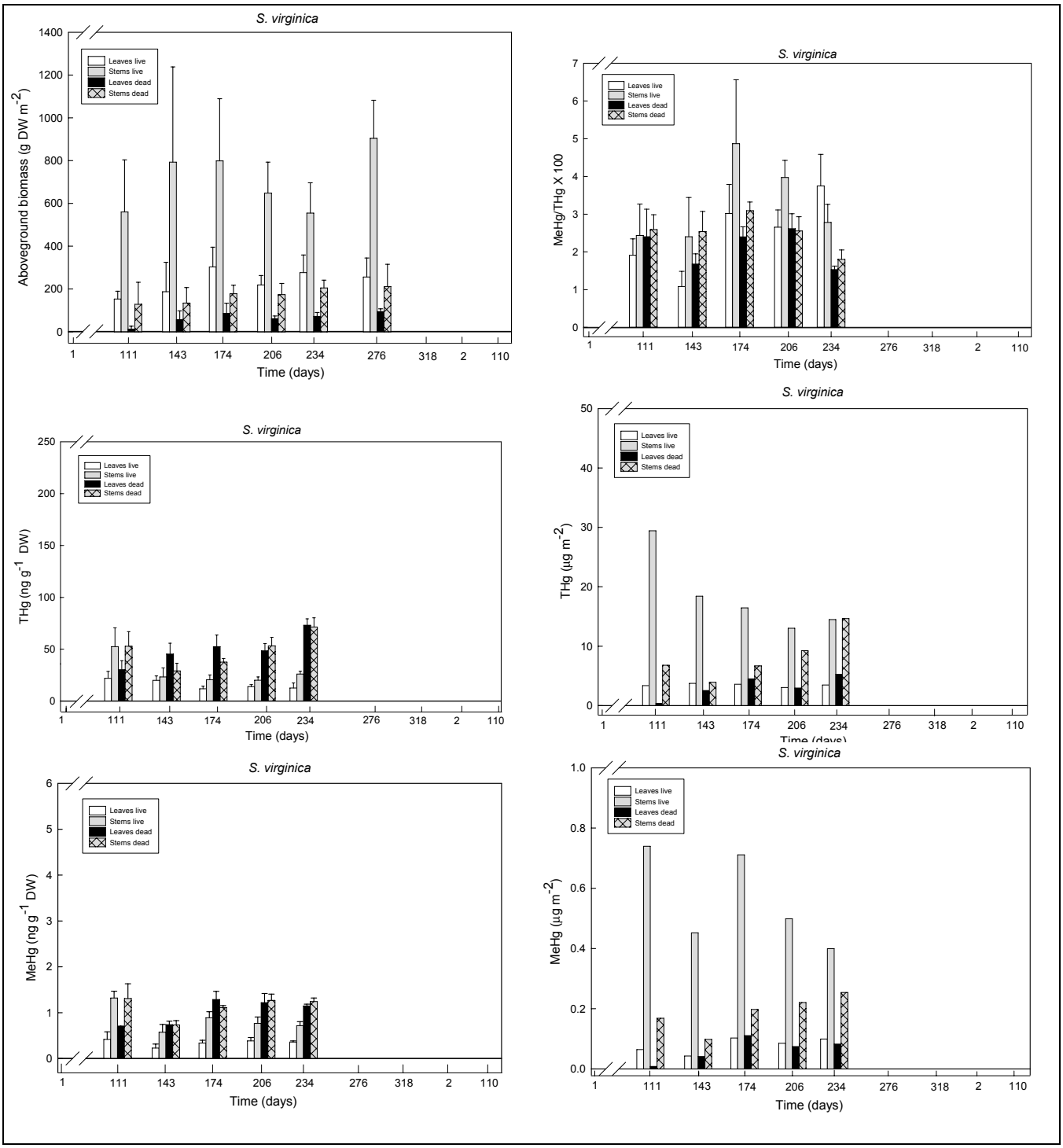

Figure 5-4. Seasonal changes in the aboveground biomass, concentrations of THg and MeHg, MeHg:THg ratio, and THg and MeHg mass of *Salicornia virginica* at low marsh site R-44 of the China Camp State Park. Mean values 2005-2006 and standard deviations (N=5).

Regression curves were fitted to the standing crop data. Fourth-order polynomial curves were the best fit for the live standing crop of *S. foliosa* and for the dead standing crop of both species. Second-order polynomial curves were the best fit for the live standing crop of *S. virginica*. The curves fitted the live standing crop data better than the dead standing crop (p-values indicated that fits were significant at the 95% confidence level). However, the curve fitted to the live *S. foliosa* standing crop underestimated the maximum by 28%. These regression equations, of which the coefficients are provided in Table 5-3, can be used to estimate standing crop for biomass of *S. foliosa* and *S. virginica* at related sites. The dead *S. foliosa* standing crop fitted the regression equation to a limited extent ($p>0.05$, $R^2 = 0.30$), and, therefore, estimates made using this equation may deviate from actual dead standing crop.

Table 5-3. Coefficients of equations representing the curves of live and dead standing crop for *Spartina foliosa* and *Salicornia virginica* at the low marsh site R-44 of the China Camp State Park (for the means of seven replicates). Fourth-order polynomials fitted the live standing crop of *Spartina foliosa* and dead standing crops of both plant species according to the equation $Y = A + BX + CX^2 + DX^3 + EX^4$. A second-order polynomial fitted the live standing crop of *Salicornia virginica*, according to the equation $Y = A + BX + CX^2$. The p statistic gives the p-value of the estimated regression line through the sample points; the R^2 statistic indicates the fraction of the variability in biomass explained by the fitted model.

Species	A	B	C	D	E	p	R^2
S. foliosa							
Living	177.94	-35.72	0.55	-0.23×10^{-2}	0.30×10^{-5}	0.021	0.83
Dead	212.18	-8.18	0.11	-0.05×10^{-2}	0.06×10^{-5}	0.282	0.30
S. virginica							
Living	237.45	7.88	-0.02			0.010	0.71
Dead	156.46	-3.24	0.04	-0.01×10^{-2}	0.02×10^{-5}	0.052	0.72

Mercury and methylmercury concentrations in plant tissues

The seasonal changes in the concentrations of mercury species are shown in Figures 5-3 and 5-4. The numerical values are provided in Tables A5-1, A5-2, A5-3, and A5-4.

Mercury species concentrations were generally higher in *S. foliosa* than in *S. virginica*, except in stems where they were higher in *S. virginica*. In *S. foliosa*, the mean THg concentrations ranged from 11.29 to 33.83 ng g^{-1} DW in live leaves; from 10.13 to 13.21 ng g^{-1} DW in live stems; from 102.30 to 158.00 ng g^{-1} DW in dead leaves; and from 139.40 to 210.40 ng g^{-1} DW in dead stems. In *S. virginica*, the mean THg concentrations ranged from

11.90 to 21.91 ng g^{-1} DW in live leaves; from 23.23 to 52.54 ng g^{-1} DW in live stems; from 30.25 to 73.10 ng g^{-1} DW in dead leaves; and from 29.14 to 71.38 ng g^{-1} DW in dead stems.

In *S. foliosa*, the mean MeHg concentrations ranged from 0.26 to 0.53 ng g^{-1} DW in live leaves; from 0.20 to 0.34 ng g^{-1} DW in live stems; from 1.10 to 2.11ng g^{-1} DW in dead leaves; and from 2.92 to 210.4.44 ng g^{-1} DW in dead stems. In *S. virginica*, the mean MeHg concentrations ranged from 0.23 to 0.42 ng g^{-1} DW in live leaves; from 0.72 to 1.32 ng g^{-1} DW in live stems; from 0.69 to 1.29 ng g^{-1} DW in dead leaves; and from 0.73 to 1.32 ng g^{-1} DW in dead stems.

The greatest MeHg:THg ratios in both plant species were found to be 0.0455 in live stems of *S. foliosa* in mid-August and 0.0487 in live stems of *S. virginica* at the beginning of June.

In dead plant matter, the THg and MeHg concentrations almost always exceeded those in live plant matter and were particularly elevated in *S. foliosa*. Concentrations were usually lower in the leaves than in the stems of both species. In the live standing crop, the THg concentration was usually greater in the leaves than in the stems of *S. foliosa*, whereas the reverse was true in *S. virginica*. The MeHg concentration was usually greater in the leaves than in the stems of both plant species.

The consistently greater mercury species concentrations in dead plant material may be due to one or more of the following four reasons, listed by Gallagher and Kibby (1980): (1) Dead tissues are more porous than live tissues, and, therefore, interstitial spaces may be more readily contaminated with sediment. (2) The same porous structure may provide surfaces for sorption of salts from the flooding seawater. (3) Decomposition may selectively remove other components, including water (see also Chapter 6 of this report). (4) Microbes may be associated temporarily with the dead plants resulting in the precipitation of metals in tissues (Chapter 6 this report). Elevated trace metal and mercury species levels in dead tissues (as opposed to live tissues) of salt marsh plants were also reported by Williams and Murdock (1972), Gallagher and Kibby (1980), and Price (2005).

Net primary production, mortality, fragmentation/leaching, and consequences for the fluxes of mercury species

The collected data on live standing crop, dead standing crop, and dead biomass disappearance were used to calculate net primary production, mortality, and fragmentation/leaching of biomass. These data were coupled with the data on seasonal changes in mercury species concentrations in tissues to calculate three fluxes of mercury species in the conceptual model represented in Figure 5-5, as follows:

1. Uptake--Transfer from the marsh substrate to live shoots includes both current transfers from soil through roots to shoots and those coming from mercury species stored in belowground plant parts.
2. Mortality--Transfer via this process begins the flow through the detrital food web.
3. Fragmentation, Leaching and Excretion--This complex of processes includes losses involving passive leaching of mercury species from the dead plants, excretion by the organisms associated with that community, and fragmentation. In this study, no distinction between these components was made. Leaching of mobile ions, such as potassium, can be rapid; however, the fragmentation pathway might be more important for elements forming structural or storage compounds in plants.

A representative data set for dry matter flux in *S. foliosa* is shown in Figure 5-6. Net production (NP) equals the change in standing crop in the live component ($L_{t2} - L_{t1}$) plus that lost to mortality ($M_{t1\text{-}t2}$) during the time period, both in g DW m^{-2}.

$$NP = \left(L_{t2} - L_{t1}\right) + M_{t1-t2} \tag{5-1}$$

Loss from the attached dead plant community (FLE) equals the dead biomass of plant material present at the beginning of the time period (D_{t1}) less than that present at the end (D_{t2}) plus that added to the dead plant community by mortality during the time interval ($M_{t1\text{-}t2;}$ measured on the Lomnicki plots).

$$FLE = \left(DB_{t1} - DB_{t2}\right) + M_{t1\text{-}t2} \tag{5-2}$$

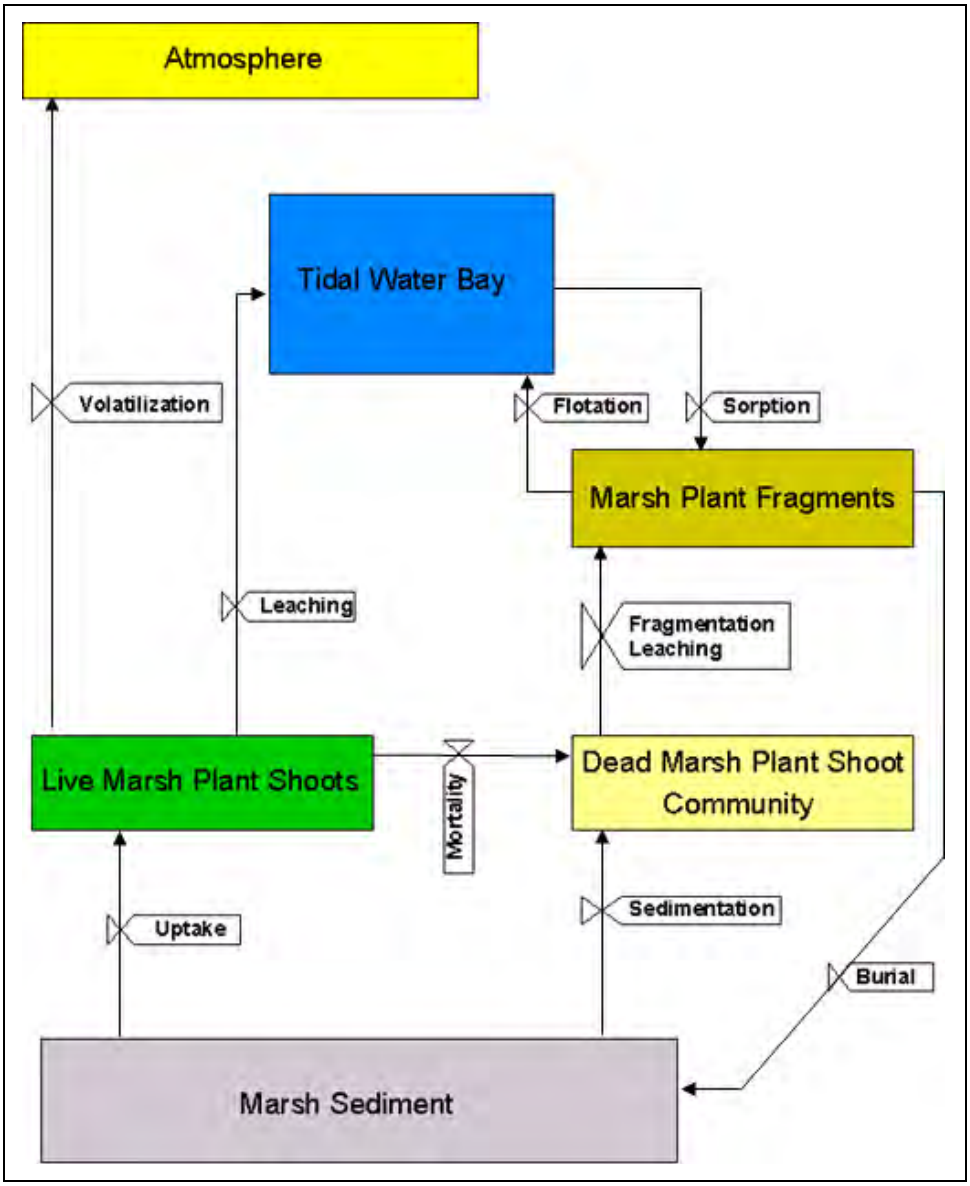

Figure 5-5. Conceptual model of the role of marsh plants as vectors in mercury species dynamics.

A representative data set for the flux of THg in *S. foliosa* is shown in Figure 5-7. Similar to the approach described above, uptake (U) equals the change in the mercury species contained in standing crop in the live component ($L_{t2} - L_{t1}$) plus that lost to mortality ($M_{t1\text{-}t2}$) during the time period, all in μg THg m^{-2}.

$$U = \left(L_{t2} - L_{t1}\right) + M_{t1-t2} \tag{5-3}$$

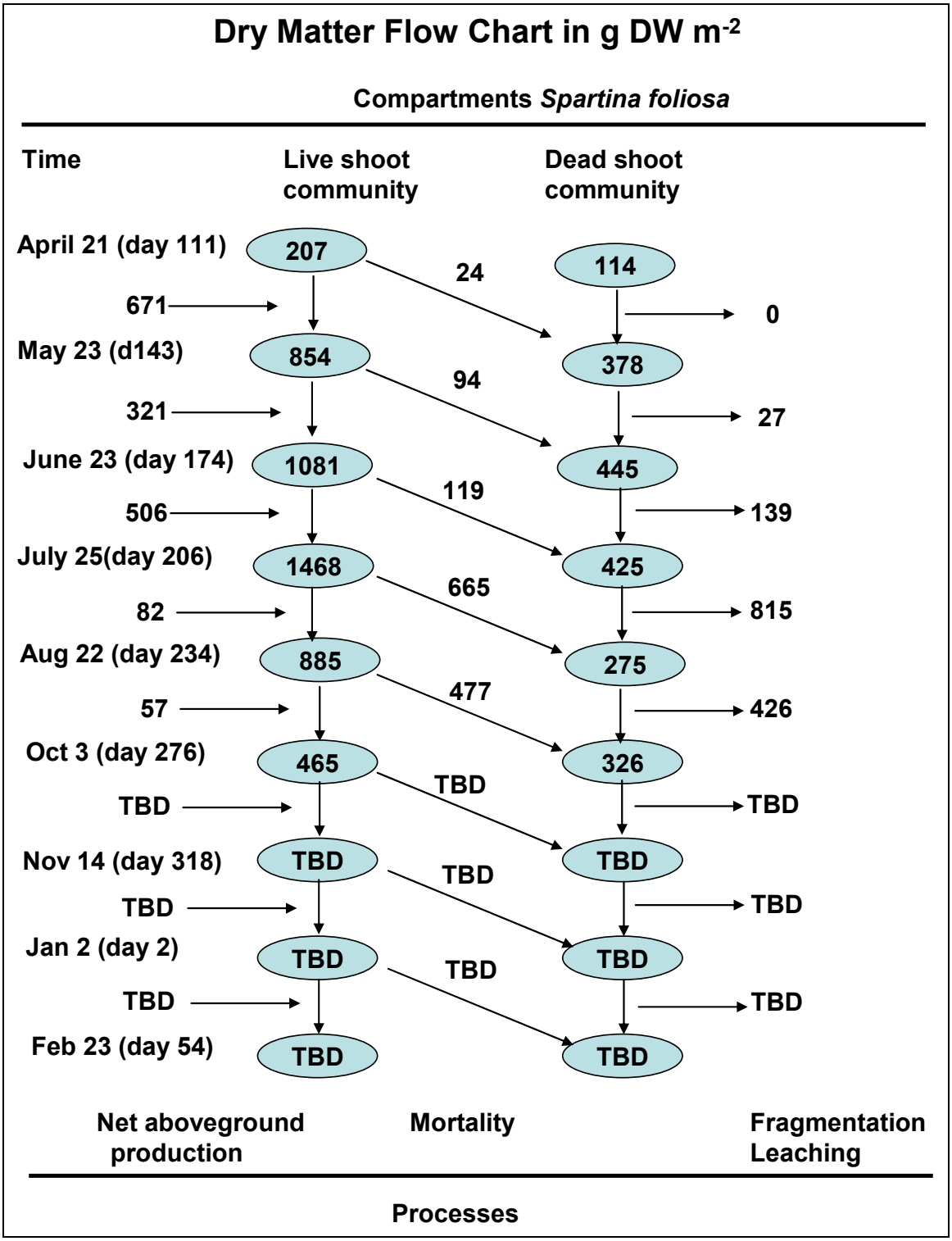

Figure 5-6. Flow chart of the flux of dry matter through live *Spartina foliosa* and the community associated with the attached dead plants at low marsh site R-44 of the China Camp State Park. Dates are followed by Julian day numbers between parentheses. Mean values 2005.

Loss from the attached dead plant community (FLE) equals the dead biomass of plant material present at the beginning of the time period (D_{t1}) less than that present at the end (D_{t2}) plus that added to the dead plant community by mortality during the time interval ($M_{t1-t2;}$ measured on the Lomnicki-plots). Mortality is calculated by multiplying the separately measured mortality mass in g DW m^{-2} by the mercury species concentrations in µg g^{-1} DW of the live shoots, the loss (FLE) in µg THg m^{-2}.

$$FLE = \left[\left(MB_{t1-t2} + DB_{t1}\right) - DB_{t2}\right] CD_{t1} \qquad (5\text{-}4)$$

Diagrams such as the Figures 5-6 and 5-7 were prepared for the fluxes of dry matter and mercury species of *S. foliosa* and *S. virginica*. The individual fluxes for the different time periods can be summed to estimate the annual net production, mortality, dry matter loss, and the annual uptake and loss numbers that represent estimates of the amount of mercury species vectored through the marsh plants (Table 5-1 and Table 5-2). These data are representative for the natural cycle of transfer of mercury species through the vegetation in an established coastal marsh on San Pablo Bay. Both plant species exhibit great primary production rates in May and June and significant fragmentation/leaching rates in May and July (Figures 5-8 and 5-9).

The dataset is still incomplete, but from the data collected thus far the following is apparent. In the period between 21 April and 22 August annual net primary production in *S. foliosa* was approximately 1,499 g DW m^{-2} (Table 5-1). The latter value is probably close to actual net primary production in this plant species, as inferred from the regression line fitted to the aboveground live standing crop (Figure 5-2). In the same period, 26.173 µg THg m^{-2} and 0.588 µg MeHg m^{-2} were taken up. Assuming that the uptake in this period represents about 75% of the total annual uptake, as demonstrated in a similar study on trace metal uptake in other coastal plants in a nearby Oregon marsh (Gallagher and Kibby 1980), annual uptakes of 34.897 µg THg m^{-2} and 0.784 µg MeHg m^{-2} were tentatively estimated. Loss by fragmentation and leaching is expected to approximate uptake in established vegetation.

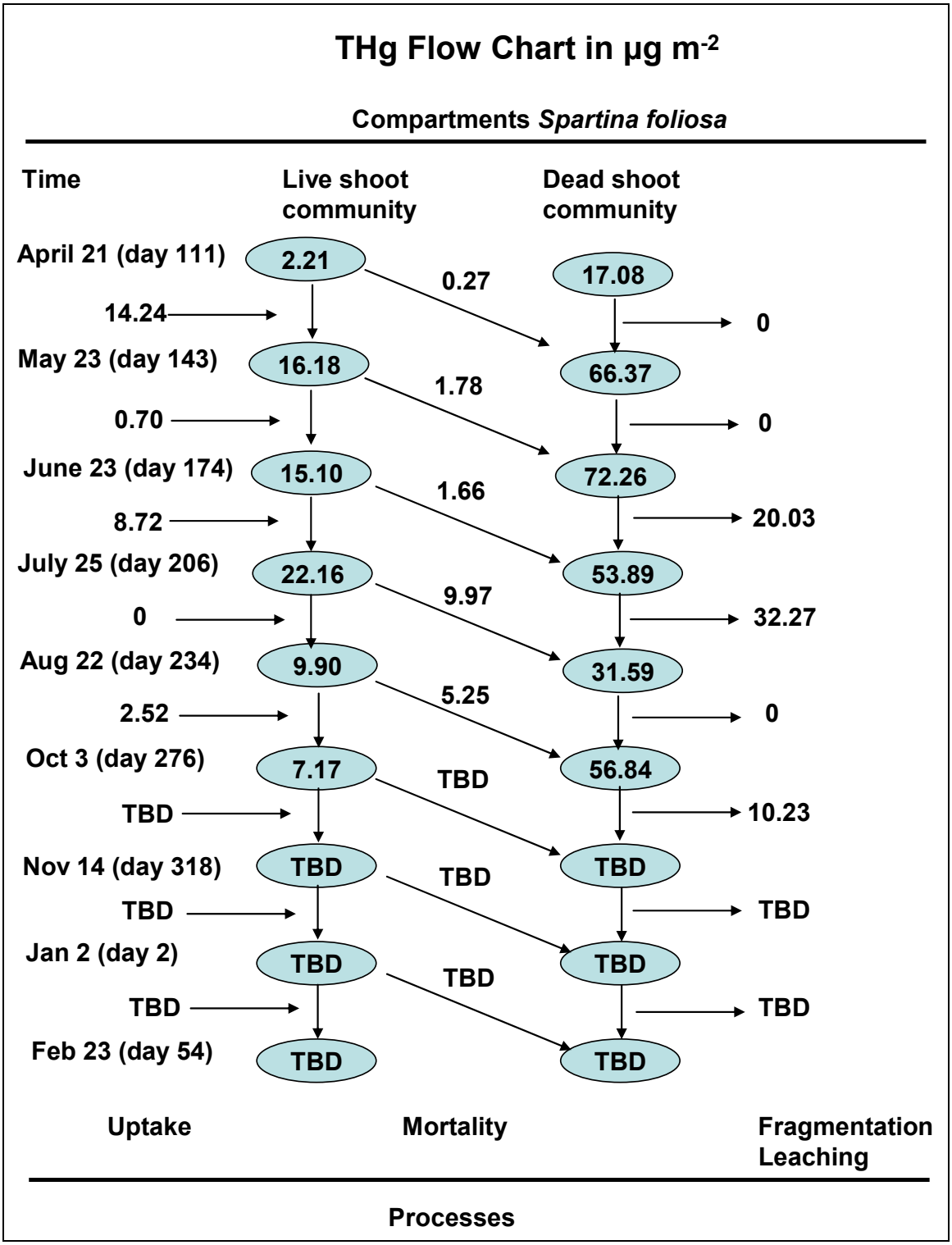

Figure 5-7. Flow chart of the flux of mercury through live *Spartina foliosa* and the community associated with the attached dead plants at low marsh site R-44 of the China Camp State Park. Dates are followed by Julian day numbers between parentheses. Mean values 2005.

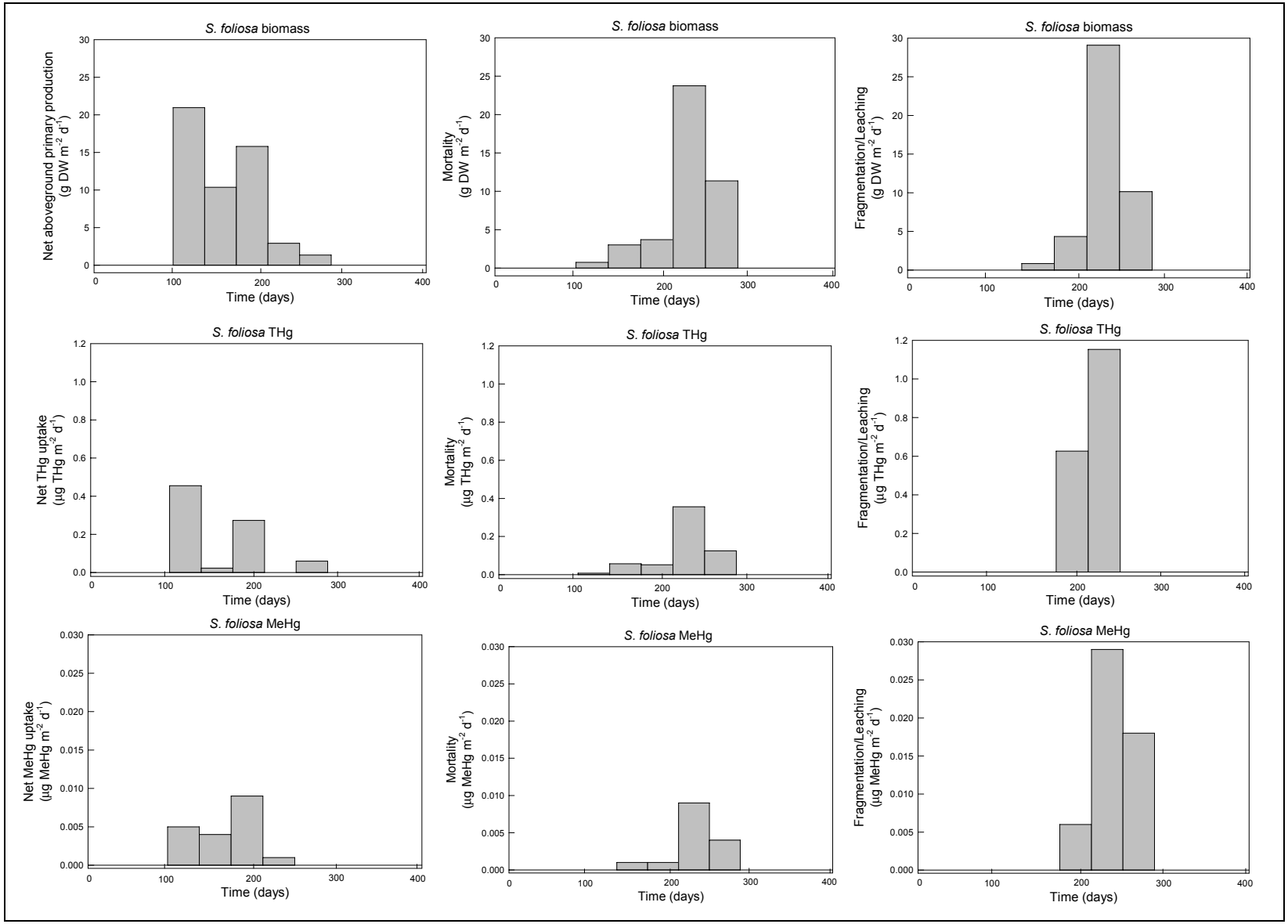

Figure 5-8. Seasonal changes in the estimated net aboveground production, uptake rates of THg and MeHg, and the mortality and fragmentation/leaching rates of *Spartina foliosa* at low marsh site R-44 of the China Camp State Park. Mean values 2005.

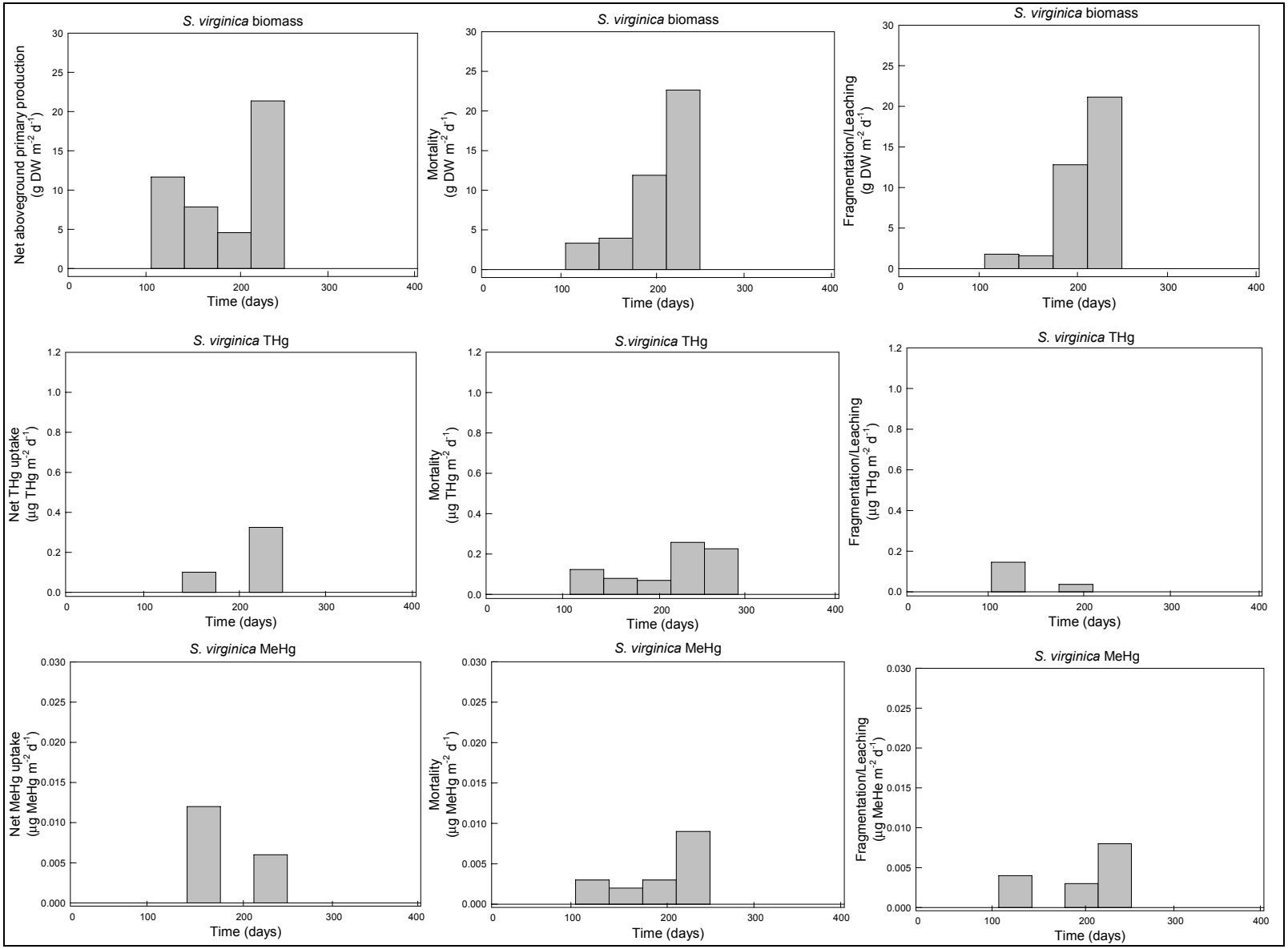

Figure 5-9. Seasonal changes in the estimated net aboveground production, uptake rates of THg and MeHg, and the mortality and fragmentation/leaching rates of *Salicornia virginica* at low marsh site R-44 of the China Camp State Park. Mean values 2005.

Following the same reasoning, in the period between 21 April and 22 August annual net primary production in *S. virginica* was approximately 1,361 g DW m^{-2}. The latter value is probably less than actual net primary production in this plant species, as inferred from the regression line fitted to the aboveground live standing crop (Figure 5-2). In the same period, 9.422 µg THg m^{-2} and 0.018 µg MeHg m^{-2} were taken up, tentatively resulting in annual uptakes of 12.562 µg THg m^{-2} and 0.024 µg MeHg m^{-2}, with loss by fragmentation and leaching being about equal to annual uptake. Because periodic uptake, fragmentation and leaching rates in *S. virginica* were usually a factor of 2 to 3 less than in *S. foliosa*, annual uptake and loss rates of mercury species are expected to be also about a factor of 2 to 3 less than those of *S. foliosa*.

The preliminary primary production estimates resulting from the current study of 1,499 g DW m^{-2} for *S. foliosa* and 1,361 g DW m^{-2} for *S. virginica* have been compared to other production estimates for San Francisco Bay tidal marshes (Table 5-4). For *S. foliosa* the estimate is similar to the net production measured in Tolay Creek on San Pablo Bay, and for *S. virginica* it is in the same range as reported for Petaluma River and Creekside Park. The live aboveground biomass values of *S. foliosa* were similar to values reported for *Spartina alterniflora* marshes along the east coast of North America (reviewed by Hussey and Long 1982) and The Netherlands (Groenendijk 1984) but less than the extremely large peak standing crops of 2,000 and 3,000 g m^{-2} found in American salt marshes of more southern latitudes. The live aboveground biomass values of *S. virginica* were in the same order of magnitude as found in more southern coastal marshes in California by Zedler et al. (1980) and Onuf (1987), ranging from 412 to 1,046 g DW m^{-2}.

Annual mass balances

Based on the tentative estimates of annual uptake and loss of mercury species through vegetation, the overall potential input of mercury species by the studied plant species from sediment into the food web, expressed on a same-size area basis, would be greater from *S. foliosa* than by *S. virginica*.

Table 5-4. Summary of estimated annual net primary production (NPP) of *Spartina foliosa* and *Salicornia virginica* in San Francisco Bay tidal marshes. Most studies use end-of-season biomass to estimate primary production, except those reported by Josselyn (1983) which are estimated using the Smalley method, and Best (this report) which are estimated using a combination of the methods of Smalley and Wiegert-Evans, modified by Lomnicki.

Location	Year	NPP (g DW m^{-2})	Quadrat Size (m^2)	Quadrats per Station	Sampling Frequency per Year	Reference
S. foliosa						
Tolay Creek San Pablo Bay	1968	1,400	0.25	5	52	Cameron (1972)
Mare Island, San Pablo Bay	1972	274	0.125	8	1	Mahall and Park (1976a)
Petaluma River	1972	689	0.125	8	1	Mahall and Park (1976a)
Creekside Park, Corte Madera Creek	1982	950	0.20	5	7	Josselyn (1983)
Corte Madera Bay	1982	710-1,120	0.20	5	7	Josselyn (1983)
China Camp State Park	2005-6	1,499	0.026	7	9	Best (This Report)
S. virginica						
Tolay Creek San Pablo Bay	1968	1,050	0.25	5	52	Cameron (1972)
Mare Island, San Pablo Bay	1972	820-958	0.125	8	2	Mahall and Park (1976a)
Petaluma River	1972	590	0.125	8	2	Mahall and Park (1976a)
Petaluma River	1979	604-1,462	0.25	10	2	Balling and Resh (1983)
Muzzi Marsh, Corte Madera Bay	1982	950-1,500	0.10	10	2	Josselyn (1983)
Creekside Park	1982	600-1,000	0.10	4	7	Josselyn (1983)
China Camp State Park	2005-6	1,361	0.026	7	9	Best (this report)

S. foliosa has an annual net primary production of 14,499 kg DW ha^{-1} and uptake of 0.348 g THg ha^{-1} and 0.008 g MeHg ha^{-1} (Table 5-5). *S. virginica* has an annual net primary production of 13,610 kg DW ha^{-1} and uptake of 0.094 g THg ha^{-1} and 0.002 g MeHg ha^{-1} (Table 5-5). The estimated uptake and loss rates of THg are low compared to loss rates with particulate plant matter reported for other metals (Cd, Pb, Cr, Cu, and Ni) in a *Spartina alterniflora*-predominated marsh on the Atlantic coast, where loss rates ranged from 17 to 779 g ha^{-1} (Kraus 1988). In the latter study, the importance of excretion of metals, including mercury through salt glands was emphasized.

Table 5-5. Annual net primary production and mercury species mass balances.

Compartment	Net Primary Production (kg DW ha^{-1})	Plant Uptake/Loss		Volatilization (g THg ha^{-1})	Deposition (g THg ha^{-1})
		(g THg ha^{-1})	(g MeHg ha^{-1})		
Spartina foliosa	14,990	0.348	0.008	0.518	23.20
Salicornia virginica	13,610	0.094	0.0002	0.518	23.20
Fresh water	-	-	-	0.066	23.20

Scaling up of the net primary production and biomass loss rates and mercury species uptake and loss rates to the 203-ha surface area of the HAAF would result in the following tentative estimates:

1. A completely *S. foliosa*-vegetated HAAF-size system would have an annual net primary production and similar biomass loss rate of 3,045 × 10^3 kg DW, a THg uptake and loss rate of 70.64 g, and a MeHg uptake and loss rate of 1.62 g.
2. In contrast, a *S. virginica*-vegetated HAAF-size system would have an annual net primary production and similar biomass loss rate of 2,858 × 10^3 kg DW, a THg uptake and loss rate of 19.08 g, and a MeHg uptake and loss rate of 0.04 g.

As pointed out earlier, this approach emphasizes the relationships between concentrations of mercury species in sediment and those in particulate plant material, but it does not take gaseous transpiration (volatilization) of mercury in the form of Hg^0 into account. Volatilization from vegetation was recently measured in the freshwater wetlands in the Everglades and ranged from 17 to 31 ng THg m^{-2} h^{-1} (Lindberg et al. 2002). Assuming a mean volatilization rate of 24 ng THg m^{-2} h^{-1}, a 12-h light day, and a 180-d growth season, annual volatilization above a wetland vegetation would be 51,837 ng m^{-2} or 0.518 g THg ha^{-1} (Table 5-5). Reasoning along these lines, volatilization above a completely vegetated HAAF system would be $\geq$105 g THg y^{-1}. Volatilization above fresh water was 8 to 15 times lower than above vegetation, i.e., 1 to 2 ng THg m^{-2} h^{-1} (Lindberg et al. 2002). Conservatively assuming a mean volatilization rate of 1.5 ng THg m^{-2} h^{-1}, a 12-h light day and 365-d year, annual volatilization above a completely inundated system would be 6,567 ng m^{-2} or 0.066 g THg ha^{-1} (Table 5-5) and for a HAAF-size system 13.3 g THg y^{-1}. The estimated volatilization above the vegetation is above the range, and above the water

close to the lower limit of the range of 6,664 to 24,600 ng THg m^{-2} y^{-1} estimated by Conaway et al. (2003) above San Francisco Bay. These volatilization values are great when one compares them with the recently measured annual THg deposition of 23,200 ng THg m^{-2} in the San Francisco Bay area (Tsai and Hoenicke 2001). The estimates would be equivalent to an annual deposition of 0.232 g THg ha^{-1} or 47.1 g THg for a HAAF-size system. A completely vegetated HAAF has the potential to volatilize all of THg that would be deposited on a HAAF-size surface area. The estimated volatilization rates above the vegetation are greater than the net uptake and loss rates through leaching and fragmentation in *S. foliosa* and *S. virginica*, and, if true, would add significantly to the mercury uptake rates and to a larger scale mass balance of the system. However, the volatilization rates measured in the Everglades are exceptionally great and represent a subtropical ecosystem vegetated by cattails. Actual rates for HAAF are presumably less than those observed in Florida because cattails have high evapotranspiration rates and temperatures in subtropical Florida are higher than in San Pablo Bay.

Entry of mercury into the food web

The actual effects of the inputs of mercury-species-containing plant-derived particulate matter into the food webs would depend on trophic level, food preference, seasonal cycle of the consumer, total sediment surface area vegetated, location of the vegetation in the marsh landscape (elevation relative to sea level, distance to subtidal area), and estuary-bay landscape. Since the levels of mercury species in dead plant material greatly exceed those in live plant material (on a dry weight basis), detritivores would ingest greater mercury concentrations than herbivores, and consumers of *S. foliosa* would ingest more MeHg than those of *S. virginica*. The trophic relationships within the marsh-dependent food web and tentative fate of mercury species at various trophic levels have been explored and are further discussed in Chapter 7.

Conclusions

1. Salt marsh vegetation differentially takes up THg and MeHg from the sediment.
2. *S. foliosa* has a greater annual net primary production and uptake of THg and MeHg than *S. virginica*.
3. Plant litter contains greater levels of THg and MeHg than live plant biomass, potentially forming a source of exposure for detritivores.

POINT OF CONTACT CHAPTER 5:

Dr. Elly P. H. Best
U.S. Army Engineer Research and Development Center
Environmental Laboratory, Vicksburg, MS
Ph: 601-634-4246; E-mail: elly.p.best@erdc.usace.army.mil

6 Dynamics of Mercury, Methylmercury, and Stable Isotope Signatures in Decomposing Macrophytes from a Tidal Marsh on San Pablo Bay

Introduction

The contamination of fish with monomethylmercury (MeHg) has created great interest in mercury cycling and speciation in the environment. Atmospheric deposition of MeHg has been implicated in elevated levels of Hg in fish of Scandinavian lakes (Hultberg et al. 1994). In North America, lakes receive comparatively small amounts of atmospheric MeHg but contain fish whose MeHg burdens make them unsuitable for human consumption. A correlation between the proportion of catchment area that is wetland which is immediately adjacent to a lake and the concentration of MeHg in fish was established by Driscoll et al. (1994) for Adirondack lakes. Wetlands contain considerable stores of MeHg in both peat and pore water (Heyes 1996; St. Louis et al. 1994, 1996; Best et al. 2005; Chapter 4 of this report), and wetlands in general have been identified as sources of MeHg to downstream lakes. Although the importance of wetlands as sources of MeHg has been realized, studies of the internal cycling of Hg or production of MeHg within wetlands were only recently initiated. MeHg concentrations are also elevated in fish of newly formed reservoirs, where the source is thought to be large amounts of decomposing plant material due to flooding (Bodaly et al. 1984). The MeHg concentration of fish in limnocorrals was experimentally enhanced by the addition of vegetation or soil (Ramlal et al. 1987). Both additions also increased the methylation rate of added ^{203}Hg while decreasing oxygen levels. This suggests a relationship between greater rates of Hg methylation, anoxic decomposition, and elevated levels of MeHg in fish. Ramlal's study indicates that the increase in Hg methylation cannot be linked directly to the elevated MeHg levels in fish since the added ^{203}Hg is potentially more available for methylation than the THg in soil and vegetation. The study also did not account for presence of MeHg in plants (Moore et al. 1995). Decomposition may occur in wetlands under aerobic and anaerobic conditions. The primary methylators of Hg are SRB (Compeau and Bartha 1985; King et al. 2000; Macalady et al. 2000; Batten and Scow 2003), which are considered

primarily as anaerobes. However, SRB have also been detected under aerotolerant aerobic conditions (Hines et al. 1999; Ito et al. 2002; Okabe et al. 1999). It is possible that during the decomposition process of fresh plant material, under the largely anoxic conditions that exist in the near-surface saturated wetlands soils and at the bottom of reservoirs, the Hg stored in and on plant material is methylated as suggested also by the authors in Chapter 5 of this report. Another possibility would be that shading by the vegetation canopy would reduce photodemethylation. This would explain why wetlands and reservoirs are sources of MeHg. If pre-existing MeHg is released from the plant material after flooding, the mass of tissue MeHg should decrease during decomposition. However, if the methylation of inorganic Hg in the decomposing plant litter occurs through methylation, the mass of tissue MeHg will increase.

Salt marsh plants may be a factor in mercury bioaccumulation in the food webs of the salt marsh as well as the adjacent part of the bay. It appears that many animals preferentially consume macrophyte detritus as opposed to fresh material (Mann 1988). Microbial utilization may represent a major sink for marsh primary production (Zedler 1982). Aquatic food webs are fueled by primary producers from marsh and open water (Kwak and Zedler 1997) in Southern California, while food webs of tidal salt marshes along the northern Pacific coast are detritus-based (Sibert 1977; Naiman and Sibert 1979). In the current study, stable isotope ratios were used to explore their value as identifier of food source for consumers. Stable isotope ratios reflect the nutrients assimilated, rather than the material ingested, and characterize the diet over a greater time period than traditional methods such as gut content analysis (Peterson and Fry 1987). In freshwater systems, usually the stable isotope ratios of carbon and nitrogen suffice, but in estuarine and marine systems the stable isotope ratio of sulfur adds considerably to explaining the composition of the food web which is tied to food sources from fresh or saline water (Hobson 1999; Kwak and Zedler 1997; Lubetkin and Simenstad 2004). Carbon isotope ratios have been reported to behave conservatively, because they change about 1‰ during trophic transfer, thus serving as a source indicator (Fry and Sherr 1984). Plants exhibiting a C_4 photosynthetic pathway, e.g., *Spartina foliosa*, have distinctly greater (~10‰) carbon isotope ratios than C_3 plants, e.g., *Salicornia virginica* (O'Leary 1981). The nitrogen isotopic ratio is widely used as a trophic level indicator, because the isotope ratios change on average by 3‰ during trophic transfer (Minagawa and Wada 1984). The sulfur isotopic ratio did not show a

significant shift per trophic level in studies published so far (Peterson et al. 1986; Peterson and Howarth 1987; Fry 1988, 1991; Hesslein et al. 1993; Michener and Schell 1994). For this study, the stable isotopes of carbon, nitrogen, and sulfur were determined.

Objectives

In the present study, three questions are addressed:

1. How rapidly does salt marsh vascular plant dry mass decrease when decomposing under controlled environmental conditions representative for those in the field?
2. Is mercury stored in and on the surface of the plant material methylated during the decomposition process?
3. Can stable isotope signatures serve as indicators for the utilization of decomposing salt marsh vascular plant material in food chains?

Study site

The Hamilton Army Airfield (HAAF) Wetlands Restoration Site on San Pablo Bay is part of the San Francisco Baylands. It is located in the North Bay. The Baylands consist of the shallow water habitats around the San Francisco Bay. The Baylands ecosystem includes the areas of maximum and minimum tidal fluctuations, adjacent habitats, and their associated plants and animals. The boundaries of the ecosystem vary with the bay-ward and landward movements of fish and wildlife that depend upon the Baylands for survival. Many habitats of the Baylands are wetlands. Habitat goals selected for the planned restored HAAF wetland, with a surface area of 203 ha, include the restoration of tidal marshes, with natural transitions into upland areas with seasonal wetlands. The restored HAAF area is expected to increase the habitat of the regionally rare and protected clapper rail and salt marsh harvest mouse because it is adjacent to existing populations, will contain a large tidal wetland, and is remote from predator outposts and corridors (San Francisco Bay Area Wetlands Ecosystem Goals Project 1999).

The test site representative for the tidal part of HAAF was situated at the HAAF bay edge (SM-10; 38° 03.116′ N, 122° 29.55′ W; Figure 6-1). The nearby tidal salt marsh at the China Camp State Park (R44; 38° 00.411′ N, 122° 28.758′ W), chosen as a reference, covers 45 ha (Hopkins and Parker 1984) and is frequently immersed by tidal waters (salinity 25-32‰;

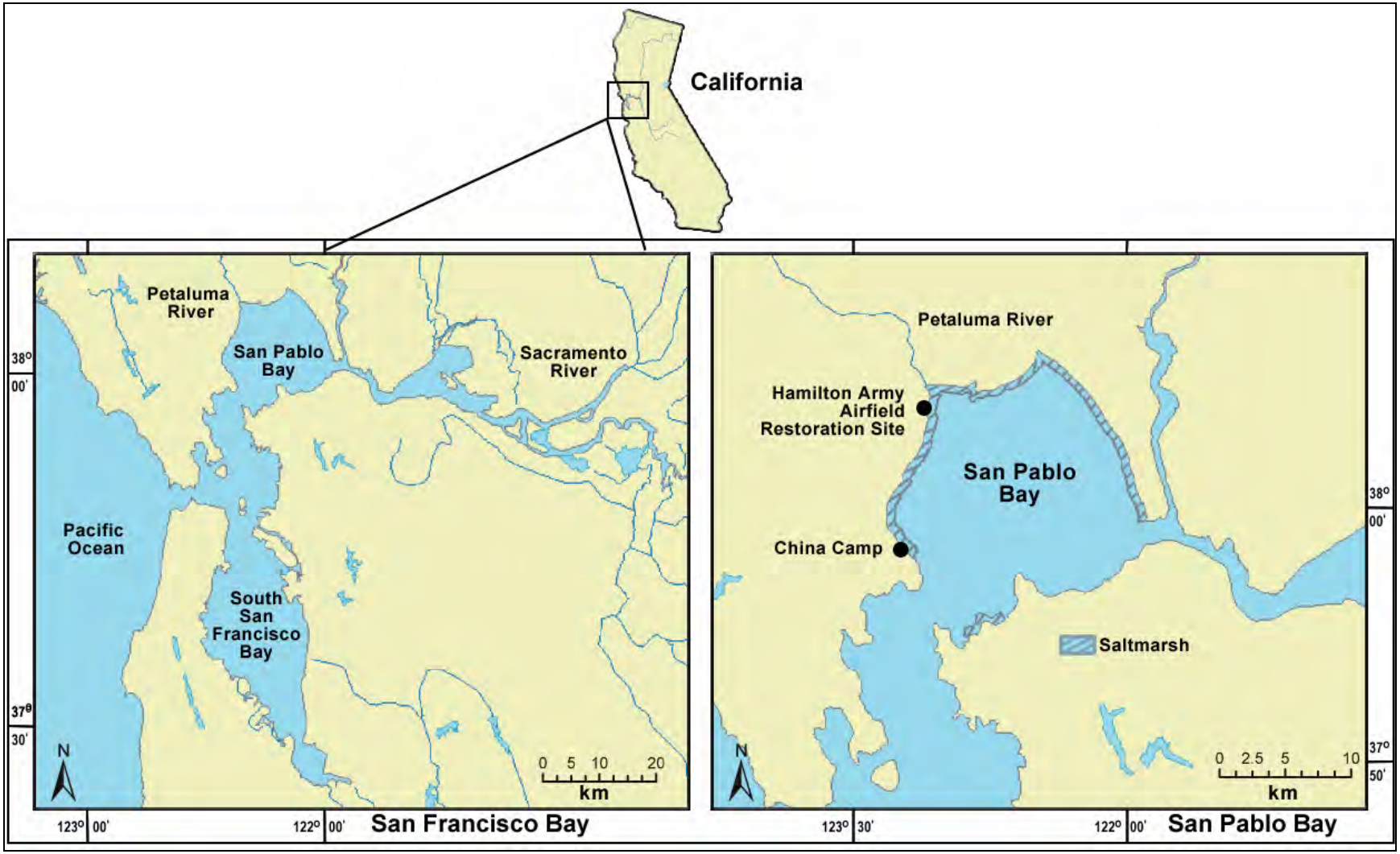

Figure 6-1. Site map showing the location of San Pablo Bay within San Francisco Bay (left) and the location of the Hamilton Army Airfield Restoration Site and the China Camp reference site (right).

Figure 6-1). The tidal salt marsh at China Camp is predominated by *Spartina foliosa (Pacific cordgrass)* on the low marsh between mean tidal level (MTL) and mean high water level (MHW), and by *Salicornia virginica* (common pickleweed) at somewhat higher levels and above MHW.

Materials and methods

Materials

Plant litter

Large samples of standing aboveground, scenesced, biomass of *S. foliosa* and *S. virginica* were collected from the tidal marsh at the China Camp State Park reference site on 26 March 2004 (Currin et al. 1995; Figure 6-2). The samples were dried to constant weight at 60 °C to minimize errors in weighing. The dry litter was clipped into approximately 4-cm-long pieces with scissors, mixed, and stored until use (Figure 6-2).

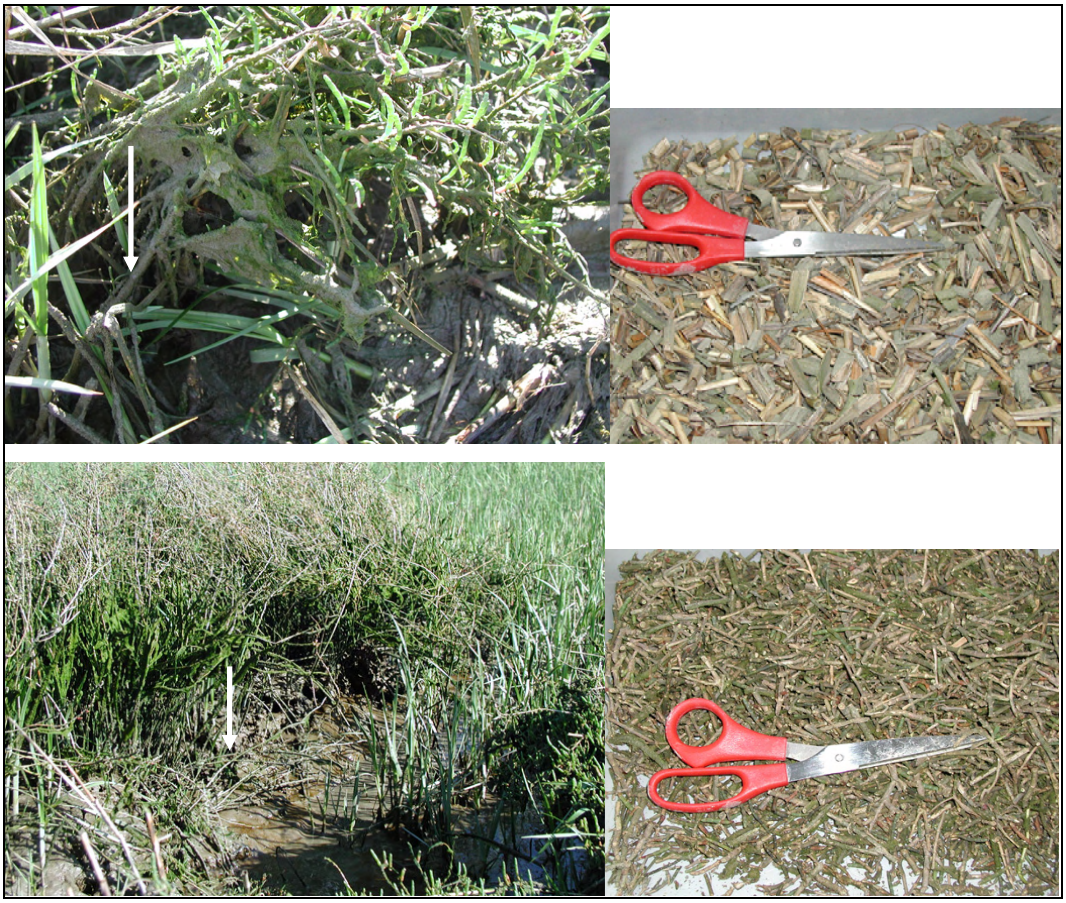

Figure 6-2. *Spartina foliosa* (upper) and *Salicornia virginica* (lower) in March 2004. Standing, scenesced aboveground parts sampled marked by arrows (left). Materials were dried and clipped prior to incubation (right).

Portions of plant litter, originating from these relatively homogeneous batches, were placed loosely into nylon gauze (1-mm mesh-size, 15 × 15 cm litter bags) and closed by a string.

Water

Common microorganisms in the water of San Pablo Bay were included in all treatments. The water for the incubations was freshly collected from the upcoming tide at China Camp on 26 March 2004. It was shipped on ice to the Environmental Laboratory, ERDC. Vicksburg, MS, stored under refrigeration, and used without prior treatment for the incubation within 3 days after collection. A 700-mL volume was placed in each vessel.

Sediment

Common microorganisms in the sediment of the China Camp State Park reference site were also included in all treatments. Sediment (0-10 cm) was excavated, shipped on ice to the Environmental Laboratory, ERDC, Vicksburg, MS, and stored under refrigeration until use within 3 days of collection. Approximately 2 kg WW was mixed thoroughly in a plastic tray using a scoop, and 50 g WW (equivalent to 20 g DW) was placed in each vessel.

Incubations

Dry mass weighing 12 to 15 g per plant species, per vessel, was incubated in the laboratory in vessels containing water and sediment under aerobic and under anaerobic conditions. Litter bags were placed into 2-L plexi-glass cylindrical vessels (0.125-m diameter) containing the sediment and water. The vessels were closed with a gas-tight lid. The litter bags were situated on small stainless-steel wire-mesh tables inside the vessels, and water and sediment were mixed continuously using a magnetic stirrer that kept water and sediment mixed by the stir bar inside the vessels without moving and damaging the litter bags. The aerobic series of vessels was aerated twice a week by sparging enough air into the aqueous phase to bring the oxygen concentration to a level of 7.1 mg L^{-1} (verified by oxygen measurements). In the anaerobic series of vessels, the aqueous phase was sparged twice a week with oxygen-free nitrogen to decrease the oxygen levels to ≤0.1mg L^{-1}. Vessels were incubated in a walk-in growth chamber illuminated with 500-600 μE m^{-2} s^{-1} at the top of the vessels (in the order

of 25% of full sunlight at noon of a bright summer day) at a 14-h photoperiod and temperature of 22 °C–26 °C (Figure 6-3).

Sample collection

Three samples/litter bags of each plant species were retrieved on five occasions during a 150-day period. The plant materials were dried to constant weight at 70 °C, weighed, and ground in a IKA mill (Janke & Kunkel, Wilmington, NC). Oxygen levels of the aqueous phase were measured before each sparging, for verification of the sparging treatment, and at the end of the incubation period, using Clark-type electrodes (YSI Model 59). Oxygen concentrations in the water of the aerobic series fluctuated between 7.1 and 0.2 mg L^{-1} between sparges. The pH was measured initially and at the end of the incubation period.

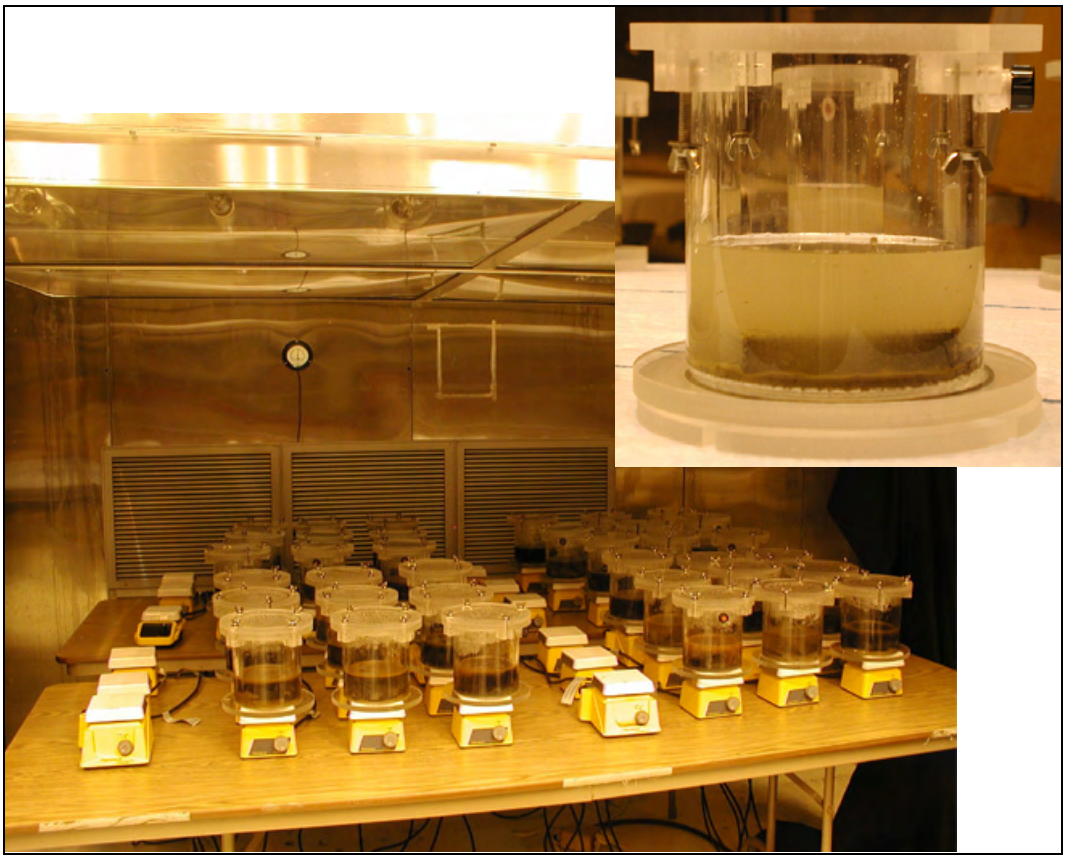

Figure 6-3. Incubations of *Spartina foliosa* and *Salicornia virginica* plant materials in litter bags with sediment and seawater in the laboratory under aerobic and anaerobic conditions.

Methods

Mercury species, elemental, and stable isotope determinations

Total mercury. THg was determined by isotope dilution ICP/MS after Hintelmann and Ogrinc (2003) in H_2SO_4/HNO_3 digests using continuous-flow cold-vapor generation with ICP/MS detection (Finnigan MAT, Model Element 2). For internal standard $^{201}Hg^{2+}$ was added. The acidified samples were continuously mixed with a solution of stannous chloride by means of a peristaltic pump. The formed mercury vapor was separated from the liquid in a gas-liquid separator (Model L1-2), and the elemental mercury was swept into the plasma of the ICP/MS. The following isotopes of Hg were measured: ^{201}Hg (internal standard) and ^{202}Hg (to calculate ambient total Hg).

Methylmercury. MeHg was determined according to Hintelmann and Evans (1997). For this, a 0.2-g sample was weighed into 30-mL Teflon vials and suspended with an additional 10 mL of distilled water. $CH_3{}^{201}HgCl$ (55 pg) was added as an internal standard. After 200 µL of H_2SO_4 (9 M) and 500 µL of KCl (20%) were added, the vessel was placed into a heating block at 140 °C. MeHg was distilled from the sample under a supporting nitrogen stream (80 mL min^{-1}) over a period of approximately 60-90 min per sample.

A reaction vessel was filled with 100 mL Milli-Q water, and the distillate was added for measurement of MeHg. About 0.2 mL of acetate buffer (2 M) was added to adjust the pH to 4.9. Sodium tetraethylborate (100 µL, 1% w/v) was added and the solution sat at room temperature for 20 min while the tetraethylborate reacted. Tenax adsorber traps were connected to the reaction vessel and the generated methylethylmercury was purged for 20 min from the solution using nitrogen (200 mL min^{-1}) and collected on the Tenax trap. Finally, all mercury species were thermally desorbed from the trap (250 °C), separated by gas chromatography, and quantified by ICP/MS (Micromass Platform). The following isotopes of Hg were measured: ^{201}Hg (internal standard) and ^{202}Hg (to calculate ambient MeHg). Peak areas were used for quantification, and concentrations of individual isotopes were calculated as described in Hintelmann and Ogrinc (2003).

Mercury analysis QA/QC. For each batch of samples the following set of QA/QC samples was measured: three reagent blanks (THg) or bubbler blanks (MeHg), and a certified reference material (IAEA 356 marine sediment and MESS-3 marine estuary sediment for sediment analysis and NIST 1515 apple leaves for plant analysis). Individual distillation yields were determined using the added internal ^{201}Hg isotope standard. Typically, one triplicate sample was analyzed (i.e., triplicate distillation or digestion) per batch.

Elemental and stable isotope analysis. The analyses of carbon, nitrogen, sulfur concentrations, and the determinations of their stable isotope ratios in organic matter were carried out using a Costech (Costech Analytical, Valencia, CA) 4010 ECS Elemental Analyzer with a 50-sample autosampler and CNHS detection, Conflo interface, Isodat data program, and Isotope Ratio Mass Spectrometer (IRMS). Analyses involved complete combustion of the sample to a gas and separation of the pure gases (CO_2, N_2 and SO_2; Fry and Sherr 1984; Peterson and Fry 1987). A pure gas was then introduced into an IRMS, and the isotopic composition was quantified relative to a standard reference material. Standards were carbon in PeeDee Belemnite for ^{13}C, atmospheric nitrogen for ^{15}N, and sulfur in the Canyon Diablo meteorite for ^{34}S. Results for each elemental stable isotope were expressed in difference from the standard (δ) as parts per thousand (‰):

$$\delta X = [(Rsample/Rstandard)-1] \times 10^3$$

where X is ^{13}C, ^{15}N, or ^{34}S, and R is the corresponding ratio of $^{13}C/^{12}C$, $^{15}N/^{14}N$, or $^{34}S/^{32}S$. The δ values denote a greater proportion of the heavy isotope. Standard deviations of $\delta^{13}C$, $\delta^{15}N$, and $\delta^{34}S$ replicate analyses of the standards and the dry samples were 0.2‰, 0.2‰, and 0.5‰, respectively.

Details of the determinations of Hg species and elemental and stable isotope determinations are provided in the Chapters 3 and 4.

Microbial biomass determinations using polar lipid fatty acid methylester analysis

PLFAME analysis has been detailed elsewhere (Fredrickson et al. 1986). Briefly, 2 g (WW) samples were collected from the litter bags and from the original batches of fresh plant material and sediment prior to incubation.

All samples were lyophilized. These samples were extracted for 3 h at room temperature in 6 mL of a mixture of dichloromethane:methanol:water (1:2:0.8, v:v:v). Amino-propyl solid phase extraction columns (Supelco, Bellefonte, PA) were used to separate the total lipid into neutral, glyco- and polar lipid fractions. Phospholipid fatty acid methyl esters (from the polar lipid fraction) were prepared for gas chromatography/mass spectrometry (GC/MS) by mild alkaline methanolic transesterification. The resulting phospholipid fatty acid methyl esters were dissolved in hexane containing methyl nonadecanoate (50 pmol μL^{-1}) as an internal standard. Then these esters were analyzed using a gas chromatograph equipped with a 50 m × 0.25 mm (ID) DB-1 capillary column (0.1-µm film thickness, J&W Scientific, Folsom, CA) and a flame ionization detector. Peak identities were confirmed using a gas chromatograph-mass selective detector (Hewlett Packard GC6890-5973 MSD) with electron impact ionization at 70 eV. Areas under the peaks were converted to concentrations, summed, and then normalized to the gram weight extracted for biomass determinations. For community comparisons, the percentage contribution of each peak was calculated and then normalized using an arcsine square root transformation. The following SRB were distinguished by their characteristic FA biomarkers: *Desulfobacter hydrogenophilus* and *Desulfobacterium autotrophicum* by 10-Methyl 16:0 (10Me16:0) and *Desulfovibrio desulfuricans* by iso17:0 (i17:0) (Boon et al. 1977; Taylor and Parkes 1983; Vainshtein et al. 1992). *Desulfobacter* and *Desulfobacterium* biomasses are indistinguishable from each other with this biomarker approach, and, therefore, their combined biomass is further referred to as *Desulfobacter* biomass in this chapter. For comparison with literature data, 1 pmole PLFAME is considered as equivalent to 2.5×10^4 microbial cells. For further identification of phylogenic groups, oligonucleotide probes may be suitable to be used in the future (Daly et al. 2000).

Statistical analysis

Statistical analyses were conducted with the software STATGRAPHICS Plus for Windows version 32S package (Manugistics, Rockville, MD). Normal distribution of the data was tested using the Shapiro-Wilk's test. Analysis of variance (ANOVA) was expanded with a multiple range test using Fisher's least significant difference procedure. The p-value in the ANOVA is a measure of the significance of the analysis; it was set at a 95% confidence level (p value of ≤ 0.05). Regression analyses were conducted using the least squares method. The p-value in the regression model was set at a 95% confidence level (p value of ≤ 0.05) unless stated otherwise.

The R^2-value of the regression model indicates the proportion of the variance explained by the model. Regression models explaining at least 50% of the variability in the data set, i.e., $R^2>0.50$, were considered as providing a good fit.

Results and discussion

Change in dry mass

Dry mass loss differed significantly between both plant species, as demonstrated by ANOVA ($p<0.001$). Therefore, further analyses of data sets for each plant species were conducted separately.

S. foliosa litter lost 58% and 66% mass within 150 days. Mass decreased initially exponentially, but increased somewhat at the end of the 150-day period. Therefore, a polynomial model fitted the data better than an exponential model (Figure 6-4). Mass loss was greatest during the initial ten days of incubation. Mass loss was significantly faster under aerobic than under anaerobic conditions (Figure 6-4; Table 6-1).

S. virginica litter lost 83% and 84% mass within 150 days. Mass loss in this litter also was greatest during the initial ten days of incubation but significantly slower under aerobic than under anaerobic conditions (Figure 6-5; Table 6-2).

Patterns differed between both species, in that mass was lost more slowly in *S. foliosa* than in *S. virginica*, and mass loss was greater under aerobic than in anaerobic conditions in *S. foliosa*, but less under aerobic than anaerobic conditions in *S. virginica*. Remaining mass patterns were similar in both plant species, in that mass decreased initially exponentially and increased slightly at the end of the incubation period. The latter increase was attributed to adsorption of sediment-microbial aggregates moved by the stir bars inside the incubators. Mass loss was significantly affected by incubation time, oxygen concentration in the water, C:N ratio, the concentrations of THg and MeHg, and the MeHg:THg ratio of the litter (ANOVA; $p<0.001$).

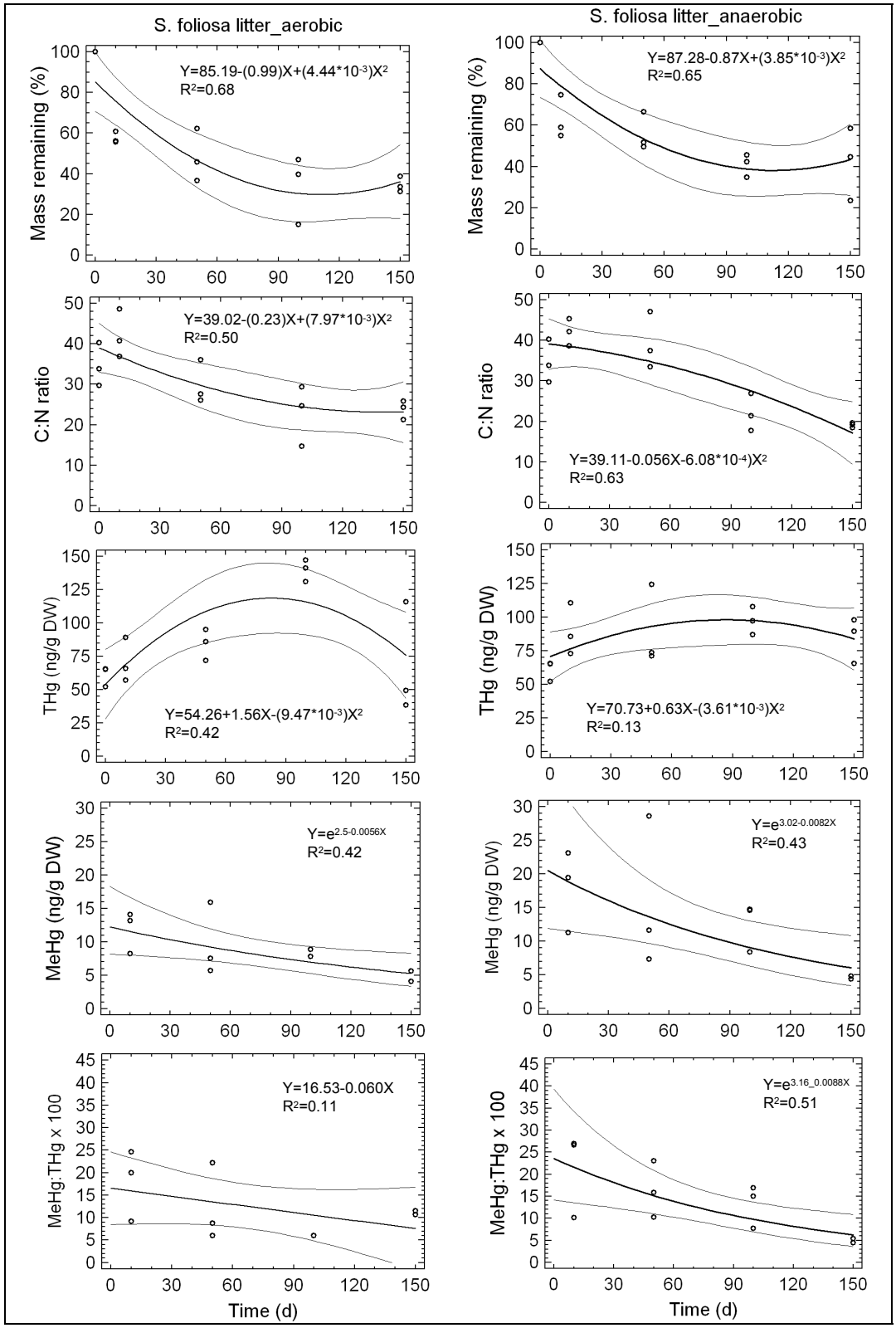

Figure 6-4. Changes over time of mass loss, C:N ratio, concentrations of THg and MeHg, and MeHg:THg ratio in decomposing litter of *Spartina foliosa*. Lines represent regression lines and 95% confidence limits. Regression equation and proportion of variance explained (R^2) by the fitted model indicated.

Table 6-1. Changes in decomposing plant litter of *Spartina foliosa* under aerobic and anaerobic conditions: mass, THg, MeHg concentrations, and MeHg:THg ratio. Values of sediment and 0.7 L water inoculum at the beginning of the experiment are given for reference. Mean values and standard deviations (N=3).

Incubation Period (days)	Mass		THg (ng g^{-1} DW)	MeHg (ng g^{-1} DW)	MeHg:THg Ratio (x100)
	(g DW)	(% Initial)			
S. foliosa, t_0	12.2 (1.7)	100 (0)	60.9 (7.6)	1.0 (0.0)	1.7 (0.3)
Aerobic					
10	7.0 (0.3)	57.5 (2.8)	70.8 (16.6)	11.8 (3.2)	17.9 (7.9)
50	5.8 (1.6)	48.2 (12.9)	84.3 (11.8)	9.7 (5.5)	12.3 (8.7)
100	4.1 (2.0)	33.9 (16.8)	139.9 (8.2)	8.3 (0.7)	6.0 (0.0)
150	4.2 (0.5)	34.5 (3.9)	67.8 (41.9)	4.9 (1.1)	11.1 (0.6)
Anaerobic					
10	7.6 (1.3)	62.8 (10.4)	89.8 (19.1)	17.9 (6.1)	21.2 (9.6)
50	6.8 (1.1)	55.9 (9.2)	89.6 (30.1)	15.9 (11.3)	16.4 (6.4)
100	4.9 (0.6)	40.8 (5.6)	97.4 (10.4	12.6 (3.6)	13.2 (4.8)
150	5.1 (2.1)	42.2 (17.6)	84.2 (16.9)	4.6 (0.3)	4.9 (0.6)
Sediment inoculum	20.0		297.0 (42.5)	1.2 (0.1)	0.4 (0.0)
Water inoculum[1]	NA	NA	463.0 (53.7)	1.10 (0.18)	0.2 (0.0)

[1] units ng L^{-1}. NA = not applicable.

Changes in total mercury and methylmercury concentrations in the decomposing litter

In *S. foliosa* litter, the THg concentration increased under aerobic conditions from 61 ng g^{-1} DW initially to 140 ng THg g^{-1} DW after 100 days of incubation, and decreased subsequently (Figure 6-4, Table 6-1). To a lesser extent, an increased THg concentration also occurred during incubation under anaerobic conditions. The total mass of THg contained in the litter decreased over time. The MeHg concentration in the litter increased strongly during the first 10 days of incubation and decreased exponentially thereafter. The initial increase was far less under aerobic conditions (from 1.0 to 11.8 ng MeHg g^{-1} DW) than under anaerobic conditions (from 1.0 to 17.9 ng g^{-1} DW; Figure 6-4, Table 6-1). The initial THg and MeHg concentrations in the incubation water at the beginning of the experiment were elevated compared to median values determined in surface waters of San Francisco Bay (9 ng THg L^{-1} and 0.0435 ng MeHg L^{-1} in bulk water) (SFEI 2004).

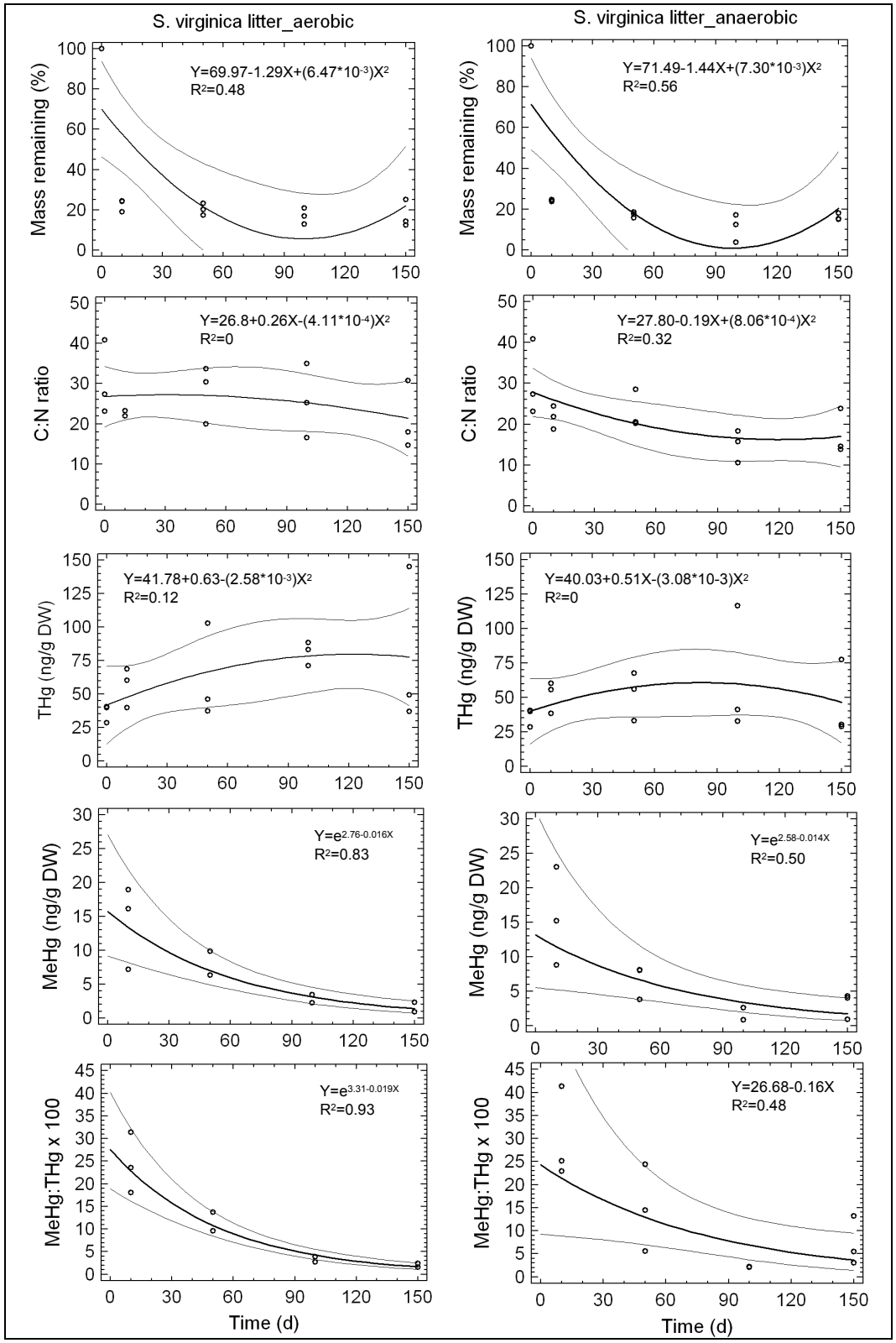

Figure 6-5. Changes over time of mass loss, C:N ratio, concentrations of THg and MeHg, and MeHg:THg ratio in decomposing litter of *Salicornia virginica*. Lines represent regression lines and 95% confidence limits. Regression equation and proportion of variance explained (R^2) by the fitted model indicated.

Table 6-2. Changes in decomposing plant litter of *Salicornia virginica* under aerobic and anaerobic conditions: mass, THg, MeHg concentrations, and MeHg:THg ratio. Values of sediment and 0.7 L water inoculum at the beginning of the experiment are given for reference. Mean values and standard deviations (N=3).

Incubation Period (days)	Mass		THg (ng g^{-1} DW)	MeHg (ng g^{-1} DW)	MeHg:THg Ratio (x100)
	(g DW)	(% Initial)			
S. virginica, t_0	14.2 (1.8)	100 (0)	36.2 (6.8)	1.0 (0.0)	2.9 (0.6)
Aerobic					
10	3.2 (0.4)	22.5 (3.0)	56.2 (14.8)	14.1 (6.1)	24.3 (6.7)
50	2.9 (0.4)	20.2 (2.9)	62.0 (35.5)	8.1 (2.5)	11.7 (2.9)
100	2.4 (0.6)	16.8 (4.0)	80.8 (8.9)	2.8 (0.8)	3.3 (0.8)
150	2.5 (1.0)	17.3 (6.9)	77.0 (59.2)	1.6 (1.0)	2.0 (0.6)
Anaerobic					
10	3.4 (0.1)	24.2 (0.5)	51.5 (11.6)	15.7 (7.1)	29.8 (10.1)
50	2.5 (0.2)	17.3 (1.5)	52.1 (17.6)	6.6 (2.5)	14.8 (9.4)
100	1.6 (1.0)	11.0 (6.9)	63.5 (46.1)	1.7 (1.2)	2.2 (0.1)
150	2.3 (0.2)	16.1 (1.6)	45.6 (27.8)	3.0 (1.9)	7.2 (5.3)
Sediment inoculum	20.0		297.0 (42.5)	1.2 (0.1)	0.4 (0.0)
Water inoculum[1]	NA	NA	463.0 (53.7)	1.10 (0.18)	0.2 (0.0)

[1] units mg L^{-1}; NA = not applicable.

This finding suggests that the water used for the experiment contained elevated concentrations of colloidal mercury species given off by mud flats that became submerged during the upcoming tide (Choe et al. 2003a, 2003b). However, this is the water that inundates the litter that stays in the marsh and further decomposes on site. The pH in the incubation water decreased (Table 6-3), indicating microbial organic acid formation. The total mass of MeHg contained in the incubated litter increased from an initial 12.2 ng to 82.6 ng (aerobic) and 136 ng (anaerobic) after 10 days, and decreased subsequently to 20.6 ng (aerobic) and 23.5 ng (anaerobic) after 150 days of incubation. The MeHg:THg ratio (in percent THg) increased initially rapidly from 1.7 to 17.9 and decreased subsequently to 11.1 under aerobic conditions, increasing initially to 21.2 and decreasing subsequently to 4.9 under anaerobic conditions. The increase of MeHg contained in the litter after 10-day incubation greatly exceeded the quantities added with the bay water and sediment and were, therefore, attributed to microbial activity.

Table 6-3. Changes in oxygen concentration and pH of the seawater in which the plant litter of *Spartina foliosa* decomposed. Mean values and standard deviations (N=3) of 3-day observations during incubation.

Incubation Period (days)	Oxygen Concentration (mg L^{-1})	pH
Water *S. foliosa*, t_0	7.1 (0.0)	7.5 (0.0)
Aerobic		
10	6.1 (0.9)	7.3 (0.4)
50	2.8 (3.5)	7.2 (0.4)
100	4.0 (2.8)	6.9 (0.1)
150	4.9 (0.3)	7.0 (0.0)
Anaerobic		
10	0.1 (0.1)	6.9 (0.4)
50	0.3 (0.1)	7.0 (0.2)
100	0.2 (0.1)	7.1 (0.2)
150	0.3 (0.2)	7.1 (0.5)

In *S. virginica* litter, the THg concentration increased under aerobic conditions from 36 ng g^{-1} DW initially to 81 ng THg g^{-1} DW after 100 days of incubation, and decreased subsequently. An increased THg concentration occurred also during incubation under anaerobic conditions, but to a lesser extent (Figure 6-5, Table 6-2). The MeHg concentration in the litter increased strongly during the first 10 days of incubation, and decreased exponentially thereafter. The initial increase was similar under aerobic and anaerobic conditions (from 1.0 to 14-16 ng MeHg g^{-1} DW; Figure 6-5, Table 6-2). The pH in the incubation water decreased (Table 6-4), which indicates microbial organic acid formation. The total mass of tissue MeHg in the incubated litter increased from an initial 14.2 ng to 45.1 ng (aerobic) and 53.4 ng (anaerobic) after 10 days, and decreased subsequently to 4.0 ng (aerobic) and 6.9 ng (anaerobic) after 150 days of incubation.

The MeHg:THg ratio (in percent THg) initially increased strongly from 2.9 to 24.3 and decreased subsequently to 2.0 under aerobic conditions, increasing initially to 29.8 and decreasing subsequently to 7.2 under anaerobic conditions. As in *S. foliosa* litter, the increase of MeHg contained in the litter after 10-day incubation greatly exceeded the quantities added with the bay water and sediment and were attributed to microbial activity.

Table 6-4. Changes in oxygen concentration and pH of the seawater in which the plant litter of *Salicornia virginica* decomposed. Mean values and standard deviations (N=3) of 3-day observations during incubation.

Incubation Period (days)	Oxygen Concentration (mg L^{-1})	pH
Water *S. virginica*, t_0	7.1 (0.0)	7.5 (0.0)
Aerobic		
10	5.3 (0.3)	6.9 (0.1)
50	6.5 (2.1)	7.3 (0.2)
100	7.4 (0.4)	7.3 (0.2)
150	7.2 (0.9)	7.3 (0.3)
Anaerobic		
10	0.1 (0.0)	6.6 (0.2)
50	0.9 (0.1)	7.1 (0.2)
100	1.9 (0.9)	7.8 (0.1)
150	1.8 (0.7)	7.2 (0.1)

Among both litter types, *S. foliosa* litter initially had a greater THg and lower MeHg concentration than *S. virginica* litter at 60.9 ng THg and 1.0 ng MeHg g^{-1} DW versus 36.2 ng THg and 2.0 ng MeHg g^{-1} DW. The MeHg content of the decomposing plant litter was elevated to greater levels in *S. foliosa* than in *S. virginica*, and the content remained elevated over the whole 150-day incubation period, while the MeHg content in decomposing *S. virginica* litter decreased to values below initial readings between 50 and 100 incubation days. The methylation of *S. foliosa* litter (C_4 plant) was slightly greater than of *S. virginica* litter (C_3 plant), but this difference was smaller than found between C_3 and C_4 plants in an Amazonian floodplain lake possibly because of the warmer climate in the latter case (Acha et al. 2005). Litter of both plant species can act as a transient source of MeHg, the amount depending on litter quantity, environmental conditions (oxygen level) and stage within the decomposition process (time). The latter confirms results of an earlier study in a freshwater marsh by Heyes et al. (1998).

Changes in stable isotope ratios and elemental concentrations in the decomposing litter

The initial elemental and stable isotope compositions of *S. foliosa* were characteristic for this plant species. The elemental concentrations for C, N, and S were 318.7, 9.3, and 2.1 mg g^{-1} DW, respectively (Table 6-5).

Table 6-5. Changes in decomposing plant litter of *Spartina foliosa* under aerobic and anaerobic conditions: concentrations and stable isotope ratios of carbon, nitrogen, sulfur, and C:N ratio. Values of sediment inoculum at the beginning of the experiment are given for reference. Mean values and standard deviations (N=3).

Incubation Period (days)	Carbon (mg g^{-1}DW)	Nitrogen (mg g^{-1}DW)	Sulfur (mg g^{-1}DW)	$\delta^{13}C$ (‰)	$\delta^{15}N$ (‰)	$\delta^{34}S$ (‰)	C:N Ratio
S. foliosa, t_0	318.7(32.3)	9.3 (0.7)	2.1 (0.2)	-15.6 (0.6)	7.7 (0.9)	8.7 (1.6)	34.6(5.3)
Aerobic							
10	321.2 (18.3)	7.7 (0.6)	3.5 (1.0)	-15.5 (0.2)	3.8 (0.8)	8.1 (0.6)	42.0 (6.0)
50	283.2 (34.9)	9.8 (2.5)	4.4 (2.0)	-15.9 (0.2)	2.7 (1.3)	11.6 (3.0)	29.9 (5.4)
100	228.9 (22.5)	11.1 (5.1)	6.4 (1.8)	-16.9 (1.0)	2.5 (1.1)	7.4 (3.1)	22.9 (7.5)
150	294.0 (45.5)	12.5 (2.8)	7.1 (1.6)	-15.7 (0.5)	2.2 (0.4)	5.7 (1.7)	23.8 (2.3)
Anaerobic							
10	292.3 (32.0)	6.9 (0.2)	5.3 (1.3)	-14.2 (0.3)	5.2 (1.7)	5.4 (1.4)	42.1 (3.4)
50	303.7 (25.8)	7.9 (1.8)	6.3 (0.7)	-15.0 (0.5)	3.1 (0.3)	10.4 (3.1)	39.3 (7.0)
100	285.0 (45.7)	13.1 (0.9)	8.3 (1.4)	-16.1 (0.7)	2.4 (0.9)	12.4 (1.0)	22.0 (4.6)
150	254.8 (53.6)	13.3 (2.4)	10.4 (3.3)	-15.6 (0.6)	2.1 (0.3)	12.1 (2.2)	19.0 (0.6)
Sediment inoculum	22.5 (1.2)	2.7 (0.1)	0.9 (0.0)	-22.7 (0.1)	4.1 (1.0)	10.2 (0.5)	8.4 (0.1)

The stable isotope ratios were 15.6‰ $\delta^{13}C$, 7.7‰ $\delta^{15}N$, and 8.7‰ $\delta^{34}S$. In this litter, the concentration of C decreased slightly over time, but those of N and S increased by a factor of about 2. At the end of the 150-day incubation period, the C:N ratio had decreased from 34.6 initially to 23.8 in the aerobic litter and to 19.0 in the anaerobic litter. The changes in stable isotopic ratios for ^{13}C, ^{15}N, and ^{34}S in the litter followed characteristic patterns. $\delta^{13}C$ remained almost constant around -15.6‰, which is typical for a C_4 plant. $\delta^{15}N$ decreased from 7.7‰ to 2.1-2.2‰, maximally 5.5‰ or a factor of 3 to 4, in aerobic and anaerobic litter, decreasing faster in aerobic than in anaerobic litter. The $\delta^{34}S$ had increased after 50-day incubation from 8.7‰ initially to 11.6‰ and decreased subsequently to 5.7‰ in the aerobic litter, but increased to maximally 12.4‰ in the anaerobic litter (Figure 6-6 and Table 6-6).

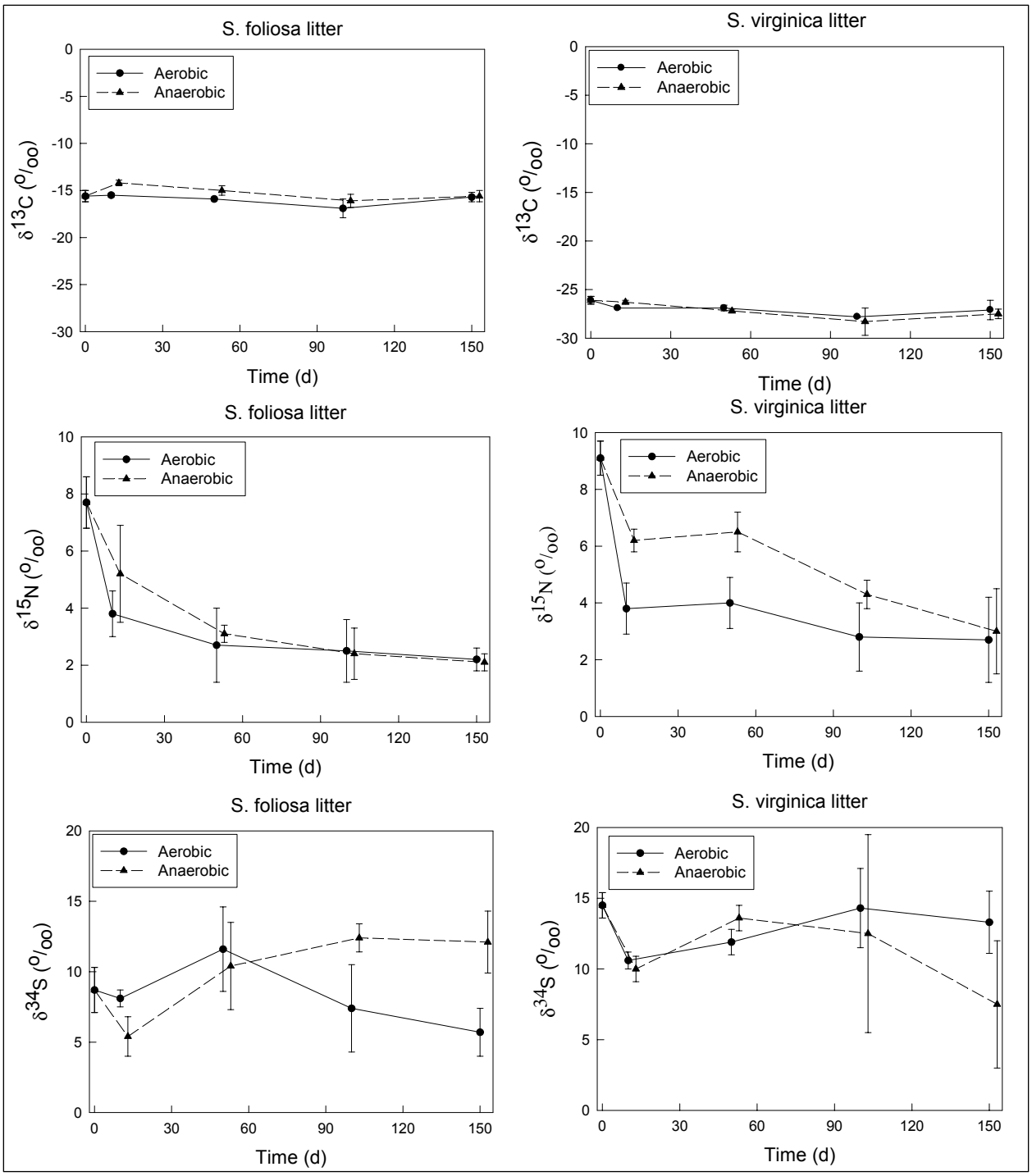

Figure 6-6. Changes in stable isotope means ($\delta^{13}C$, $\delta^{15}N$, and $\delta^{34}S$) of decomposing litter of *Spartina foliosa* (left-hand side) and *Salicornia virginica* (right-hand side) under aerobic and anaerobic conditions. Mean values and standard deviations (N=3).

Table 6-6. Changes in decomposing plant litter of Salicornia virginica under aerobic and anaerobic conditions: concentrations and stable isotope ratios of carbon, nitrogen, sulfur, and C:N ratio. Values of sediment inoculum at the beginning of the experiment are given for reference. Mean values and standard deviations (N=3).

Incubation Period (days)	Carbon (mg g^{-1}DW)	Nitrogen (mg g^{-1}DW)	Sulfur (mg g^{-1}DW)	$\delta^{13}C$ (‰)	$\delta^{15}N$ (‰)	$\delta^{34}S$ (‰)	C:N ratio
S. virginica, t_0	353.0 (23.0)	12.2 (2.7)	4.5 (0.4)	-26.1 (0.4)	9.1 (0.6)	14.5 (0.9)	30.4 (9.3)
Aerobic							
10	295.5 (7.2)	13.2 (0.7)	5.6 (1.0)	-26.9 (0.1)	3.8 (0.9)	10.6 (0.6)	22.3 (0.8)
50	291.3 (31.7)	10.9 (3.3)	4.7 (2.8)	-26.9 (0.3)	4.0 (0.9)	11.9 (0.9)	28.0 (7.2)
100	225.5 (76.1)	8.9 (0.4)	4.1 (0.8)	-27.8 (0.1)	2.8 (1.2)	14.3 (2.8)	25.6 (9.3)
150	310.3 (92.7)	11.1 (2.2)	3.7 (0.9)	-27.1 (1.0)	2.7 (1.5)	13.3 (2.2)	21.1 (8.5)
Anaerobic							
10	280.1 (28.4)	13.0 (0.4)	6.8 (0.8)	-26.3 (0.2)	6.2 (0.4)	10.0 (0.9)	21.7 (2.8)
50	288.5 (23.1)	12.7 (1.7)	10.5 (2.0)	-27.2 (0.2)	6.5 (0.7)	13.6 (0.9)	23.1 (4.8)
100	161.5 (38.7)	11.0 (1.2)	4.3 (1.0)	-28.3 (1.4)	4.3 (0.5)	12.5 (7.0)	14.8 (4.0)
150	226.1 (85.2)	12.9 (1.9)	7.6 (2.8	-27.5 (0.5)	3.0 (1.5)	7.5 (4.5)	17.4 (5.6
Sediment inoculum	22.5 (1.2)	2.7 (0.1)	0.9 (0.0)	-22.7 (0.1)	4.1 (1.0)	10.2 (0.5)	8.4 (0.9)

The initial elemental and stable isotope composition of *S. virginica* was also characteristic for this plant species, and differed greatly from that of *S. foliosa*. The elemental concentrations for C, N, and S were 353.0, 12.2, and 4.5 mg g^{-1} DW, respectively (Table 6-6). The stable isotope ratios were -26.1‰ $\delta^{13}C$, 9.1‰ $\delta^{15}N$, and 14.5‰ $\delta^{34}S$. In this litter, the C concentration decreased slightly over time, the N concentration oscillated around the initial value of 12.2, and the S concentration increased up to 10 days under aerobic and up to 50 days under anaerobic conditions but then decreased (Table 6-6). At the end of the 150-day incubation period, the C:N ratio had decreased from 30.4 initially to 21.1 in the aerobic litter and 17.4 in the anaerobic litter. The changes in stable isotopic ratios for ^{13}C, ^{15}N, and ^{34}S in the litter followed characteristic patterns. $\delta^{13}C$ remained almost constant around -26.1‰, which is typical for a C_3 plant.

$\delta^{15}N$ decreased from 9.1‰ to 2.7-3.0‰, i.e., by 6.4‰ or a factor of 3 to 4, in aerobic and anaerobic litter, decreasing faster in aerobic than in anaerobic litter. $\delta^{34}S$ decreased up to 50-day incubation from initially 14.5‰ to 10.0-10.6‰ but subsequently increased to levels measured

initially in the aerobic litter. Levels decreased in the anaerobic litter to 7.5‰ (Figure 6-6; Table 6-6).

The elemental and stable isotope ratio signatures of both litter types were different initially and changed via species-characteristic patterns during the decomposition process. The C:N ratio generally decreased during decomposition and exceeded the value of 35 only in *S. foliosa* litter in the period between initial and 10 to 50 days of decomposition. A C:N ratio of $\geq$35 is attributed to the C-rich structural carbohydrates in higher plant tissue, which are considered to be of low food quality for animals (Elser et al. 2000). Thus, *S. foliosa* litter may be considered as having a lower food quality than *S. virginica* litter during part of the decomposition process.

Changes in microbial biomass in the decomposing litter

The total microbial biomass in *S. foliosa* litter was elevated initially, with 779,200 pg PLFAME g^{-1} DW (Table 6-7; Figure 6-7). SRB contributed about 20% to the microbial biomass at the beginning of decomposition.

Table 6-7. Changes in decomposing plant litter of *Spartina foliosa* under aerobic and anaerobic conditions: total microbial biomass, and relative contributions of sulfur reducing microbial strains. Polar lipid fatty acid methylester content (PLFAME) is taken as a measure for total microbial biomass. Values of sediment and water inoculum at the beginning of the experiment are given for reference. Mean values and standard deviations (N=3).

Incubation Period (days)	Microbial Biomass (pmole g^{-1} DW)	*Desulfobacter* (relative abundance)	*Desulfovibrio* (relative abundance)
S. foliosa, t_0	779,200 (490,400)	18.5 (1.6)	0.3 (0.3)
Aerobic			
10	1,027,000 (234,800)	20.2 (1.1)	6.0 (0)
50	1,526,000 (821,600)	14.6 (3.1)	0.01.4 (0.2)
100	1,414,000 (810,200)	19.3 (3.4)	0.02.0 (0.7)
150	972,600 (481,800)	14.4 (2.8)	0.01.6 (0.2)
Anaerobic			
10	737,600 (299, 400)	21.0 (1.6)	0.00.6 (0.1)
50	857,700 (730,400)	13.9 (0.4)	0.01.7 (0.4)
100	2,397,000 (810, 600)	13.1 (1.6)	0.02.5 (0.1)
150	638,400 (292,800)	14.8 (0.9)	0.01.8 (0.3)
Sediment inoculum	54,050 (28,570)	17.0 (2.3)	0.02.6 (0.2)
Water inoculum[1]	17,380 (9,481)	28.2 (11.4)	0 (0)

[1] Unknown volume of seawater collected on 0.45-µm glass fiber filter and lyophilized.

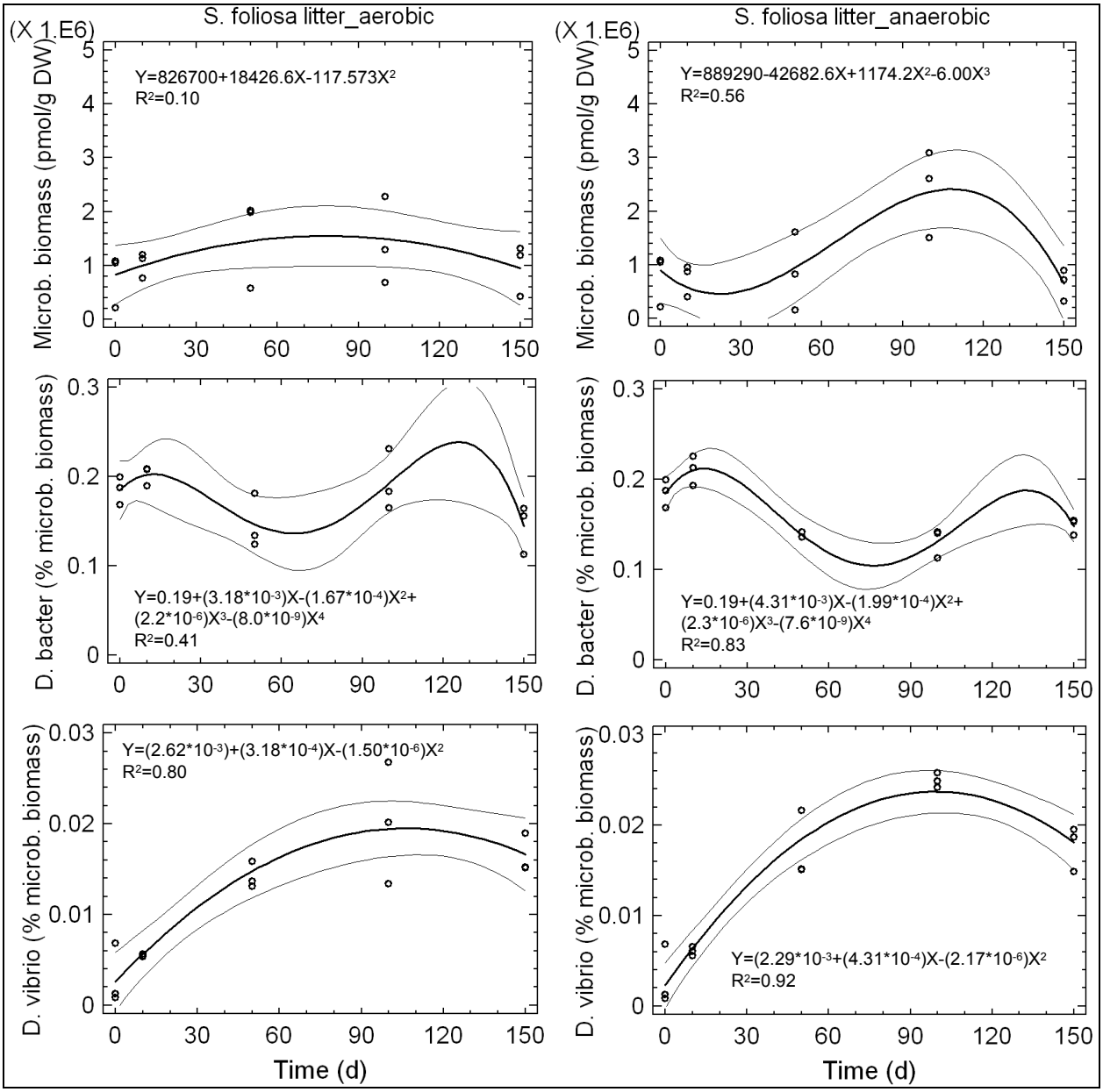

Figure 6-7. Changes over time of microbial biomass and relative contributions of sulfur reducing bacterial strains in decomposing litter of *Spartina foliosa*. Lines represent regression lines and 95% confidence limits. Regression equation and proportion of variance explained (R^2) by the fitted model indicated.

Microbial biomass increased up to 100-day incubation and decreased subsequently. The increase was less under aerobic than under anaerobic conditions. Of both SRB groups identified, the *Desulfobacter* biomass usually exceeded that of *Desulfovibrio* by a factor of 5-20.

The SRB patterns differed as the biomass of *Desulfobacter* followed a wave pattern, whereas that of *Desulfovibrio* increased up to 100-day incubation

and decreased subsequently. In the course of the decomposition process, the biomass of both *Desulfobacter* and *Desulfovibrio* contributed relatively more to total microbial biomass in litter of *S. foliosa* than in litter of *S. virginica*.

The total microbial biomass in *S. virginica* litter initially was far greater than in the *S. foliosa* litter, at 5,786,000 pmole PLFAME g^{-1} DW or a factor of 7.4 (Table 6-8; Figure 6-8). SRB contributed also about 20% to the microbial biomass in plant litter at the beginning of incubation. Microbial biomass was lower during the decomposition of litter than initially, reaching maximally 50% of initial values. Of both SRB groups distinguished, the *Desulfobacter* biomass usually exceeded that of *Desulfovibrio* by a factor of 5-20 as in *S. foliosa*. The SRB patterns differed in that *Desulfobacter* biomass followed a wave pattern, whereas *Desulfovibrio* biomass increased up to 100-day incubation and decreased subsequently.

Table 6-8. Changes in decomposing plant litter of *Salicornia virginica* under aerobic and anaerobic conditions: total microbial biomass, and relative contributions of sulfur reducing microbial strains. Polar lipid fatty acid methylester content (PLFAME) is taken as a measure for total microbial biomass. Values of sediment and water inoculum at the beginning of the experiment are given for reference. Mean values (SD; N=3).

Incubation Period (days)	Microbial Biomass (pmole g^{-1} DW)	*Desulfobacter* (relative abundance)	*Desulfovibrio* (relative abundance)
S. virginica, t_0	5,786,000 (3,899,000)	20.1 (0.6)	0.1 (0)
Aerobic			
10	1,540,000 (181,800)	21.8 (2.1)	0.4 (0)
50	949,700 (502,200)	13.2 (0.4)	0.6 (0)
100	1,514,000 (353,300)	16.2 (2.3)	1.3 (0.5)
150	428,200 (290,200)	12.0 (1.0)	0.8 (0.1)
Anaerobic			
10	1,438,000 (896,200)	22.0 (1.0)	0.3 (0)
50	1,504,000 (361,700)	11.5 (0.6)	0.7 (0.1)
100	2,795,000 (2,046,000)	15.2 (0.8)	1.1 (0.7)
150	584,900 (50,450)	14.5 (1.1)	0.8 (0)
Sediment inoculum	54,050 (28,570)	17.0 (2.3)	2.6 (0.2)
Water inoculum[1]	17,380 (9,481)	28.2 (11.4)	0 (0)

[1] Unknown volume of seawater collected on 0.45-µm glass fiber filter and lyophilized.

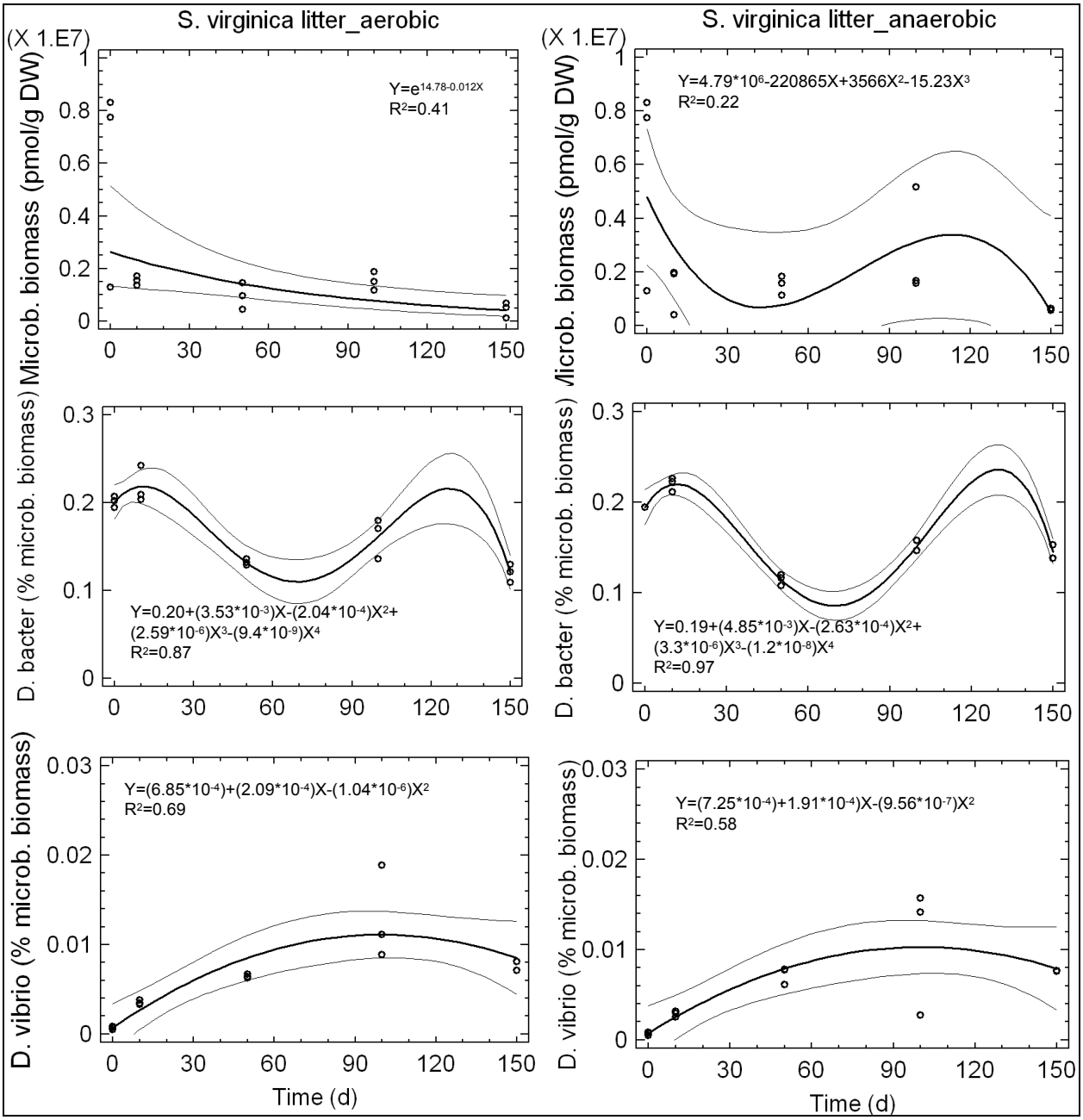

Figure 6-8. Changes over time of microbial biomass and relative contributions of sulfur reducing bacterial strains in decomposing litter of *Salicornia virginica*. Lines represent regression lines and 95% confidence limits. Regression equation and proportion of variance explained (R^2) by the fitted model indicated.

At that time, the oxygen concentration in the incubation water of the aerobic and anaerobic series differed greatly (0.2 to 7.4 mg O_2 L^{-1}) and pH decreased during decomposition (Table 6-3, Table 6-4). It is possible that one characteristic common to both litter types—the N content—may be the cause of this difference.

The total microbial biomass in the sediment was far lower than in both litter types at the beginning of incubation. In sediment it was a factor of 14 (Table 6-8) lower than in *S. foliosa* litter, and a factor of 107 (Table 6-8) lower than in *S. virginica* litter. The total microbial biomass in the sediment amounted to 13.5×10^8 cells g^{-1} DW, with 2.7×10^8 cells g^{-1} DW attributed to SRB. SRB contributed about 20% to the microbial biomass in sediment at the beginning of the incubation period. In the current study, the SRB, composed partly by methylating bacteria, originated largely from the litter itself, 10% from the sediment in the *S. foliosa* series, and 1% from the sediment in the *S. virginica* series, with a negligible inoculum from the San Pablo Bay water. The contribution of 2.7×10^8 SRB cells g^{-1} DW to the total microbial biomass in the sediment found in the present study is similar to an earlier estimate of about 2.5×10^8 cells g^{-1} DW pertaining to the nearby Hoffman salt marsh (Murray and Horne 1979).

Potential impact of decomposing macrophyte litter on food chains

On a square meter basis, the decomposing plant litter of *S. foliosa* forms a larger potential source of MeHg for food chain organisms than that of *S. virginica*. This is because the MeHg concentration in *S. foliosa* was elevated to greater levels, remained elevated over the whole 150-day decomposition period, and annual fragmentation of dead plant material was relatively greater (Chapter 5). The MeHg content in decomposing *S. virginica* litter decreased below initial values between 50 and 100 days of decomposition, and fragmentation was relatively lower (Chapter 4). However, on a system basis, the actual impact of MeHg from decomposing plant litter on food chain would be determined by the total amount of litter produced by either plant species, the time at which it would become available for the food chain, the situation of the *S. foliosa* and *S. virginica* vegetation zones within the landscape of the marsh itself and of the adjacent part of the bay, as well as the preference and life cycle of the various detritivores and consumers of the food chain. In the case of China Camp, the temporarily increased MeHg portion of THg in the decomposing plant litter may impact the food web within the marsh itself (with molluscs and crabs being abundant, Chapter 7) and the nearshore fish consumers (Chapter 7).

Conclusions

1. Plant materials decomposed with different rates, with a dry weight loss of maximally 66% in *S. foliosa* and 84% in *S. virginica*. Oxygen concentration affected decomposition rates differentially. Aerobic conditions increased mass loss in *S. foliosa* litter but decreased it in *S. virginica* litter.
2. The THg concentration in the litter increased during the decomposition process, but the total THg mass contained in the litter did not. The temporarily increased MeHg content in the decomposing plant litter, up to concentrations of 17.9 ng g^{-1}, supports the hypothesis that THg in and on the surface of the plant litter is methylated during the decomposition process, when in contact with site-characteristic sediment and water. However, in later phases of the decomposition process, the MeHg concentration decreased and, thus, demethylation of MeHg occurred also under both aerobic and anaerobic conditions. This phenomenon indicates that plant litter from coastal marshes can act as a transient source of MeHg, the amount depending on litter quantity and quality (plant species), environmental conditions (oxygen level), and stage within the decomposition process (time).
3. Among the stable isotope ratios determined, the $\delta^{13}C$ ratio proved to be a reliable indicator of the plant material source, since $\delta^{13}C$ remained stable at approximately 15.6‰ in *S. foliosa* litter and approximately 26.1‰ in *S. virginica* litter. Shifts in the $\delta^{15}N$ ratios were greater than 3-3.6 ‰ considered as indicative for trophic transfer by one level and typical for specialized diets within food webs (Minagawa and Wada 1984; Fry 1988).
4. The C:N ratio generally decreased during decomposition and exceeded the value of 35 only in *S. foliosa* litter in the period between initial period and 10 to 50 days of decomposition. A C:N ratio of $\geq$35 is considered to be indicative of low food quality for animals. Thus, *S. foliosa* litter may be considered as having a lower food quality than *S. virginica* litter during part of the decomposition process.

POINT OF CONTACT CHAPTER 6:

Dr. Elly P. H. Best
U.S. Army Engineer Research and Development Center
Environmental Laboratory, Vicksburg, MS
Ph: 601-634-4246; E-mail: elly.p.best@erdc.usace.army.mil

7 Mercury Dynamics in Food Webs Associated with Tidal Salt Marshes on San Pablo Bay

Introduction

Long-term goals for San Francisco Bay development include extensive wetland restoration. The current wetlands bordering San Pablo Bay are to be increased from 16,200 ha to 42,525 ha by the year 2055 (San Francisco Bay Area Wetlands Ecosystem Goals Project 1999). Dikes currently protect most of the areas targeted for restoration, which have subsided considerably due to drying and oxidation of the soils. Considerable amounts of material are required to raise the elevation of subsided areas to a level that would allow colonization by macrophytes, which, in turn, would trap sediment required to sustain the elevation of the wetland. For example, the Hamilton Army Airfield site, where the restoration of a tidal wetland is planned, will require approximately 8.1 million cubic meters of material. The reestablishment of wetlands in the San Francisco SF Bay Delta system using dredged sediment has the potential for mobilizing mercury present in the sediments. The origin of this contamination in the SF Bay system is largely from the historic mining of mercury in the nearby coastal mountains. The THg levels in San Francisco Bay sediment range from 400 to 1,080 ng g^{-1} DW. This has resulted in total sedimentary THg levels at or greater than those in sediments relative to other aquatic ecosystems perceived to present a Hg environmental toxicity risk (e.g., the Everglades).

The introduction of inorganic mercury to any wetland environment raises concerns related to the production of MeHg. Wetland conditions can be conducive to the production of MeHg, and certain natural wetlands have been identified as contributors of MeHg to downstream lakes and streams (St. Louis et al. 1994, 1996; Rudd 1995; Hurley et al. 1995; Branfireun et al. 1996, 1998), and as potential contributors to estuaries (Marvin-DiPasquale et al. 2003; Davis et al. 2003; Best et al. 2005). MeHg is the most toxic Hg species and cause of the greatest concern. MeHg is a potent toxin that efficiently biomagnifies in food webs. Impaired reproduction is one of the most sensitive toxicological responses, with effects occurring at very low dietary concentrations. In birds, the documented effects of Hg on

reproduction range from embryo lethality to sublethal behavioral changes in juveniles at low dietary exposure. Reproductive effects in birds typically occur at about 20% of the concentrations that cause mortality in adult birds (Scheuhammer 1991). Fish reproduction can also be very sensitive to MeHg (Wiener and Spry 1996), but data on exposures and sensitivities specific to the San Francisco Bay-Delta are not available. Aquatic systems tend to have greater rates of Hg bioaccumulation and biomagnification than terrestrial systems (USEPA 1997). Several factors contribute to this difference. Fish store most Hg as MeHg in their muscle, whereas mammals and birds store much of their MeHg burden in feathers and fur, items poorly digested or rarely consumed (and affording mammals and birds a Hg excretory pathway unavailable to fish). Aquatic systems have more complex food webs and more trophic levels, and the primary producers in aquatic systems may themselves accumulate more Hg from water and sediment than do soil-based primary producers in terrestrial systems (USEPA 1997). Top predators in aquatic systems are, therefore, at greatest risk from Hg bioaccumulation. Within the San Francisco Bay area several fish species currently have significantly enhanced Hg levels that exceed the threshold for human health concern (SFEI 2005a; data 2000). Since fish usually belong to the higher trophic levels of a food chain, it is important to quantify if and how food webs in the marsh itself and in the adjacent bay are impacted by MeHg production within the marsh, ultimately causing these elevated Hg body burdens in fish. This knowledge could contribute to the knowledge base needed to design and manage wetlands targeted at minimizing MeHg production.

The food web within Pacific coastal marshes as in Atlantic coastal marshes is primarily detritus-based, with microbes, insects, and amphipods being the most important heterotrophs. Once detrital material leaves the attached dead plant community (dead plants plus the community of microorganisms), the food web in the Northwest marshes may include copepods, mollusks, and salmonid fishes (Sibert 1977). In addition, a strong food web linkage between salt marsh plants and nearshore fish consumers has been argued for many North American coastal ecosystems, including the Atlantic and the Pacific Northwest (Naiman and Sibert 1979; Kistritz and Yesaki 1979; Wainwright et al. 2000). In contrast, other researchers report that coastal and estuarine food webs are fueled by algal production, i.e., either phytoplankton (Nixon et al. 1976; Haines 1977; Gleason and Wellington 1988; Kimmerer 2004), submersed macrophytes, epiphytes and macroalgae (Simenstad and Wissmar 1985), or epibenthic

microalgae (Sullivan and Moncreiff 1990). A food web analysis of Southern California coastal wetlands indicates that salt marsh plants can be the major organic matter source for fish, and macroalgae for invertebrates and selected bird species, but that in the absence of abundant marsh plants inputs of macroalgae and microalgae support fishes (Kwak and Zedler 1997). A more recent food web study of a San Francisco Bay tidal salt marsh confirms the similarity in structure between Atlantic and gulf coast food webs, with the exception of compartmentalization of the marsh plain food web separate from the low marsh and slogh food web (Grenier 2004).

Quantitative knowledge about food web structure has practical applications in measuring the effects of anthropogenic inputs such as the bioaccumulation of contaminants in higher order predators (Cabana and Rasmussen 1994). Such information also allows assessing the impacts of introduced species, and comparison of food webs geographically and temporally, as may be needed to assess restoration and conservation efforts or to test the effects of climate change. Consumer diets, organic matter sources, and trophic levels can be estimated using empirically determined tracer levels in mixing models. Consumer stable isotope ratios reflect their foods (Peterson and Fry 1987; Sackett 1989) and trophic position in the food web, with fractionation rates of less than 1‰ per trophic level for $\delta^{13}C$ (Peterson and Fry 1987; Post 2002), 3 -3.6‰ per trophic level for $\delta^{15}N$ (Peterson and Fry 1987; Fry 1988; Post 2002; or more, according to McCutchan et al. 2003) and no significant change in $\delta^{34}S$ (Peterson et al. 1986; Peterson and Howarth 1987; Fry 1988, 1991; Michener and Schell 1994). The resolution of organic matter sources is more powerful when multiple isotopes are used simultaneously, but the mathematics can be difficult to implement. The scope of many multiple food source mixing models is limited by the sources and tracers (1-2 sources, 1-2 tracers), or the models focus on trophic structure rather than flow reconstruction, although some models do allow for a more complex set of potential sources. In many cases this modeling is an overly simplistic way of partitioning food resources, particularly in estuarine systems, which can have multiple source inputs (Peterson and Howarth 1987; Cifuentes et al. 1988; Fry 1988). A set of two complementary mixing models has been identified, i.e., SOURCE and STEP, that use linear programming techniques with multiple tracers, to estimate the dominant primary producer sources of consumers, and their diets and trophic levels, regardless of the number of sources and trophic steps (Lubetkin and Simenstad 2004).

Objectives

The present study was designed to do the following:

1. Identify organic matter sources that support consumers in San Pablo Bay tidal salt marshes.
2. Identify trophic linkages between salt marsh habitats and bay habitats.
3. Quantify the bioaccumulation of Hg species.
4. Evaluate the trophic pathways leading to toxicity in higher trophic levels in San Pablo Bay food webs.

Such knowledge is critical to define food web support functions that may be required for effective restoration and mitigation projects. If salt marsh habitat for endangered species, such as the California clapper rail (*Rallus longirostris obsoletus*) or California black rail (*Laterallus jamaicensis coturniculus*) is planned, their dependency on shallow waters must be known. Also, for projects to provide fish habitat, it must be known if it is sufficient to provide an open water channel or bay, or whether vegetated salt marsh should be included, and where the potential toxicity pathways originate.

In this chapter, a description is presented of the predominant species, their stable isotope signatures, and their mercury species contents, with reference to the predominant trophic groups in which they may belong. A modeling analysis to (1) identify the dominant sources of organic matter supporting the food web, (2) determine the sequence of trophic steps, and (3) evaluate the specific predator-prey linkages is expected to be carried out as a follow-up of the current study and the results will be reported in a subsequent report.

Study sites

The Hamilton Army Airfield (HAAF) Wetlands Restoration Site on San Pablo Bay is part of the San Francisco Baylands. It is located in the North Bay. The Baylands consist of the shallow water habitats around the San Francisco Bay between the maximum and minimum elevations of the tides (Figure 7-1). The Baylands ecosystem includes the areas of maximum and minimum tidal fluctuations, adjacent habitats, and their associated plants and animals. The boundaries of the ecosystem vary with the bayward and landward movements of fish and wildlife that depend upon the Baylands for survival. Many habitats of the Baylands are wetlands. Habitat goals

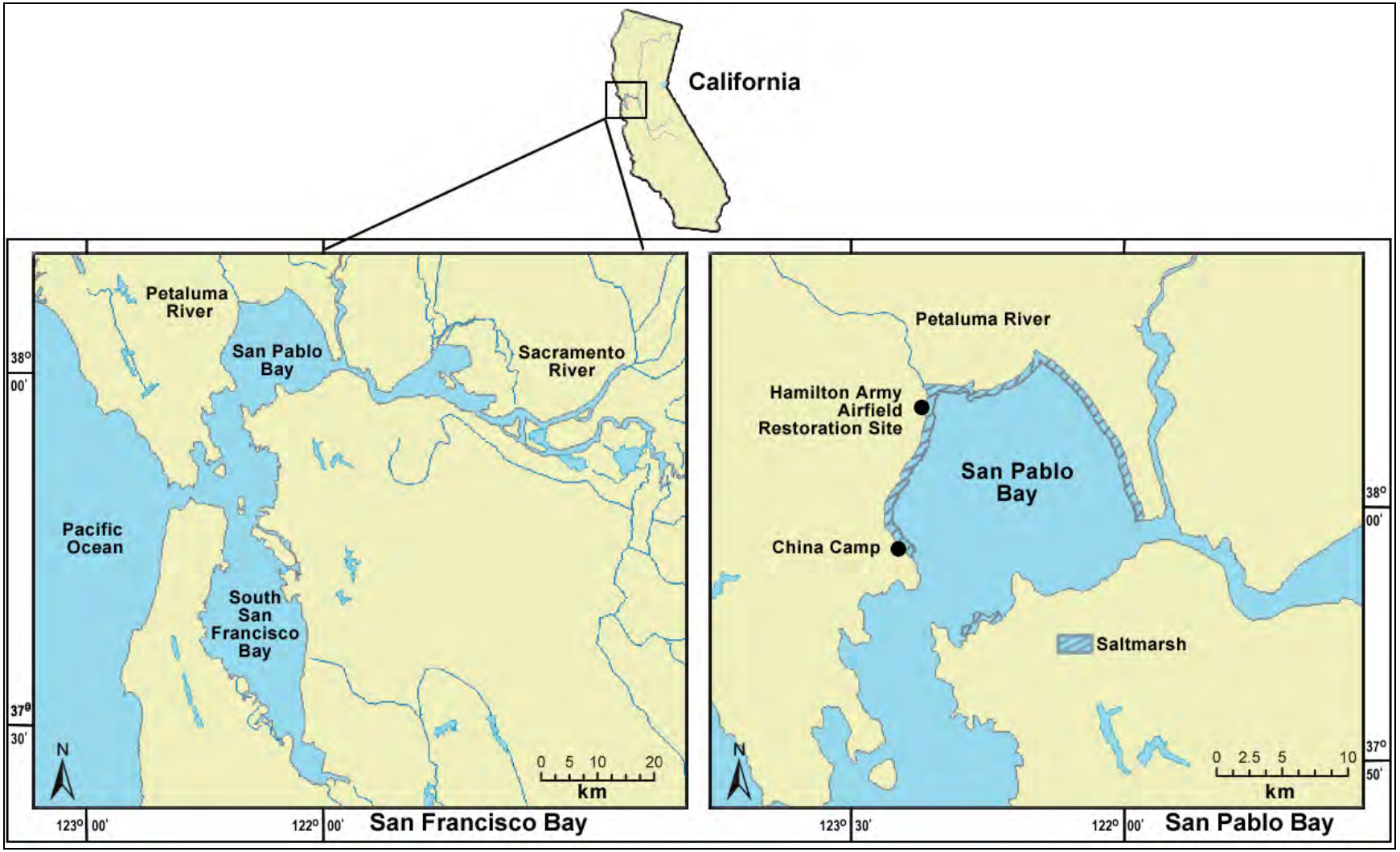

Figure 7-1. Site map showing the location of San Pablo Bay within San Francisco Bay (left) and the location of the Hamilton Army Airfield Restoration Site and the China Camp reference site (right).

selected for the planned restored HAAF wetland, with a surface area of 203 ha, include the restoration of tidal marshes, with natural transitions into upland areas with seasonal wetlands. The restored HAAF area is expected to increase the habitat of the regionally rare and protected clapper rail and salt marsh harvest mouse because it is adjacent to existing populations, will contain a large tidal wetland, and is remote from predator outposts and corridors (San Francisco Bay Area Wetlands Ecosystem Goals Project 1999).

For studies aimed at providing baseline information on tidal wetlands relevant for the future HAAF wetland, the nearby tidal salt marsh at the China Camp State Park was chosen as a reference (Figure 7-1). In this tidal salt marsh, traversed by several tidal channels, *Spartina foliosa* (Pacific cordgrass) and S*alicornia virginica* (common pickleweed) are the dominant plant species. *S. foliosa* is usually the primary colonizer on the tidal mud flats that fringe the tidal marsh plain, and it occurs in virtually pure stands on the low marsh between Mean Tidal Level (MTL) and Mean High Water Level (MHW). At somewhat higher elevations near and above MHW, *S. foliosa* intermixes and gradually yields to *S. virginica*. At high tidal salt marsh, between about MHW and the maximum extent of the tides, *S. virginica* is found in association with peripheral halophytes including *Distichlis spicata* (saltgrass) and *Atriplex triangularis* (fathen). The history, physical setting, and ecological relationships in several Baylands ecosystems have been outlined in San Francisco Bay Area Wetlands Ecosystem Goals Project (1999).

Materials and methods

Field collection

For the current food web study, samples were collected in the tidal marsh at the reference site China Camp State Park (R-44; 38° 00.411′ N, 122° 28.758′ W) and the adjacent area of San Pablo Bay. The following organic materials were collected within the listed time frames. Particulate organic matter (POM) suspended in the water column was collected and analyzed as a potentially important link in the food web. Water samples were collected in July 2005 from (1) the bay adjacent to the China Camp marsh site R-44, and (2) a large marsh pool located on the high marsh for subsequent analysis of suspended particulate matter (Figure 7-2). Suspended POM for the analysis of stable isotopes and Hg species was sampled by collecting two 1-L surface water samples in each habitat type. The samples were

temporarily stored in glass jars on ice during transport, and subsequently water was filtered over 0.45-µm glass fiber filters under gentle vacuum in the laboratory. The samples contained a mixture of plankton and detritus.

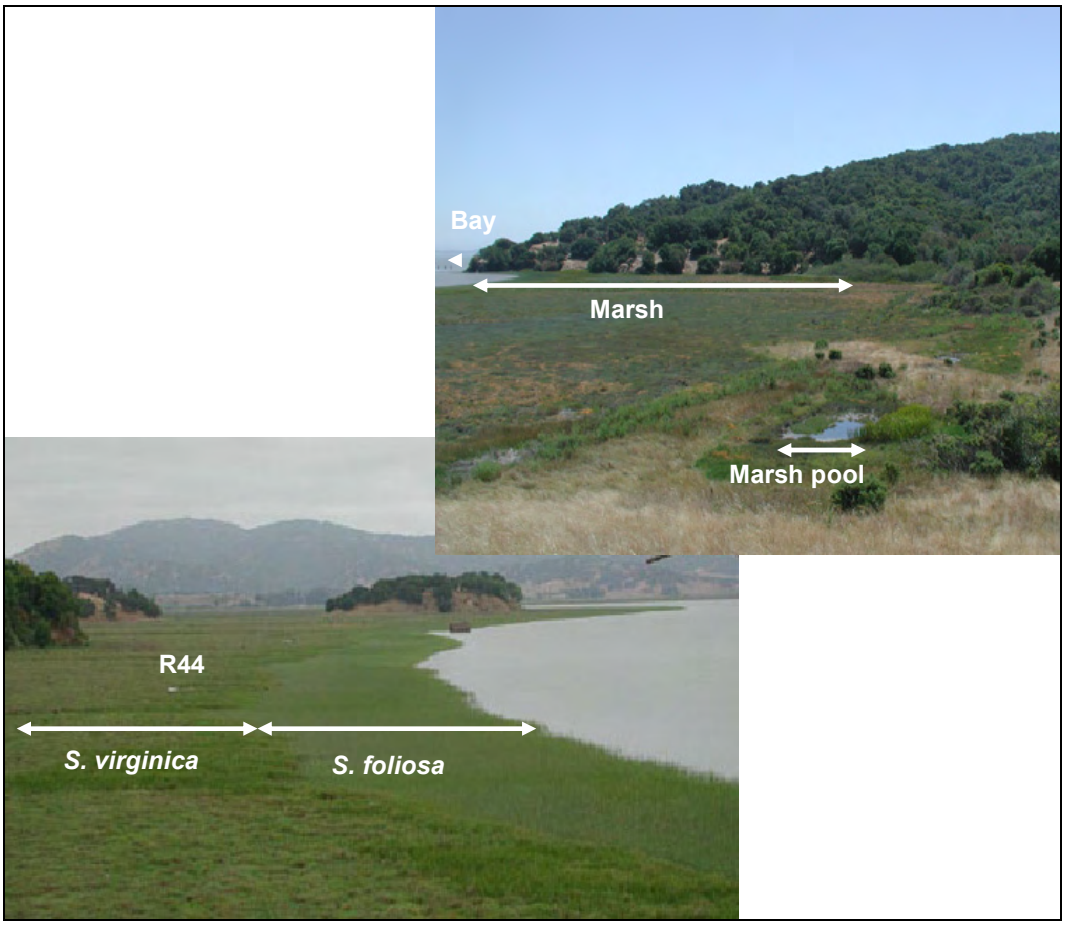

Figure 7-2. Habitat types at the China Camp State Park from which samples were collected (upper). Reference site and zones dominated by *Spartina foliosa* and *Salicornia virginica*, respectively, marked (lower).

Phytoplankton samples were collected in July 2005 from the bay adjacent to the China Camp marsh site R-44 and from the same marsh pool as POM, located in the high marsh (Figure 7-3), for the analysis of stable isotopes and Hg species. Samples were collected from the bay by pulling a standard 363-µm nitex mesh plankton net (equipped with a 540-µm mesh-bucket) over a distance of about 1 mile through the bay water behind a small Boston Whaler, and from the marsh pool, by pulling the plankton net manually through the water over variable distances. The suspensions were temporarily stored in glass jars on ice during transport, and subsequently lyophilized in the laboratory. The samples contained largely plankton.

Figure 7-3. Sites of phytoplankton collection in San Pablo Bay (upper) and of phytoplankton and filamentous algae in the marsh pool of the China Camp site (mid and lower). Approximate locations marked by arrows.

The following three distinct marsh microalgal groups were collected in July 2005: two groups of epipelic algae from the low marsh, i.e., one group dominated by diatoms (red-brown color), a second group dominated by cyanobacteria (*Microcystis* sp.), and a third group of filamentous algae from the marsh pond. The epipelic microalgae were sampled quantitatively between the macrophytic vegetation (Figure 7-4) by pressing a 2.5-cm diameter glass petri dish upside down into the sediment, excising the upper 0.5-cm sediment layer by insertion of a flat glass plate underneath the petri dish, and collection of the sediment contained in the dish.

Figure 7-4. Site of epipelic algae collection of the China Camp site. One cyanobacteria-dominated location marked by an arrow.

The filamentous algae were gathered by hand from the marsh pool and transferred into plastic bags (Figure 7-3). Macroalgae, including *Ulva* and *Phucus* sp., were collected by hand from the tidal and intertidal zones of the rocky shore adjacent to the R-44 China Camp site (Figure 7-3-upper, marked by an arrow), and transferred into plastic bags. Of the salt marsh vascular plant materials, the live shoots of *S. foliosa* and *S. virginica* collected in June 2003 and July 2004 were used. In addition, two *S. foliosa* and two *S. virginica* samples from HAAF, collected in July 2005, were used to enable analysis of 5 or 6 replicates. The latter shoot samples did not differ significantly in stable isotope signatures and mercury species from the other samples of the same species. Shoots of saltgrass (*Distichlis spicata)* and arrowleaf saltbush (*Atriplex triangularis)* were collected in July 2005 – the latter two species have been cited as potentially important in San Francisco Bay marsh food webs (San Francisco Bay Area Wetlands Ecosystem Goals Project 1999). All plant materials were stored on ice during transport and subsequently lyophilized in the laboratory.

Vascular plant litter was collected as standing dead *S. foliosa* and *S. virginica* materials in March 2004. Decomposition of the latter material was also studied experimentally by incubation up to 150 days under aerobic and anaerobic conditions (Chapter 6). Freshly collected plant litter and litter incubated for 150 days under aerobic and anaerobic conditions were included in the current food chain analysis.

Four invertebrate species were collected in July 2005 from adjacent bay sediments by boat at high tide using a Birge-Ekman dredge, i.e., Chinese

clams (*Potamocorbula amurensis)*, Baltic clams (*Macoma baltica)*, pile worms (*Nereis vexillosa)*, and an unidentified worm species. The sediment samples were sieved on site, the animals were freed from adhering sediments by rinsing them with seawater, temporarily stored in glass jars on ice during transport, and subsequently lyophilized in the laboratory. Four other invertebrate species were hand-collected from the marsh in 2004, i.e., a tiger beetle (*Cicindela* sp.) and an unidentified snail in February, and amphipods (*Orchestia traskiana)* and ribbed mussels (*Geukinsia demissa*) in February, May, and September 2004. Shrimp, starry flounder (*Platichthys stellatus*), and most arrow gobies (*Clevelandia ios*) and sculpins (*Leptocottus armatus*) were collected in February, May, and September 2004 from the adjacent bay by boat at high tide using a 3-m otter trawl. Most crabs (yellow shore crab or *Hemigrapsus oregonensis* and European green crab or *Carcinus maenas*) and a few gobies and sculpins were collected at the same points in time using 1-m-long, standard, minnow traps placed in first-order tidal creeks over a 24-h tidal cycle. Invertebrates and fish were stored on ice during transport. These samples were frozen until further processing in the laboratory.

Frozen specimens of mammals and birds were obtained as follows: *Reithrodontomys raviventris* (salt marsh harvest mouse): provided by U.S. Fish and Wildlife Service, Ashland, OR; Code MAM1528, found dead in coastal marsh HAAF, 22 December 2004. *Microtus californicus* (California vole): provided by SFEI, Oakland, CA; ID No. 5-juvenile, found dead in coastal marsh of China Camp, 14 July 2000. *Melospiza melodia samuelis* (Song sparrow): provided by SFEI, Oakland, CA; ID No. 2, juvenile, 3, 4, found dead in coastal marsh of China Camp, on, respectively, 25 May 2002, 1 June 2000, and 29 March 2000. *Laterallus jamaicensis coturniculus* (California black rail): provided by SFEI, Oakland, CA; ID No. 1, juvenile found dead in coastal marsh China Camp, 25 April 2002.

Laboratory processing

The salinity of the water samples used to quantify POM was measured in the field. Salinity was 24‰ in the bay water and 23‰ in the salt pond water. Particulate matter removed from the filtrate was rinsed with 10% hydrochloric acid (HCl) under gentle vacuum filtration to dissolve calcium carbonate ($CaCO_3$) that may have been present, followed by a distilled water rinse. The filters were lyophilized and then sealed in a glass vial for

later elemental and isotope analysis. Shells were removed from shellfish, and muscle tissues were excised from fish, mammals, and birds. All animal samples were lyophilized.

Elemental and stable isotope analysis

The natural stable isotopes of carbon and nitrogen have been used successfully to describe the structure of food webs, to indicate the apparent trophic level at which a particular organism operates, and to define the number of steps in the food chains of complex food webs (Michener and Schell 1994). The analyses of carbon, nitrogen, sulfur concentrations and the determinations of their stable isotope ratios in organic matter were carried out using a Costech (Costech Analytical, Valencia, CA) 4010 ECS Elemental Analyzer with a 50-sample autosampler and CNHS detection, Conflo interface, Isodat data program, and Isotope Ratio Mass Spectrometer (IRMS). Analyses involved complete combustion of the sample to a gas and separation of the pure gases (CO_2, N_2, and SO_2; Fry and Sherr 1984; Peterson and Fry 1987). A pure gas was then introduced into an IRMS, and the isotopic composition was quantified relative to a standard reference material. Standards were carbon in PeeDee Belemnite for ^{13}C, atmospheric nitrogen for ^{15}N, and sulfur in the Canyon Diablo meteorite for ^{34}S. Results for each elemental stable isotope were expressed in difference from the standard (δ) as parts per thousand (‰):

$$\delta X = [(Rsample/Rstandard)-1] \times 10^3,$$

where X is ^{13}C, ^{15}N, or ^{34}S, and R is the corresponding ratio of $^{13}C/^{12}C$, $^{15}N/^{14}N$, or $^{34}S/^{32}S$. The δ values denote a greater proportion of the heavy isotope. Standard deviations of $\delta^{13}C$, $\delta^{15}N$, and $\delta^{34}S$ replicate analyses of the standards and the dry samples were 0.2‰, 0.2‰, and 0.5‰, respectively.

Total mercury determinations

Total Hg was determined by isotope dilution ICP/MS after Hintelmann and Ogrinc (2003) in H_2SO_4/HNO_3 digests using continuous-flow cold-vapor generation with ICP/MS detection (Finnigan MAT, Model Element 2). $^{201}Hg^{2+}$ was added as internal standard. The acidified samples were continuously mixed with a solution of stannous chloride by means of a peristaltic pump. The formed mercury vapor was separated from the liquid in a gas-liquid separator (Model L1-2) and the elemental mercury

swept into the plasma of the ICP/MS. The following isotopes of Hg were measured: ^{201}Hg (internal standard) and ^{202}Hg (to calculate ambient THg).

Methylmercury determinations

MeHg was determined as described elsewhere (Hintelmann and Evans 1997; Hintelmann and Nguyen 2005). For this, tissue samples were digested by adding either 5 mL of KOH/MeOH (20% w/v) or 5 mL HNO_3 (4 M), and heating overnight at 50 °C. $CH_3{}^{201}HgCl$ was added as an internal standard. Appropriate sample aliquots (0.050 – 1.0 mL) were added to Milli-Q in gas-wash bottles, neutralized with 20% KOH or 1 M HCl, and the pH was adjusted to 4.9 using 0.2 mL of 2 M acetate. Sodium tetraethylborate (100 µL, 1% w/v) was added, and the solution sat at room temperature for 20 min while the tetraethylborate reacted. Tenax adsorber traps were connected to the reaction vessel and the generated methylethylmercury was purged from the solution using nitrogen (200 mL min^{-1}) and collected on the Tenax trap. Finally, all mercury species were thermally desorbed from the trap (250 °C), separated by gas chromatography, and quantified by ICP/MS (Micromass Platform). The following isotopes of Hg were measured: ^{201}Hg (internal standard) and ^{202}Hg (to calculate ambient MeHg). Peak areas were used for quantification and concentrations of individual isotopes were calculated as described in Hintelmann and Ogrinc (2003).

Mercury analysis QA/QC

For each batch of samples, the following set of QA/QC samples was measured: three reagent blanks (THg) or bubbler blanks (MeHg), and a certified reference material (IAEA 356 marine sediment and MESS-3 marine estuary sediment for sediment analysis and NIST 1515 apple leaves for plant analysis). Individual distillation yields were determined using the added internal ^{201}Hg isotope standard. Typically, one triplicate sample was analyzed (i.e., triplicate distillation or digestion) per batch.

Statistical comparisons and models

Analysis of variance (ANOVA) was used to compare isotope ratios for each element among producer groups and between consumer groups within the China Camp marsh and adjacent San Pablo Bay area. A nested ANOVA was used to compare isotope ratios from each element among producer groups, with individual taxa (or types) of producers nested within six

broader producer groups (POM, phytoplankton, marsh microalgae, bay macroalgae, marsh vascular plants, and marsh vascular plant litter). If that ANOVA detected a significant producer group main effect, then significant pairwise differences among producer group means were detected using a Fisher multiple comparison procedure. A nested ANOVA was also used to compare isotope ratios from each element among consumer groups, with individual taxa (or types) of producers nested within four broader producer groups (invertebrates, fishes, mammals, and birds).

Associations among producer and consumer isotopic distributions will be explored to identify the most important organic matter sources, and then multiple-source mixing models (Lubetkin and Simenstad 2004; Fry and Sherr 1984) will be used to approximate the relative inputs of each source into the food web of the China Camp marsh and adjacent San Pablo Bay area. Two complementary mixing models will be used, i.e., SOURCE and STEP, which use linear programming techniques with multiple tracers, to estimate the dominant primary producer sources of consumers, and their diets and trophic levels, regardless of the number of sources and trophic steps. SOURCE will be used to estimate consumers' direct and indirect uptake of autotrophic sources and their trophic levels. STEP will be used to estimate the consumers' diet, which may include autotrophs and/or heterotrophs. Similar two-source models have been used to explore food web relationships by Haines (1976); Hughes and Sherr (1983); and Van Dover et al. (1992), and three source models by Kwak and Zedler (1997).

Results

Particulate matter isotopic composition

The salinities of 23‰ and 24‰ measured in the surface water of both the marsh pool and bay water indicated that the water was brackish. The stable isotope ratios of the POM samples varied more between habitats, i.e., bay and marsh pool, than between sites within the same habitat (Table 7-1). Within habitats, $\delta^{13}C$ varied maximally 0.8‰, δ^{15}1.3‰, and $\delta^{34}S$ 0.9‰, while between habitats, variations were 2.5‰ for $\delta^{13}C$, 2.5‰ for $\delta^{15}N$, and 3.1‰ for $\delta^{34}S$. POM mean δ-values of the SF Bay were greater for all three elements than those of the marsh pool, despite the similarities in isotopic ratios of the water in the bay and marsh pool itself (Table 7-1).

Table 7-1. Stable isotope ratios of suspended particulate organic material (POM), primary producers, and vascular plant litter (including habitat type, where sampled) collected from the China Camp marsh and adjacent San Pablo Bay area. Data are sample size (N) and mean values (standard deviations). Results of ANOVA followed by Fisher's multiple comparison procedure to detect significant differences ($p<0.05$) among isotope ratio means ($\delta^{13}C$, $\delta^{15}N$, and $\delta^{34}S$) of organic material groups indicated. Organic material groups followed by the same letter are not significantly different according to this procedure.

Organic Material Type/Species	Habitat Type	N	$\delta^{13}C$ (‰)	$\delta^{15}N$ (‰)	$\delta^{34}S$ (‰)
Particulate organic matter			AB	AB	CD
POM	Bay	2	-24.2 (0.2)	5.9 (0.8)	16.5 (0.9)
POM	Marsh pool	2	-21.7 (0.8)	3.4 (1.3)	13.4 (0.8)
Phytoplankton			A	BC	A
SF Bay	Bay	2	-29.5 (3.9)	12.2 (0.6)	11.9 (0.1)
Marsh	Marsh pool	3	-23.0 (0.1)	4.9 (0.3)	3.6 (2.1)
Marsh microalgae			BC	A	AB
Diatom sp.	Low-mid marsh	3	-20.2 (0.2)	4.4 (1.1)	5.6 (0.4)
Cyanobacteria sp.	Low-mid marsh	3	-20.9 (1.3)	4.4 (0.4)	7.6 (1.4)
Filamentous sp.	Marsh pool	3	-16.9 (0.9)	2.0 (1.3)	13.7 (4.7)
Bay macroalgae			C	D	D
Ulva sp.	Bay	3	-15.6 (0.4)	13.5 (0.2)	18.2 (0.7)
Fucus sp.	Bay	3	-16.7 (0.7)	14.4 (1.3)	17.6 (0.4)
Marsh vascular plants			AB	BC	BC
Spartina foliosa (C_4)	Low marsh	6	-14.8 (0.5)	8.8 (3.0)	7.8 (4.2)
Salicornia virginica (C_3)	Mid marsh	5	-27.7 (0.9)	6.4 (1.5)	12.9 (1.2)
Distichlis spicata (C_4)	High marsh	3	-14.8 (0.3)	5.1 (0.2)	14.5 (0.2)
Atriplex triangularis (C_3)	High marsh	3	-27.4 (0.4)	2.7 (1.1)	16.6 (0.3)
Marsh vascular plant litter			ABC	C	BC
Spartina foliosa (C_4)	Low marsh	3	-15.6 (0.6)	7.7 (0.9)	8.7 (1.6)
Salicornia virginica (C_3)	Mid marsh	3	-26.1 (0.4)	9.1 (0.6)	14.6 (0.9)

Primary producer isotopic composition

Between-taxa variation in isotope ratios of primary producers was substantial, but within-taxa δ-values were similar (Table 7-1). Although sample sizes varied among taxa, most standard deviations of mean δ-values were less than 2.0‰, and only two exceeded 4.0‰ (i.e., $\delta^{34}S$ of filamentous microalage and of *Spartina foliosa*).

The isotope ratios of the five primary producer groups and of POM were calculated from the isotope ratios of the taxa and of the bay and marsh pool POM (Figure 7-5). The isotope ratios of the primary producers appeared to be less related to habitat than to organismal characteristics. Mean values in POM and other primary producers ranged from -16.1‰ (±2.0) to -25.6‰ (±2.2) for $\delta^{13}C$, and from 6.9‰ (±1.7) to 17.9‰ (±1.6) for $\delta^{34}S$ (Figure 7-5). Mean $\delta^{13}C$ (±SE) values were most depleted in phytoplankton (-25.6 ± 2.2‰), and the range of $\delta^{13}C$ values in phytoplankton partly overlapped with those in POM (-23.0 ± 2.4‰), marsh vascular plants (-20.8 ± 1.2‰), and litter (-20.8 ± 2.0‰). Mean $\delta^{13}C$ (±SE) values were least depleted bay macroalgae (-16.1 ± 2.0‰), and the range of $\delta^{13}C$ values in bay macroalgae partly overlapped with those in marsh microalgae (-19.3 ± 1.6‰) and litter (-20.8 ± 2.0‰). Mean $\delta^{34}S$ (±SE) values were significantly greater in bay macroalgae (17.9 ± 1.6‰) than those in phytoplankton, microalgae, vascular plants, and litter, but its range partly overlapped with the $\delta^{34}S$ (±SE) range in POM (14.9 ± 1.9‰; Figure 7-5).

Mean $\delta^{34}S$ (±SE) values were least in phytoplankton (6.9 ± 1.7‰), and the range of $\delta^{34}S$ values in phytoplankton partly overlapped with those in marsh microalgae (8.9 ± 1.3‰). The ranges of $\delta^{34}S$ values in marsh microalgae (8.9 ± 1.3‰) partly overlapped with those in marsh vascular plants (12.0 ± 0.9‰) and litter (11.6 ± 1.6‰).Mean $\delta^{15}N$ (±SE) values were significantly greater in bay macroalgae (13.9 ± 1.0‰) than those in POM, phytoplankton, marsh microalgae, vascular plants and litter (Figure 7-5). The range of $\delta^{15}N$ values in the marsh microalgae (mean±SE; 3.6 ± 0.8‰) partly overlapped the range of POM (4.6 ± 1.2‰), those of POM partly overlapped the range in phytoplankton (7.8 ± 1.1‰) and marsh macrophytes (6.3 ± 0.6‰). The range of $\delta^{15}N$ in the marsh vascular plant litter (mean±SE; 8.4 ± 1.0‰) partly overlapped with those in the marsh vascular plants and phytoplankton.

Two groups were distinguished among the primary producers based on their characteristic $\delta^{13}C$ values. The group with the most depleted ^{13}C values, ranging from -27 to -20, included microalgae (phytoplankton, diatoms, and cyanobacteria), and both C_3 marsh macrophytes, *S. virginica* and *Atriplex triangularis*. The group with the least depleted ^{13}C values, ranging from -17 to -15‰, included filamentous, macroalgae, and both C_4 marsh macrophytes, *S. foliosa* and *Distichlis spicata* (Table 7-1).

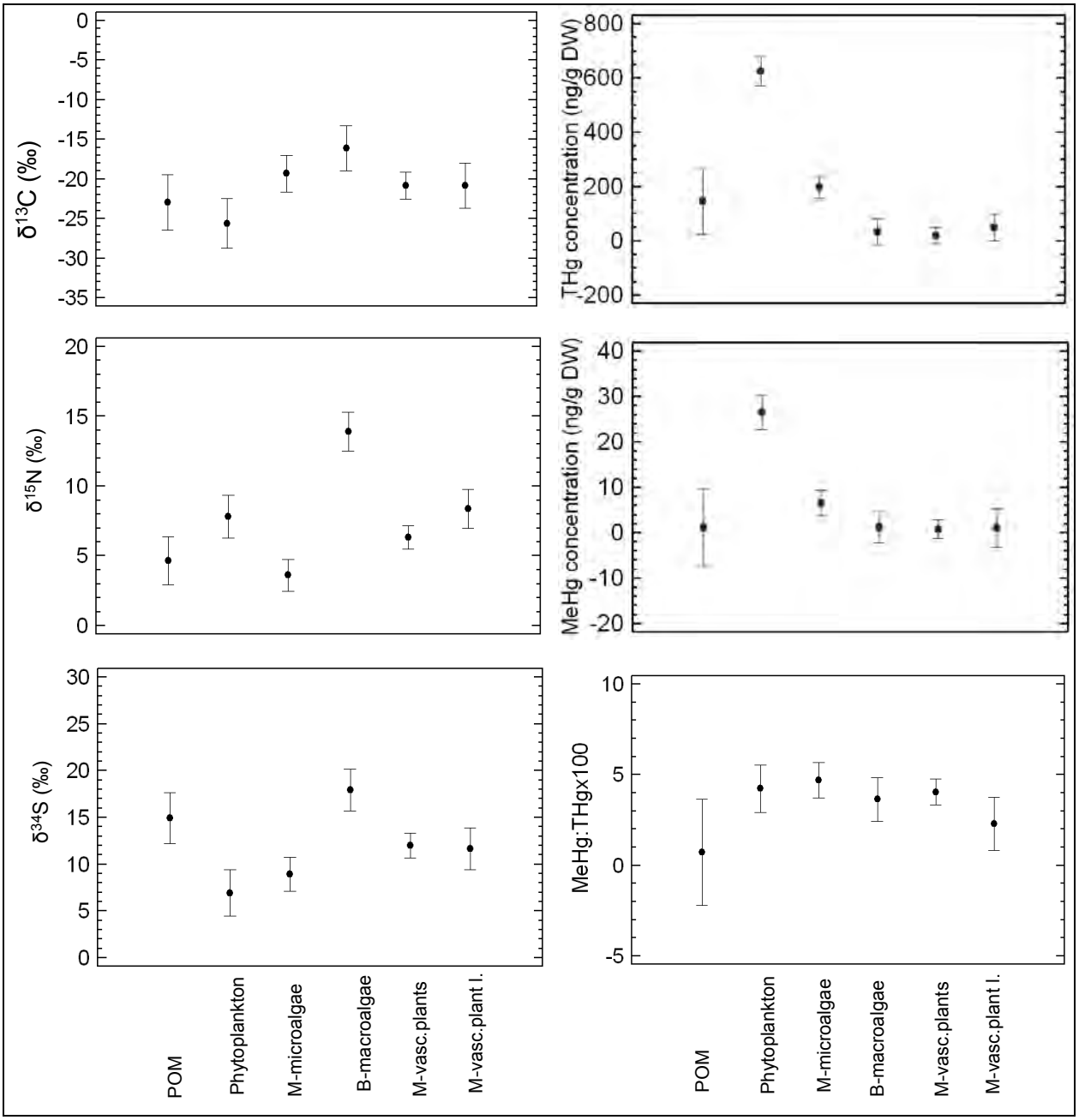

Figure 7-5. Stable isotope ratios, THg and MeHg concentrations, and MeHg:THg ratios of organic material groups collected from the China Camp marsh and adjacent San Pablo Bay area. Data are mean values and Least Significant Differences. Sample sizes given in Table 7-1. Abbreviations: POM = particulate organic material; M = marsh; B = bay; vasc. = vascular; vasc.plant l. = vascular plant litter. Isotopic signatures water types: Bay, $\delta^{13}C$ -13.89 ± 1.51‰, $\delta^{15}N$ -18.38 ± 0.73‰, $\delta^{34}S$ 20.59 ± 0.05‰; marsh pool, $\delta^{13}C$ -13.35 ± 0.98‰, $\delta^{15}N$ -14.81 ± 11.97‰, $\delta^{34}S$ 21.98 ± 0.62‰.

Primary producers from the bay, phytoplankton and macroalgae, had $\delta^{15}N$ values > 10‰, while those from the marsh were more depleted and ranged from 2 to 9‰. The primary producers (except the filamentous algae) from the marsh pool and from the low-mid marsh had more depleted (lower) $\delta^{34}S$ values, ranging from 3 to 8‰ (phytoplankton, diatoms, cyanobacteria, and *S. foliosa*), than those from the bay and mid- and high-marsh, ranging from 12 to 18‰ (bay phytoplankton and macroalgae, and *S. virginica*, *D. spicata* and *A. triangularis*). POM and *S. virginica* litter also had elevated $\delta^{34}S$ values. All elemental contents of producers and POM are provided in Table A7-1.

Consumer isotopic composition

Invertebrate isotope ratios were variable among species but included a more narrow range overall compared to primary producers and POM (Table 7-2). Mean invertebrate values (±SE) were -20.1‰ (±0.5) for $\delta^{13}C$, 12.1‰ (±0.4) for $\delta^{15}N$, and 14.2‰ (±0.4) for $\delta^{34}S$ (Figure 7-6). Exceptional isotope ratios in invertebrates were found for $\delta^{13}C$ and $\delta^{15}N$ in all species from the low marsh (the tiger beetle *Cicindela* sp., an unidentified snail, the amphipod *Orchestia traskiana*, and two filter-feeding bivalves *Geukinsia demissa*, and *Potamocorbula amurensis*), but for $\delta^{34}S$ only in *Cicindela*.

The variation in fish isotope ratios was less than that in invertebrates in general and similar to that in the bay invertebrates (Table 7-2). Mean fish values (±SE) were -17.5‰ (±0.7) for $\delta^{13}C$, 15.8‰ (±0.6) for $\delta^{15}N$, and 12.7‰ (±0.6) for $\delta^{34}S$. There was little overlap in the ranges of isotope ratios spanned by invertebrates compared to those spanned by fishes. In general, fishes were enriched in $\delta^{13}C$ and $\delta^{15}N$ and had similar $\delta^{34}S$ ratios compared to several invertebrate species. Mean invertebrate values (±SE) were -20.0‰ (±0.5) for $\delta^{13}C$, 12.1‰ (±0.4) for $\delta^{15}N$, and 14.2‰ (±0.4) for $\delta^{34}S$.

The isotope ratios in the two mammals sampled, i.e., a saltmarsh harvest mouse (*Reithrodontomys raviventris*) from the nearby HAAF fringe marsh, and a California vole (*Microtus californicus*) from China Camp, were similar (Table 7-2). Mean mammal values (±SE) were -23.1‰ (±2.2) for $\delta^{13}C$, 11.6‰ (±1.9) for $\delta^{15}N$, and 14.8‰ (±1.9) for $\delta^{34}S$ (Table 7-2).

Table 7-2. Stable isotope ratios of invertebrate, fish, mammals, and avian consumers (including habitat type, where sampled) collected from the China Camp marsh, HAAF, and adjacent San Pablo Bay area. Data are sample size (N) and mean values (standard deviations). Results of ANOVA followed by Fisher's multiple comparison procedure to detect significant differences ($p<0.05$) among isotope ratio means ($\delta^{13}C$, $\delta^{15}N$, and $\delta^{34}S$) of consumer groups indicated. Consumer groups followed by the same letter are not significantly different according to this procedure.

Consumer Group/Species	Habitat Type	N	$\delta^{13}C$ (‰)	$\delta^{15}N$ (‰)	$\delta^{34}S$ (‰)
Invertebrates			A	A	A
Cicindela sp. (Tiger beetle)	Low marsh	1	-22.3	2.2	6.7
Snail sp.	Low marsh	1	-25.5	4.1	10.2
Orchestia traskiana (Amphipod)	Low marsh	6	-22.5 (1.2)	8.0 (1.3)	17.2 (0.5)
Geukinsia demissa (Ribbed mussel)	Bay	9	-23.1 (1.1)	11.1 (1.2)	15.5 (1.3)
Potamocorbula amurensis (Chinese clam)	Bay	1	-20.9	11.6	13.3
Macoma baltica (Baltic clam)	Bay	3	-18.0 (2.6)	13.1 (0.8)	11.9 (1.0)
Nereis vexillosa (Pile worm)	Bay	2	-15.8 (0.5)	14.2 (0.0)	11.4 (2.0)
Worm sp.	Bay	2	-17.1 (0.2)	14.9 (0.5)	10.4 (3.1)
Hemigrapsus oregonensis (Yellow shore crab)	Bay	2	-16.0 (1.0)	13.5 (0.9)	15.7 (0.7)
Carcinus maenas (European green crab)	Bay	8	-19.0 (3.5)	14.1 (1.4)	15.4 (0.7)
Shrimp sp.	Bay	6	-19.6 (0.4)	15.4 (1.6)	14.7 (1.4)
Fishes			B	B	A
Platichthys stellatus (Starry flounder)	Bay	8	-18.3 (3.8)	15.3 (1.5)	11.8 (1.6)
Clevelandia ios (Arrow goby)	Bay	3	-14.8 (1.6)	15.6 (1.2)	12.7 (0.6)
Leptocottus armatus (Pacific staghorn sculpin)	Bay	9	-17.6 (2.6)	16.3 (1.2)	13.5 (0.7)
Mammals			A	A	A
Reithrodontomys raviventris (Salt marsh harvest mouse)	High marsh	1	-23.1	12.7	14.9
Microtus californicus (California vole)	High marsh	1	-23.2	10.7	14.7
Birds			A	AB	A
Melospiza melodia samuelis (Song sparrow)	High marsh	3	-20.6 (0.8)	12.7 (0.0)	15.0 (0.2)
Laterallus jamaicensis coturniculus (California black rail)	Marsh	1	-24.8	13.5	15.8

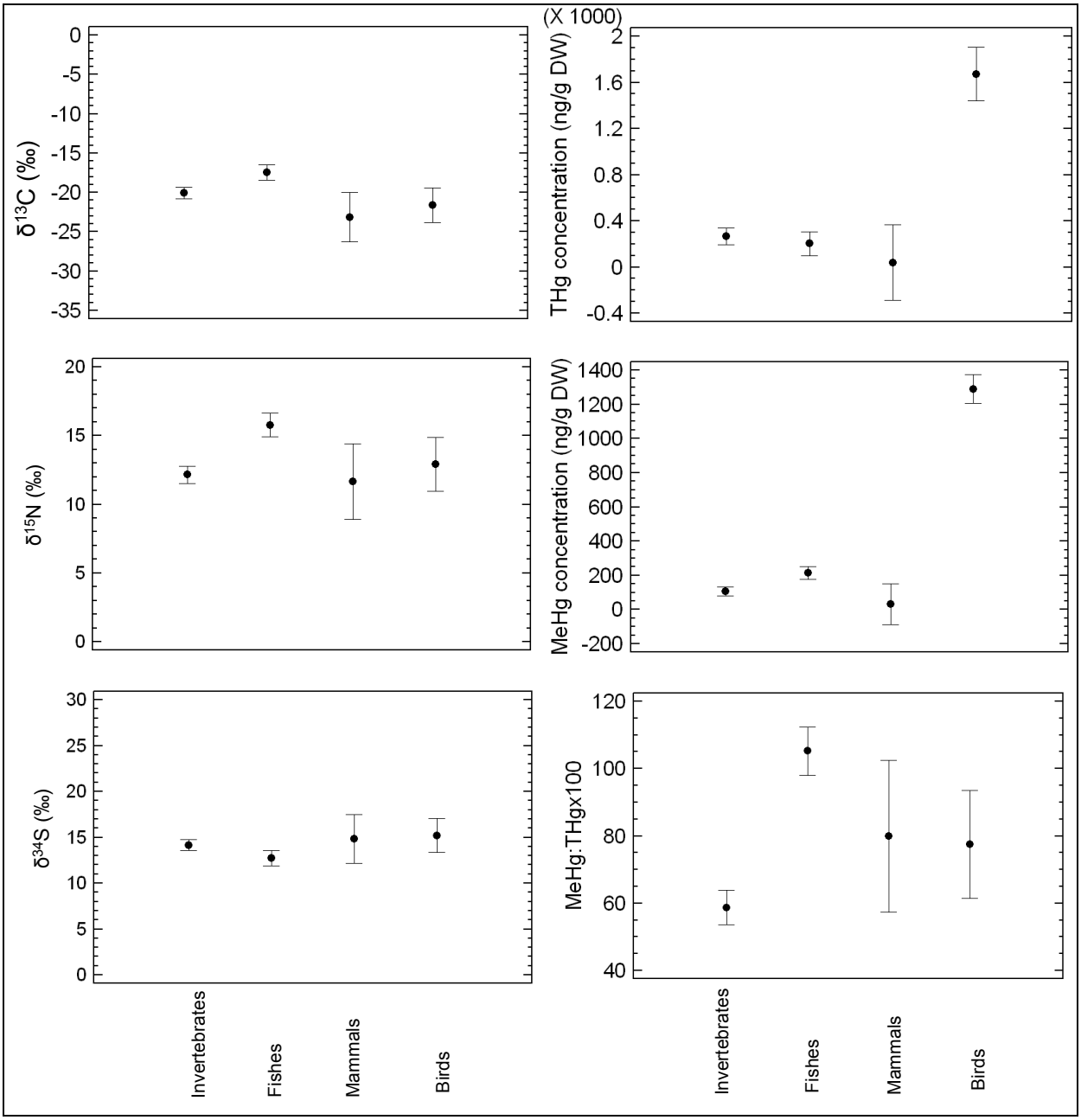

Figure 7-6. Stable isotope ratios, THg and MeHg concentrations, and MeHg:THg ratios of consumer groups collected from the China Camp marsh and adjacent San Pablo Bay area. Data are mean values and least significant differences. Sample sizes given in Table 7-2.

There was considerable overlap in the ranges of isotope ratios spanned by mammals and invertebrates. Absolute differences in mean δ values of invertebrates and mammals were 3.0‰ for $\delta^{13}C$, 0.4‰ for $\delta^{15}N$, and 0.6‰ for $\delta^{34}S$. Mean mammal $\delta^{13}C$ and $\delta^{34}S$ values were most closely associated with the isotope ratios of the C_3 vascular plants from the mid and high marsh, i.e., *S. virginica* and *A. triangularis*, but their $\delta^{15}N$ values of 10.7-12.7 ‰ were at least a factor of 1.7 greater.

The isotope ratios in the two birds sampled from China Camp, i.e., a song sparrow (*Melospiza melodia samuelensis)* and a California black rail (*Laterallus jamaicensis coturniculus*) were distinct from one another (Table 7-2). Absolute differences in their mean δ-values were 4.2‰ for $\delta^{13}C$, 0.8‰ for $\delta^{15}N$, and 0.8‰ for $\delta^{34}S$. Mean bird values (±SE) were -22.1‰ (±1.4) for $\delta^{13}C$, 12.2‰ (±0.8) for $\delta^{15}N$, and 15.1‰ (±1.3) for $\delta^{34}S$ (Figure 7-6). The isotope ratios of *M. melodia samuelensis,* a seed and insect consumer, were most closely associated with the isotope ratios of the C_3 vascular plants from the mid and high marsh, i.e., *S. virginica* and *A. triangularis*, but their $\delta^{15}N$ values of 15.0‰ were at least a factor of 2.3 greater.

The isotopic ratios of *L. jamaicensis coturniculus,* a carnivore, were most closely associated with selected low-marsh and bay invertebrates. All elemental contents of consumers are provided in Table A7-2.

Associations among producer and consumer ratios

Nitrogen isotopic distributions can be useful indicators of trophic position in marine ecosystems, where ^{15}N enrichment increases predictably with trophic level of consumers (Peterson and Fry 1987; Fry 1988, 1991). Thus, the univariate plot of $\delta^{15}N$ values of consumers from the China Camp marsh and adjacent San Pablo Bay area provided a progressive ranking of trophic position. By incorporating a generalized trophic enrichment factor of 3.6‰ (Fry 1988), the number of trophic levels (food chain length) and consumer trophic positions were approximated. This analysis indicated a total of four trophic levels for the China Camp marsh and adjacent San Pablo Bay area food web (Figure 7-7). The primary consumer trophic level (TL 2: 7.8‰ ≤ $\delta^{15}N$<11.4‰) encompassed one invertebrate species, *Orchestia traskiana*, and one mammal, *Microtus californicus*. Two invertebrate species with $\delta^{15}N$ values less than 7.8‰ were found, i.e., a *Cicindela* species and a snail. These species are obligate herbivores, and their exceptionally low $\delta^{15}N$ values may be due to a potential preference for plants with low $\delta^{15}N$ values, which may be a species like *A. triangularis* for *Cicindela* sp. and marsh pool filamentous algae for the snail (Table 7-1).

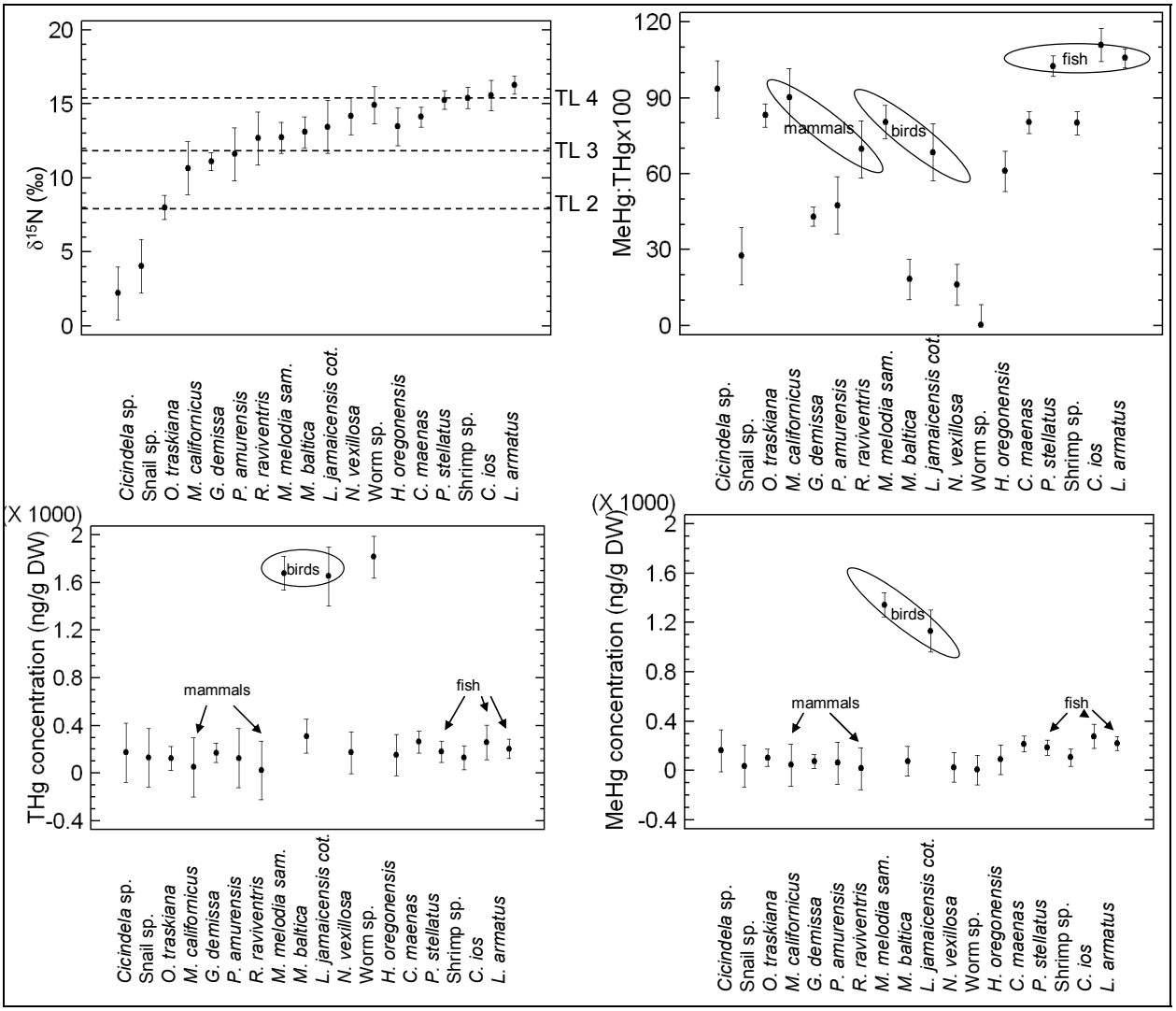

Figure 7-7. Trophic level estimation for invertebrates, fish, and avian consumers collected from the China Camp marsh and adjacent San Pablo Bay area based on mean (± standard error of the mean) ranked nitrogen isotopic distributions ($\delta^{15}N$)-Upper left-hand side. Hg species and MeHg:THg ratios presented to enable relating trophic level following $\delta^{15}N$ ranking to MeTHg ratio. Sample sizes given in Table 7-3. Abbreviations: TL = Trophic Level.

The second consumer trophic level (TL 3: 11.4‰ ≤ $\delta^{15}N$ < 15.0‰) encompassed seven invertebrate species, one mammal, *R. raviventris*, and both birds (Table 7-2). Shrimp had a $\delta^{15}N$ value of 15.4‰, which is close to the upper boundary of TL 3 and the lower boundary of TL 4. The third consumer trophic level (TL 4; $\delta^{15}N$ ≥ 15.0‰ and <18.8‰) encompassed three fish species. The maximum $\delta^{15}N$ value of 16.3‰ lies near the margin of trophic levels 3 and 4 (15‰), suggesting that only three trophic levels may exist in this particular aquatic food web.

Dual isotope biplots indicated associations among isotopic distributions of producers and consumers (Figure 7-8). Among dual isotope biplots, the $\delta^{13}C$ versus $\delta^{34}S$ is considered the most informative in resolving food web structure because of a high ratio of among- to within-producer isotope ratio variation with minimal isotopic fractionation associated with trophic transfers (Peterson et al. 1985; Peterson and Fry 1987). The $\delta^{13}C$ versus $\delta^{34}S$ plot from the China Camp marsh and adjacent San Pablo Bay area food web indicated the following:

1. Ratios of the bay-associated invertebrates *M. Baltica*, *N. vexillosa*, unidentified worm species, *H. Oregonensis*, *C. maenas*, shrimp, and all fish primarily distributed intermediate between those of macroalgae, C_4 grasses, and marsh pool-filamentous algae.
2. Ratios of all marsh-associated invertebrates *O. traskiana*, *G. demissa*, the bay-associated invertebrate *P. amurensis*, both mammals and both birds, and the exceptional *Cicindela* sp. and snail species largely distributed intermediate between those of marsh pool-phytoplankton, marsh pool-POM, bay-POM, and marsh-diatoms, and marsh–cyanobacteria.
3. Ratios of none of the consumers matched those of the C_3 marsh plants and the bay-phytoplankton. The relative depletion of *S. virginica* live and litter materials, of *A. triangularis*, and of the bay phytoplankton in ^{13}C suggests minimal food web support from these sources. However, even though these plant species may contribute little to the entire food web, they could be an important food source for niche organisms. Dual isotope biplots of $\delta^{13}C$ versus $\delta^{15}N$ values (Figure 7-8) confirmed results from the $\delta^{13}C$ versus $\delta^{34}S$ plots described above.

In summary, trends in the collective isotopic distributions suggest that inputs from bay macroalgae, C_4 grasses, marsh-diatoms, marsh-cyanobacteria, and marsh-pool filamentous algae provide the organic matter that forms the base of the food web, supporting invertebrates, fishes, mammals, and birds. These producers together occupy four habitat types, i.e., the bay, the low-, mid-, and high-salt marsh. However, it remains to be demonstrated if connectivity between these habitats exists.

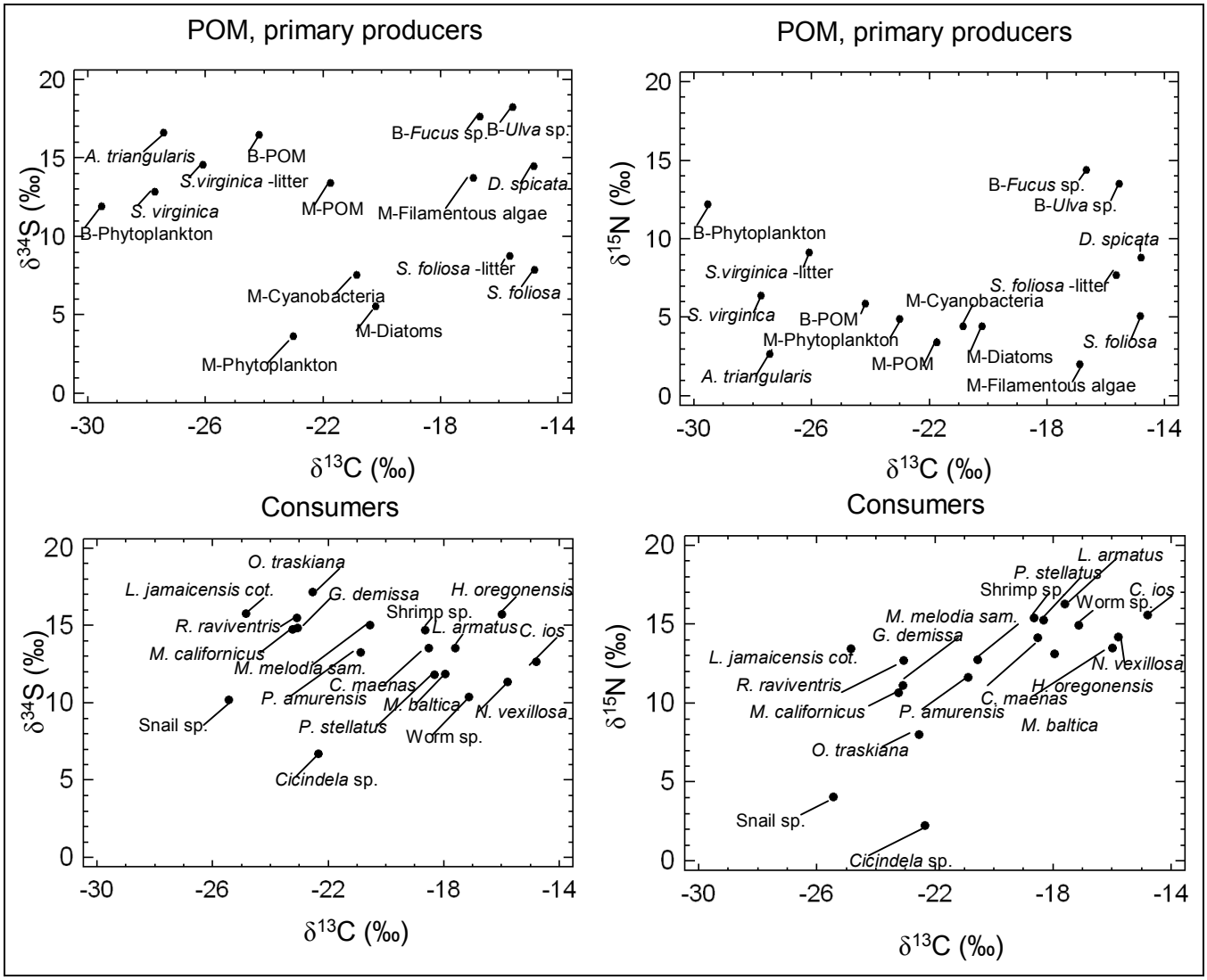

Figure 7-8. Dual isotope plots of $\delta^{13}C$, $\delta^{15}N$, and $\delta^{34}S$ mean values for particulate organic matter (POM), primary producers, and consumers collected from the China Camp marsh and adjacent San Pablo Bay area. Abbreviations: B = bay; M = marsh.

Further analysis of the associations among producers and consumers will be performed using multiple-source mixing models (Lubetkin and Simenstad 2004) to approximate the relative input of each source into the food web of the China Camp marsh and adjacent San Pablo Bay area. Following this different approach, the consumers will be organized by their position in the food web in terms of their diets, rather than by habitat (Table 7-3).

Table 7-3. Estimated trophic levels for invertebrate, fish, mammals, and avian consumers collected from the China Camp marsh, HAAF, and adjacent San Pablo Bay area, calculated using SOURCE and STEP with $\delta^{13}C$, $\delta^{15}N$, and $\delta^{34}S$.

Consumer Group/Species	Habitat Type	SOURCE	STEP
Herbivores			
Microtus californicus (California vole)	High marsh	TBD	TBD
Reithrodontomys raviventris (Salt marsh harvest mouse)	High marsh	TBD	TBD
Snail sp.	High marsh	TBD	TBD
Suspension feeders			
Geukinsia demissa (Ribbed mussel)	Bay	TBD	TBD
Potamocorbula amurensis (Chinese clam)	Bay	TBD	TBD
Macoma baltica (Baltic clam)	Bay	TBD	TBD
Suspension-deposit feeders			
Nereis vexillosa (Pile worm)	Bay	TBD	TBD
Shrimp sp.	Bay	TBD	TBD
Deposit feeders			
Orchestia traskiana (Amphipod)	Low marsh	TBD	TBD
Worm sp.	Bay	TBD	TBD
Omnivores			
Hemigrapsus oregonensis (Yellow shore crab)	Bay	TBD	TBD
Carcinus maenas (European green crab)	Bay	TBD	TBD
Predators			
Leptocottus armatus (Pacific staghorn sculpin)	Bay	TBD	TBD
Clevelandia ios (Arrow goby)	Bay	TBD	TBD
Platichthys stellatus (Starry flounder)	Bay	TBD	TBD
Cicindela sp. (Tiger beetle)	Low marsh	TBD	TBD
Laterallus jamaicensis coturniculus (California black rail)	Marsh	TBD	TBD
Melospiza melodia samuelis (Song sparrow)	High marsh	TBD	TBD

Abbreviation: TBD= to be determined.

Mercury species concentrations and MeHg:THg ratios in producers and consumers

Mean THg and MeHg concentrations of primary producers and POM appeared also to be less related to habitat than to organismal characteristics, just like the isotopic ratios. Both these concentrations showed a similar pattern, in that levels were greatest in phytoplankton (ranges 578 to 654 ng THg g^{-1} DW, and 16.9 to 41.0 ng MeHg g^{-1} DW), intermediate in

POM and marsh microalgae (ranges 38 to 276 ng THg g^{-1} DW, and 1.05 to 8.87 ng MeHg g^{-1} DW), and least in marsh vascular plants (live and litter) and bay macroalgae (ranges 9 to 61 ng THg g^{-1} DW, and 0.30 to 1.48 ng MeHg g^{-1} DW; Table 7-4, Figure 7-2). The MeHg:THg ratio was significantly greater in phytoplankton and marsh microalgae than in marsh vascular plant litter, with the other groups having intermediate MeHg:THg ratios.

Table 7-4. THg, MeHg, and MeHg:THg ratios of suspended particulate organic material (POM), primary producers, and vascular plant litter (including habitat type, where sampled) collected from the China Camp marsh and adjacent San Pablo Bay area. Data are sample size (N) and mean values (standard deviations). Results of ANOVA followed by Fisher's multiple comparison procedure to detect significant differences ($p<0.05$) among Hg species means of organic material groups indicated. Organic material groups followed by the same letter are not significantly different according to this procedure. ND = not determined.

Organic Material Type/ Species	Habitat Type	N	THg (ng g^{-1} DW)	MeHg (ng g^{-1} DW)	MeHg : THg (x 100)
Particulate organic matter			AB	AB	A
POM	Bay	2	144	1.05	0.73
POM	Marsh pool	2	ND	ND	ND
Phytoplankton			C	C	A
SF Bay	Bay	2	578 (45)	41.0 (7.32)	7.16 (1.82)
Marsh	Marsh pool	3	654 (36)	16.9 (15.00)	2.29 (1.10)
Marsh microalgae			B	B	A
Diatom sp.	Low-mid marsh	3	273 (4)	8.87 (1.08)	3.25 (0.42)
Cyanobacteria sp.	Low-mid marsh	3	276 (10)	7.45 (2.57)	2.68 (0.86)
Filamentous sp.	Marsh pool	3	38 (11)	2.98 (0.58)	8.13 (1.75)
Bay macroalgae			A	AB	A
Ulva sp.	Bay	3	40 (13)	1.48 (0.19)	3.97 (1.42)
Fucus sp.	Bay	3	26 (3)	0.85 (0.08)	3.32 (0.17)
Marsh vascular plants			A	A	A
Spartina foliosa (C_4)	Low marsh	6	19 (7)	0.76 (0.31)	4.02 (0.73)
Salicornia virginica (C_3)	Mid marsh	5	21 (10)	1.02 (0.42)	5.29 (2.69)
Distichlis spicata (C_4)	High marsh	3	23 (2)	0.61 (0.07)	2.73 (0.35)
Atriplex triangularis (C_3)	High marsh	3	9 (2)	0.30 (0.02)	3.36 (0.73)
Marsh vascular plant litter			A	AB	A
Spartina foliosa (C_4)	Low marsh	3	61 (8)	0.97 (0.02)	1.67 (0.33)
Salicornia virginica (C_3)	Mid marsh	3	36 (7)	0.96 (0.02)	2.88 (0.61)

Among the primary producers and POM, two groups were distinguished based on their MeHg:THg ratios. The group with the greatest MeHg:THg ratio, ranging from 7 to 8, included bay phytoplankton and marsh pool filamentous algae (Table 7-4). The other group with a MeHg:THg ratio of 1 to 5 included all other primary producers, POM, and marsh vascular plant litter. The relatively large standard errors of the mean for three groups were caused (1) in POM by lack of replicates; (2) in bay macroalgae by one *Ulva* sample with an unusually elevated THg concentration and, thus, a far lower Me:THg ratio than the other macroalgal samples; and (3) in marsh vascular plant litter by inclusion of samples in different decomposition phases with their inherent MeHg:THg ratios (see Chapter 6).

Mean THg levels were significantly greater in birds (1,670 ng g^{-1} DW) than in all other consumer groups with (Figure 7-3). The mean THg levels in the other consumer groups were far less, notably 274 ng g^{-1} in invertebrates, 185 ng g^{-1} in fish, and 27 ng g^{-1} in mammals. However, the mean THg level in birds was even exceeded by the THg concentration of 1,820 ng g^{-1} DW in an unidentified worm species from the bay (Table 7-5). The MeHg levels in birds (1,280 ng g^{-1}) were also significantly greater than in the other consumer groups (Figure 7-3). The mean MeHg levels in the other consumer groups were far less than those for THg, notably 190 ng g^{-1} in fish, 119 ng g^{-1} in invertebrates, and 17 ng g^{-1} in mammals.

Among the consumers, the greatest MeHg:THg ratio was found in fish, where almost 100% of THg had accumulated in the form of MeHg. MeHg:THg ratios in the other consumer groups decreased in the order of birds and mammals with 75%> and invertebrates with 64% (Figure 7-3). There was a scale difference between the overall mean MeHg:THg ratio in primary producers and in consumers of a factor of 12.

Ranking the consumers into their approximate trophic levels based on their $\delta^{15}N$ values (Figure 7-4, upper left side) did not indicate an increase in MeHg concentration with increasing trophic level for most consumers (Figure 7-4, lower right side). Fish ranked at the greatest, fourth, trophic level and also exhibited elevated MeHg levels (mean MeHg level 215 ng g^{-1} DW). Although birds ranked below fish at the third trophic level, they demonstrated by far the greatest MeHg concentrations (mean MeHg level 1,290 ng g^{-1}DW). Mammals ranked at a trophic level less than both other consumer groups and exhibited less MeHg concentrations (mean MeHg level 199 ng g^{-1}DW). Other phenomena of interest were (1) the only insect

Table 7-5. THg, MeHg, and MeHg:THg ratios of invertebrate, fish, mammals, and avian consumers (including habitat type, where sampled) collected from the China Camp marsh, HAAF, and adjacent San Pablo Bay area. Data are sample size (N) and mean values (standard deviations). Results of ANOVA followed by Fisher's multiple comparison procedure to detect significant differences ($p<0.05$) among Hg species means of consumer groups. Consumer groups followed by the same letter are not significantly different according to this procedure.

Consumer Group/Species	Habitat Type	N	THg (ng g^{-1} DW)	MeHg (ng g^{-1} DW)	MeHg:THg (x100)
Invertebrates			A	A	A
Cicindela sp. (Tiger beetle)	Low marsh	1	173	161	93.4
Snail sp.	Low marsh	1	131	36.0	27.5
Orchestia traskiana (Amphipod)	Low marsh	6	126 (26)	103 (13.70)	83.1 (7.55)
Geukinsia demissa (Ribbed mussel)	Bay	9	171 (55)	74.6 (29.17)	43.1 (3.94)
Potamocorbula amurensis (Chinese clam)	Bay	1	127	60.5	47.5
Macoma Baltica (Baltic clam)	Bay	3	310 (198)	76.7 (53.13)	18.3 (4.69)
Nereis vexillosa (Pile worm)	Bay	2	174 (31)	26.2 (17.61)	16.2 (13.04)
Worm sp.	Bay	2	1,815 (626)	6.50 (2.10)	0.40 (0.26)
Hemigrapsus Oregonensis (Yellow shore crab)	Bay	2	152 (20)	90.4 (23.87)	61.1 (23.78)
Carcinus maenas (European green crab)	Bay	8	263 (137)	216 (118.28)	80.3 (10.31)
Shrimp sp.	Bay	6	119 (34)	90.7 (28.10)	76.0 (5.39)
Fishes			A	B	C
Platichthys stellatus (Starry flounder)	Bay	8	181 (37)	186 (39.47)	103 (4.24)
Clevelandia ios (Arrow goby)	Bay	3	258 (201)	276 (195.86)	111 (7.63)
Leptocottus armatus (Pacific staghorn sculpin)	Bay	9	205 (83)	220 (98.60)	106 (6.31)
Mammals			A	A	AB
Reithrodontomys raviventris (Salt marsh harvest mouse)	High marsh	1	25	17.5	69.7
Microtus californicus (California vole)	High marsh	1	50	44.9	90.1
Birds			B	C	A
Melospiza melodia samuelis (Song sparrow)	High marsh	3	1,678 (588)	1,342.93 (448.01)	80.5 (1.57)
Laterallus jamaicensis coturniculus (California black rail)	Marsh	1	1,652	1,130	68.5

analyzed, *Cicindela* sp., exhibited a strongly elevated MeHg level, potentially causing elevated MeHg concentrations in insectivorous consumers; (2) the invertebrate species exhibited MeHg concentrations that showed a large between-species variation, but narrow within-species variation. These results indicate also, just as the stable isotope ratios, that the associations between species are more defined by their diets rather than by habitat. Further analysis of the associations among producers and consumers using multiple-source mixing models (Lubetkin and Simenstad 2004) to approximate the relative inputs of each source into the food web of the China Camp marsh and adjacent San Pablo Bay area is expected to elucidate these relationships.

General discussion

Numerous studies of Atlantic and Gulf of Mexico salt marshes, when employing only a single stable isotope, reported various influences of vascular plants and algae as organic matter sources supporting salt marsh food webs. In general, these studies suggest that *S. foliosa* detrital inputs to the food web are dominant in supporting consumers in Atlantic coastal salt marshes, but phytoplankton or benthic algae may be equally important sources in gulf systems. The role of terrestrial input and C_3 plant contributions to these food webs could not be resolved by single isotope approaches, but may be important in some marshes (as discussed by Kwak and Zedler 1997).

Application of multiple stable isotopes (^{13}C, ^{15}N, and ^{34}S) to identify sources of organic matter in salt marsh food webs has provided more conclusive results and allowed the consideration of more producers relative to those studies applying a single isotope. Multiple stable isotope research in salt marshes of Massachusetts and Georgia (Atlantic Coast) indicated that *S. alterniflora* and algae may be almost equally important contributors to those food webs, with the balance shifting depending on location in the marsh, feeding mode, size, and trophic position of consumers (Peterson et al. 1985, 1986; Peterson and Howarth 1987). Conversely, multiple isotope evidence from Louisiana and Mississippi (gulf coast) salt marshes suggest that *S. alternoflora* is not an important source of organic matter in those systems and that the food webs are primarily supported by benthic and planktonic algae (Fry 1983; Sullivan and Moncreiff 1990).

The results of the current preliminary analysis of organic matter sources that support the consumers within the China Camp marsh and in the adjacent San Pablo Bay indicate that a mixture of inputs from bay macroalgae, C_4 grasses, and marsh microalgae may provide the organic matter that forms the base of the food web, while phytoplankton appears not to be a major contributor to the marsh food web. Whether the results of the current study agree with those reported in the only other food web study of the more southern, California coastal marshes of the Tijuana Estuary and San Dieguito Lagoon (Kwak and Zedler 1997), or with the contrasting results of the study by Grenier (2004) on a similar San Francisco Bay marsh as included in the current study remains to be demonstrated. The results of the current study are in contrast to those reported by Spiker and Schemel (1979), indicating that in San Francisco Bay $\delta^{13}C$ analyses revealed that *S. foliosa* was not an important source of detritus in the large estuarine system.

Success in identifying sources (primary producers) of organic matter in a food web depends upon the ability to differentiate potential sources isotopically. This differentiating ability diminishes as additional sources are considered and isotopic distributions overlap. California coastal wetlands are generally small compared with those associated with most Atlantic and Gulf of Mexico shores (Kwak and Zedler 1997). On the western coast, the gradient between land and sea is steep and the intertidal zone is small. The Pacific coast is a high energy zone and marshes can only develop in embayments. High salt marsh habitat lies within meters of intertidal channels or bays. Thus, producers associated with all marsh habitats must be considered as potential sources of organic matter for the aquatic food web.

Wetland conditions can be conducive to MeHg production, and certain wetlands have been identified as potential contributors of estuaries (Heyes 1996; St. Louis et al. 1994, 1996; Best et al. 2005). Hg concentrations increase with each step in the food chain through biomagnification. Therefore, species at the top of a food chain, e.g., humans and fish-consuming wildlife, receive the greatest Hg exposure. An interim fish consumption advisory for humans was issued for the San Francisco Estuary due to concern over human exposure to MeHg (Office of Environmental Health Hazard Assessment 1994). Following USEPA guidance (USEPA 1995), a Hg screening value of 230 ng g^{-1} WW (equivalent to 2,300 ng g^{-1} DW) was calculated (SFEI 1999). This means that samples with Hg concentrations above the screening value pose a potential human health concern. THg

concentrations in all consumer samples collected in the current study, including fish, were below this screening value, and, thus did not pose a direct threat to human health. However, whether or not the measured Hg species levels pose a toxicity threat for the food web in the China Camp marsh and adjacent bay area still has to be determined. A potentially fruitful approach would be to follow bioaccumulation and reproduction in caged sentinel organisms on selected locations within the marsh and bay over a suitable period of time and collecting sufficient information on diet and environmental factors affecting net MeHg production to explain spatial and seasonal effects in sentinel response. The Hg levels determined in the current study were far greater than those in another, freshwater, marsh system of the Everglades where extensive food chain studies have been conducted (Loftus 2000). In the latter system, pilot experiments were undertaken to quantify toxicity in fish by Hg species in the marsh.

In order to manage coastal wetland fishes and birds, it is critical to understand how the different habitats that provide foods are coupled with habitats that support spawning and nursery functions and provide nesting, resting, and refuge areas. Tidal systems have a large potential for significant linkages between marshes, channels, and bays, with two-way exchanges of consumers and foods being possible. This means that fishes and birds may move into the marsh and feed, and foods may move into the channels and bay to be consumed. Current results indicate that a mixture of input from bay macroalgae, C_4 grasses, marsh diatoms and cyanobacteria, and marsh-pool filamentous algae may provide the organic matter that forms the base of the food web. The study also supports this linkage and confirms that these habitats should be managed as a single ecosystem. Knowledge that this link exists is important for the planning of habitat enhancement and restoration projects.

Conclusions

1. Trends in the collective isotopic distributions suggest that inputs from bay macroalgae, C_4 grasses, marsh diatoms, marsh cyanobacteria, and marsh pool filamentous algae provide the organic matter that forms the base of the food web, supporting invertebrates, fishes, mammals, and birds.
2. These producers together occupy four habitat types, i.e., the bay, the low-, mid-, and high-salt marsh. It remains to be demonstrated if connectivity between these habitats exists.
3. Mean THg and MeHg concentrations of primary producers and POM appeared to be less related to habitat than to organismal characteristics.

Levels were greatest in phytoplankton (ranges 578 to 654 ng THg g^{-1} DW and 16.9 to 41.0 ng MeHg g^{-1} DW), intermediate in POM and marsh microalgae (ranges 38 to 276 ng THg g^{-1} DW and 1.05 to 8.87 ng MeHg g^{-1} DW), and least in marsh vascular plants (live and litter) and bay macro-algae (ranges 9 to 61 ng THg g^{-1} DW and 0.30 to 1.48 ng MeHg g^{-1} DW). The MeHg:THg ratio was significantly greater in phytoplankton and marsh microalgae than in marsh vascular plant litter, with the other groups having intermediate MeHg:THg ratios. Among the primary producers and POM, two groups were distinguished based on their MeHg:THg ratios. The group with the greatest MeHg:THg ratio, ranging from 7 to 8, included bay phytoplankton and marsh pool filamentous algae. The other group with a MeHg:THg ratio of 1 to 5 included all other primary producers, POM, and marsh vascular plant litter.

4. Mean THg levels were significantly greater in birds (1,670 ng g^{-1} DW) than in all other consumer groups. The mean THg levels in the other consumer groups were far less, notably 274 ng g^{-1} in invertebrates, 185 ng g^{-1} in fish, and 27 ng g^{-1} in mammals. However, the mean THg level in birds was even exceeded by the THg concentration of 1,820 ng g^{-1} DW in an unidentified worm species from the bay. The MeHg levels in birds (1,290 ng g^{-1}) were also significantly greater than in the other consumer groups. The mean MeHg levels in the other consumer groups were far less than those for THg, notably 190 ng g^{-1} in fish, 119 ng g^{-1} in invertebrates, and 17 ng g^{-1} in mammals. Among the consumers, the greatest MeHg:THg ratio was found in fish, where almost 100% of THg had accumulated in the form of MeHg. MeHg:THg ratios in the other consumer groups decreased in the order of birds and mammals with 75% and invertebrates with 64%. There was a scale difference between the overall mean MeHg:THg ratio in primary producers and in consumers of a factor of 12.
5. Ranking the consumers into their approximate trophic levels based on their $\delta^{15}N$ values did not indicate an increase in MeHg concentration with increasing trophic level for most consumers. Fish ranked at the greatest, fourth, trophic level and also exhibited elevated MeHg levels (mean MeHg level 215 ng g^{-1} DW). Although birds ranked below fish at the third trophic level, they demonstrated by far the greatest MeHg concentrations (mean MeHg level 1,290 ng g^{-1} DW). Mammals ranked at a trophic level less than both other consumer groups and exhibited less MeHg concentrations (mean MeHg level 199 ng g^{-1} DW). Further analysis of the associations among producers and consumers using multiple-source mixing models (Lubetkin and Simenstad 2004) to approximate the relative inputs of each source into the food web of the China Camp marsh and adjacent San Pablo

Bay area is expected to elucidate these relationships. Following this different approach, the consumers will be organized by their position in the food web in terms of their diets, rather than by habitat.

POINT OF CONTACT CHAPTER 7:

Dr. Elly P. H. Best
U.S. Army Engineer Research and Development Center
Environmental Laboratory, Vicksburg, MS
Ph: 601-634-4246; E-mail: elly.p.best@erdc.usace.army.mil

8 Bioavailability of Sediment-Associated Mercury to Macrobenthos

Introduction

Estuarine sediments are considered a sink for mercury, and Hg uptake from sediment is a major route of Hg transfer to the biota in aquatic systems. Sediment-associated inorganic Hg and monomethylmercury (MeHg) are bioavailable for assimilation into invertebrates (Gagnon and Fisher 1997; Mason and Lawrence 1999; Lawrence and Mason 2001) and are, therefore, a primary source of Hg transferred to fish and piscivorous birds (Jackson 2001; Chan et al. 2003). Multiple factors control Hg bioavailability and, therefore, this relevant parameter cannot be estimated using total sediment concentrations as the sole determinant (Lawrence and Mason 2001). Heavy metal bioavailability and bioaccumulation potential are positively correlated with the rate of contaminant accumulation in laboratory exposures (e.g., Gillis et al. 2004; van Straalen et al. 2005; Gust and Fleeger 2005).

Intertidal sediments at Hamilton Army Airfield (HAAF) and China Camp present a significant and bioavailable source of Hg to the sediment-feeding benthic bent-nosed clam *Macoma nasuta* in laboratory exposures (Best et al. 2005). This chapter presents results of further investigation of the bioavailability of Hg in sediments from San Pablo Bay salt marshes to another benthic invertebrate, the polychaete worm *Nereis virens*.

To restore wetlands at HAAF, the area will require additional material to elevate the site to the point where typical marsh vegetation can colonize and the natural sediment trapping, marsh-building physical dynamics can proceed. Such a restoration effort would include addition of locally dredged sediment to raise the topography relative to sea level. The higher level may result in changes to the pre-restoration potential of sediment Hg and MeHg to accumulate in the benthic biota. It was postulated that adequate estimates of Hg bioavailability in a post-restoration HAAF marsh may be attained by using a local restored marsh, the Sonoma Baylands, as a surrogate.

The bioavailability of sediment-associated THg and MeHg from the HAAF bay edge, China Camp State Park, and, respectively, the natural and restored salt marshes of the Sonoma Baylands were assessed. The more landward part of the Sonoma Baylands was restored in 1998, using both deep anthropogenic dredged sediment and post-construction, naturally deposited, allochthonous sediment. Comparison of the bioavailability of Hg and MeHg from those intertidal sediments is expected to provide an insight on whether Hg bioavailability will change after undergoing a restoration effort.

In addition, this chapter presents results of an expanded investigation in reducing the Hg bioavailability by sediment treatment using granular activated carbon (GAC). Early results (Best et al. 2005) indicated that GAC reduces the bioavailability of spiked, labile, but not of environmentally contaminated Hg species to a benthic invertebrate. In the present study, the effect of increasing the contact time of GAC and HAAF sediment on the bioavailability of Hg species is addressed.

Objectives

The objectives of this study were to quantify the following:

1. The uptake kinetics of THg and MeHg to an intertidal benthic invertebrate in HAAF sediments using bioaccumulation methods
2. The effects of salt marsh restoration activities on the bioavailability of mercury species in the sediment using Sonoma Baylands as representative for a restored marsh
3. The effects of contact time on Hg bioavailability reduction by GAC addition to HAAF sediments.

Study sites

The HAAF and the Sonoma Baylands are located on San Pablo Bay, California. The Baylands ecosystem includes the areas of maximum and minimum tidal fluctuations, adjacent habitats, and their associated plants and animals. The boundaries of the ecosystem vary with the bayward and landward movements of fish and wildlife that depend upon the Baylands for survival. Many habitats of the Baylands are wetlands. A detailed description of the sites and locations is presented in Chapter 3.

Methods

Experimental organisms

The marine, sediment-dwelling polychaete worm, *N. virens,* was used in all experiments. Worms purchased from a commercial vendor (Aquatic Research Organisms, Hampton, NH) were collected from an intertidal location and shipped overnight to ERDC, Vicksburg, MS. Upon arrival, worms were acclimated to 20 °C in 30‰ artificial seawater over a period of 2 to 3 days. Worms weighing between 1 and 3 g were used in the bioaccumulation experiments.

Sediment sampling

Sediment samples were collected on 27 July 2004 in the mudflats adjacent to tidal marshes at the reference site in the China Camp State Park R-44, the HAAF bay edge site SM-10, and the natural and the restored Sonoma Bayland salt marshes.

Several undisturbed 10.5-cm-diameter sediment cores were collected from a boat. The upper 10-cm layers were pooled and stored in an ice-cooled-one-gallon bucket. The buckets were deep-frozen with dry ice and shipped overnight to the Environmental Laboratory at ERDC, Vicksburg, MS. The contents of the buckets were stored at -80 °C until further use.

Uptake kinetics experiment

The bioavailability of Hg was assessed by measuring the uptake kinetics of THg and MeHg in *N. virens,* using bioaccumulation methods (USEPA and USACE 1998; ASTM 2000).

The uptake kinetics of THg and MeHg were investigated using sediment collected from the HAAF, China Camp, Sonoma Marsh, and Sonoma Baylands sites, and time-series exposures. Sediment from each site was added to 20 replicate 1-L beakers. Each beaker received the volume of sediment corresponding to 75 g DW and 800 mL of 30‰ artificial seawater (ASW; Instant Ocean, OH). Beakers were maintained at 20 °C in a temperature-controlled water bath under constant trickle aeration. After 48 h, one worm was added to each beaker. The water in each beaker was renewed three times weekly to maintain adequate water quality and no supplemental food source was provided. To determine uptake rate

kinetics, worms from three replicates were sampled after 7, 14, 28, and 56 days of exposure.

To derive kinetics parameters for THg and MeHg, 56-day accumulation data for both THg and MeHg were fit to a two-compartment model (Gillis et al. 2004)

$$\frac{dC_a}{dt} = k_u C_s - k_e C_a$$

in which C_a is the tissue concentration (ng per g wet wt), k_u is the conditional uptake clearance rate coefficient (g sediment dry wt per g tissue wet wt day^{-1}), and C_s is the concentration in the sediment (ng per g dry wt) and k_e is the conditional elimination rate coefficient (day^{-1}). C_a and C_s were measured, k_u was calculated, and the above equation was then solved for k_e.

Bioavailability reduction experiment

Sediment from the HAAF site was used to test the effects of GAC on the bioaccumulation of THg using a recently developed approach (Best et al. 2005; Zimmerman et al. 2004; Millward et al. 2005). Activated carbon is a heat-activated carbon substrate of both high surface area and high affinity for non-polar and ionic compounds and has been suggested as a viable sorbent for the removal of contaminants from gaseous, aqueous, and sediment phases (Millward et al. 2005). Approximately 600 g WW of HAAF sediment was placed into each of two sealable jars. GAC was added to one jar at 3.4% on a dry weight basis. Both GAC-amended and control sediments were then sealed and tumbled for 1 week to facilitate mixing. Following mixing, the contents of each jar were then divided between five replicate beakers and 800 mL of overlying water (30‰ ASW) was added. Before animals were added, the beakers were maintained at 20 °C for 84 days under gentle aeration using a fine bubble stream, and with 50% water exchange once a week. This period was designed to enable contacting of Hg-contaminated sediment and GAC under a redox and oxygenation regime similar to those in the field.

At termination of the 84-day contact period, single adult *N. virens* were added to each beaker and were maintained at 20 °C for 56 days. Water was renewed three times a week, as in the uptake experiment, and no supplemental food was provided. Worms were removed from the sediment after

a sediment exposure period of 56 days, and the tissue and sediment samples were frozen prior to analysis for THg.

Chemical analyses of invertebrate tissue

Total mercury

USEPA method 7421 was used (USEPA 1992, 1994). Worms were thoroughly ground in a stainless steel mixer prior to the dissolution process. Approximately a 0.2-g sample of the tissue was heated at 115 °C with sulfuric acid and nitric acid for 1 h or until the tissue dissolved. Subsequently, 50 mL of water was carefully added to the acidic mixture followed by an excess of potassium permanganate. This mixture was heated at 95 °C for 1 h. The excess potassium permanganate was reduced with hydroxylamine hydrochloride and sodium chloride solution. Mercury was determined using a CETAC M-6000A Atomic Absorption Mercury Analyzer. Typical reporting and method detection limits for this sample size are 0.025 and 0.005 ng g^{-1}, respectively.

Methylmercury

Methods were modified after Bloom (1989), Horvat et al. (1993), Hammerschmidt et al. (2004), and St. Louis et al. (2001). Worms were blended using a stainless steel mixer. Approximately 0.2 g of blended tissue was extracted and distilled from Teflon distillation vessels using a mix of H_2SO_4, KC1, H_2O, and $CuSO_4$ as the extracting and distillation solution. Samples were distilled in a 130 °C carbon block, assisted by a stream of nitrogen, until about 80% of the solution was collected in Teflon receiver bottles held just above freezing in a specially designed refrigerator. All of the connecting transfer lines for the distillation apparatus are Teflon. Then 0.5 mL of 2 M acetate buffer was added to each sample, including standard and quality control samples, after the distillates were transferred to Erlenmeyer flask reaction vessels. After that, 0.1 mL of 1% sodium tetraethyl borate was added to the reaction vessels, and the ethylation process was allowed to proceed for 20 min. At the end of the reaction period, volatile Hg compounds were purged from the reaction solution with nitrogen gas and the Hg compounds were collected on activated carbon column traps. The Hg compounds were purged from the activated carbon traps at 360 °C and allowed to pass through a gas chromatograph with an OV-3 column held isothermal at 100 °C. The effluent Hg compounds were pyrolyzed in a quartz column with quartz

wool at approximately 800 °C and the resulting Hg detected with cold-vapor atomic fluorescence spectroscopy. The typical reporting limit for this sample size is 0.05 ng g^{-1}.

Statistical analysis

Mean body burdens were compared using ANOVA and Tukey multiple comparison post hoc test using SigmaStat, version 3.0 (SPSS, Inc., Chicago, IL). Parametric comparison test assumptions were checked for violations using the Shapiro-Wilk's test for normality of residuals, and Levene median test for equality of variances. A significance level of $p < 0.05$ was used for all statistical tests.

Results and discussion

Sediment chemistry

Concentrations of THg and MeHg in the four field-collected sediments used in this study are presented in Table 8-1 and are typical for sediments commonly found in the bay area.

Table 8-1. Mean (± standard deviation; N=3) THg and MeHg concentrations in the upper 10 cm of sediment from four sites bordering San Pablo Bay.

Site	Sediment Concentration (ng g^{-1} DW)	
	THg	MeHg
HAAF	299 ± 144	1.97 ± 1.08
China Camp	362 ± 43	3.71 ± 0.73
Sonoma Marsh	358 ± 132	0.49 ± 0.09
Sonoma Baylands	296 ± 1	2.75 ± 0.20

Uptake kinetics experiment

The concentration of THg and MeHg in *N. virens* did not significantly increase during the first 28 days of the exposure to San Francisco Bay area sediments (Figures 8-1 and 8-2). The concentration of THg at exposure termination (day 56) was significantly greater than concentrations measured at days 7 and 14 in all exposures. The mean concentration of MeHg at exposure termination was greater than concentrations measured at days 7 and 14 in all exposures, but significant differences were only found for the Sonoma Marsh and Sonoma Baylands sediment exposures (Figures 8-1 and 8-2). Mean THg and MeHg body burdens determined for

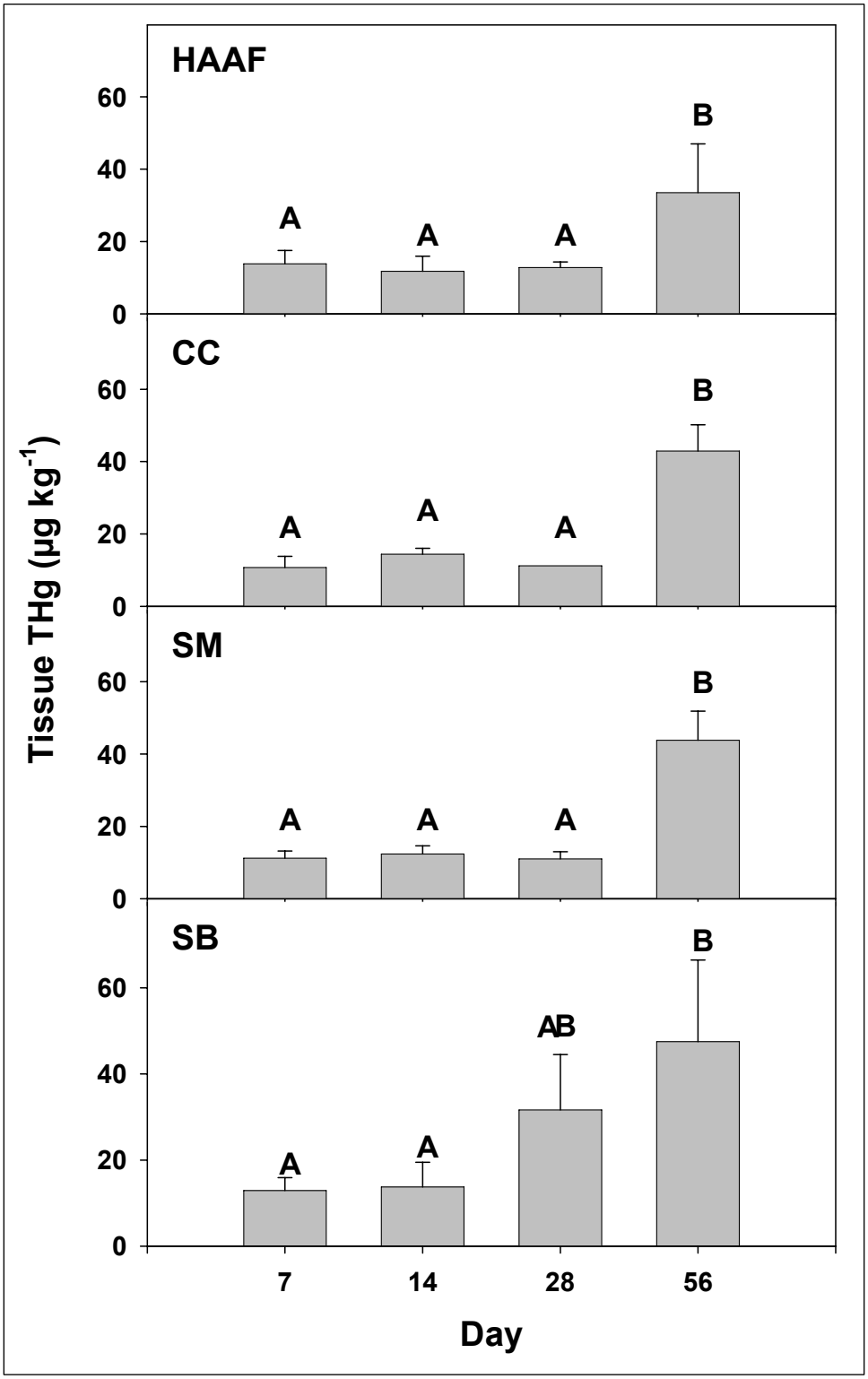

Figure 8-1. Mean body burdens of THg in *Nereis virens* exposed to Hamilton Army Airfield (HAAF), China Camp (CC), Sonoma Marsh (SM), and Sonoma Baylands (SB) sediment for increasing periods. Same letters indicate results were not significantly different by one-way ANOVA with Tukey's post hoc test ($P < 0.05$).

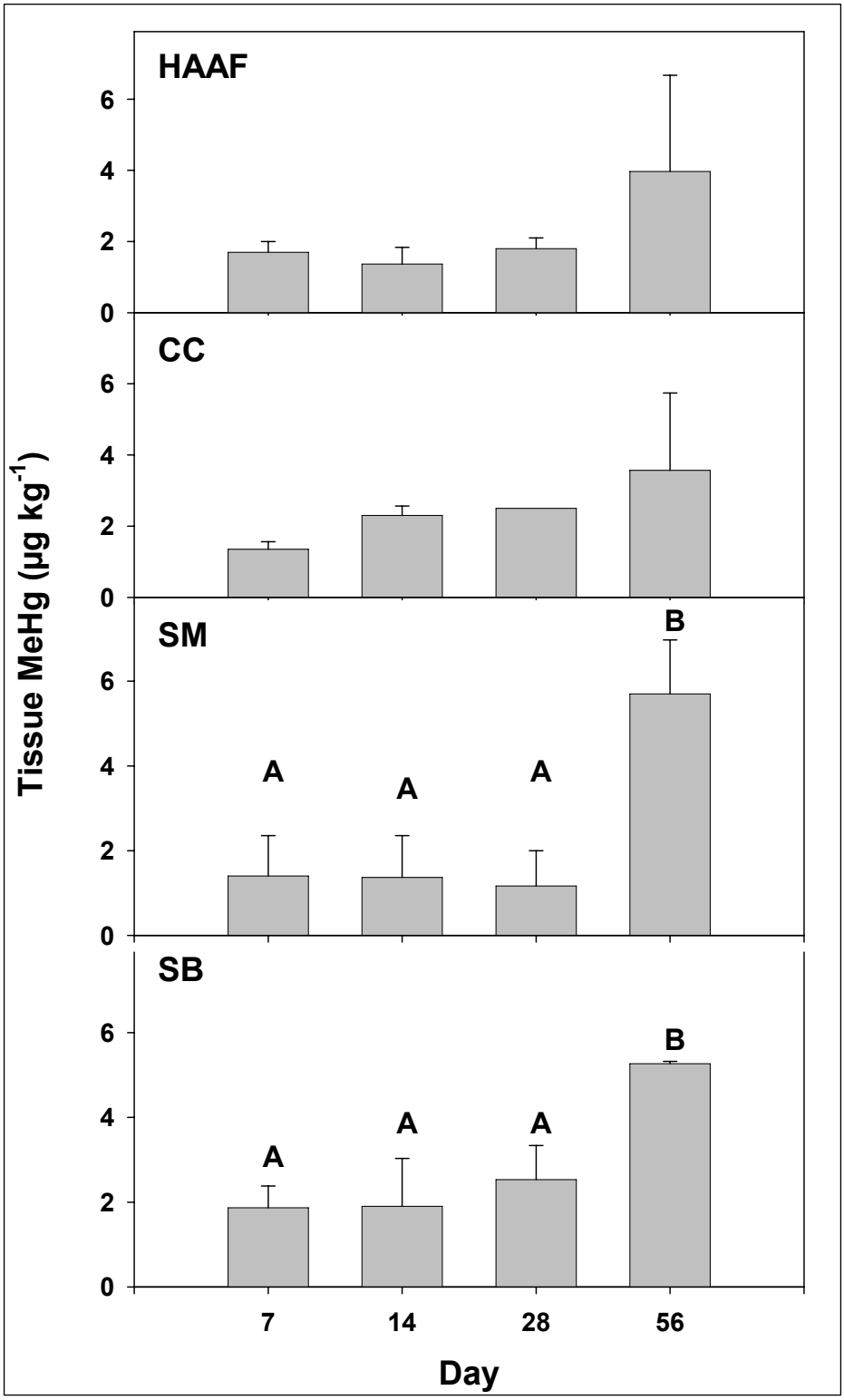

Figure 8-2. Mean body burdens of MeHg in *Nereis virens* exposed to Hamilton Army Airfield (HAAF), China Camp (CC), Sonoma Marsh (SM), and Sonoma Baylands (SB) sediments for increasing periods. Same letters indicate results were not significantly different by one-way ANOVA with Tukey's post hoc test ($P < 0.05$).

the earliest time point (7 days) of exposure is likely indistinguishable and, therefore, representative of mean background concentrations of those compounds in the field-collected worms used in this study.

Overall trends of increasing body burden of THg and MeHg were observed over 56-day exposures to San Francisco Bay area sediments. Model-fitted estimates of uptake clearance rate coefficients were derived from the time series accumulation data for THg and MeHg (Table 8-2). Uptake clearance rate coefficients and corresponding standard error were compared. The k_u estimates for Hg were similar for the HAAF, China Camp, and Sonoma Marsh sediments but were greater for the Sonoma Baylands sediment. For MeHg, k_u estimates were similar for the HAAF, China Camp, and Sonoma Baylands sediments but were greater for the Sonoma Marsh sediment. The rate of metal uptake from sediment or soil has been used as a reliable indicator of metal bioavailability (e.g., Gillis et al. 2004; van Straalen et al. 2005; Gust and Fleeger 2005). Therefore, bioavailability was greatest in the Sonoma Baylands sediment for THg and in the Sonoma Marsh sediment for MeHg.

Table 8-2. Toxicokinetic model parameters estimates for THg and MeHg calculated for *Nereis virens* exposed to Hamilton Army Airfield, China Camp, Sonoma Baylands, and Sonoma Marsh sediments.

Sediment	Uptake Rate (k_u, d^{-1})		Elimination Rate (k_e, d^{-1})			TSS_{95} (2.99/k_e)	BAF kinetic (k_u/k_e)	BAF 56-day
	Estimate	se	Estimate	se	p-Value			
THg								
HAAF	0.0026	0.0011	0.0120	0.0189	0.02	158	0.22	0.11
China Camp	0.0023	0.0008	0.0040	0.0128	0.74	234	0.58	0.12
Sonoma Marsh	0.0023	0.0007	ND	0.0122	1.00	245	ND	0.12
Sonoma Baylands	0.0041	0.0014	0.0170	0.0175	0.36	171	0.24	0.15
MeHg								
HAAF	0.0550	0.0282	0.0184	0.0258	0.49	116	2.99	2.01
China Camp	0.0650	0.0283	0.0675	0.0386	0.12	77	0.96	0.96
Sonoma Marsh	0.1795	0.0771	ND	0.0177	1.00	169	ND	11.63
Sonoma Baylands	0.0511	0.0132	0.0168	0.0127	0.22	235	3.04	1.92

Abbreviations: se = standard error; p-value = statistical significance; TSS_{95} =time for 95% steady-state concentration; BAF = bioaccumulation factor; ND = not determined.

Reports of experimentally derived uptake rates for inorganic Hg or MeHg from sediment were not found in the available literature. The rates of heavy metal uptake in *N. virens* reported for cadmium (0.34 to 0.89 g DW/g tissue DW/day) uptake from spiked sediment (Ray et al. 1980) were substantially greater than those derived for THg or MeHg in the present study. Rates of uptake of other heavy metals in *N. virens* were not found in the available literature.

Estimates of elimination rate estimates (k_e) were very slow (Table 8-2) and reliable estimates ($p > 0.1$) were only obtained for THg for HAAF sediment. Extremely slow elimination of Hg and MeHg was reported for benthic marine clams exposed to HAAF and China Camp sediments (Best et al. 2005) and to freshwater clams (Inza et al. 1998) and fish (Wang and Wong 2003) exposed to spiked water.

Visual inspection of the uptake curves indicated that at termination of the 56-d exposure *N. virens* was far from approaching steady-state for Hg and MeHg. This was confirmed by the observation that the final mercury species concentrations in animals exposed to China Camp sediment were far less than those in the field-collected related *Nereis vexillosa* specimens from the San Pablo Bay sediments adjacent to the China Camp site, which were 174 ± 31 ng THg g-1 DW and 26.16 ± 17.61 ng MeHg g-1 DW (Chapter 7). The exposure periods estimated for achieving 95% steady-state body burdens (Table 8-2) are much longer than the exposure duration used in this study and result from the extremely slow Hg and MeHg elimination in *N. virens*. The kinetically derived BAF estimates, which represent the tissue-to-sediment concentration ratio at steady state, were much greater than values empirically determined at the termination of the 56-d sediment exposure (Table 8-2). Estimates of time-to-steady-state and steady-state BAFs have great associated uncertainty since they were calculated using estimated, i.e., not measured, elimination rate estimates. Determination of elimination rates experimentally by transferring worms approaching steady-state body burdens to uncontaminated sediments is warranted for an accurate modeling of THg and MeHg toxicokinetics in invertebrates exposed to San Francisco Bay area sediment.

The near-steady-state (TSS_{95}) THg and MeHg tissue concentrations in *N. virens* (Table 8-2) were relatively similar (differences within a factor of 5 or less) to body burdens determined for crabs and mussels field-collected from the HAAF and China Camp sites in June 2003 (Best et al. 2005). The

BAF values were greater for MeHg than for THg for both *N. virens* exposed in the laboratory (this study) and field-collected crabs and mussels (Best et al. 2005) for the HAAF and China Camp sites. The laboratory-derived BAFs were greater than field-derived values (Best et al. 2005) for MeHg but were less for THg. Overall, the bioavailability of Hg and MeHg to *N. virens* in laboratory exposures appears to be similar to the bioavailability of those compounds in the field for HAAF and China Camp sediments.

Bioavailability reduction experiment

Activated carbon has a proven ability as a sorbent for Hg in the elemental, ionic, and monomethyl forms (USEPA 1997), and short-term exposures have been indicated to reduce bioavailability of labile Hg species to sediment-ingesting organisms (Best et al. 2005). Other studies have indicated that a GAC cap reduces flux of aqueous MeHg by 96% after 14-day contact time, and up to 58% of MeHg and 62% of THg can repartition from the sediment onto the sorbent after 4 months of contact (Pers. Comm. V. Magar, 2004, ENVIRON Holdings, Inc.). These data suggest that GAC addition to contaminated sediments warrants consideration as a remediation strategy to reduce the availability of Hg for uptake into organisms and for methylation by microbes.

Body burdens of THg in *N. virens* exposed to GAC-amended and non-amended (control) HAAF sediment were not significantly different (Figure 8-3). Treatment with 3.4% GAC followed by a 91-day contact period failed to promote a significant effect on the final body burden of THg or MeHg in *N. virens*, suggesting failure of that treatment to reduce the bioavailability of those contaminants (data not shown). However, exposure of *N. virens* to HAAF sediment for 56 days resulted in body burdens less than those determined during the same exposure period in the uptake kinetics experiment but similar to the apparent background concentration of those compounds in worms used in this study. Therefore, THg and MeHg may not have increased significantly above initial concentrations in *N. virens* used in the bioavailability reduction experiment. Such apparent lack of significant bioaccumulation of THg and MeHg in *N. virens* exposed to GAC-amended and non-amended HAAF sediments precluded the determination of the potential effects of GAC amendment in the bioavailability of THg and MeHg to benthic invertebrates.

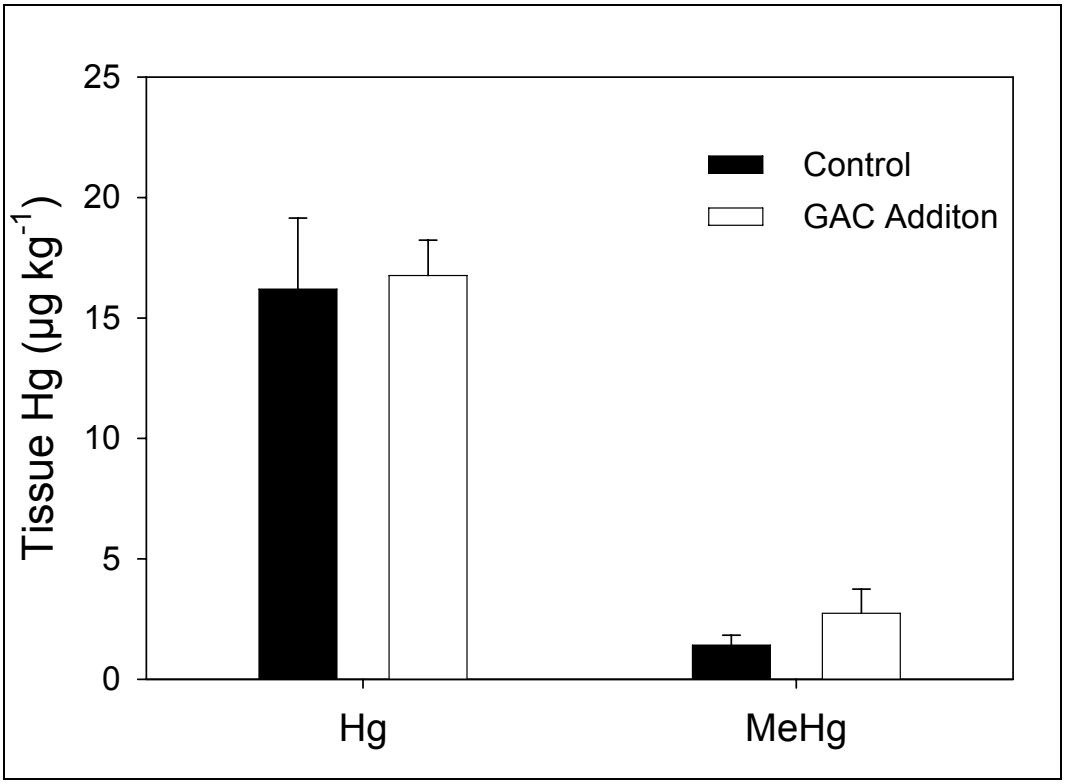

Figure 8-3. Effect of 3.4% GAC contact on the 56-d bioaccumulation of THg and MeHg in *Nereis virens.* Mean values and standard errors.

In previous work, it was demonstrated (Best et al. 2005, Chapter 6) that contacting HAAF sediment with 3.4% GAC for 16 days significantly reduced the bioavailability of spiked, labile Hg species, but not the bio-availability of aged Hg species. In those experiments it was postulated that the differential efficacy of GAC for labile versus aged Hg probably reflected a slow and/or partial release of Hg species from associations with ligands into the dissolved phase, from where they would be available for repartitioning onto the sorbent-active-surface. Such desorption-rate-limiting processes have been observed in sorbent studies with PCB-contaminated sediments (Millward et al. 2005; Zimmerman et al. 2004). The present study failed to demonstrate the potential that increased contact time from 16 to 91 days would result in improved efficacy of GAC in reducing the bioavailability of aged Hg species.

Conclusions

1. Uptake rates of THg in *N. virens* ranged from 0.0026 to 0.0041 d^{-1}, and elimination rates from 0.0040 to 0.0170 d^{-1}.

2. Uptake rates of MeHg ranged from 0.0511 to 0.1795 d^{-1}, and elimination rates from 0.0168 to 0.0184 d^{-1}. Both uptake and elimination rates were greater for MeHg than for THg.
3. The time for THg and MeHg to approach steady state in *N. virens* was relatively long (> 100 days) because of the extremely slow elimination rate for those compounds.
4. The 56-day biota to sediment accumulation factor (BAF) of THg was similar for the four sediments tested, ranging from 0.11 to 0.15. The BAF of MeHg was far greater, ranging from 0.96 to 11.63. The greatest BAF of MeHg was found in sediment from Sonoma Marsh, a marsh of natural origin. Thus, the current study does not provide evidence that marsh restoration increases the bioavailability of Hg species.
5. Addition of 3.4% GAC to THg and MeHg containing sediments did not reduce the bioavailability of mercury species to *N. virens* in laboratory exposures.

POINT OF CONTACT CHAPTER 8:

Dr. Guilherme R. Lotufo
U.S. Army Engineer Research and Development Center
Environmental Laboratory, Vicksburg, MS
Ph: 601-634-4103; E-mail: gui.lotufo@erdc.usace.army.mil

References

Acha, D., V. Iniguez, M. Roulet, J. R. D. Guimarez, R. Luna, L. Alanoca, and S. Sanchez. 2005. Sulfate-reducing bacteria in floating macrophyte rhizospheres from an Amazonian floodplain lake in Bolivia and their association with Hg methylation. *Appl. Environ. Microbiol.* 71(11):7531-7535.

American Society for Testing and Materials (ASTM). 2000. Standard guide for determination of the bioaccumulation of sediment associated contaminants by benthic invertebrates. In *Annual Book of Standards*. 11.05:1-54. West Conshohocken, Pennsylvania.

Baeyens, W., M. Leermakers, T. Papina, A. Saprykin, N. Brion, J. Noyen, M. de Gieter, and M. Elskens. 2003. Bioconcentration and biomagnification of mercury and methylmercury in North Sea and Scheldt estuary fish. *Arch. Environ. Contam. Toxicol.* 45:498-508.

Back, R. C., and C. J. Watras. 1995. Mercury in zooplankton of northern Wisconsin lakes: Taxonomic and site-specific trends. *Water Air Soil Pollut.* 80:931-938.

Balling, S. S., and V. H. Resh. 1983. The influence of mosquito control recirculation ditches on plant biomass, production, and composition in two San Francisco Bay salt marshes. *Estuarine Coastal Shelf Sci.* 16:151-161.

Batten, K. M., and K. M. Scow. 2003. Sediment microbial community composition and methylmercury pollution at four mercury mine-impacted sites. *Microb. Ecol.* 46:429-441.

Beijer, K., and A. Jernelow. 1979. Methylation of mercury in aquatic environments. In *The biogeochemistry of mercury in the environment. Topics in Environmental Health, vol.3*, ed. J. O. Nriagu, 203–210. New York: Elsevier/North-Holland.

Benoit, J. M., C. C. Gilmour, R. P. Mason, and A. Heyes. 1999. Sulfide controls on mercury speciation and bioavailability to methylating bacteria in sediment and pore waters. *Environ. Sci. Technol.* 33:951-957.

Berman, M., T. Chase, Jr., and R. Bartha. 1990. Carbon flow in mercury biomethylation by *Desulfovibrio desulfuricans*. *Environ. Microb.* 56:298-300.

Berner, R. A. 1971. *Principles of chemical sedimentology*. New York: McGraw-Hill.

Berner, R. A. 1980. *Early diagenesis: A theoretical approach*. Princeton, NJ: Princeton Univ. Press.

Best, E. P. H., H. L. Fredrickson, V. A. McFarland, H. Hintelmann, R. P. Jones, C. H. Lutz, G. A. Kiker, A. J. Bednar, R. N. Millward, R. A. Price, G. R. Lotufo, and G. L. Ray. 2005. *Pre-construction biogeochemical analysis of mercury in wetlands bordering the Hamilton Army Airfield Wetlands Restoration Site*. ERDC/EL TR-05-15. Vicksburg, MS: U.S. Army Engineer Research and Development Center.

Bloom, N. S. 1989. Determination of picogram levels of methylmercury by aqueous phase ethylation, followed by cryogenic gas chromatography with cold vapor atomic fluorescence detection. *Can. J. Fish. Aquat. Sci.* 46:1131-1140.

Bodaly, R. A., R. E. Hecky, and R. J. P. Fudge. 1984. Increases in fish mercury levels in lakes flooded by the Churchill River Diversion, Northern Manitoba. *Can. J. Fish. Aquat. Sci.* 41:682-691.

Boehn, H. L. 1971. Redox potentials. *Soil Science* 112: 39-45.

Boon, J. J., J. W. De Leeuw, G. J. Van der Hoe, and J. H. Vosjan. 1977. Significance and taxonomic value of iso and anteiso monoenoic fatty acids and branched β-hydroxy acids in *Desulfovibrio desulfuricans*. *J. Bacteriology* 129:1183-1191.

Bothner, M. H., R. A. Jahnke, M. L. Peterson, and R. Carpenter. 1980. Rate of mercury loss from contaminated estuarine sediments. *Geochim. Cosmochim. Acta* 44:273–285.

Branfireun, B. A., A. Heyes, and N. T. Roulet. 1996. The hydrology and methylmercury dynamics of a Precambrian shield headwater peatland. *Wat. Resour. Res.* 32:1785-1974.

Branfireun, B. A., D. Hilbert, and N. T. Roulet. 1998. Sinks and sources of methylmercury in a boreal catchment. *Biogeochem.* 41:277-291.

Brenner, R. C., V. S. Magar, J. A. Ickes, E. A. Foote, J. E. Abbott, L. S. Bingler, and E. A. Crecelius. 2004. Long-term recovery of PCB-contaminated surface sediments at the Sangamo-Weston Twelvemile Creek/Lake Hartwell Superfund Site. *Environ. Sci. Technol.* 15:2328-2337.

Cabana, G., and J. B. Rasmussen. 1994. Modelling food chain structure and contaminant bioaccumulation using stable nitrogen isotopes. *Nature* 372:255-257.

Cameron, G. N. 1972. Analysis of insect trophic diversity in two salt marsh communities. *Ecology* 53:58-73.

Canario, J., and C. Vale. 2004. Rapid release of mercury from intertidal sediments exposed to solar radiation: A field experiment. *Environ. Sci. Technol.* 38:3901-3907.

Chan, H. M., A. M. Scheuhammer, A. Ferran, C. Loupelle, J. Holloway, and S. Weech. 2003. Impacts of mercury on freshwater fish-eating wildlife and humans. *Hum. Ecol. Risk Assess.* 9:867-883.

Choe, K-Y, G. A. Gill, and R. D. Lehman. 2003a. Distribution of particulate, colloidal, and dissolved mercury in San Francisco Bay estuary. 1. Total mercury. *Limnol. Oceanogr.* 48:1535-1546.

Choe, K-Y, G. A. Gill, and R. D. Lehman. 2003b. Distribution of particulate, colloidal, and dissolved mercury in San Francisco Bay estuary. 2. Monomethyl mercury. *Limnol. Oceanogr.* 48:1547-1556.

Choe K.-Y., G. A. Gill, R. D. Lehman, S. Han, W. A. Heim, and K. H. Coale. 2004. Sediment–water exchange of total mercury and monomethyl mercury in the San Francisco Bay Delta. *Limnol. Oceanogr.* 49:1512 –1527.

Choi, S. C., and R. Bartha. 1993. Cobalamin-mediated mercury methylation by *Desulfovibrio desulfuricans* LS. *Environ. Microb.* 59: 290-295.

Choi, S. C., T. Chase, Jr., and R. Bartha. 1994. Metabolic pathways leading to mercury methylation in *Desulfovibrio desulfuricans* LS. *Appl. Environ. Microbiol.* 60: 4072-4077.

Cifuentes, L. A., J. H. Sharp, and M. L. Fogel. 1988. Stable carbon and nitrogen biochemistry in the Delaware estuary. *Limnol. Oceanogr.* 33:1102-1115.

Compeau, G. C., and R. Bartha. 1985. Sulphate-reducing bacteria: Principal methylators of mercury in anoxic estuarine sediment. *Appl. Environ. Microbiol.* 50:498-502.

Conaway, C. H., S. Squire, R. P. Mason, and A. R. Flegal. 2003. Mercury speciation in the San Francisco Bay estuary. *Mar. Chem.* 80:199-225.

Currin, C. A., S. Y. Newell, and H. W. Paerl. 1995. The role of standing dead *Spartina alterniflora* and benthic microalgae in salt marsh food webs: Considerations based on multiple stable isotope analysis. *Mar. Ecol. Prog. Ser.* 121:99-116.

Daly, K., R. J. Sharp, and A. J. McCarthy. 2000. Development of oligonucleotide probes and PCR primers for detecting phylogenic subgroups of sulfate-reducing bacteria. *Microbiology* 146:1693-1705.

Davis, J. A., D. Yee, J. N. Collins, S. E. Schwarzbach, and S. N. Luoma. 2003. Potential for increased mercury accumulation in the estuary food web. In *Issues in San Francisco estuary tidal wetlands restoration. San Francisco Estuary and Watershed Science*, ed. L. R. Brown, 1(1): article 4. http://repositories.cdlib.org/jmie/sfews/vol1/iss1/art4/.

Davison, W., and H. Zhang. 1994. *In situ* speciation measurements of trace components in natural waters using thin film gels. *Nature* 367:546-548.

Devereux, R., M. R. Winfrey, J. Winfrey, D. A. Stahl. 1996. Depth profile of sulfate-reducing bacterial ribosomal RNA and mercury methylation in an estuarine sediment. *FEMS Microb. Ecol.* 20: 23-31.

Divis, P., M. Leermakers, H. Docekalova, and Y. Gao. 2005. Mercury depth profiles in river and marine sediments measured by the diffusive gradients in thin films technique with two different specific resins. *Anal. Bioanal. Chem.* 382:1715-1719.

Dočekalová, H., O. Clarisse, S. Salomon, and M. Wartel. 2002. Use of constrained DET probe for a high-resolution determination of metals and anions distribution in the sediment pore water. *Talanta* 57:145-155.

Driscoll, C. T., C. Yan, C. L. Schofield, R. Munson, and H. Holsapple. 1994. The chemistry and bioavailability of mercury in Adirondack lakes. *Environ. Sci. Technol.* 28:136A-143A.

Elser, J. J., W. F. Fagan, R. F. Denno, D. R. Dobberfuhl, A. Folarin, A. Huberty, S. Interlandi, S. S. Kilham, E. MaCauley, K. L. Schulz, E. H. Siemann, and R. W. Sterner. 2000. Nutritional constraints in terrestrial and freshwater food webs. *Nature* 408:578-580.

Faulkner, S. P., W. H. Patrick, Jr., and R. P. Gambrell. 1989. Field techniques for measuring soil parameters. *Soil Sci. Soc. Am. J.* 53: 883-890.

Fredrickson, H. L., T. Cappenberg, and J. de Leeuw. 1986. Polar lipid ester-linked fatty acid composition of Lake Vechten seston: An ecological application of lipid analysis. *FEMS Microb. Ecol.* 38:381-396.

Fredrickson, H. L., J. Furey, J. W. Talley, and M. Richmond. 2004. Bioavailability of hydrophobic organic contaminants and quality of organic carbon. *Environ. Chem. Lett.* 2:77-81.

Fry, B. 1983. Fish and shrimp migrations in the northern Gulf of Mexico analyzed using stable C, N, and S isotope ratios. *Fish Bull.* 81:789-801.

_____. 1988. Food web structure on Georges Bank from stable C, N, and S isotopic compositions. *Limnol. Oceanogr.* 33:1182-1190.

_____. 1991. Stable isotope diagrams of freshwater food webs. *Ecology* 72:2292-2297.

Fry, B., and E. B. Sherr. 1984. $\delta^{13}C$ measurements as indicators of carbon flow in marine and freshwater ecosystems. *Contrib. Mar. Sci.* 27:15-47.

Gagnon, C., and N. S. Fisher. 1997. Bioavailability of sediment-bound methyl and inorganic mercury to a marine bivalve. *Environ. Sci. Technol.* 31:993-998.

Gallagher, J. L., and H. V. Kibby. 1980. Marsh plants as vectors in trace metal transport in Oregon tidal marshes. *Amer. J. Bot.* 67:1069-1074.

Gill, G. A., N. S. Bloom, S. Cappellino, C. T. Driscoll, R. Mason, and J. W. M. Rudd. 1999. Sediment–water fluxes of mercury in Lavaca Bay, Texas. *Environ. Sci. Technol.* 33:663 –669.

Gillis, P. L., D. G. Dixon, U. Borgmann, and T. B. Reynoldson. 2004. Uptake and depuration of cadmium, nickel, and lead in laboratory-exposed *Tubifex tubifex* and corresponding changes in the concentration of a metallothionein-like protein. *Environ. Toxicol. Chem.* 23:76-85.

Gilmour, C. C., and E. A. Henry. 1991. Mercury methylation in aquatic systems affected by acid decomposition. *Environ. Pollut.* 71:131-169.

Gilmour, C. C., G. S. Riedel, M. C. Ederington, J. T. Bell, J. M. Benoit, G. A. Gill, and M. C. Stordal. 1998. Methymercury concentrations and production rates across a trophic gradient in the northern Everglades. *Biogeochem.* 40:327-345.

Gleason, D. F., and G. M. Wellington. 1988. Food resources of postlarval brown shrimp (*Penaeus aztecus*) in a Texas salt marsh. *Mar. Biol.* 97:329-337.

Gobeil, C., and D. Cossa. 1993. Mercury in sediments and sediment pore water in the Laurentian Trough. *Can. J. Fish. Aquat. Sci.* 50:1794–1800.

Grenier, J. L. 2004. Ecology, behavior, and trophic adaptations of the salt marsh song sparrow *Melospiza melodia samuelis*: The importance of the tidal influence gradient. PhD diss., University of California, Berkeley.

Grenier, L., A. Melwani, J. Hunt, S. Bezalel, J. Davis, G. Ichikawa, B. Jaki, W. Heim, A. Bonnema, and M. Gassel. 2007. *California Bay-Delta Authority Fish Mercury Project Year 1 Annual Report. Sport Fish Sampling and Analysis*. CBDA Project # ERP 02D-P67. 29 May 2007.

Groenendijk, A. M. 1984. Primary production of four dominant salt-marsh angiosperms in the SW Netherlands. *Vegetatio* 57:143-152.

Gust, K. A., and J. W. Fleeger. 2005. Exposure-related effects on Cd bioaccumulation explain toxicity of Cd-phenanthrene mixtures in *Hyalella azteca*. *Environ. Toxicol. Chem.* 24:2918-2926.

Haines, E. B. 1976. Relation between the stable carbon isotope composition of fiddler crabs, plants, and soils in a salt marsh. *Limnol. Oceanogr.* 21:880-883.

_____. 1977. The origins of detritus in Georgia salt marsh estuaries. *Oikos* 29:254-260.

Hammerschmidt, C. R., W. F. Fitzgerald, C. H. Lamborg, P. H. Balcom, and P. T. Visscher. 2004. Biogeochemistry of methylmercury in sediments of Long Island Sound. *Mar. Chem.* 90:31-52.

Harmon, S. M., J. K. King, J. B. Gladden, G. T. Chandler, and L. A. Newman. 2004. Methylmercury formation in a wetland mesocosm amended with sulfate. *Environ. Sci. Technol.* 38: 650-656.

Harper, M., W. Davison, H. Zhang, and W. Tych. 1998. Solid phase to solution kinetics in sediments and soils interpreted from DGT measured fluxes. *Geochim. Cosmochim. Acta* 62:2757-2770.

Heller, A. A., and J. H. Weber. 1998. Seasonal study of speciation of mercury (II) and monomethylmercury in *Spartina alterniflora* from the Great Bay Estuary, NH. *Sci. Tot. Environm.* 221:181-188.

Hesslein, R. H., K. A. Hallard, and P. Ramlal. 1993. Replacement of sulfur, carbon, and nitrogen in tissue of growing borad whitefish (*Coregonus nasus*) in response to a change in diet traced by $\delta^{34}S$, $\delta^{13}C$, and $\delta^{15}N$. *Can. J. Fish. Aquat. Sci.* 50:2071-2076.

Heyes, A. 1996. Methylmercury in natural and disturbed wetlands. PhD diss., McGill Univ., Montreal, Canada.

Heyes, A., T. R. Moore, and J. W. M. Rudd. 1998. Mercury and methylmercury in decomposing vegetation of a pristine and impounded wetland. *J. Environ. Qual.* 27:591-599.

Hines, M. E., R. S. Evans, B. R. S. Genthner, S. G. Willis, J. N. Friedman, J. N. Rooney-Varga, and R. Devereux. 1999. Molecular phylogenetic and biogeochemical studies of sulfate-reducing bacteria in the rhizosphere of *Spartina alterniflora*. *Appl. Environ. Microbiol.* 65:2209-2216.

Hines N. A., P. L. Brezonik, and D. R. Engstrom. 2004. Sediment and porewater profiles and fluxes of mercury and methylmercury in a small seepage lake in northern Minnesota. *Environ. Sci. Technol.* 38:6610-6617.

Hintelmann, H., and R. D. Evans. 1997. Application of stable isotopes in environmental tracer studies – Measurements of monomethylmercury (CH_3Hg^+) by isotope dilution ICP-MS and detection of species transformation. *Fresenius J. Anal. Chem.* 358:378-385.

Hintelmann, H., K. Keppel-Jones, and R. D. Evans. 2000. Constants of mercury methylation and demethylation rates in sediments and comparison of tracer and ambient mercury availability. *Environ. Toxicol. Chem.* 19:2204-2211.

Hintelmann, H., and H. T. Nguyen. 2005. Extraction of methylmercury from tissue and plant samples using acid leaching. *Anal. Bioanal. Chem.* 381:360-365.

Hintelmann, H., and N. Ogrinc. 2003. Determination of stable mercury isotopes by ICP/MS and their application in environmental studies. In *Biogeochemistry of environmentally important trace elements*, ed. Y. Cai and C. O. Braids, 835:321-338. Washington, DC: ACS Symposium Series.

Hobson, K. A. 1999. Tracing origins and migration of wildlife using stable isotopes: a review. *Oecologia* 120:314-326.

Hopkins, D. R., and V. T. Parker. 1984. A study of the seed bank of a salt marsh in northern San Francisco Bay. *Amer. J. Bot.* 71:348-355.

Hornberger, M. I., S. N. Luoma, A. Van Geen, C. Fuller, and R. Anima. 1999. Historical trends of metals in the sediments of San Francisco Bay, California. *Mar. Chem.* 64: 39-55.

Horvat, M., N. S. Bloom, and L. Liang. 1993. Comparison of distillation with other current isolation methods for the determination of methyl mercury compounds in low level environmental samples. *Anal. Chim. Acta* 28:135-152.

Hughes, E. H., and E. B. Sherr. 1983. Subtidal food webs in a Georgia estuary: $\delta^{13}C$ analysis. *J. Exp. Mar. Biol. Ecol.* 67:227-242.

Hultberg, H., A. Iverfeldt, and Y-H. Lee. 1994. Methylmercury input/output and accumulation in forested catchments and critical loads for lakes in southern Sweden. In *Mercury pollution: Integration and synthesis*. ed. C. J. Watras and J. W. Huckabee, 313-331. Chelsea, MI: Lewis Publishers.

Hurley, J. P., J. M. Benoit, C. L. Babiarz, M. M. Shafer, A. W. Andren, J. R. Sullivan, R. Hammond, and D. A. Webb. 1995. Influences of watershed characteristics on mercury levels in Wisconsin rivers. *Environ. Sci. Technol.* 29:1867-1875.

Hussey, A., and S. P. Long. 1982. Seasonal changes in weight of above and below ground vegetation and dead plant material in salt marsh at Coline Point, Essex. *J. Ecol.* 70:757-771.

Inza, B., F. Ribeyre, and A. Boudou. 1998. Dynamics of cadmium and mercury compounds (inorganic mercury or methylmercury): Uptake and depuration in *Corbicula flumine*a. Effects of temperature and pH. *Aquat. Toxicol.* 43: 273-285.

Ito, T., S. Okabe, H. Satoh, and Y. Watanabe. 2002. Successional development of sulfate-reducing bacterial populations and their activities in a wastewater biofilm growing under microaerophilic conditions. *Appl. Environ. Microbiol.* 68:1392-1402.

Jackson, T. A. 2001. Variations in the isotope composition of mercury in a freshwater sediment sequence and food web. *Can. J. Fish. Aquat. Sci.* 58:185-196.

Josselyn, M. 1983. *The ecology of San Francisco Bay tidal marshes: A community profile*. FWS/OBS-83/23. Washington, DC: U.S. Fish and Wildlife Service, Division of Biological Services.

Kimmerer, W. 2004. Open water processes of the San Francisco Estuary: From physical forcing to biological responses. *San Francisco Estuary and Watershed Science* ed. L. R. Brown, 2(1): article 1. http://repositories.cdlib.org/jmie/sfews/vol2/iss1/art1/.

King, J. K., J. E. Kostka, M. E. Frischer, and F. M. Saunders. 2000. Sulfate-reducing bacteria methylate mercury at variable rates in pure cultures and in marine sediments. *Appl. Environ. Microbiol.* 66:2430-2437.

Kistritz, R. U., and I. Yesaki. 1979. Primary production, detritus flux, and nutrient cycling in a sedge marsh, Fraser River Estuary. Technical Report 17, Vancouver: Westwater Research Center, University of British Columbia.

Kraaij, R. H., J. Tolls, D. Sijm, G. Cornelissen, A. Heikens, and A. Belfroid. 2001. Effects of contact time on the sequestration and bioavailability of different classes of hydrophobic organic chemicals to benthic oligochaetes (Tubificidae). *Environ. Toxicol. Chem.* 21:752-759.

Kraus, M. L. 1988. Accumulation and excretion of five heavy metals by the saltmarsh cordgrass *Spartina alterniflora*. *Bull. New Jersey Academy Sci.* 33:39-43.

Kwak, T. J., and J. B. Zedler. 1997. Food web analysis of Southern California coastal wetlands using multiple stable isotopes. *Oecologia* 110:262-277.

Landers, J. 2005. Airfield to be buried under dredged sediment to restore wetlands. Civil Engineering News. *Civil. Eng*. 75 (10):21-22.

Lawrence, A. L., and R. P. Mason. 2001. Factors controlling the bioaccumulation of mercury and methylmercury by the estuarine amphipod *Leptocheirus plumulosus*. *Environ. Pollut.* 111:217-231.

Lindberg, S. E., W. Dong, and T. Meyers. 2002. Transpiration of gaseous elemental mercury through vegetation in a subtropical wetland in Florida. *Atmospheric Environ.* 36:5207-5219.

Loftus, W. F. 2000. Accumulation and fate of mercury in an Everglades aquatic food web. PhD diss., Florida International Univ., Miami.

Lomnicki, A., E. Bandola, and K. Jankowska. 1968. Modification of the Wiegert-Evans method for estimation of the primary production. *Ecology* 49:147-149.

Lubetkin, S. C., and C. A. Simenstad. 2004. Multi-source mixing models to quantify food web sources and pathways. *J. Appl. Ecol.* 41:996-1008.

Macalady, J. L., E. E. Mack, D. C. Nelson, and K. M. Scow. 2000. Sediment microbial community structure and mercury methylation in mercury-polluted Clear Lake, California. *Appl. Environ. Microbiol.* 66:1479-1488.

Mahall, B. E., and R. B. Park. 1976a. The ecotone between *Spartina foliosa* Trin. and *Salicornia virginica* L. in salt marshes of northern San Francisco Bay. I. Biomass and production. *J. Ecol.* 64:421-433.

_____. 1976b. The ecotone between *Spartina foliosa* Trin. and *Salicornia virginica* L. in salt marshes of northern San Francisco Bay. II. Soil water and salinity. *J. Ecol.* 64:793-809.

Mann, H. 1988. Production and use of detritus in various freshwater, estuarine, and coastal marine ecosystems. *Limnol. Oceanogr.* 33:910-930.

Marvin-DiPasquale, M. C., and J. L. Agee. 2003. Microbial mercury cycling in the sediments of the San Francisco Bay delta. *Estuaries 26:* 1517-1528.

Marvin-DiPasquale, M. C., and D. G. Capone. 1998. Benthic sulfate reduction along the Chesapeake Bay central channel. I. Spatial trends and controls. *Mar. Ecol. Prog. Ser.* 168:213-228.

Marvin-DiPasquale, M. C., and R. S. Oremland. 1998. Bacterial methylmercury degradation in Florida Everglades peat sediment. *Environ. Sci. Technol.* 32: 2556-2563.

Marvin-DiPasquale, M. C., J. L. Agee, R. M. Bouse, and B. E. Jaffe. 2003. Microbial cycling of mercury in contaminated pelagic and wetland sediments of San Pablo Bay, California. *Environ. Geol.* 43:260-267.

Mason, R. P., W. F. Fitzgerald, J. Hurley, A. K. Hanson, P. L. Donaghay, and J. M. Sieburth. 1993. Mercury biogeochemical cycling in a stratified estuary. *Limnol. Oceanogr.* 38:1227-1241.

Mason, R. P., and A. L. Lawrence. 1999. Concentration, distribution, and bioavailability of mercury and methylmercury in sediments of Baltimore Harbor and Chesapeake Bay, Maryland, USA. *Environ. Toxicol. Chem.* 18:2438-2447.

McCutchan, J. H., W. M. Lewis, Jr., C. Kendall, and C. C. McGrath. 2003. Variation in trophic shift for stable isotope ratios of carbon, nitrogen, and sulfur. *Oikos* 102:378-390.

McFarland, V. A., J. U. Clarke, C. H. Lutz, and D. K. MacMillan. 2002. *Mercury concentrations bordering the Hamilton Army Air Field Remediation Site: September 2001*. Report to USACE District, San Francisco. Vicksburg, MS: U.S. Army Engineer Research and Development Center.

_____. 2003. *Mercury Concentrations Bordering The Hamilton Army Air Field Remediation Site: February* 2003. Wet Season - Dry Season Contrast. Report to USACE District, San Francisco. Vicksburg, MS: U.S. Army Engineer Research and Development Center.

Michener, R. H, and D. M. Schell. 1994. Stable isotope ratios as tracers in marine aquatic food webs. In *Stable isotopes in ecology and environmental science,* ed. K. Lajtha and R. H. Michener, 138-157. Oxford, Great Britain: Blackwell Scientific Publishers.

Millward, R. N., T. S. Bridges, U. Ghosh, J. R. Zimmerman, and R. G. Luthy. 2005. Addition of activated carbon to sediments to reduce PCB bioaccumulation by a polychaete (*Neanthes arenaceodentata*) and an amphipod (*Leptocheirus plumulosus*). *Environ. Sci. Technol.* 39:2880-2887.

Minagawa, M., and E. Wada. 1984. Stepwise enrichment of ^{15}N along food chains: Further evidence and the relation between $\delta^{15}N$ and animal age. *Geochim. Cosmochim. Acta* 48:1135-1140.

Moore, T. R., J. L. Bubier, A. Heyes, and R. J. Flett. 1995. Methyl and total mercury in boreal wetland plants, Experimental Lakes Area, Northwestern Ontario. *J Environ. Qual.* 24:845-850.

Murray, M. A., and A. J. Horne. 1979. Studies on Hoffman salt marsh, Richmond, California. I. Initial studies on the inner marsh and its acid pollution. UCB-SERL 79-2. University of California, Richmond: Sanitary Engineering Research Laboratory.

Naiman, R. J., and J. R. Sibert. 1979. Detritus and juvenile salmon production in the Nanaimo Estuary. III. Importance of detrital carbon to the estuarine ecosystem. *J. Fish. Res. Board Can.* 36:504-520.

Nixon, S. W., C. A. Oviatt, J. Garber, and V. Lee. 1976. Diet metabolism and nutrient dynamics in a salt marsh embayment. *Ecology* 57:740-750.

Odum, E. P. 1980. The status of three ecosystem-level hypotheses regarding salt marsh estuaries: tidal subsidy, outwelling, and detritus-based food chains. In *Estuaries Perspectives*, ed. V. S. Kennedy, 485-496. New York: Academic Press.

Office of Environmental Health Hazard Assessment (OEHHA). 1994. Health advisory on catching and eating fish: Interim sport fish advisory for San Francisco Bay. http://www.oehha.ca.gov/fish/general/sfbaydelta.html

Okabe, S., T. Itoh, H. Satoh, and Y. Watanabe. 1999. Analyses of spatial distributions of sulfate-reducing bacteria and their activity in aerobic wastewater biofilms. *Appl. Environ. Microbiol.* 65:5107-5116.

O'Leary, M. H. 1981. Carbon isotope fractionation in plants. *Phytochem.* 20:553-567.

Onuf, C. P. 1987. *The ecology of Mugu Lagoon, California: An estuarine profile*. U.S. Fish and Wildlife Service Biological Report 85, 122 pp.

Oremland, R. S., C. W. Culbertson, and M. R. Winfrey. 1991. Methylmercury decomposition in sediments and bacterial cultures: Involvement of methanogens and sulfate reducers in oxidative demethylation. *Appl. Environ. Microbiol.* 57:130-137.

Orr, M., S. Crooks, and P. B. Williams. 2003. Will restored tidal marshes be sustainable? In *Issues in San Francisco estuary tidal wetlands restoration. San Francisco Estuary and Watershed Science*, ed. L. R. Brown, 1(1): article 5. http://repositories.cdlib.org/jmie/sfews/vol1/iss1/art5/.

Peterson, B., and R. W. Howarth. 1987. Sulfur, carbon and nitrogen isotopes used to trace organic matter flow in the salt-marsh estuaries of Sapelo Island, Georgia. *Limnol. Oceanogr.* 32:1195-1213.

Peterson, B. J., and B. Fry. 1987. Stable isotopes in ecosystem studies. *Annu. Rev. Ecol. Syst.* 18:293-320.

Peterson, B. J., R. W. Howarth, and R. H. Garritt. 1985. Multiple stable isotopes used to trace the flow of organic matter in estuarine food webs. *Science* 227:1361-1363.

_____. 1986. Sulfur and carbon isotopes as tracers of salt-marsh organic matter flow. *Ecology* 67:865-874.

Phillip Williams and Associates. 1998. Conceptual design for tidal wetland restoration for the Hamilton Airfield focused feasibility study. Vol. 1. Prepared for IT Corporation, 103 pp.

Post, D. M. 2002. Using stable isotopes to estimate trophic position: Models, methods and assumptions. *Ecology* 83:703-718.

Price, R. A. 2005. Spatial distribution and concentrations of mercury species in the vegetated marsh zones. In *Pre-construction biogeochemical analysis of mercury in wetlands bordering the Hamilton Army Airfield Wetlands Restoration site,* ed. E. P. H. Best, 42-48. ERDC/EL TR-05-15. Vicksburg, MS: U.S. Army Engineer Research and Development Center.

Ramlal, P. S., C. Anema, A. Furutani, R. E. Hecky, and J. W. M. Rudd. 1987. Mercury methylation and demethylation studies at southern Indian Lake, Manitoba: 1981-1983. *Can. Tech. Rep. Fish. Aquat. Sci.* 1490.

Ray, S., D. McLeese, and D. Pezzack. 1980. Accumulation of cadmium by *Nereis virens*. *Arch. Environm. Contain. Toxicol.* 9:1-8.

Robinson, J. B., and O. H. Tuovinen. 1984. Mechanisms of microbial resistance and detoxification of mercury and organomercury compounds: Physiological, biochemical, and genetic analysis. *Microbiol. Rev.* 48: 95-124.

Rudd, J. W. M. 1995. Sources of methyl mercury to freshwater ecosystems: A review. *Wat. Air Soil Pollut.* 90:697-713.

Sackett, W. M. 1989. Stable isotope studies on organic matter in the marine environment. In *Handbook of Environmental Isotope Geochemistry,* ed. P. Fritz and J. C. Fontes, 3:139-170. Amsterdam, The Netherlands: Elsevier.

San Francisco Bay Area Wetlands Ecosystem Goals Project. 1999. *Baylands ecosystem habitat goals*. First Reprint. U.S. Environmental Protection Agency, San Francisco, CA, San Francisco Bay Regional Water Quality Control Board, Oakland, CA.

San Francisco Estuary Institute (SFEI). 1999. *Contaminant concentrations in fish from San Francisco Bay, 1999*. Richmond, CA: San Francisco Estuary Institute.

San Francisco Estuary Institute (SFEI). 2004. *San Francisco estuary regional monitoring program data*. http://www.sfei.org/rmp/data.htm.

San Francisco Estuary Institute (SFEI). 2005a. The pulse of the estuary: monitoring and managing water quality in the San Francisco estuary. SFEI Contribution 411. San Francisco Estuary Institute, Oakland, CA: 26.

San Francisco Estuary Institute (SFEI). 2005b. The pulse of the estuary: monitoring and managing water quality in the San Francisco estuary. SFEI Contribution 411. San Francisco Estuary Institute, Oakland, CA: 25.

San Francisco Bay Regional Water Quality Control Board. 2006 Water quality control plan for the San Francisco Bay Basin. http://www.swrcb.ca.gov/rwqcb2/sfbaymercurytmdl.htm.

Scheuhammer, A. M. 1991. Effects of acidification on the availability of toxic metals and calcium to wild birds and mammals. *Environ. Poll.* 71:329-375.

Schroeder, W. H., and J. Munthe. 1998. Atmospheric mercury- An overview. *Atm. Environ.* 32: 809-822.

Sibert, J. 1977. Detritus-based food webs: Exploitation by juvenile chum salmon (*Oncorhynchus keta*). *Science* 196:649-650.

Simenstad, C. A., and R. C. Wissmar. 1985. δ13C evidence of the origins and fates of organic carbon in estuarine and nearshore foodwebs. *Mar. Ecol.* 22: 141-152.

Smalley, A. E. 1958. The role of two invertebrate populations, *Littorina irrorata* and *Orchelium fidicinium*, in the energy flow of a salt marsh ecosystem. PhD diss., Univ. of Georgia, Athens.

Spiker, E. C., and L. E. Schemel. 1979. Distribution and stable-isotope composition of carbon in San Francisco Bay. In *San Francisco Bay: The urbanized estuary*, ed. T. J. Conomos, 195-212. San Francisco, CA: Pacific Division, American Association for the Advancement of Science.

St. Louis, V. L., J. W. M. Rudd, C. A. Kelly, K. G. Beaty, N. S. Bloom, and R. J. Flett. 1994. The importance of wetlands as sources of methyl mercury to boreal forest ecosystems. *Can. J. Fish. Aquat. Sci.* 51:1065-1076.

St. Louis, V. L., J. W. M. Rudd, C. A. Kelly, K. G. Beaty, R. J. Flett, and N. T. Roulet. 1996. Production and loss of methylmercury and loss of total mercury from boreal forest catchments containing different types of wetlands. *Environ. Sci. Technol.* 30:2719-2729.

St. Louis, V. L., J. W. M. Rudd, C. A. Kelly, B. D. Hall, K. R. Rolfhus, K. J. Scott, S. E. Lindberg, and W. Dong. 2001. Importance of the forest canopy to fluxes of methyl mercury and total mercury to boreal ecosystems. *Environ. Sci. Technol.* 35: 3089-3098.

Sullivan, M. J., and C. A. Moncreiff. 1990. Edaphic algae are an important component of salt marsh food-webs: Evidence from multiple stable isotope analysis. *Mar. Ecol. Prog. Ser.* 62:149-159.

Summers, A. O. 1986. Organization, expression, and evolution of genes for mercury resistance. *Annu. Rev. Microbiol.* 40: 607-634.

Taylor, J., and R. J. Parkes. 1983. The cellular fatty acids of the sulphate-reducing bacteria and their activities in cyanobacterial mats of Solar Lake (Sinai, Egypt). *Appl. Environ. Microbiol.* 64:2943-2951.

Teasdale, P. R., S. Hayward, and W. Davison. 1999. In situ, high-resolution measurement of dissolved sulfide using diffusive gradients in thin films with computer-imaging densitometry. *Anal. Chem.* 71:2186-2191.

Tsai, P., and R. Hoenicke. 2001. *San Francisco Bay atmospheric deposition pilot study Part 1: Mercury*. SFEI Contribution 72. Richmond, CA: San Francisco Estuary Institute.

Ullrich, S. M., T. W. Tanton, and S. A. Abdrashitova. 2001. Mercury in the aquatic environment: A review of factors affecting methylation. *Crit. Rev. Environ. Sci. Technol.* 31:241-293.

U.S. Environmental Protection Agency (USEPA). 1992. *Mercury in solid or semisolid waste (Manual cold-vapor technique), Method 7471A, Test Methods for Evaluating Solid Waste Methods, SW-846*, Third Edition, Update II, July 1992.

_____. 1994. Mercury in solid or semi-solid waste (manual cold-vapor technique). http://www.epa.gov/epaoswer/hazwaste/test/pdfs/7471a.pdf.

_____. 1995. *Guidance for assessing chemical contaminant data for use in fish advisories: Vol. 1, fish sampling and analysis*, 2nd ed. EPA 823-R-93-002. Washington, DC: U.S. Environmental Protection Agency, Office of Water.

_____. 1997. *Mercury study report to Congress, vol. VI (final): an ecological assessment for anthropogenic mercury emissions in the United States*. EPA-425/R-97-008. Washington, DC.

U.S. Environmental Protection Agency (USEPA) and U.S. Army Corps of Engineers (USACE). 1998. *Evaluation of dredged material proposed for disposal in waters of the U.S. - Testing manual*. EPA-823-B-004. Washington, DC.

U.S. Geological Survey (USGS). 2002. Web document at http://sfbay.wr.usgs.gov/access/IntegratedScience/IntSci.html

Vainshtein, M., H. Hippe, and R. M. Kroppenstedt. 1992. Cellular fatty acid composition of *Desulfovibrio* species and its use in classification of sulfate-reducing bacteria. *Syst. Appl. Microbiol.* 15:554-556.

Valiela I, D. Rutecki, and S. Fox. 2004. Salt marshes: Biological controls in food webs in a diminishing environment. *J. Exper. Mar. Biol. Ecol.* 300:131-159.

Van Dover, C. L., J. F. Grassle, B. Fry, R. H. Garritt, and V. R. Starczak. 1992. Stable isotope evidence for entry of sewage-derived organic material into a deep-sea food web. *Nature* 360:153-156.

Van Straalen, N. M., M. H. Donker, M. G. Vijver, and C. A. M. Van Gestel. 2005. Bioavailability of contaminants estimated from uptake rates into soil invertebrates. *Environ. Pollut.* 163:409-417.

Wainwright, S. C., M. P. Weinstein, K. W. Able, and C. A. Curring. 2000. Relative importance of benthic microalgae, phytoplankton and the detritus of smooth cordgrass *Spartina alterniflora* and the common reed *Phragmites australis* to brackish-marsh food webs. *Mar. Ecol. Prog. Ser.* 200:77-91.

Walsh, C. T., M. D. Distefano, M. J. Moore, L. M. Shewchuk, and G. L. Verdine. 1988. Organization, expression, and evolution of genes for mercury resistance. *FASEB Journal* 2: 124-130.

Wang, W. X., and R. C. K. Wong. 2003. Combined effects of food quantity and quality on Cd, Cr, and Zn assimilation to the green mussel, *Perna viridis*. *J. Exp. Mar. Biol. Ecol.* 290:49-69.

Wiegert, R. G., and F. C. Evans. 1964. Primary production and the disappearance of dead vegetation on an old field in southern Michigan. *Ecology* 45:49-62.

Wiener, J. G., and D. J. Spry. 1996. Toxicological significance of mercury in freshwater fish. In *Environmental contaminants in wildlife: Interpreting tissue concentrations*, ed. W. N. Beyer, G. H. Wood, and A. W. Redmon-Norwood, 297-339. Boca Raton, FL: Lewis Publishers.

Wiener, J. G., C. G. Gilmour, and D. P. Krabbenhoft. 2003. *Mercury strategy for the Bay-Delta ecosystem: A unifying framework for science, adaptive management, and ecological restoration*. Final report to the California Bay Delta Authority for Contract 4600001642 between the Association of Bay Area Governments and the University of Wisconsin-La Crosse.

Williams, R. B., and M. B. Murdock. 1972. The potential importance of *Spartina alterniflora* in conveying zinc, manganese and iron into estuarine food chains. In *Proceedings National Symposium on Radioecology, Washington, DC*, ed. D. J. Nelson and F. C. Evans, 431-439. U.S. Atomic Energy Commission.

Windham, L., J. S. Weis, and P. Weis. 2001. Patterns and processes of mercury release from leaves of two dominant salt marsh macrophytes, *Phragmites australis* and *Spartina alterniflora*. *Estuaries* 24: 787-795.

Zedler, J. B. 1982. The ecology of Southern California coastal salt marshes: A community profile. FWS/OBS-81/54. Washington, DC: U.S. Fish and Wildlife Service.

Zedler, J. B., T. Winfield, and P. Williams. 1980. Salt marsh productivity with natural and altered tidal circulation. *Oecologia* 44:236-240.

Zhang, H., and W. Davison. 1995. Performance characteristics of diffusion gradients in thin films for the *in situ* measurement of trace metals in aqueous solution. *Anal. Chem.* 67:3391-3400.

Zhang, H., W. Davison, S. Miller, and W. Tych. 1995. In situ high resolution measurements of fluxes of Ni, Cu, Fe, and Mn and concentrations of Zn and Cd in porewaters by DGT. *Geochim. Cosmochim. Acta* 59:4181-4192.

Zhang, H., and W. Davison. 1999. Diffusional characteristics of hydrogels used in DGT and DET techniques. *Anal. Chim. Acta* 398:329-340.

Zimmerman, J. R., U. Ghosh, R. G. Luthy, R. N. Millward, and T. S. Bridges. 2004. Addition of carbon sorbents to reduce bioavailability of PAH and PCB in marine sediments: Physicochemical tests. *Environ. Sci. Technol.* 38:5458-5464.

Appendix A

Table A5-1. Seasonal changes in biomass of *Spartina foliosa* at low marsh site R-44 of the China Camp State Park.

Date	Tissue	Plant Biomass (g DW m^{-2})			Ash-450 (% DW)	
		Leaves	Stems	Shoots	Leaves	Stems
21 April 05	Live	97.22 (34.40)	109.69 (39.61)	206.91 (72.59)	8.99 (0.88)	9.91 (0.90)
	Dead	47.29 (12.37)	66.26 (33.14)	113.55 (34.94)	35.50 (5.34)	40.93 (9.47)
23 May 05	Live	349.89 (102.67)	503.94 (165.64)	853.83 (188.51)	10.60 (1.02)	11.80(0.86)
	Dead	167.87 (27.95)	209.82 (75.43)	377.69 (67.79)	45.02 (6.11)	52.77 (7.58)
23 June 05	Live	346.13 (51.36)	735.26 (188.00)	1081.39 (235.02)	13.47 (1.76)	9.84 (0.96)
	Dead	231.00 (51.62)	214.24 (49.56)	445.24 (84.54)	48.00 (4.42)	50.68 (11.05)
25 July 05	Live	367.31 (106.20)	1,101.16 (241.75)	1,468.47 (332.28)	14.98 (1.59)	10.78 (0.91)
	Dead	278.20 (36.27)	146.87 (24.22)	425.07 (35.90)	49.25 (5.53)	54.38 (2.80)
23 August 05	Live	208.71 (72.09)	676.73 (175.39)	885.43 (244.89)	13.76 (1.71)	9.43 (0.71)
	Dead	194.59 (74.69)	80.66 (32.37)	275.24 (63.25)	44.60 (6.21)	55.14 (12.18)
3 October 05	Live	102.49 (36.30)	362.76 (80.83)	465.24 (80.20)	14.05 (1.57)	11.01 (1.68)
	Dead	192.15 (58.73)	133.78 (53.80)	325.93 (81.20)	46.72 (7.27)	65.70 (5.56)
14 November 05	Live	TBD	TBD	TBD	TBD	TBD
	Dead	TBD	TBD	TBD	TBD	TBD
2 January 06	Live	TBD	TBD	TBD	TBD	TBD
	Dead	TBD	TBD	TBD	TBD	TBD
23 February 06	Live	TBD	TBD	TBD	TBD	TBD
	Dead	TBD	TBD	TBD	TBD	TBD

Note: TBD = to be determined.

Mean values 2005-2006 and standard deviations (N=7). Belowground biomass was 1,184.65 ± 470.43 g DW m^{-2} on 25 July 2005 (N=3).

Table A5-2. Seasonal changes in the concentrations of THg, MeHg, and MeHg:THg ratio in biomass of *Spartina foliosa* at low marsh site R-44 of the China Camp State Park.

Date	Tissue	THg (ng g^{-1} DW)		MeHg (ng g^{-1} DW)		MeHg:THg Ratio (x100)		THg (µg m^{-2})	MeHg (µg m^{-2})
		Leaves	Stems	Leaves	Stems	Leaves	Stems	Shoots	Shoots
21 April 05	Live	11.29 (3.07)	10.13 (7.63)	0.36 (0.43)	0.20 (0.06)	2.93 (2.83)	2.64 (1.20)	2.21	0.06
	Dead	158.0 (36.01)	145.0 (44.33)	1.10 (0.37)	2.92 (1.04)	0.72 (0.31)	2.03 (0.36)	17.08	0.25
23 May 05	Live	24.17 (2.73)	15.30 (3.64)	0.26 (0.05)	0.26 (0.03)	1.08 (0.17)	1.61 (0.24)	16.18	0.22
	Dead	145.4 (24.63)	200.0 (39.23)	2.06 (0.83)	3.96 (0.51)	1.48 (0.73)	2.09 (0.54)	66.37	1.18
23 June 05	Live	22.61 (4.49)	9.89 (2.91)	0.36 (0.10)	0.26 (0.02)	1.54 (0.27)	2.62 (0.41)	15.10	0.32
	Dead	152.0 (13.20)	173.4 (45.97)	1.57 (0.12)	4.44 (0.64)	1.05 (0.15)	2.96 (0.63)	72.26	1.31
25 July 05	Live	20.73 (3.48)	13.21 (2.49)	0.50 (0.02)	0.34 (0.03)	2.37 (0.28)	2.05 (0.85)	22.16	0.56
	Dead	120.1 (16.67)	139.4 (13.46)	2.11 (0.20)	3.79 (1.16)	1.68 (0.16)	2.63 (0.62)	53.89	1.14
23 August 05	Live	20.96 (2.97)	8.17 (3.28)	0.53 (0.02)	0.33 (0.06)	2.66 (0.27)	4.55 (0.76)	9.98	0.33
	Dead	102.3 (15.70)	144.9 (33.67)	1.74 (0.15)	2.92 (0.65)	1.64 (0.09)	2.16 (0.23)	31.59	0.57
3 October 05	Live	33.87 (10.75)	10.21 (3.17)	TBD	TBD	TBD	TBD	TBD	TBD
	Dead	149.3 (28.93)	210.4 (20.27)	TBD	TBD	TBD	TBD	TBD	TBD
14 November 05	Live	TBD	TBD	TBD	TBD	TBD	TBD	TBD	TBD
	Dead	TBD	TBD	TBD	TBD	TBD	TBD	TBD	TBD
2 January 06	Live	TBD	TBD	TBD	TBD	TBD	TBD	TBD	TBD
	Dead	TBD	TBD	TBD	TBD	TBD	TBD	TBD	TBD
23 February 06	Live	TBD	TBD	TBD	TBD	TBD	TBD	TBD	TBD
	Dead	TBD	TBD	TBD	TBD	TBD	TBD	TBD	TBD

Note: TBD = to be determined.

Mean values 2005-2006 and standard deviations (N=5). THg and MeHg contents in belowground biomass on 25 July 2005 to be determined.

Table A5-3. Seasonal changes in biomass of *Salicornia virginica* at low marsh site R-44 of the China Camp State Park.

Date	Tissue	Plant Biomass (g DW m^{-2})			Ash-450 (% DW)	
		Leaves	Stems	Shoots	Leaves	Stems
21 April 05	Live	153.32 (36.25)	560.29 (243.50)	713.60 (253.09)	28.74 (1.43)	16.98 (3.86)
	Dead	12.54 (13.37)	128.63 (102.94)	141.17 (115.09)	21.00 (0.47)	18.11 (2.55)
23 May 05	Live	187.49 (137.63)	793.26 (445.23)	980.75 (570.56)	26.19 (2.22)	10.43 (2.45)
	Dead	55.88 (42.08)	134.48 (72.13)	190.36 (110.80)	17.99 (2.31)	12.90 (3.26)
23 June 05	Live	303.19 (92.33)	798.80 (290.74)	1,101.99 (359.26)	26.90 (2.82)	10.30 (1.61)
	Dead	85.79 (48.08)	178.02 (40.09)	263.82 (73.11)	20.36 (3.70)	14.76 (1.73)
25 July 05	Live	219.38 (43.96)	648.28 (144.53)	867.67 (153.55)	34.48 (1.76)	12.45 (2.57)
	Dead	61.11 (12.70)	173.91 (52.13)	235.02 (58.17)	27.18 (1.71)	23.66 (3.53)
23 August 05	Live	276.73 (82.15)	554.89 (141.71)	831.62 (201.27)	34.52 (2.87)	12.03 (1.11)
	Dead	72.10 (18.05)	205.15 (36.26)	277.25 (50.71)	27.35 (1.11)	24.76 (0.71)
3 October 05	Live	255.99 (88.96)	904.29 (177.98)	1,160.29 (183.82)	38.63 (1.27)	11.62 (1.77)
	Dead	94.44 (13.25)	211.38 (103.89)	305.82 (107.23)	35.74 (3.14)	31.21 (6.14)
14 November 05	Live	TBD	TBD	TBD	TBD	TBD
	Dead	TBD	TBD	TBD	TBD	TBD
2 January 06	Live	TBD	TBD	TBD	TBD	TBD
	Dead	TBD	TBD	TBD	TBD	TBD
23 February 06	Live	TBD	TBD	TBD	TBD	TBD
	Dead	TBD	TBD	TBD	TBD	TBD

Note: TBD = to be determined.

Mean values 2005-2006 and standard deviations (N=7). Belowground biomass was 3147.81 ± 1543.82 g DW m^{-2} on 25 July 2005 (N=3).

Table A5-4. Seasonal changes in the concentrations of THg, MeHg, and MeHg:THg ratio in biomass of *Salicornia virginica* at low marsh site R-44 of the China Camp State Park.

Date	Tissue	THg (ng g^{-1} DW)		MeHg (ng g^{-1} DW)		MeHg:THg Ratio (x100)		THg (µg m^{-2})	MeHg (µg m^{-2})
		Leaves	Stems	Leaves	Stems	Leaves	Stems	Shoots	Shoots
21 April 05	Live	21.91 (6.72)	52.54 (17.99)	0.42 (0.16)	1.32 (0.12)	1.91 (0.43)	2.44 (0.68)	32.80	0.80
	Dead	30.25 (3.55)	52.83 (12.85)	0.69 (0.01)	1.31 (0.26)	2.40 (0.30)	2.59 (0.32)	7.17	0.18
23 May 05	Live	19.99 (4.20)	23.23 (8.69)	0.23 (0.07)	0.57 (0.14)	1.08 (0.33)	2.40 (0.85)	22.18	0.50
	Dead	45.28 (8.53)	29.14 (7.33)	0.74 (0.06)	0.73 (0.08)	1.68 (0.22)	2.54 (0.43)	6.45	0.14
23 June 05	Live	11.90 (2.54)	20.59 (4.66)	0.34 (0.05)	0.89 (0.11)	3.02 (0.63)	4.87 (1.38)	20.06	0.81
	Dead	52.43 (11.3)	37.59 (3.54)	1.29 (0.15)	1.11 (0.04)	2.40 (0.22)	3.09 (0.19)	11.19	0.31
25 July 05	Live	13.89 (1.98)	20.09 (3.21)	0.39 (0.06)	0.77 (0.11)	2.65 (0.37)	3.97 (0.37)	16.07	0.58
	Dead	48.47 (6.97)	53.21 (8.26)	1.22 (0.16)	1.27 (0.11)	2.61 (0.33)	2.55 (0.31)	12.22	0.30
23 August 05	Live	12.54 (4.93)	26.07 (2.75)	0.36 (0.02)	0.72 (0.07)	3.75 (0.68)	2.78 (0.39)	17.94	0.50
	Dead	73.10 (6.25)	71.38 (8.82)	1.15 (0.03)	1.24 (0.06)	1.53 (0.07)	1.80 (0.20)	19.91	0.34
3 October 05	Live	TBD	TBD	TBD	TBD	TBD	TBD	TBD	TBD
	Dead	TBD	TBD	TBD	TBD	TBD	TBD	TBD	TBD
14 November 05	Live	TBD	TBD	TBD	TBD	TBD	TBD	TBD	TBD
	Dead	TBD	TBD	TBD	TBD	TBD	TBD	TBD	TBD
2 January 06	Live	TBD	TBD	TBD	TBD	TBD	TBD	TBD	TBD
	Dead	TBD	TBD	TBD	TBD	TBD	TBD	TBD	TBD
23 February 06	Live	TBD	TBD	TBD	TBD	TBD	TBD	TBD	TBD
	Dead	TBD	TBD	TBD	TBD	TBD	TBD	TBD	TBD

Note: TBD = to be determined.

Mean values 2005-2006 and standard deviations (N=5). THg and MeHg contents in belowground biomass on 25 July 2005 to be determined.

Table A7-1. C, N, and S contents of suspended particulate organic material (POM), primary producers, and vascular plant litter (including habitat type where sampled) collected from the China Camp marsh and adjacent San Pablo Bay area. Data are sample size (N), mean values, and standard deviations.

Material	Habitat Type	N	C (mg kg^{-1})	N (mg kg^{-1})	S (mg kg^{-1})
Particulate organic matter					
POM	Bay	2	15.0 (0)	2.07 (0.17)	5.18 (0.62)
POM	Marsh pool	2	52.5 (21.1)	8.79 (2.15)	4.38 (1.53)
Phytoplankton					
SF Bay	Bay	2	179 (18.5)	30.0 (2.52)	4.01 (0.14)
Marsh	Marsh pool	3	105 (8.28)	17.1 (0.60)	9.33 (1.58)
Marsh microalgae					
Diatom sp.	Mid marsh	3	31.1 (1.84)	4.62 (0.34)	2.56 (0.36)
Cyanobacteria sp.	Mid marsh	3	39.8 (4.58)	4.63 (0.45)	3.29 (0.41)
Filamentous sp.	Marsh pool	3	214 (14.6)	21.7 (4.00)	14.5 (0.57)
Bay macroalgae					
Ulva sp.	Bay	3	271 (23.7)	34.0 (4.00)	13.6 (1.32)
Fucus sp.	Bay	3	342 (14.2)	18.4 (0.32)	13.5 (4.41)
Marsh vascular plants					
*Spartina foliosa** (C_4)	Low marsh	6	365 (14.3)	11.5 (2.93)	2.68 (0.86)
*Salicornia virginica** (C_3)	Mid marsh	5	371 (17.4)	12.5 (4.40)	2.70 (0.16)
Distichlis spicata (C_4)	High marsh	3	391 (7.48)	9.00 (1.94)	1.49 (0.03)
Atriplex triangularis (C_3)	High marsh	3	332 (22.9)	10.4 (2.90)	2.04 (0.46)
Marsh vascular plant litter					
Spartina foliosa (C_4)	Low marsh	3	319 (32.2)	9.27 (0.73)	2.08 (0.22)
Salicornia virginica (C_3)	Mid marsh	3	353 (23.0)	12.2 (2.72)	4.50 (0.40)

Table A7-2. C, N, and S contents of invertebrate, fish, mammals, and avian consumers (including habitat type where sampled) collected from the China Camp marsh, HAAF*, and adjacent San Pablo Bay area. Data are sample size (N), mean values, and standard deviations.

Species	Habitat Type	N	C (mg kg^{-1})	N (mg kg^{-1})	S (mg kg^{-1})
Invertebrates					
Cicindela sp. (Tiger beetle)	Low marsh	1	470 (0.00)	91.4 (0.00)	3.27 (0.00)
Snail sp.	Low marsh	1	439 (0.00)	76.8 (0.00)	3.77 (0.00)
Orchestia traskiana (Amphipod)	Low marsh	6	365 (27.2)	73.5 (3.55)	5.16 (1.35)
Geukinsia demissa (Ribbed mussel)	Bay	9	403 (27.2)	74.3 (5.33)	9.46 (0.92)
Potamocorbula amurensis (Chinese clam)	Bay	1	359 (0.00)	83.5 (0.00)	12.6 (0.00)
Macoma baltica (Baltic clam)	Bay	3	344 (68.9)	65.6 (7.75)	6.57 (1.24)
Nereis vexillosa (Pile worm)	Bay	2	342 (35.2)	79.6 (2.97)	11.0 (1.11)
Worm sp.	Bay	2	280 (16.7)	67.0 (3.63)	8.98 (1.28)
Hemigrapsus oregonensis (Yellow shore crab)	Bay	2	349 (3.99)	88.7 (3.20)	9.98 (0.55)
Carcinus maenas. (European green crab)	Bay	8	360 (41.1)	93.5 (19.9)	8.44 (2.97)
Shrimp sp.	Bay	6	424 (33.1)	125 (10.7)	8.85 (1.48)
Fishes					
Platichthys stellatus (Starry flounder)	Bay	8	461 (16.9)	138 (8.01)	8.59 (1.39)
Clevelandia ios (Arrow goby)	Bay	3	436 (8.66)	134 (5.36)	10.5 (0.55)
Leptocottus armatus (Pacific staghorn sculpin)	Bay	9	455 (15.0)	137 (2.71)	12.0 (1.62)
Mammals					
Reithrodontomys raviventris *(Salt marsh harvest mouse)	High marsh	1	441 (0.00)	114 (0.00)	7.13 (0.00)
Microtus californicus (California vole)	High marsh	1	492 (0.00)	93.6 (0.00)	7.30 (0.00)
Birds					
Melospiza melodia samuelis (Song sparrow)	High marsh	3	476 (4.93)	124 (3.53)	8.95 (0.43)
Laterallus jamaicensis coturniculus (California black rail)	Unknown	1	490 (0.00)	121 (0.00)	8.62 (0.00)

REPORT DOCUMENTATION PAGE

Form Approved
OMB No. 0704-0188

Public reporting burden for this collection of information is estimated to average 1 hour per response, including the time for reviewing instructions, searching existing data sources, gathering and maintaining the data needed, and completing and reviewing this collection of information. Send comments regarding this burden estimate or any other aspect of this collection of information, including suggestions for reducing this burden to Department of Defense, Washington Headquarters Services, Directorate for Information Operations and Reports (0704-0188), 1215 Jefferson Davis Highway, Suite 1204, Arlington, VA 22202-4302. Respondents should be aware that notwithstanding any other provision of law, no person shall be subject to any penalty for failing to comply with a collection of information if it does not display a currently valid OMB control number. **PLEASE DO NOT RETURN YOUR FORM TO THE ABOVE ADDRESS.**

1. REPORT DATE *(DD-MM-YYYY)*
September 2007

2. REPORT TYPE
Interim report

3. DATES COVERED *(From - To)*

4. TITLE AND SUBTITLE

Pre-Construction Biogeochemical Analysis of Mercury in Wetlands Bordering the Hamilton Army Airfield (HAAF) Wetlands Restoration Site. Part 2

5a. CONTRACT NUMBER

5b. GRANT NUMBER

5c. PROGRAM ELEMENT NUMBER

6. AUTHOR(S)

Elly P. H. Best, Herbert L. Fredrickson, Holger Hintelmann, Olivier Clarisse, Brian Dimock, Charles H. Lutz, Gui R. Lotufo, Rod N. Millward, Anthony J. Bednar, and John S. Furey

5d. PROJECT NUMBER

5e. TASK NUMBER

5f. WORK UNIT NUMBER

7. PERFORMING ORGANIZATION NAME(S) AND ADDRESS(ES)

U.S. Army Engineer Research and Development Center
Environmental Laboratory
3909 Halls Ferry Road, Vicksburg, MS 39180-6199

8. PERFORMING ORGANIZATION REPORT NUMBER

ERDC/EL TR-07-21

9. SPONSORING / MONITORING AGENCY NAME(S) AND ADDRESS(ES)

U.S. Army Corps of Engineers
Washington, DC 20314-1000;
U.S. Army Engineer Research and Development Center
3909 Halls Ferry Road, Vicksburg, MS 39180-6199

10. SPONSOR/MONITOR'S ACRONYM(S)

11. SPONSOR/MONITOR'S REPORT NUMBER(S)

12. DISTRIBUTION / AVAILABILITY STATEMENT

Approved for public release; distribution is unlimited.

13. SUPPLEMENTARY NOTES

14. ABSTRACT

Over 90% of the coastal wetlands in San Francisco Bay have been lost since the industrial revolution. With funding from the Long Term Management Strategy team, the U.S. Army Corps of Engineers (USACE) is working with the San Francisco Basin Regional Water Board, California State Coastal Conservancy, and San Francisco Bay Conservation and Development Commission to reconstruct wetlands at the former Hamilton Army Airfield (HAAF) on San Pablo Bay. This 203-ha site will provide tidal habitat to endangered species such as the clapper rail and the saltmarsh harvest mouse. Because HAAF has subsided well below mean sea level, it will require 8.1 million cubic meters of material to elevate the site to the point where emergent marsh vegetation can become established. This is a critical process that will reestablish natural sediment trapping, marsh building, and physical dynamics. However, wetlands are generally considered a source of monomethylmercury (MeHg) production, and the association of mercury with gold mining legacies of the Bay Basin raises particular concerns. HAAF represents only 203 ha of the additional 26,325 ha of wetlands to be established around the bay between 2005 and 2055. Means to mitigate MeHg magnification in bay aquatic food webs are needed not only for HAAF but other SF Bay restoration sites as well. Those means are currently unknown.

(Continued)

15. SUBJECT TERMS
See reverse.

16. SECURITY CLASSIFICATION OF:			**17. LIMITATION OF ABSTRACT**	**18. NUMBER OF PAGES**	**19a. NAME OF RESPONSIBLE PERSON**
a. REPORT	**b. ABSTRACT**	**c. THIS PAGE**			**19b. TELEPHONE NUMBER** *(include area code)*
UNCLASSIFIED	UNCLASSIFIED	UNCLASSIFIED		221	

14. ABSTRACT

This interim technical report describes studies primarily performed in 2004 and 2005 and completed in the first half of 2006. Work during this period focused on (1) site-specific rates of methylation and demethylation, as well as characterizations of sedimentary microbial communities; (2) mercury dynamics in decomposing plant litter; (3) mercury dynamics in food webs; and (4) bioavailability of sediment-associated mercury of existing marsh sediments to macrobenthos. A new time-integrative method for measuring and monitoring mercury cycle-related biogeochemical parameters in marshes was developed, and the role of marsh vegetation as a vector in mercury species transport was quantified.

15. SUBJECT TERMS (Concluded)

Bioaccumulation
Bioavailability
Coastal wetlands restoration
Decomposition
Demethylation
Food chain
Macrophytes
Management
Mass balance
Mercury
Methylation
Model
Monitoring
Monomethylmercury
Plant litter
Salicornia virginica
Salt marsh
San Francisco Bay
San Pablo Bay
Sediment
Spartina foliosa
Stable isotopes
Tidal marsh